Analytic continuations and integrability for the KPZ universality class with open boundaries

Ulysse Godreau

▶ **To cite this version:**

Ulysse Godreau. Analytic continuations and integrability for the KPZ universality class with open boundaries. Physics [physics]. Université Paul Sabatier - Toulouse III, 2022. English. NNT : 2022TOU30157 . tel-03924807

HAL Id: tel-03924807
https://theses.hal.science/tel-03924807

Submitted on 5 Jan 2023

HAL is a multi-disciplinary open access archive for the deposit and dissemination of scientific research documents, whether they are published or not. The documents may come from teaching and research institutions in France or abroad, or from public or private research centers.

L'archive ouverte pluridisciplinaire **HAL**, est destinée au dépôt et à la diffusion de documents scientifiques de niveau recherche, publiés ou non, émanant des établissements d'enseignement et de recherche français ou étrangers, des laboratoires publics ou privés.

Université Fédérale
Toulouse Midi-Pyrénées

THÈSE

En vue de l'obtention du
DOCTORAT DE L'UNIVERSITÉ DE TOULOUSE
Délivré par l'Université Toulouse 3 - Paul Sabatier

Présentée et soutenue par

Ulysse GODREAU

Le 23 septembre 2022

Prolongements analytiques et intégrabilité pour la classe d'universalité KPZ avec bords

Ecole doctorale : **SDM - SCIENCES DE LA MATIERE - Toulouse**

Spécialité : **Physique**

Unité de recherche :
LPT - Laboratoire de Physique Théorique

Thèse dirigée par
Sylvain PROLHAC

Jury

M. Jan DE GIER, Rapporteur
Mme Véronique TERRAS, Rapporteure
M. Malte HENKEL, Examinateur
M. Reda CHHAIBI, Examinateur
M. Luigi CANTINI, Examinateur
M. Sylvain PROLHAC, Directeur de thèse
M. Pierre PUJOL, Président

Abstract The asymmetric simple exclusion process (ASEP) is a stochastic model featuring particles with contact interactions hopping randomly on a one dimensional lattice. Despite its simplicity, it possesses many interesting theoretical characteristic, as a generically non equilibrium steady state, complex hydrodynamics properties and connections with the KPZ universality class. The fact that it is exactly solvable by various methods makes it a model of choice to further our understanding of out-of-equilibrium statistical physics. If many results are known for the ASEP on a infinite lattice, much less is known for the process in finite volume. In this thesis we consider the totally asymmetric case (TASEP) with open boundary conditions of the process. We obtain exact expressions for the spectral gaps of an operator giving access to the fluctuations of the current of particle in regimes of the model relevant to KPZ universality in the large system size limit. Our derivation of the eigenstates of the TASEP is based on the systematic construction of the analytic continuations of expressions previously known for the ground state of the process, and are validated by Bethe ansatz. Connections are made with existing results for the exclusion process with periodic boundary conditions.

Résumé Le processus d'exclusion simple asymétrique (ASEP) est un modèle stochastique dans lequel des particules présentant des interactions de contact se déplacent aléatoirement sur un réseau unidimensionel. Malgré la simplicité de sa définition, de nombreuses propriétés théoriques telles que le fait qu'il présente un état stationnaire hors-équilibre ou les liens qui le relient à la classe d'universalité KPZ en font un des modèles les plus étudiés en physique statistiques. Il est de plus intégrable par ansatz de Bethe et son état stationnaire peut être calculé explicitement par ansatz matriciel, de sorte qu'il permet de dériver des résultats exacts pour la classe d'universalité KPZ. Dans cette thèse nous considérons le cas totalement asymétrique (TASEP) du processus avec des conditions aux bords ouvertes. Nous obtenons des expressions exactes pour les premiers états excités d'un opérateur donnant accès aux fluctuations du courant de particules en temps fini dans la limite thermodynamique, pour des régimes du système présentant des propriétés universelles caractéristiques de la classe KPZ. Notre méthode de calcul des états propres du TASEP ouvert est fondée sur le calcul systématique du prolongement analytique d'expressions déjà connues pour l'état stationnaire du processus, obtenue par une généralisation de l'ansatz matriciel. Ces résultats sont ensuite validés et partiellement démontré par l'étude asymptotiques des équations de Bethe du processus.

Contents

Remerciements

Je tiens tout d'abord à remercier Jan de Gier et Véronique Terras d'avoir bien voulu relire avec beaucoup d'attention cette thèse en qualité de rapporteurs, ainsi que Luigi Cantini, Reda Chhaibi, Malte Henkel et Pierre Pujol d'avoir accepté d'être membres de mon jury.

Toute ma gratitude va à Sylvain Prolhac qui a encadré cette thèse et en a conçu le projet. Sa bienveillance, sa disponibilité et son immense maîtrise scientifique ont permis au présent travail d'exister. Ce fut une chance rare et une joie d'avoir pu travailler avec lui durant trois ans.

Je ne saurais trop remercier les membres et personnels du LPT et de l'ex-IRSAMC qui m'ont acccompagné au cours de ma thèse, en particulier Malika Bentour, Sandrine Le Magoarou, Nicolas Elefantis, Nicolas Destainville, Jérôme Cuny et Bertrand Georgeot.

Salut enfin, et fraternellement merci à tou.te.s les doctorant.es et postddoc passé par le 3R1 au cours de ces trois années.

Introduction

In the endeavour to derive general laws and methods to understand physical systems composed of many interacting elements, statistical physics has come to identify two general categories of systems namely *equilibrium* and *non-equilibrium* ones. The first category encompasses all systems which in the long time limit evolve freely into a steady state that is macroscopically at rest, meaning that all macroscopic quantities do not evolve anymore. These equilibrium steady states can be characterized at the microscopic level by the detailed balance condition : the net probability fluxes between any microscopic configurations of the system vanish. As a consequence of detailed balance, the probability distribution of the system's microscopic configuration depends only on a few macroscopic quantities such as energy, temperature, or the value of various external fields. Moreover, the general form of this probability distribution is universal, and can be cast for any equilibrium system into a Gibbs-Boltzmann law. On the other hand, non-equilibrium systems breaking detailed balance have a much more complex steady state distribution. The existence of net probability fluxes manifest itself notably through macroscopic currents of energy or particle within the system, which makes their phenomenology much richer and complex. The pursuit of a generalization of the equilibrium formalism to non-equilibrium system is the object of considerable work, which produced several result of great generality, as fluctuation relations, or the introduction of large deviation functions and functionals as generalization of the Gibbs-Boltzmann distribution.

Another general problematic of statistical physics is to determine to what extent systems and models with different microscopic behaviour can be considered as *essentially similar* at macroscopic scales, considering that a proper description of statistical systems should be as independent as possible of their microscopic details. This idea was made precise and quantitative with the introduction by Kadanov and Wilson of the *renormalization group* formalism. It appears that under a systematic coarse-graining procedure, large sets of different models become similar at large scale to a single renormalization *fixed point* capturing their essential macroscopic behaviour. All models converging to the same fixed point are then said to belong to the same universality class. The idea of universality is best illustrated, for equilibrium systems, by the two dimensional Ising model which is arguably the simplest representative of a vast universality class encompassing many two dimensional systems of particles with local interactions. Typically universal properties which manifest for all models in the same class are the scaling laws of macroscopic quantities in the vicinity of critical points or the normalized statistics of the fluctuations of fields describing the coarse-grained state of a model.

Among the continuum of models of a given universality class, some outstanding cases occupy a favored position, being exactly solvable by a happy mathematical accident. These so-called *integrable models* are characterized by a large number of conserved quantities which considerably constrains their behaviour and allows the exact computation of their dynamics by more or less systematic methods. Among these models one finds several well known classical or quantum one dimensional models like the Lieb-Liniger model and the XXX and XXZ spin chains, or two-dimensional models like the six and eight vertex models or the Ising model. The identification of an integrable model within a universality class allows the derivation of very general results from a single mathematically tractable representative.

In regards of what was just said, the asymmetric simple exclusion process (ASEP), which will be the object of all attention in the present work, appears as an object of choice to further our understanding of statistical physics beyond equilibrium. The exclusion process is a purely stochastic model in which particles randomly hop, with a preferred direction, from one site to another of a discrete lattice with the unique constraint that a site is occupied by at most one particle, resulting in particle-particle interactions. It is indeed one the simplest statistical models breaking the detailed balance

condition, and displays, despite the simplicity of its definition, complex hydrodynamics features and non-trivial statistical properties. ASEP also belongs to the Kardar-Parisi-Zhang (KPZ) universality class, a large category of non-equilibrium models in which a growing *height function* can be defined (typically describing an interface between two phases of the system). All models in the KPZ class are characterized by common scaling properties of their associated height functions, as well as common non-Gaussian distributions of the local fluctuations of this function. The number of models known to belong to the KPZ class or experimental systems exhibiting KPZ behviour has been steadily growing until now, coming from as seemingly unrelated contexts as cell colony growing, disordered quantum systems, integrable non-linear oscillator chains, deposition models of growing interfaces, phase transitions in liquid crystals, slow combustion of paper or quantum-gate circuits. The exclusion process being integrable by Bethe ansatz, it is an ideal tool to derive exact results for the whole KPZ class.

If many results have been established for the ASEP on a infinite lattice, much less is known about the ASEP in finite volume with periodic or open boundary conditions. The purpose of this work is to contribute to fill this gap by computing the eigenstates of the infinitesimal generator of the exclusion process in the regime relevant to KPZ universality. More precisely, we compute the eigenvalues of an operator $M(\mu)$, called throughout this work the *deformed Markov matrix* of the process related to the cumulant generating function of the current of particles. This quantity is of special interest as the mapping from the exclusion process to an interface growth model translating properties of the ASEP into universal KPZ properties is done by considering the time integrated local currents of particles through the lattice of sites.

In terms of method, our approach relies crucially on the analyticity of the eigenstates of an operator with respect to a given parameter upon which it depends. More specifically, the main results of this thesis, which are exact expressions for higher eigenstates of the above-mentioned operator $M(\mu)$, will be obtained by analytic continuation of a given ground-state eigenvalue of this operator.

Let us briefly outline the content of this thesis

Chapter 1 is devoted to a general presentation of the exclusion process and its relations with the KPZ universality class. After providing a formal definition of the model and reviewing the physical application and issues related to it, we introduce the mathematical tools and concepts needed to study the fluctuations of the current through the chain. We then briefly introduce the KPZ universality class to set the scene for our results and justify their relevance

In chapter 2 we focus on the integrable techniques used to compute the eigenvalues and eigenstates of the evolution operators of the exclusion process. After presenting the Matrix product ansatz of Derrida Evans Hakim and Pasquier for the steady state of the open ASEP, we go one with the derivation of the Bethe ansatz equation for the periodic exclusion process as a warm up, and then the derivation of the Bethe equation for the open TASEP by the algebraic Bethe ansatz. We give some justification for a second set of Bethe equations for the open TASEP, that is used in the rest of the thesis, although strictly speaking these equation (and the results derived from them) are conjectural.

Chapter 3 is essentially a technical preparation for the result stated in the next chapter. Starting with a mathematical introduction to the notions of analytic continuation and Riemann surfaces which are their natural domain of definition, we gather the rather lengthy computations of the analytic continuations of the functions related to the eigenstates of the operators we are interested in.

In chapter 4 we state our own results, published in [41] and [40], namely the explicit and exact expressions of the spectral gaps of the deformed Markov operator $M(\mu)$ for different scalings of the boundary parameters of the model, in terms of the functions constructed in chapter 3.

Chapter 1

The totally asymmetric simple exclusion process - presentation and general results

In this chapter the reader is introduced to the asymmetric simple exclusion process. After defining the model and some of its variants in first section 1.1, we start by providing some motivations for our work coming from various context in physics in section 1.2. We then set up the formalism used throughout this thesis to study the fluctuations of the current, introducing notably the deformed matrix $M(\mu)$ of the current for the exclusion process, and give an overview of the phenomenology of the open chain in the totally asymmetric cases by a mean field approach in 1.3. Note that the exact computation of the stationary state of the open ASEP will be done in chapter 2.

The second part of the chapter consists of a brief introduction to the KPZ equation and universality class and its connection with the exclusion process in section 1.5. We finally give an overview of the results currently known about the fluctuations of the density and current of particles in the periodic in section 1.6 and open TASEP in section 1.7.

1.1 Definition of the model and variants

The open ASEP and TASEP

The open asymmetric simple exclusion process [84, 31, 81] is a continuous time Markov process defined on a one dimensional lattice. Each site of the lattice can be in two states, empty or occupied by one particle. Each particle in the system may hop from site i to the site $i+1$ on its right with rate p and to the site $i-1$ on its left with rate q, if the destination sites are empty. The hopping processes occur independently for each particle with exponential waiting time. More precisely, each particle is associated with a Poisson process with unit rate which triggers a hopping event. The direction of the hop is then selected with probabilities p and q and the particle then moves only if the destination site is empty.

Several geometries of the lattice can be considered. One can first define the exclusion process on an infinite chain of sites, in which case the system has an infinite number of possible configurations. The large time behaviour of the model in this case typically depends on the initial configuration of the chain, see figure 1.1 for a representation of the most commonly used initial conditions for the infinite ASEP. The exclusion process can also be defined on a finite size lattice of L site with periodic boundary condition. In the exclusion process on a ring (or with periodic boundary conditions), the site L is connected to the site 1 and the number of particles N on the chain is fixed, so that the system has $\binom{L}{N}$ possible configurations corresponding to the choices of position of the particles on the lattice. One can finally define the exclusion process with open boundaries. Each end of the chain is then connected to a reservoir of particles, so that a particle may enter site 1, if empty, with rate α and a particle at site 1 may exit the system with probability γ. Similarly, a particle at site L may exit the system with rate β or enter site L from the right reservoir with rate δ. Several special cases can also be considered depending on the values of the parameters. The case $p = q = 1/2$ – with $\alpha = \beta = \gamma = \delta = 1/2$ for the open chain – defines the symmetric exclusion process (SSEP) which is special as in this case the

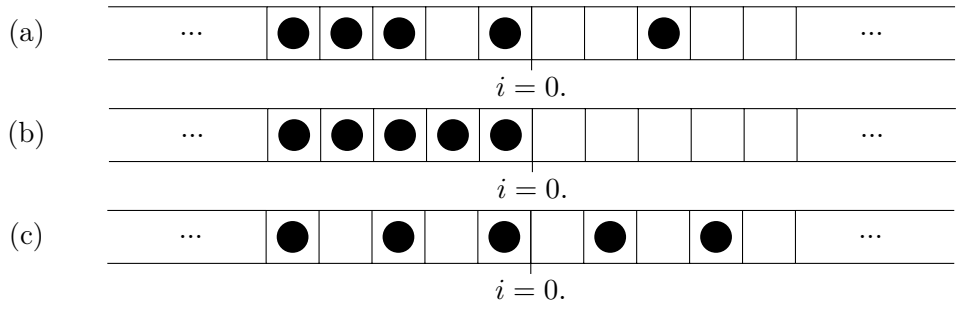

Figure 1.1: Several initial conditions for the infinite line TASEP. (a) Poisson (or stationary), sites are randomly occupied of free with a density of particle of one half (b) domain wall, all sites on the left of 0 are occupied (c) alternating, sites are alternatively occupied or free.

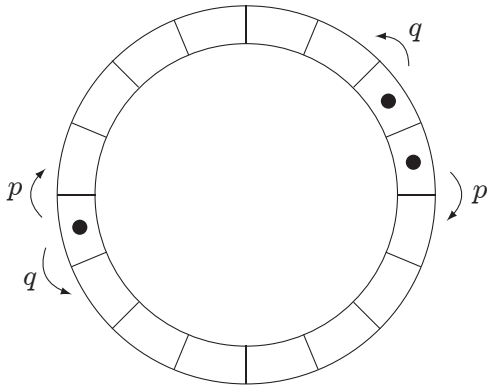

Figure 1.2: Rules of the dynamics of the ASEP with periodic boundary conditions

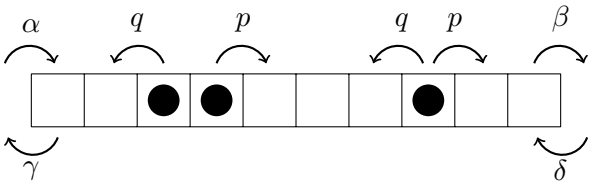

Figure 1.3: Rules of the dynamics of the open ASEP with open boundaries

system evolves to an equilibrium steady state (see below). The totally asymmetric case, which is the object of attention of the present work, is obtained when the motion of the particles is unidirectional. The backward hopping, entry and exit rates q, δ, γ are then set to zero. Up to a rescaling of the time variable t, the forward hopping rate can be set to $p = 1$.

The exclusion process is a purely stochastic process, and has no underlying Hamiltonian structure for instance. It is described by a set of configurations $\mathcal{S}$, each configuration $\mathcal{C} \in \mathcal{S}$ being defined by the sequence of of occupation numbers $(n_i)_{i \in \text{lattice}}$ with $n_i = 1$ if the i-th site is occupied and $n_i = 0$ if its is empty. For the infinite line ASEP, the infinite configuration space is thus $\mathcal{S} = \{0, 1\}^{\mathbb{Z}}$, while $\mathcal{S} = \{0, 1\}^L$ for the periodic or open ASEP on a chain of L sites. The dynamics of the model is fully encoded by the data of the transition rates $W(\mathcal{C} \to \mathcal{C}')$ which are the probabilities per unit time for the system in configuration $\mathcal{C}$ to switch to configuration $\mathcal{C}'$. The state of the system at any time is fully characterized by the probabilities $P_t(\mathcal{C})$ of being in configuration $\mathcal{C}$ at time t. Given an initial probability distribution $P_{t=0}(\mathcal{C})$, the time evolution of the probabilities $P_t(\mathcal{C})$ is given by the master

equation

$$\frac{d}{dt}P_t(\mathcal{C}) = \sum_{\mathcal{C}'} W(\mathcal{C}' \to \mathcal{C})P_t(\mathcal{C}') - W(\mathcal{C} \to \mathcal{C}')P_t(\mathcal{C}) \ . \tag{1.1}$$

The exclusion process reaches in the long time limit a unique stationary distribution $P^*(\mathcal{C})$ satisfying

$$\sum_{\mathcal{C}'} W(\mathcal{C}' \to \mathcal{C})P^\star(\mathcal{C}') - W(\mathcal{C} \to \mathcal{C}')P^\star(\mathcal{C}) = 0 \ , \tag{1.2}$$

The existence and unicity of the stationary distribution is guaranteed by the ergodicity or irreducibility of the process, that is by the fact that any configuration of the system can be reached from any other in finite time along a trajectory in configuration space with non zero probability. This property implies in turn that the time average of any function of the system's state over a single realization of the process coincides with the ensemble average of the same function at fixed t over many realization of the process.

The stationary distribution of the periodic ASEP will be computed in 1.3.2. The exact stationary distribution on configurations of the open ASEP will be derived in 2.1. Let us first give some motivations for the study of the exclusion process

1.2 Motivations and background

Non-equilibrium steady states

Statistical physics is broadly concerned with the study of systems possessing a large number of possible internal configurations, called *microstates* – so large a number that the resolution of the full dynamics of these systems down to the elementary level is not feasible in practice. However, the physical quantities of interest which are accessible to observation are typically many-to-one functions on the set of microstates, so that it is often possible to elucidate the macroscopic behavior of the system by adopting a probabilistic description of the microstate level, once it settles into a time-independent stationary state. This is done by surmising a probability measure on the configuration space (or set of microstates), the values of macroscopic observables being then obtained as an *ensemble* average over the configuration space of the value realized by each configuration.

The first step in that direction was taken in the 1860s when Boltzmann conjectured that all accessible microstates of an isolated system – constrained by the value of globally conserved quantities – have the same probability in the long time limit, which defines the *microcanonical ensemble*. The generalization of this approach to the case of systems weakly coupled to thermal baths and particles reservoirs led to the introduction of the *canonical* and *grand-canonical* ensembles with the corresponding Gibbs measure on configuration space, which are since the backbone of equilibrium statistical physics.

However, not all physical systems are amenable to this approach. In order to apply the powerful ensemble formalism to a given system, it has to settle into an *equilibrium* steady-state. Let us consider a system with a finite set of possible (microscopic) configurations $\mathcal{S} = \{\mathcal{C}\}$, following a Markovian dynamics. Assuming that the system reaches a unique stationary state characterized by a stationary distribution $P^*(C)$, its state is an equilibrium state if it satisfies the additional *detailed balance* property

$$W(\mathcal{C} \to \mathcal{C}')P^\star(\mathcal{C}) = W(\mathcal{C}' \to \mathcal{C})P^\star(\mathcal{C}') \ , \tag{1.3}$$

which is a sufficient but much stronger condition for the stationarity of $P^*(\mathcal{C})$. The detailed balance condition can be defined in a more general way directly from the transition rates of the process [51]. Let

$$\mathcal{L} : \mathcal{C}_1 \to \mathcal{C}_2 \to \ ... \ \to \mathcal{C}_N - 1 \to \mathcal{C}_1 \tag{1.4}$$

$$\mathcal{L}^{\text{rev}} : \mathcal{C}_1 \to \mathcal{C}_{N-1} \to \ ... \ \to \mathcal{C}_2 \to \mathcal{C}_1 \tag{1.5}$$

be a loop in configuration space and its reversed analogue. Considering the product of the transition rates along the loop $\Pi[\mathcal{L}] = \prod_{i=1}^{N-1} W(\mathcal{C}_i \to \mathcal{C}_{i+1})$, the set of rates defining the Markov process is said

to satisfy the detailed balance condition if $\Pi[\mathcal{L}] = \Pi[\mathcal{L}^{\text{rev}}]$ for all loops, in which case the stationary distribution of the process is at equilibrium.

No general framework comparable to the ensembles of equilibrium statistical mechanics exists at the time for system exhibiting non-equilibrium steady states. Yet these systems are ubiquitous in nature, and possess a much richer phenomenology than the all in all very narrow category of equilibrium systems. A way of dealing with non-equilibrium statistical systems in the absence of unified theoretical framework is to build one's intuition by closely studying *toy models*.

In this regard, (T)ASEP is one the simplest interacting many-body models breaking detailed-balance [1], yet it displays many features broadly characteristic of non-equilibrium models, including long range correlations in the steady state (while the dynamics only relies on nearest neighbour interactions), finite currents of particles in the steady state and non-Gaussian fluctuations of the observables (current and density of particles).

Biological transport and traffic modeling

The asymmetric exclusion process and its generalizations find direct applications in the modelization of several transport phenomena involving interacting particles.

The first ASEP-like model was introduced in 1968 [59] to study the dynamics of ribosomes on a mRNA chain in order to understand the kinetic of the translation of genetic code into proteins. This physical situation contains indeed the main ingredients that define the exclusion process. The particles, here ribosomes, are bound to a one dimensional chain (the mRNA) which is discrete by nature as it is divided into codons. Ribosomes cannot overtake each others and move along the mRNA in a preferred direction imposed by the direction of reading of the gene encoded by the mRNA. The mRNA threads being finite and bounded, one has to consider the ASEP with open boundaries specifically. Some refinement can be added to the vanilla ASEP to make it more realistic in regard of its application to genetic translation [18]: particle may be longer than one site to take into account the fact that ribosomes occupy a space larger that one codon; the translation of some segments can be longer than others, so that one has to consider inhomogeneous hopping rates, *i.e* site-dependent p and q. One can also consider dynamics with random attachment and evaporation of particles in the bulk of the chain [67].

Another prominent application in biology is the transport of ions or light molecules through pores across cell walls [18]. This phenomenon raises interesting theoretical questions as the transport in these channel is known to be sudiffusive, *i.e.* the the mean square displacement of a particle scales like $\langle x^2 \rangle \ll t$. Pores can be considered as one dimensional as they often have a diameter close to the typical size of the particles they carry. Apart from their diffusive behaviour, the particles are subject to a driving by a difference of electrical potential between the two ends of the channel, hence the asymmetry of their motions, and short range repulsion between each others, hence the exclusion constraint. Relevant generalizations in this context include the several species ASEP to describe the transport of protons in ionic channels through the *water wire* model [19].

Among direct applications of the exclusion process one can also mention traffic modeling. An important feature of traffic flow is the formation and long time stability of shocks, that is abrupt transitions between zones of low and high density of vehicles (which typically mark the end of a traffic jam). Shocks are also found in the phenomenology of the exclusion process, and are known to generally emerge from a non-linear relation between the local density and current of particles on a chain. In the case of the TASEP, the exact phase diagram and density profiles are known as a function of the boundary rates which makes it an appropriate toy model to study traffic flow [46, 80].

KPZ universality

The KPZ equation is a stochastic differential equation first introduced in 1986 by Kardar, Parisi and Zhang [50] that describes the evolution of a *height field* $h(x,t)$ defined on a one dimensional space.

[1] for generic values of the parameters, with the exception of the cases where $\alpha\beta = \gamma\delta q^{L-1}$ see section 1.4.4

A more thorough summary on KPZ universality will be given in section 1.5, here we just present briefly the context of the KPZ class and its connection with the exclusion process. The KPZ equation writes

$$\frac{\partial h}{\partial t} = \nu \frac{\partial^2 h}{\partial x^2} + \frac{\lambda}{2}\left(\frac{\partial h}{\partial x}\right)^2 + \eta(x,t) \tag{1.6}$$

where $\eta(x,t)$ is a Gaussian white noise with average zero and correlation $\langle \eta(x,t)\eta(x',t')\rangle = 2D\delta(x-x')\delta(t-t')$. The KPZ equation describes the growth of a one dimensional interface between two phases, subject to random fluctuations and diffusive smoothing. The non linear term accounts for the fact that the interface grows in the direction locally normal to the surface. The KPZ equation describes a large variety of discrete interface growth model and is observed experimentally in many different contexts. The KPZ equation itself is actually the prototype of a wide class of models, the *KPZ universality class*[86, 21]. All models in this class are associated with height functions $h(x,t)$ which are known or conjectured to converge to a unique fluctuation field $\mathfrak{h}(x,t)$, the *KPZ fixed point*, under the KPZ so-called $1:2:3$ scaling [2]

$$\epsilon^{\alpha} h(\epsilon^{-z}t, \epsilon^{-1}x) - C_\epsilon t \quad \text{with} \quad \epsilon \to 0 \tag{1.7}$$

where C_ϵ is some model dependent drift velocity, $\alpha = 1/2$ is the *roughness exponent* and $z = 3/2$ is the *dynamic exponent*. These last two exponent are universal and characterize the KPZ class. From a more phenomenological point of view, if we denote by $w(L,t)$ the root-mean-square of the height function of some growth model in the KPZ class defined on an interval of size L

$$w(L,t) = \sqrt{\frac{1}{L}\int_0^L (h(x,t) - \overline{h}(t))^2 dx} \qquad \text{where} \quad \overline{h}(t) = \frac{1}{L}\int_0^L h(x,t)\mathrm{d}x \tag{1.8}$$

then w follows a scaling relation of the *Family-Vicsek* type :

$$\langle w(L,t)\rangle \sim L^{\alpha} f\left(\frac{t}{L^z}\right) \tag{1.9}$$

where the scaling functions f is such that

$$\begin{aligned} &f(u) \sim u^{\beta} && \text{for } u \ll 1 \quad \text{and} \quad \beta = \frac{\alpha}{z} \\ &f(u) \sim \text{const} && \text{for } u \gg 1 \end{aligned}$$

In other word, the roughness of the interface described by the model first grows like $w \sim t^{\beta}$ before saturating at a value $w_{\text{sat}} \sim L^{\alpha}$ after a typical time $t_{\text{sat}} \sim L^z$. Equivalently, starting from an uncorrelated initial height function $h(x, t=0)$, the typical correlation length ξ increases as $\xi \sim t^{1/z}$ before saturating at the whole system's size L for $t \gg t_{\text{sat}}$. Besides these scaling exponent, models in the KPZ class are also characterized by universal probability distributions of their fluctuations connected to the theory of random matrices, see 1.5

The exclusion process can be mapped to an interface growth model belonging to the KPZ universality class, known in the literature as the *corner growth* model (see figure 1.4). In fact, most results known about the KPZ class come from the study of discrete particle models, among which ASEP occupy a prominent place. Apart from ASEP, the KPZ equation is known to describe the limit behaviour of several other discrete models of interface growth like the polynuclear growth model or the Eden deposition model [45, 2]. In terms of experimental realization, KPZ behaviour has been observed in various contexts. Historically, the scaling exponents α and z have first been observed in the case of mutant bacteria colonies [48] - the interface being the limit of the growing colony, see figure 1.5. The non-Gaussian character of the fluctuations of an interface associated with KPZ scaling was then observed for the combustion front in the case of the flame-less combustion of paper [63]. More recently, observations of the boundary between two turbulent phases in nematic liquid crystal flows [87] gave access not only to the dynamic exponents but also to the predicted universal probability distribution functions of the KPZ class, see figure 1.5 From a broader theoretical point of view, KPZ behaviours

[2] The scaling exponents of $h{:}x{:}t$ indeed have a $1:2:3$ ratio

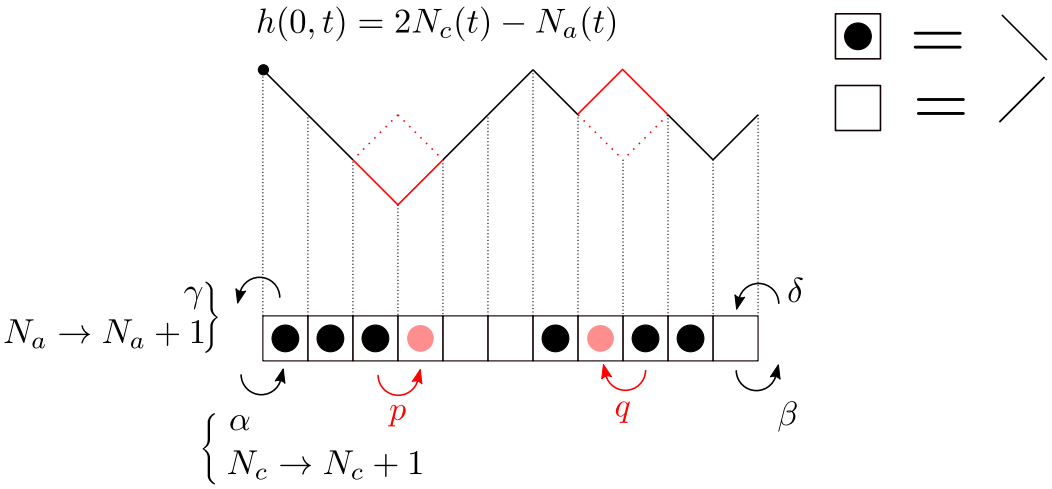

Figure 1.4: Schematic representation of the corner growth model corresponding to open ASEP. Each site is associated with a segment of slope -1 if the site is occupied and 1 if the site is empty. When a particle hops to the right, the local minimum above the bounds that is crossed is filed with a square and becomes a local maximum, and conversely a square is removed above a bound when it is crossed by a particle hopping to the left (if $q \neq 0$). The value of the height function $h(0,t)$ at the left boundary is set to twice the number of particle created at site 1 (with rate α) minus the number of particle annihilated (with rate γ), so that the height function on the interior of the interval is not affected by the transitions occurring at the boundary.

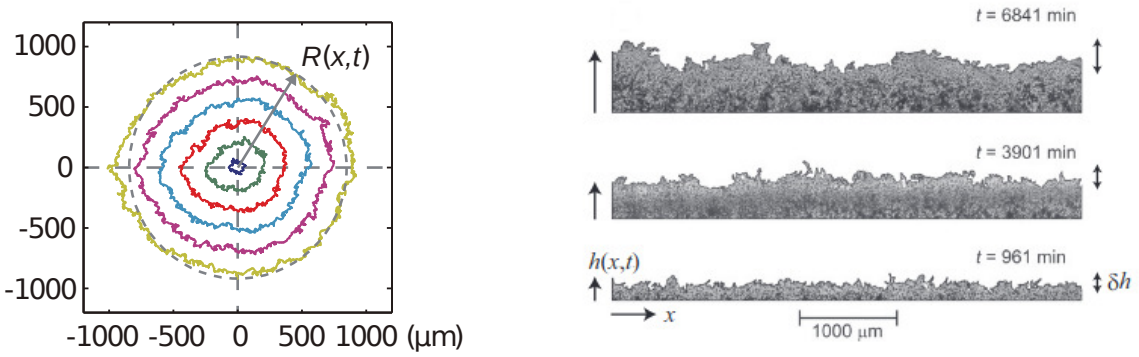

Figure 1.5: Two experimental realization of KPZ behaviour. Left : sketch of the boundary between a stable (inside) and metastable (outside) turbulent phase in a thin layer of nematic liquid crystal excited by an oscillating electric field at time intervals of $5s$ (reproduced from [87]). This experiment by Takeuchi and Sano was the first to recover the statistics of the KPZ fluctuation for a flat and circular interface. Right: time evolution of a colony of cancerous cell on a flat substrate (reproduced from [86]). The roughness of the front of cells follows a KPZ scaling.

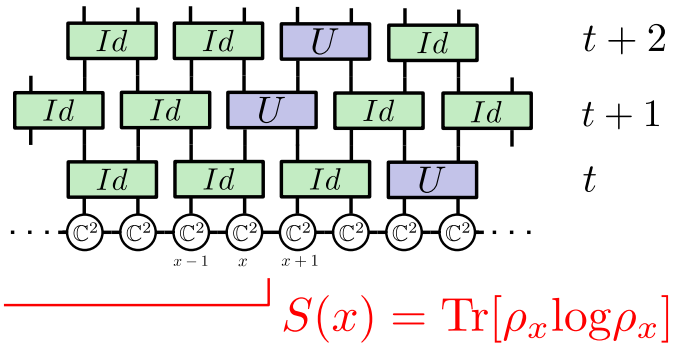

Figure 1.6: Schematic representation of the random quantum circuit considered in [64]. At each time step, two neighbours on a chain of spin-$\frac{1}{2}$ are randomly selected and are coupled through a random unitary operator. The height function considered is the Von Neumann entanglement entropy $S(x)$ which measures the entanglement between the part of the chain on the left of site x and the part on the right. This height function follows KPZ universal fluctuations, which can be understood by mapping the quantum circuit dynamics to an interface growth model.

are encountered in the theory of generalized hydrodynamics for integrable models. The purpose of generalized hydrodynamics is to describe the large scale behaviour of integrable systems by studying fields and current of conserved quantities [33]. In particular, it is possible to combine the several locally conserved charge of an integrable system into normal modes which evolves independently. In this context, it has been shown for instance that the normal modes of the current of conserved quantities in generic chains of non-linear oscillators satisfies the KPZ equation [85].

As for specifically quantum manifestations of KPZ physics, numerical evidences show that the entanglement entropy of a chain of spins-$\frac{1}{2}$ coupled by random unitary operators displays KPZ fluctuations[64], see figure 1.6. The Heisenberg XXZ spin chain also displays KPZ scaling of the correlations of the average magnetization in the high temperature limit, which has been observed both in simulations and experimentally [58, 79, 43]. The conductance of a sample of atoms described by the Anderson model [69] also follows KPZ scaling and fluctuations in the strongly localized limit.

1.3 Dynamics of the model and stationary state

1.3.1 Markov matrix of the ASEP and general properties of the steady state

As mentioned in the first section of this chapter, the time evolution of the system's probability distribution is described by the master equation

$$\frac{d}{dt}P_t(\mathcal{C}) = \sum_{\mathcal{C}'} W(\mathcal{C}' \to \mathcal{C})P_t(\mathcal{C}') - W(\mathcal{C} \to \mathcal{C}')P_t(\mathcal{C}) \tag{1.10}$$

with transition rates $W(\mathcal{C} \to \mathcal{C}')$ given by the dynamics of the model. The configuration of the system and the master equation can be represented in a more convenient way. Considering the case of the open TASEP, we associate with each site a vector space $\mathbb{C}_i^2$ with basis $\{|0\rangle, |1\rangle\}$, where $|0\rangle$ represent an empty site and $|1\rangle$ an occupied site. The full state space of the system is thus the 2^L dimensional tensor product $\bigotimes_{i=1}^{L} \mathbb{C}_i^2$, and a configuration is represented by a tensor product of local configuration $|\mathcal{C}\rangle = |n_1\rangle \otimes |n_2\rangle \ldots \otimes |n_L\rangle$. The state of the system at any time t is then fully characterized by the state vector

$$|P_t\rangle = \sum_{\mathcal{C} \in \mathcal{S}} P_t(\mathcal{C}) |\mathcal{C}\rangle \tag{1.11}$$

where $\mathcal{S}$ is the set of all configurations. A basis $\mathcal{B}$ of the configuration space of the whole system is given by the family of all vector corresponding to a single configuration, with the corresponding list of

occupation numbers ordered in lexicographic order:

$$\mathcal{B} = \left\{ |00,....,00\rangle, |00,....,01\rangle, |00,....,10\rangle, ..., |11,....,10\rangle, |11,...,11\rangle \right\} \tag{1.12}$$

In the case of the open ASEP, defining the local matrices

$$C_1 = \begin{pmatrix} -\alpha & \gamma \\ \alpha & -\gamma \end{pmatrix} \qquad m = \begin{pmatrix} 0 & 0 & 0 & 0 \\ 0 & -q & p & 0 \\ 0 & q & -p & 0 \\ 0 & 0 & 0 & 0 \end{pmatrix} \qquad D_L = \begin{pmatrix} -\delta & \beta \\ \delta & -\beta \end{pmatrix} \tag{1.13}$$

one defines the Markov matrix [3]

$$M = C_1 + \sum_{i=1}^{L-1} m_{i,i+1} + D_L \ , \tag{1.14}$$

where the matrices $m_{i,i+1}$ act as m on the local spaces $\mathbb{C}_i^2 \otimes \mathbb{C}_{i+1}^2$ and as the identity elsewhere, and matrices C_1 and D_L act only on sites 1 and L respectively.

$$m_{i,i+1} = \underbrace{\mathrm{Id} \otimes \ ... \ \otimes \mathrm{Id}}_{i-1} \otimes m \otimes \underbrace{\mathrm{Id} \otimes \ ... \ \otimes \mathrm{Id}}_{L-i-1} \ . \tag{1.15}$$

The matrix m is understood here as acting on the tensor product of two local spaces $\mathbb{C}^2 \otimes \mathbb{C}^2$, with basis $\{|00\rangle, |01\rangle, |10\rangle, |11\rangle\}$. Equivalently, the Markov matrix can be written as

$$M = \sum_{\mathcal{C} \neq \mathcal{C}'} W(\mathcal{C}' \to \mathcal{C}) \, |\mathcal{C}\rangle \langle \mathcal{C}'| - \sum_{\mathcal{C}} r(\mathcal{C}) \, |\mathcal{C}\rangle \langle \mathcal{C}| \tag{1.16}$$

where

$$r(\mathcal{C}) = \sum_{\mathcal{C}' \neq \mathcal{C}} W(\mathcal{C} \to \mathcal{C}') \tag{1.17}$$

is the exit rate from the configuration $\mathcal{C}$, so that the probability of the waiting time $t_w(\mathcal{C})$ for the system in configuration $\mathcal{C}$ to hop to another configuration is exponentially distributed as

$$P(t_w(\mathcal{C}) = t) = \mathrm{e}^{-r(\mathcal{C})t} \tag{1.18}$$

The master equation of the process then writes

$$\frac{d}{dt} |P_t\rangle = M \, |P_t\rangle \tag{1.19}$$

Note that up to a rescaling of the time variable, it is always possible to set $p = 1$ and $q < 1$, which is the convention that we will use in what follows [4]. In the totally asymmetric case, the Markov matrix writes

$$C_1 = \begin{pmatrix} -\alpha & 0 \\ \alpha & 0 \end{pmatrix} \qquad m = \begin{pmatrix} 0 & 0 & 0 & 0 \\ 0 & 0 & 1 & 0 \\ 0 & 0 & -1 & 0 \\ 0 & 0 & 0 & 0 \end{pmatrix} \qquad D_L = \begin{pmatrix} 0 & \beta \\ 0 & -\beta \end{pmatrix} \ . \tag{1.20}$$

The solution of the master equation (1.19) for any $t \geq 0$ formally writes

$$|P_t\rangle = \mathrm{e}^{tM} \, |P_0\rangle \tag{1.21}$$

[3] Properly speaking, M is referred to, in the mathematics literature as the *transition rate matrix* or *infinitesimal generator* of the process, as the entries of a proper Markov matrix are supposed to add up to one. However, by a slight abuse of language, we will designate it as a Markov matrix

[4] the reverse case with $q = 1$ and $p < 1$ is completely equivalent by left right symmetry

A first property of the ASEP with finite size is that, starting from any configuration $\mathcal{C}_i$ it is possible to reach any other configuration $\mathcal{C}_f$ in a finite number of transition with non-zero rates $W(\mathcal{C} \to \mathcal{C}')$. This property, namely the *irreducibility* of the Markov process, implies by the Perron-Frobenius theorem that the open ASEP is ergodic: the evolution of the system with any initial probabilities will converge in the long time limit to a unique steady states with stationary probability vector $|P^\star\rangle$ (or *stationary measure*) satisfying the condition.

$$M\,|P^\star\rangle = 0 \tag{1.22}$$

As explained in the first section, this stationary state is in general [5] a non-equilibrium steady state, which breaks the detailed balance condition. Indeed, the asymmetry of the hopping rates implies that even for the one particle case, the process is not reversible, *i.e.* trajectories in the configuration space do not have the same probabilities as their reversed counterparts. A direct consequence of this fact is that, since the Markov matrix M is not symmetric or similar to a symmetric matrix, its spectrum is complex.

The stationary state corresponds to the eigenvalue 0 of M, all other eigenvalues of M having negative real part. Of special interest is the the eigenvalue with second largest real part, referred to as the *gap* of the process. Indeed, designating the eigenvalues of M (ordered by decreasing real part) by $\{E_n\}$ and the corresponding eigenvectors by $\{|\psi_n\rangle\}$, the time evolution of the probability vector (1.21) writes

$$|P_t\rangle = \left(\sum_{n=0}^{2^L-1} |\psi_n\rangle\,\langle\psi_n|\,\mathrm{e}^{E_n t}\right)|P_0\rangle \tag{1.23}$$

$$= \langle P^*|P_0\rangle\,|P^\star\rangle + \mathrm{e}^{E_1 t}\,\langle\psi_1|P_0\rangle\,|\psi_1\rangle + o\left(\mathrm{e}^{E_1 t}\right) \tag{1.24}$$

so that the gap controls the relaxation to the stationary state. In particular, the typical relaxation time to the stationary state is $1/E_1$. In the case of the periodic TASEP of size L, the gaps scales like $\frac{1}{L^{3/2}}$ in the maximal current phase (see 1.3.3 so that the relaxation time scales like $L^{3/2}$, in accordance with the facts that it belongs to the KPZ universality class. As for the open TASEP, several scaling are found for the gap depending on the values of the boundary rates.

We also define two time dependent macroscopic variables of the system's state. Let N_t be number of particles present on the chain at time t (of course it is a fixed quantity in the case of the periodic ASEP), an $Q_t^{(i)}$ the number of particle which have algebraically crossed the bond between site i and site $i+1$ up to time t, with $Q_t^{(0)}$ the number of particle entering at site 1 minus the number of particle removed and similarly for $Q_t^{(L)}$. One can also conveniently define the total number of particle having crossed any bond in the system

$$Q_t = \sum_{i=0}^{L} Q_t^{(i)}\ . \tag{1.25}$$

The time integrated current $Q_t^{(i)}$ is also interpreted as the value of the height function of the corner growth model over site i (see figure 1.4), so the study of this observable is of primary interest in relation with KPZ universality. With these definitions, the stationary average density ρ and average current J are then defined as

$$\rho = \lim_{t\to\infty} \frac{\langle N_t\rangle}{t} \tag{1.26}$$

$$J = \lim_{t\to\infty} \frac{\langle Q_t^{(0)}\rangle}{t} \tag{1.27}$$

Note that the bound i where the number of crossing is counted has no effect on the value of J. For the ring ASEP, it is implied by the translation symmetry of the chain. In the case of open ASEP, since

[5] with the exception of the symmetric case, with $p = q$ and $\alpha/\gamma = \delta/\beta$

the number of particle is conserved in the bulk (outside boundary sites), the number of particle having crossed any bond in the system in the long t limit is equal to $Q_t^{(0)}$.

The stationary probabilities of configurations can be computed exactly for the exclusion process. Before describing the stationary state of the open TASEP in detail, let us work out the much simpler case of the periodic TASEP

1.3.2 Steady state of the periodic ASEP

In order to compute the stationary measure for the ASEP on a ring, let us first define $N_c(\mathcal{C})$ as the number of clusters in the configuration $\mathcal{C}$, that is the number of set of adjacent particles separated by empty sites on the chain. Starting from any configuration, the possible transition exiting this configuration are, for each cluster, the ones where the rightmost particle of the cluster hops to the right, with rate p and where the leftmost particle hops to the left, whit rate q. Thus the probability per unit time of exiting the configuration $\mathcal{C}$ is $(p+q)N_c(\mathcal{C})$. By counting in the same fashion the number of configurations from which a configuration $\mathcal{C}$ with a given $N_c(\mathcal{C})$ can be reached, we see that $(p+q)N_c(\mathcal{C})$ is also equal to the sum of the incoming rates to configuration $\mathcal{C}$, that is

$$\sum_{\mathcal{C}\neq\mathcal{C}'} W(\mathcal{C}\to\mathcal{C}') = \sum_{\mathcal{C}\neq\mathcal{C}'} W(\mathcal{C}'\to\mathcal{C}) = (p+q)N_c(\mathcal{C}) \tag{1.28}$$

Thus, equation (1.2) is satisfied for a uniform probability measure $P(\mathcal{C}) = \frac{1}{\mathrm{Card}(\mathcal{S})}$:

$$\sum_{\mathcal{C}\neq\mathcal{C}'} (W(\mathcal{C}\to\mathcal{C}') - W(\mathcal{C}'\to\mathcal{C}))\frac{1}{\mathrm{Card}(\mathcal{S})} = 0 \tag{1.29}$$

The Perron-Frobenius theorem then ensures that this solution is the unique stationary measure of the periodic ASEP. The stationary measure for the periodic ASEP with L sites and N particles is:

$$P^*(\mathcal{C}) = \frac{1}{\binom{L}{N}} \,. \tag{1.30}$$

In particular, the non-equilibrium character of the stationary distribution is obvious, as the net probability current $pP(\mathcal{C}) - qP(\mathcal{C}')$ between two configuration $\mathcal{C}$ and $\mathcal{C}'$ related through the dynamics by a single hop of one particle is non-zero if $p \neq q$. We can now compute the stationary average current J in the system. Let us denote by n_i the occupation number of site i, such that $n_i = 1$ if the site is occupied and $n_i = 0$ if the site is empty. During a infinitesimal time interval dt, the average increase of the integrated current through the bond $1 \to 2$ is

$$\langle dQ_t^{(1)}\rangle = Jdt = dt\,\Big[pP(n_1=1,n_2=0) - qP(n_1=0,n_2=1)\Big] \tag{1.31}$$

$$J = p\langle\tau_1(1-n_2)\rangle - q\langle(1-n_1)\tau_2\rangle \tag{1.32}$$

the average current is thus expressed as a function of the stationary correlation of the occupation numbers of adjacent sites. Since the stationary measure of the periodic ASEP is uniform, they are easily computed. The number of configuration with $(n_1 = 1, n_2 = 0)$ is the same as the one with $(n_1 = 0, n_2 = 1)$ and is $\binom{L-2}{N-1}$, so that (1.32) writes

$$J = (p-q)\frac{\binom{L-2}{N-1}}{\binom{L}{N}} = (p-q)\frac{N(L-N)}{L(L-1)} \tag{1.33}$$

In the large L and N limit, with $\rho = N/L$ the density of particle, the current has limit

$$\lim_{L,N\to\infty} J = (p-q)\rho(1-\rho) \,. \tag{1.34}$$

Writing the conservation of the number of particles as a continuity equation on the fields $\rho(x,t)$ and $J(x,t)$ with $x = i/L$, the evolution of the density as $L \to \infty$ is given by the inviscid Burger equation

$$\frac{\partial \rho}{\partial t} = (p-q)\frac{\partial}{\partial t}[\rho(1-\rho)] \tag{1.35}$$

Which is the leading order deterministic part of the evolution of the density. The study of the fluctuations of the current around its average value in the stationary state, as well as its relaxation to this value requires much more involved techniques, that will be sketched in section 1.6.

1.3.3 Steady state of the open ASEP in the thermodynamic limit

The stationary measure on configurations of the ASEP with open boundaries is more complex than the one of the periodic model, and we will outline its computation in chapter 2. It is however possible to compute the stationary values of the current and density, as well as the density profile in the chain in large system size limit by a mean field approach [10], which we will do here following [55].

Let us write $\langle 1|$ the vector with all coordinates set to 1 in the configuration basis. A configuration is represented by a the sequence $\{n_i\}_{i\leq L}$ of the occupation numbers. By tracing the master equation (1.19) on all configuration for which $n_i = 1$ for a given site i we obtain the evolution of the average density at site i. We also set $p = 1$ for convenience. Projecting on the vector $\langle 1|\,\delta_{n_i,1}$ we obtain

$$\frac{\mathrm{d}}{\mathrm{d}t}\langle n_i\rangle = \langle 1|\,\delta_{n_i,1} M\,|P_t\rangle \tag{1.36}$$

$$= J_{i-1} - J_i \tag{1.37}$$

with local currents (setting $p = 1$)

$$J_0 = \alpha\langle 1-n_1\rangle - \gamma\langle n_1\rangle \tag{1.38}$$

$$J_i = \langle n_{i-1}(1-n_i)\rangle - q\langle n_i(1-n_{i-1})\rangle \tag{1.39}$$

$$J_L = \beta\langle n_L\rangle - \delta\langle 1-n_L\rangle \tag{1.40}$$

which simply expresses the conservation of particles in the system. Here again, the computation of the local currents requires the knowledge of the correlations between the occupation numbers of adjacent sites. In order to obtain a closed equation for the evolution of the average density, we will make the mean field approximation that neighbouring densities are uncorrelated

$$\langle n_i n_{i+1}\rangle = \langle n_i\rangle\langle n_{i+1}\rangle \tag{1.41}$$

This bold assumption is obviously wrong, as the exclusion interaction between neighbouring particles is expected to introduce strong correlations between local densities. However it gives the correct result for the stationary values of average quantities up to subleading terms with respect to the system size [6], so that our approach is valid in the limit $L \to \infty$. Equation (1.37) implies, since all derivatives vanish in the stationary state, that all local current J_i are identical. Equation (1.39) then writes

$$J = \langle n_{i-1}\rangle(1-\langle n_i\rangle) - q\langle n_i\rangle(1-\langle n_{i-1}\rangle) \tag{1.42}$$

In order to compute the thermodynamic limit, we write $\langle n_i\rangle = \rho(x)$ with $x = \frac{i-1/2}{L}$ and rescale the time as $t \to Lt$ so that in the limit $L \to \infty$ equations (1.37) and (1.42) become

$$\frac{\mathrm{d}\rho}{\mathrm{d}t} = -\frac{\partial J}{\partial x} = 0 \tag{1.43}$$

$$J = (1-q)\rho(1-\rho) - \frac{1+q}{2L}\frac{\partial \rho}{\partial x} \tag{1.44}$$

where we kept the second term in $1/2L$ in the expression of the current because the equation would otherwise yield a homogeneous density profile, incompatible with unequal boundary rates. We now

[6] The correlation functions have been exactly computed in [32]

have an autonomous system of equations for ρ and J that needs to be completed with appropriate boundary conditions. Assuming that the boundary values $\rho_0 = \rho(0)$ and $\rho_1 = \rho(0)$ of $\rho(x)$ depend only on the value of the transition rates at end sites, we consider a density locally uniform at the ends of the chain, so that equations (1.38) and (1.40) write

$$\alpha(1-\rho_0) - \gamma\rho_0 = (1-q)\rho_0(1-\rho_0) \tag{1.45}$$
$$\beta\rho(1) - \delta(1-\rho_1) = (1-q)\rho_1(1-\rho_1) \tag{1.46}$$

and the the boundary conditions for the density write

$$\rho_0 = \frac{1}{1+a} \qquad \rho_1 = \frac{1}{1+b} \tag{1.47}$$

with

$$a = \frac{1}{2\alpha}\left[1-q-\alpha+\gamma+\sqrt{(1-q-\alpha+\gamma)^2+4\alpha\gamma}\right] \tag{1.48}$$
$$b = \frac{1}{2\beta}\left[1-q-\beta+\delta+\sqrt{(1-q-\beta+\delta)^2+4\beta\delta}\right] \tag{1.49}$$

In the totally asymmetric case, these expressions reduce to

$$a = \frac{1}{\alpha} - 1 \qquad b = \frac{1}{\beta} - 1 \tag{1.50}$$

These boundary densities can be interpreted as the effective density of particle reservoirs connected at both ends of the system. We can now solve equations (1.43) and (1.44) by fixing the current J, determining the corresponding density profiles $\rho(x)$ and then use boundary conditions to find out the values of boundary rates compatible with these ρ and J.

From equation (1.44) we see that $\partial_x\rho$ has to be of order L if the difference between $(1-q)\rho(1-\rho)$ and J is finite, which is only possible on a region of size scaling like L^{-1}, otherwise it would imply a diverging density. Thus, these equations describe the formation of a shock, that is a steep transition (a discontinuity as $L \to \infty$) between regions of unequal density. As we will see, these shocks are located at the boundaries in most case except on a specific line of the phase diagram.

The maximum of $(1-q)\rho(1-\rho)$ is $\frac{1-q}{4}$ attained for $\rho = \frac{1}{2}$ thus the current is bounded between 0 and $\frac{1-q}{4}$ and there is a value $\rho_- < \frac{1}{2}$ of the density such that

$$J = (1-q)\rho_-(1-\rho_-)\ . \tag{1.51}$$

Outside the regions where its gradient is extensive, the density is then approximately equal to ρ_- or $\rho_+ = (1-\rho_-)$ from equation (1.44). When the gradient term is finite, its sign depends on the value of the density:

$$\frac{\partial\rho}{\partial x} < 0 \quad \text{when} \quad \rho < \rho_- \tag{1.52}$$
$$\frac{\partial\rho}{\partial x} > 0 \quad \text{when} \quad \rho_- < \rho < \rho_+ \tag{1.53}$$
$$\frac{\partial\rho}{\partial x} < 0 \quad \text{when} \quad \rho_+ < \rho \tag{1.54}$$

Thus, the value ρ_+ is an attractive point for the variation of the density with respect to x and ρ_- is repulsive. Integrating equation (1.44), we find

$$\left(\frac{\rho-\rho_+}{\rho-\rho_-}\right)\left(\frac{\rho_0-\rho_-}{\rho_0-\rho_+}\right) = \exp\left(-2L(\rho_+-\rho_-)\frac{1-q}{1+q}x\right) \tag{1.55}$$

Checking this expression against the boundary conditions, the only possible cases - which correspond to different phases of the system, are the following

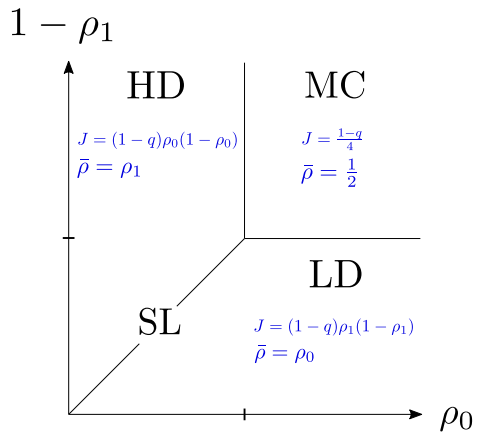

Figure 1.7: Phase diagram of the open ASEP with respect to the boundary parameters (1.47), with the corresponding values of current J and bulk average density $\bar{\rho}$. The phases are: MC maximal current, HD high density, LD low density, SL shock line.

- $\rho_0 = \rho_-$ and $\rho_1 < \rho_+$, which implies $\rho < \frac{1}{2}$ and $\rho_1 < 1 - \rho_0$. This is the *low density* phase. The rate of particle creation at the left boundary is significantly lower than the rate of annihilation at the right boundary, so that the left reservoir impose its density to the system with a low value and a steep boundary layer on the right interpolates between the bulk density ρ_- and the reservoir density ρ_1.
- $\rho_0 > \rho_-$ and $\rho_1 = \rho_+$, which implies $\rho_1 > \frac{1}{2}$ and $\rho_0 > \rho_+$. This the *high density* phase. Here the rate of particle creation at the left boundary is larger than the rate of annihilation at the right so the right reservoir imposes its density to the system, with a large value and the boundary layer is located at the left end of the chain.
- $\rho_0 > \frac{1}{2}$ and $\rho_1 < \frac{1}{2}$. In this case, since the density must increase between ρ_- and ρ_+ by (1.53), one is left with $\rho_+ = \rho_- = \frac{1}{2}$. This is the *maximal current phase*, as $J = \frac{q-1}{4}$ is the largest value allowed for the current. The density is uniformly equal to $\rho = \frac{1}{2}$ apart from boundary layers at both ends of the system
- $\rho_0 = \rho_-$ and $\rho_1 = \rho_+$, which requires $\rho_0 = \rho_1 < \frac{1}{2}$. This is the *shock line*, as the domain wall between the low density region with $\rho(x) = \rho_-$ and the high density region with $\rho(x) = \rho_+$ is located (anywhere) in the bulk of the system. A more refined analysis shows that the position of this shock follows a Brownian random walk.

The others cases are ruled out by the constraints on the sign of $\partial_x \rho$. All this is summarized in the the phase diagram 1.7. Note that in the totally asymmetric case, the boundary conditions reduce to

$$\rho_0 = \alpha \qquad 1 - \rho_1 = \beta \tag{1.56}$$

In parameter space (ρ_0, ρ_1), the transition between the maximal current and the high/low density phases are continuous in both the current and the average density. The transition across the shock line is continuous in the current and discontinuous in the average density. The mean-field approximation allowed us to obtain the correct values for the mean current and density of the stationary state in the large system size limit. However it cannot give us any information on the statistics of the fluctuations around these values or on the relaxation to the steady state.

1.4 Fluctuations of the current and deformed Markov matrix

We will now introduce the tools needed to study the fluctuations of the current, and more specifically the *deformed Markov matrix* of the exclusion process. The following computations are classical results from the theory of large deviations of Markov processes, which are introduced in references [90] and [89] and that we present here following [55].

1.4.1 Deformed Markov matrix of a time additive observable

For the sake of generality, let us first consider a time additive observable $O_t = \mathcal{O}[\mathcal{C}(t)]$ [7] of a Markov process, where $\mathcal{C}(t)$ is the configuration of the system at time t. If the trajectory $\mathcal{C}(t)$ of the system is the time-concatenation of two trajectories $\mathcal{C}_1$ and $\mathcal{C}_2$ up to time t'

$$\mathcal{C}(t) = \begin{cases} \mathcal{C}_1(t) & \text{if} \quad 0 \leq t \leq t_1 \\ \mathcal{C}_2(t) & \text{if} \quad t_1 \leq t \leq t' \end{cases} \qquad t \leq t' \tag{1.57}$$

the time additivity of O_t means that $O'_t = \mathcal{O}[\mathcal{C}_1(t)] + \mathcal{O}[\mathcal{C}_2(t)]$. We are interested in the statistics of O_t at any time and more specifically in deriving the scaled cumulant generating function of O_t as a random variable, defined by

$$E(\mu) = \frac{1}{t} \log \langle \mathrm{e}^{\mu O_t} \rangle \ . \tag{1.58}$$

Let us moreover assume that O_t is modified only when the system undergoes a transition between two configuration, *i.e.* that O_t remains constant on time interval where the system stays in the same configuration $\mathcal{C}$. Denoting by $\mathcal{I}(\mathcal{C}, \mathcal{C}')$ the increment of O_t caused by the transition $\mathcal{C} \to \mathcal{C}'$. We can then write O_t as

$$O_t = \sum_{i=1}^{N} \mathcal{I}(\mathcal{C}_{i-1}, \mathcal{C}_i) \tag{1.59}$$

where $(\mathcal{C}_0, ...\mathcal{C}_N)$ is the sequence of the configuration occupied by the system up to time t. The moment generating function of O_t writes

$$\langle \mathrm{e}^{\mu O_t} \rangle = \int \mathrm{e}^{\mu \mathcal{O}[\mathcal{C}(t)]} P[\mathcal{C}(t)] \mathcal{D}[\mathcal{C}(t)] \tag{1.60}$$

where $\mathcal{D}[\mathcal{C}(t)]$ is the measure on the space of trajectories. Denoting by $(t_0, ..., t_N)$ the sequence of waiting time in the configurations $(\mathcal{C}_0, ..., \mathcal{C}_N)$, the probability of a given trajectory writes

$$P[\mathcal{C}(t)] = \mathrm{e}^{t_N r(\mathcal{C})} \prod_{i=1}^{N} W(\mathcal{C}_{i-1} \to \mathcal{C}_i) \mathrm{e}^{r(\mathcal{C}_{i-1}) t_{i-1}} \tag{1.61}$$

where the exit rate $r(\mathcal{C})$ is as defined by (1.17). The integrand of the path integral (1.60) then writes

$$\mathrm{e}^{\mu \mathcal{O}[\mathcal{C}(t)]} P[\mathcal{C}(t)] = \mathrm{e}^{-\int_{\tau=0}^{t} r(\mathcal{C}(\tau)) \mathrm{d}\tau} \prod_{i=1}^{N-1} W(\mathcal{C}_i \to \mathcal{C}_{i+1}) \mathrm{e}^{\mu \mathcal{I}(\mathcal{C}_i, \mathcal{C}_{i+1})} \ . \tag{1.62}$$

We now introduce the *deformed Markov matrix* $M(\mu)$ defined by [8]

$$M(\mu) = \sum_{\mathcal{C}' \neq \mathcal{C}} \mathrm{e}^{\mu \mathcal{I}(\mathcal{C}, \mathcal{C}')} W(\mathcal{C} \to \mathcal{C}') \left| \mathcal{C}' \right\rangle \langle \mathcal{C}| - \sum_{\mathcal{C}} r(\mathcal{C}) \left| \mathcal{C} \right\rangle \langle \mathcal{C}| \ . \tag{1.63}$$

Let $|P_t(\mu)\rangle$ be the vector solution to the master equation (1.19) where M has been replaced by $M(\mu)$. Then the coordinates $\langle \mathcal{C}_N | P_t(\mu) \rangle$ are the probabilities of the trajectories ending in configuration $|\mathcal{C}_N\rangle$ multiplied by a factor $\mathrm{e}^{\mu O_t}$ (which is the quantity averaged in the expression (1.60):

$$|P_t(\mu)\rangle = \mathrm{e}^{tM(\mu)} |P_0(\mu)\rangle = \sum_{\mathcal{C}} \int \mathrm{e}^{\mu \mathcal{O}[\mathcal{C}(t)]} P[\mathcal{C}(t)] \mathcal{D}[\mathcal{C}(t)] \left| \mathcal{C} \right\rangle \tag{1.64}$$

[7] The square brackets indicate that $\mathcal{O}$ is a functional of the trajectory of the system in configuration space, *i.e.* the value of O_t depends on the whole history of the system up to time t.

[8] One should note that $M(\mu)$ is not the infinitesimal generator of a stochastic process anymore, as the sum of its column elements do not add up to zero.

Thus, the moment generating function of O_t is obtained by averaging this last expression over the configurations of the system at time t, that is by projecting $|P_t(\mu)\rangle$ on the uniform vector $|1\rangle$:

$$\langle \mathrm{e}^{\mu O_t} \rangle = \langle 1 | P_t(\mu) \rangle = \langle 1 | \, \mathrm{e}^{tM(\mu)} \, | P_0 \rangle \tag{1.65}$$

Denoting by $\{E_n(\mu)\}_{0 \leq n < 2^N}$ the eigenvalues of $M(\mu)$ ordered by decreasing real part and $\{|\psi_n(\mu)\rangle\}$ the associated eigenvectors, this last expression writes

$$\langle \mathrm{e}^{\mu O_t} \rangle = \langle 1 | \left(\sum_{n=0}^{2^L-1} |\psi_n(\mu)\rangle \langle \psi_n(\mu)| \, \mathrm{e}^{E_n(\mu)t} \right) |P_0\rangle \tag{1.66}$$

Although the matrix $M(\mu)$ is not a stochastic matrix for $\mu \neq 0$, it is still a positive matrix for real values of μ, so that the Perron-Frobenius still ensures that the eigenvalue $E_0(\mu)$ with largest real part is real and non-degenerate. Taking the logarithm, we obtain in the limit $t \to \infty$

$$\frac{1}{t} \log \langle \mathrm{e}^{\mu O_t} \rangle = E_0(\mu) + \frac{1}{t} \log \left(\langle 1 | \psi_n(\mu) \rangle \right) \langle P_0 | \psi_n(\mu) \rangle) + o(\frac{1}{t}) \tag{1.67}$$

$$\lim_{t \to \infty} \frac{1}{t} \log \langle \mathrm{e}^{\mu O_t} \rangle \approx E_0(\mu) \; . \tag{1.68}$$

We have shown that the eigenvalue with largest real part of the deformed Markov matrix is the scaled generating function of the cumulants of its associated observable O_t in the steady state. In what follows, we will designate the eigenstate with eigenvalue E_0 as the *ground state* of the process, and the variable μ as the *fugacity*.

1.4.2 Deformed Markov matrix of the current

Let us now specify this construction in the case of the time and space integrated current Q_t of the open ASEP defined by (1.25). The increment $\mathcal{I}(\mathcal{C}, \mathcal{C}')$ of Q_t during a transition is $+1$ if a particle hops to the right during the transition and -1 if it hops to the left. Since any transition from one configuration to another involves a particle crossing a bond in the system, the current counting deformed Matrix associated to Q_t writes

$$M(\mu) = M_0 + \mathrm{e}^{\mu} M_+ + \mathrm{e}^{-\mu} M_- \tag{1.69}$$

where M_+ is the matrix whose non-zero coordinates are the rates $M_{\mathcal{C},\mathcal{C}'}$ of transition where a particle hops to the right in the chain, M_- gathers similarly the rates of the transitions implying of a particle hoping to the left and M_0 is the diagonal matrix of exit rates from each configuration, so that the original Markov matrix $M = M_0 + M_+ + M_-$ is obtained for $\mu = 0$. In terms of local update operators, $M(\mu)$ is also the tensor product of the following deformed local matrices

$$C_1(\mu) = \begin{pmatrix} -\alpha & \gamma \mathrm{e}^{-\mu} \\ \alpha \mathrm{e}^{\mu} & -\gamma \end{pmatrix} \qquad m(\mu) = \begin{pmatrix} 0 & 0 & 0 & 0 \\ 0 & -q & p\mathrm{e}^{\mu} & 0 \\ 0 & q\mathrm{e}^{-\mu} & -p & 0 \\ 0 & 0 & 0 & 0 \end{pmatrix} \qquad D_L(\mu) = \begin{pmatrix} -\delta & \beta \mathrm{e}^{\mu} \\ \delta \mathrm{e}^{-\mu} & -\beta \end{pmatrix} \tag{1.70}$$

One can also define the deformed Markov matrix associated to the integrated current $Q_t^{(i)}$ through a specific bond in the chain in a similar way as

$$M^{(i)}(\mu) = M_0^{(i)} + \mathrm{e}^{\mu} M_+^{(i)} + \mathrm{e}^{-\mu} M_-^{(i)} \tag{1.71}$$

where the matrices $M_+^{(i)}$ and $M_-^{(i)}$ contain the elements of M accounting for a particle crossing the bond between site i and $i+1$ (from the left and the right respectively) and $M_0^{(i)}$ all other elements. Defining $R_i(\lambda)$ as the diagonal matrix with coefficients

$$R_i(\lambda)_{\mathcal{C},\mathcal{C}} = \begin{cases} \mathrm{e}^{\lambda} & \text{if} \quad n_i = 1 \quad \text{with} \quad \mathcal{C} = (n_1, ..., n_L) \\ 1 & \text{otherwise} \end{cases} \tag{1.72}$$

It is straightforward to show that

$$[R_{i+1}(\mu)...R_j(\mu)]^{-1}\, M^{(i)}(\mu)\, [R_{i+1}(\mu)...R_j(\mu)] = M^{(j)}(\mu) \quad \text{if} \quad j > i \tag{1.73}$$

$$U^{-1} M^{(i)}(\mu) U = M\left(\frac{\mu}{L+1}\right) \tag{1.74}$$

$$\text{with} \quad U = \left(\prod_{k=i+1}^{L} R_k\left(\frac{L-i-k}{L-i}\mu\right)\right)\left(\prod_{k=1}^{i} R_k\left(-\frac{k-1}{i}\mu\right)\right)$$

so that all Markov matrices deformed with respect to local currents are related to one another and to the deformed Markov matrix of the space integrated current (up to a rescaling of the variable μ) by similarity transformations. Being interested in the eigenstates of these matrix, we are then free to choose the most convenient to work with, as the fluctuations of the total integrated currents are similar to those on a single site.

1.4.3 Interpretation of the eigenvectors and large deviations of the current

We showed that the generating function of the cumulants of the current in the steady state can be obtained as the eigenvalue of $M(\mu)$ with largest real part. The corresponding eigenvector $|P(\mu)\rangle$ is also physically relevant. For $\mu = 0$ the coordinates of $|P_t\rangle$ are simply the stationary probabilities of each configuration. For finite values of μ, $|P(\mu)\rangle$ is also the probability distributions of the configurations conditioned on the value of the average current realized during the evolution of the system. To show this, we need to introduce some notions from the theory of large deviations.

A parameter dependent random variable A_t (typically a stochastic process) is said to follow a large deviation principle with *rate function* $g(s)$ if its probability distribution satisfies

$$\lim_{t\to\infty} \frac{1}{t} \log P(A_t = s) = g(s)\ . \tag{1.75}$$

In other words, for large values of the parameter t, the best approximation of the probability distribution of A_t is given by the exponential of the rate function $P(A_t = s) \approx \mathrm{e}^{-tg(s)}$. It is then a classical result of the theory, known as the Gärtner-Ellis theorem, that the scaled cumulant generating function of A_t defined by

$$E(\mu) = \frac{1}{t} \log\langle \mathrm{e}^{\mu A_t}\rangle \tag{1.76}$$

is the *Legendre transform* of $g(s)$, that is

$$E(\mu) = \max_s[\mu s - g(s)] \tag{1.77}$$

or equivalently, if g is strictly convex

$$E(\mu) = \mu s^* - g(s^*) \quad \text{where} \quad g'(s^*) = \mu\ . \tag{1.78}$$

The Legendre transform is involutive (again, provided g and E are strictly convex), so that

$$g(s) = s\mu^* - E(\mu^*) \quad \text{where} \quad E'(\mu^*) = s\ . \tag{1.79}$$

Assuming now that the time averaged current $q_t = Q_t/t$ [9] follows a large deviation principle with rate function g, let us consider trajectories of the system during which the average current has value $q_t = \bar{\jmath}$, so that $Q_t = \bar{\jmath} t$. The joint probability that the system is at time t in configuration $\mathcal{C}$ with $q_t = \bar{\jmath}$ writes

$$P\big[\mathcal{C}(t) = \mathcal{C}\ \&\ q_t = \bar{\jmath}\big] = P\big[\mathcal{C}(t) = \mathcal{C} | q_t = \bar{\jmath}\big] P\big[q_t = \bar{\jmath}\big] \tag{1.80}$$

$$\approx P\big[\mathcal{C}(t) = \mathcal{C} | q_t = \bar{\jmath}\big] \mathrm{e}^{-tg(\bar{\jmath})} \tag{1.81}$$

[9] We reserve the notation J for the ensemble average of q_t in the steady state over all histories of the system. Here, we are considering fluctuations of the current, that is values of q_t departing from J for an extensive period of time

where the second equality comes from the large deviation principle. The probability $P\big[\mathcal{C}(t)\big]$ in expression (1.64) can be written by tracing out the conditional probability $P\big[\mathcal{C}(t) = \mathcal{C} \mid q_t = \bar{\jmath}\big]$ over the realizations of $\bar{\jmath}$:

$$P\big[\mathcal{C}(t)\big] = \int_{-\infty}^{\infty} P\big[\mathcal{C}(t)|\bar{\jmath}\big]\,\mathrm{d}\bar{\jmath} \tag{1.82}$$

so that (1.64) (in the case where the observable is the current) writes

$$|P_t(\mu)\rangle = \mathrm{e}^{tM(\mu)}\,|P_0(\mu)\rangle = \sum_{\mathcal{C}} \int \mathcal{D}[\mathcal{C}(t)] \int_{-\infty}^{\infty} \mathrm{d}\bar{\jmath}\; \mathrm{e}^{t(\mu\bar{\jmath}-g(\bar{\jmath}))} P\big[\mathcal{C}(t)|\bar{\jmath}\big]\,|\mathcal{C}\rangle \ . \tag{1.83}$$

Evaluating the integral of $\bar{\jmath}$ with a saddle point approximation, we obtain

$$\int_{-\infty}^{\infty} \mathrm{d}\bar{\jmath}\; \mathrm{e}^{t(\mu\bar{\jmath}-g(\bar{\jmath}))} P\big[\mathcal{C}(t)|\bar{\jmath}\big] \approx \mathrm{e}^{tE(\mu)} P\big[\mathcal{C}(t)|\bar{\jmath}\big] \quad \text{with} \quad \bar{\jmath} = E'(\mu) \tag{1.84}$$

Taking the limit $t \to \infty$ in (1.83) we finally get

$$\langle \mathcal{C}|P(\mu)\rangle = P\Big(\mathcal{C}_{stat} = \mathcal{C} \mid \bar{\jmath} = E'(\mu)\Big) \tag{1.85}$$

so that the coordinates of $|P(\mu)\rangle$ are the probability of the configurations $\mathcal{C}_{stat}$ in the stationary state conditioned on the fact the current during the evolution of the process was equal to $E'(\mu)$.

In particular, it is possible to show that the function $E(\mu)$ is convex [11], so that imposing a large value of μ amounts to condition the evolution to a large value of the current.

1.4.4 Gallavoti-Cohen symmetry

As we mentioned earlier, the out-of-equilibrium character of the asymmetric exclusion process originates in the lack of time reversibility of the dynamics. More precisely, considering a trajectory $\mathcal{C}(t)$ of the system in configuration space, let is define its time reversal $\mathcal{C}^R(t)$:

$$\mathcal{C}(t) : \mathcal{C}_0,\ t_0 \to \mathcal{C}_2,\ t_2 \to \quad ... \quad \to \mathcal{C}_N,\ t_N \tag{1.86}$$

$$\mathcal{C}^R(t) : \mathcal{C}_N,\ t_N \to \mathcal{C}_{N-1},\ t_{N-1} \to \quad ... \quad \to \mathcal{C}_0,\ t_0\ . \tag{1.87}$$

then in general $P[\mathcal{C}(t)] \neq P[\mathcal{C}^R(t)]$. The lack of time-reversibility can be measured quantitatively by introducing the *entropy production* of the process as

$$S\left[\mathcal{C}(t)\right] = \log\left(\frac{P\left[\mathcal{C}(t)\right]}{P\left[\mathcal{C}^R(t)\right]}\right) \tag{1.88}$$

The entropy creation is a time-additive observable that can be treated by the approach we presented in 1.4.1, from which one can deduce the celebrated *fluctuation theorem* [34]

$$\frac{P(s)}{P(-s)} = \mathrm{e}^{-ts} \tag{1.89}$$

for $t \to \infty$ where s is the time intensive entropy creation $s = S\left[\mathcal{C}(t)\right]/t$. The fluctuation theorem can be seen as a generalization of the second principle of thermodynamics, stating that the relative probability of a negative entropy creation is finite but vanishes in the long time limit. It is in fact a consequence of a general *Gallavoti-Cohen symmetry* which is valid for any time additive observable of any stochastic process. With $M(\sigma)$ the Markov matrix of the exclusion process deformed with respect to the entropy creation [55],

$$M(\sigma) = \sum W(\mathcal{C} \to \mathcal{C}')^{1+\sigma} W(\mathcal{C}' \to \mathcal{C})^{-\sigma}\,|\mathcal{C}\rangle\,\langle\mathcal{C}'|\ , \tag{1.90}$$

one checks that $M(\sigma) = M(-1-\sigma)^{\mathrm{T}}$, so that the spectrum $\{E_n(\mu)\}_n$ globally satisfies the Gallavotti-Cohen symmetry

$$\{E_n(\sigma)\}_n = \{E_n(-1-\sigma)\}_n \ . \tag{1.91}$$

The Gallavotti-Cohen symmetry is arguably one of the most general and foundational results known for non-equilibrium statistical systems. Let us consider now the integrated current through the left boundary of the ASEP chain $Q_t^{(0)} = \mathcal{Q}^{(0)}[\mathcal{C}(t)]$. $\mathcal{Q}$ is odd under time reversal so that it also quantifies the irreversibility of the process,

$$\mathcal{Q}^{(0)}[\mathcal{C}(t)] = -\mathcal{Q}^{(0)}\left[\mathcal{C}^R(t)\right] \ . \tag{1.92}$$

A result similar to (1.91) can be derived for the current counting Markov matrix $M(\mu)$. For the open ASEP, the Gallavotti-Cohen symmetry writes [29]

$$E(\mu) = E(\mu_0 - \mu) \qquad \text{with} \qquad \mu_0 = \log\left(\frac{\gamma\delta}{\alpha\beta}\right) + (L-1)\log(q) \ . \tag{1.93}$$

This relation is most easily derived from the Bethe ansatz equations, derived in 2.3 which are symmetric under the transformation $\mu \to \mu_0 - \mu$. The condition $\frac{\gamma\delta}{\alpha\beta}q^{L-1} = 1$ implies detailed balance for the process, in which case $\mu_0 = 0$. It encompasses notably the SSEP case.

1.5 KPZ universality

In this section we will summarize some results currently known about the KPZ universality class. Starting with the KPZ equation itself, we will then define the KPZ universality class. After outlining the connection between the exclusion process and the KPZ class (first in the case of the infinite lattice), we will recall the probability distributions found for the fluctuations of the KPZ class and finally present the connections of the ASEP in finite volume (periodic and open) with the KPZ class.

1.5.1 The KPZ equation and fixed point

We gave the expression of the KPZ equation in the first section of this chapter (1.6). Let us briefly give some motivations for this expression. One is interested in obtaining a dynamic equation for the growth of an interface on some d-dimensional substrate, described by a height function $h(\mathbf{x}, t)$ with $\mathbf{x} \in \mathbb{R}^d$ and $t \in \mathbb{R}^+$. The growth of the interface is driven by an uncorrelated random noise $\eta(\mathbf{x}, t)$ which may correspond to, say, random deposition of particles in solution above the interface, or nucleation events occurring independently on the interface (in the case of a biological system for instance). The interface is also assumed to be subject to some kind of surface tension which tend to smoothen irregularities. We expect moreover the equation to be invariant under time translation, space rotations, space translation and global height shift $h \to h + h_0$. The simplest equation compatible with these conditions is the *Edward-Wilkinson* equation (EW) [2]

$$\frac{\partial}{\partial t}h(\mathbf{x}, t) = v_0 + \nu_0\nabla^2 h + \eta(\mathbf{x}, t) \tag{1.94}$$

with

$$\langle\eta(\mathbf{x}, t)\rangle = 0 \qquad \text{and} \qquad \langle\eta(x, t)\eta(x', t')\rangle = 2D\delta(x - x')\delta(t - t') \ . \tag{1.95}$$

The constant drift v_0 can be eliminated from the equation by a Galilean transformation $h \to h + v_0 t$. The equation could include higher (even order) space derivatives, however they are not relevant under rescaling. As we mentioned in introduction, the universality of such an equation is expressed through its invariance under rescaling

$$x \to \epsilon x \qquad t \to \epsilon^z t \qquad \delta h \to \epsilon^\alpha \delta h \qquad \text{with} \qquad \delta h = h(\mathbf{x}, t) - \bar{h}(t) \tag{1.96}$$

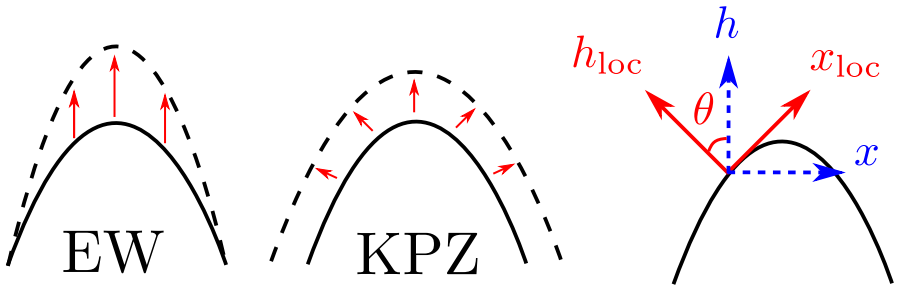

Figure 1.8: Sketch of the direction of growth of an interface described by the Edwards-Wilkinson equation (left) in the vertical direction only, and by the KPZ equation (right), in the direction locally orthogonal to the surface. On the right, sketch of the the local normal coordinates $(\mathbf{x}_{loc}, h_{loc})$ used in the derivation of the KPZ equation (1.98).

where $\bar{h}$ is the mean height and z and α are the dynamics exponents that characterize a given universality class. Imposing this invariance on the Edward-Wilkinson equation we find

$$\alpha = \frac{2-d}{2} \qquad z = 2\,, \tag{1.97}$$

which are the exponents of the EW universality class. Although many models do indeed belong to this class, the applications of the EW equation in the context of interface growth are rather limited as it describes an interface growing solely in the vertical direction. However, one expects a growing surface to grow in the direction locally normal to the interface, which is not vertical if the interface possesses a slope. Let us then consider a small piece of interface with tangential and normal coordinates $(\mathbf{x}_{loc}, h_{loc})$, which grows locally by the EW equation, see figure 1.8. These local coordinates relate to the global ones $(\mathbf{x}, h)$ as

$$\mathrm{d}h = \frac{\mathrm{d}h_{loc}}{\cos\theta} = \mathrm{d}h_{loc}\sqrt{1+(\nabla h)^2} \qquad \mathrm{d}\mathbf{x} = \frac{\mathbf{x}_{loc}}{\sqrt{1+(\nabla h)^2}} \tag{1.98}$$

where θ is the angle of the interface with the horizontal axis. Inserting the change of coordinate $(\mathbf{x}_{loc}, h_{loc})$ into the EW equation (1.94) and keeping only the lowest order non linear term, *i.e.* setting $\sqrt{1+(\nabla h)^2} \approx 1 + \frac{1}{2}(\nabla h)^2$ one gets

$$\frac{\partial}{\partial t} h(\mathbf{x},t) = v_0 + \nu\nabla^2 h + \frac{\lambda}{2}\left(\nabla h\right)^2 + \eta(\mathbf{x},t) \tag{1.99}$$

which is precisely the KPZ equation in any dimension, with a constant drift v_0 which can also be removed by a Galilean transformation. We justified the introduction of a non linear term $(\nabla h)^2$ by a geometric argument, however it may have other physical origins, so that the factor λ is a free parameter of the equation. Higher order non-linearities are not relevant under rescaling, as Kardar, Parisi and Zhang showed in their 1986 paper [50] which introduced the equation. Let us now determine the scaling exponents of the KPZ class by inserting the height function $h_\epsilon(\mathbf{x},t) = \epsilon^\alpha h(\epsilon^{-1}\mathbf{x}, \epsilon^{-z}t)$ rescaled according to the transformation (1.96) in equation (1.99). We find:

$$\frac{\partial}{\partial t} h_\epsilon(\mathbf{x},t) = \epsilon^{z-2}\nu\nabla^2 h_\epsilon + \frac{\lambda}{2}\epsilon^{\alpha+z-2}\left(\nabla h_\epsilon\right)^2 + \epsilon^{\frac{z}{2}-\frac{d}{2}-\alpha}\eta(\mathbf{x},t)\,. \tag{1.100}$$

There is no way to have all powers of ϵ vanish, so that the KPZ equation is not invariant under rescaling. However one can define the exponents α and z such that the height function has a non-trivial limit under rescaling, different from the Edward-Wilkinson solution. It can be shown that for $d = 1$, the following probability distribution of the height is a stationary measure for the KPZ equation:

$$P\left[h(x,t)\right] \propto \exp\left[-\int \mathrm{d}x \frac{\nu}{D}(\nabla h)^2\right] \tag{1.101}$$

which is the probability distribution function of a spatial *two-sided Brownian motion*, which rescales as $h \to \epsilon^{1/2} h$ under the scaling transformation $x \to \epsilon^{-1} x$, so that $\alpha = \frac{1}{2}$. Then, the only choice ensuring that no term in (1.100) blow up and that not all term vanish as $\epsilon \to 0$ is to set $z = \frac{3}{2}$. Thus we recover the values

$$\alpha = \frac{1}{2} \qquad z = \frac{3}{2} \tag{1.102}$$

of the KPZ universality class. Note that no exact values are known for $d = 2$, as the distribution (1.101) is not a stationary measure anymore for $d > 1$ [86]. The limit of the KPZ height function under rescaling with these exponents is the *KPZ fixed point* [21, 62]

$$\mathfrak{h}(x,t) = \lim_{\epsilon \to 0} \ \epsilon^{\alpha} \left(h(\epsilon^{-1} x, \epsilon^{-z} t) - C_\epsilon t \right) \tag{1.103}$$

where C_ϵ depends on the initial and boundary conditions [10]. The renormalized height function (1.103) satisfies the KPZ equation with rescaled parameter $\nu \to \epsilon^1 / 2\nu$ and $D \to \epsilon^{1/4}$. One should be aware that the limit of (1.100) when $\epsilon \to 0$

$$\frac{\partial}{\partial t} h(\mathbf{x}, t) = \frac{\lambda}{2} \left(\nabla h \right)^2 \ , \tag{1.104}$$

called the *inviscid Burger equation*, is not satisfied by the KPZ fixed point $\mathfrak{h}(x,t)$. The KPZ equation itself should be thought about as a crossover between two universality class, the EW class where $\lambda \to 0$ and the KPZ one where $\lambda \to \infty$, meaning that the non-linearity is primarily relevant, over the diffusion term. These two universality class correspond to both fixed point of the renormalization procedure of the KPZ equation and height function, with the EW fixed point being repulsive while the KPZ fixed point is attractive.

Finally, as a consequence of the Brownian nature of the stationary solution, the KPZ equation as defined by (1.99) is in fact ill-defined, since the derivative of a Brownian motion is a singular distribution, whose square $(\partial_x h)^2$ is not defined. Thus, most results known about the KPZ equation and its scaling limits are actually rigorously derived from its mapping to the *stochastic heat equation* (SHE). Given a height function $h(x,t)$ we define its *Hopf-Cole transform* as

$$Z(x,t) = \exp\left[\frac{\lambda}{2\nu} h(x,t) \right] \ . \tag{1.105}$$

Then if $Z(x,t)$ is solution to the stochastic heat equation with multiplicative noise writing

$$\frac{\partial}{\partial t} Z(x,t) = \nu \frac{\partial^2}{\partial x^2} Z(x,t) + \frac{\lambda}{2\nu} \ Z(x,t) \eta(x,t) \ , \tag{1.106}$$

the function $h(x,t)$ is formally solution to the KPZ equation. Interestingly, evaluating the the n-point functions $\langle Z(x_1,t) Z(x_2,t) ... Z_(x_n,t) \rangle$ (where the brackets denote ensemble averages over realizations of the noise) of the solution of the stochastic heat equation using the Feynman-Kac formula, one finds that the n-point function can be computed as the wave function of the n particles δ-Bose gas, or attractive Lieb-Liniger model, which is exactly solved by coordinate Bethe ansatz. This method, known as the replica Bethe ansatz, was used in [15] to compute the exact probability distribution of the KPZ height function with narrow wedge initial conditions (see below).

1.5.2 Connection of the exclusion process with the KPZ equation and universality class

We will now briefly present the link between the ASEP and KPZ equation and universality class. More precisely we will show that the asymmetric exclusion process can be mapped to an interface growth model, with the corresponding height function $h^{\mathrm{ASEP}}(x,t)$ defined below being solution, in the large

[10] More generally, C_ϵ is a non-universal parameter : if the height function is constructed as the large system size limit of a discrete model in the KPZ class, C_ϵ will depend on the model

system size limit, of the KPZ equation under the weak asymmetry scaling $\sigma = p - q = \epsilon^{1/2}$ and usual 1:2:3 scaling [8]. Explicitly, the rescaled function

$$h_\epsilon(x,t) = \epsilon^{1/2}\left(h_\sigma^{\mathrm{ASEP}}\left(\epsilon^{-1}x, \frac{\epsilon^{-3/2}t}{\sigma}\right) - \frac{t}{2}\right) \qquad \text{with} \quad \sigma = p - q = \epsilon^{1/2} \tag{1.107}$$

is solution to the KPZ equation with $\nu = 1/2$ and $\lambda = D = 1$, when $\epsilon \to 0$. When the asymmetry parameter σ is fixed to $\sigma = 1$, that is in the totally asymmetric case, the plain 1:2:3 scaling is recovered and the height function is described by the KPZ fixed point.

The height function h^{ASEP} is defined by mapping the ASEP to the corner growth model, that was defined in figure 1.4 for the open ASEP. It is possible to define the corner growth model in a similar way for the infinite line ASEP on $\mathbb{Z}$ by setting at 0 the initial height above the bond from site -1 to 0. In this case, the fluctuation of the height profile around its mean value depends on the initial condition.

The connection of ASEP to the KPZ class was first conjectured when exact results on the fluctuation of the current for the exclusion process became available. The fact that it provides an exact solution to the KPZ equation was later proved by Bertini and Giacomin in [8]. In what follows, we will just give a non-rigorous proof that the Hopf-Cole transform of the ASEP height function is solution to a discrete version of the stochastic heat equation, following [21].

Let us consider the ASEP on the infinite line. We denote the occupation numbers by the centered variables $\eta_t(x)$ such that

$$\eta_t(x) = \begin{cases} -1 & \text{if site x is occupied} \\ 1 & \text{if site x is empty} \end{cases} . \tag{1.108}$$

The height function above bond $i-1 \to i$ can then be written as

$$h_\sigma^{\mathrm{ASEP}}(i,t) = \begin{cases} 2N(t) + \sum_{0<y\leq i}\eta_t(y) & i > 0 \\ 2N(t) & i = 0 \\ 2N(t) - \sum_{0<y\leq i}\eta_t(y) & i < 0 \end{cases} \tag{1.109}$$

where $N(t)$ is the net number of particle having crossed the bond between sites -1 and 0 and the index $\sigma = p - q$ indicates that the function depends on the asymmetry through the dynamics. We then introduce the rescaled variable under KPZ scaling

$$x = \epsilon^{-1}X \qquad t = \epsilon^{-3/2}T \tag{1.110}$$

and the Hopf-Cole transform of the height function

$$Z_\epsilon(X,T) = \exp\left[\lambda_\epsilon h_\sigma^{\mathrm{ASEP}}\left(\epsilon^{-1}X, \frac{\epsilon^{-3/2}T}{\sigma}\right) - \nu_\epsilon\frac{\epsilon^{-3/2}T}{\sigma}\right] \tag{1.111}$$

where λ_ϵ and ν_ϵ are parameters that we leave undefined for now. This function is affected by three different factors during an instant dT:

i) a particle hops to the right, and the height function is increased as $h_\sigma(x,t) \to h_\sigma(x,t) + 2$ so that $Z_\epsilon \to \mathrm{e}^{2\lambda_\epsilon}Z_\epsilon$. The rate at which this event happens, in term of rescaled time T, is

$$r_\epsilon^+(X,T) = \frac{\epsilon^{-3/2}}{\sigma}\frac{p}{4}(1-\eta_t(x))(1+\eta_t(x+1)) . \tag{1.112}$$

ii) A particle hops to the left, so that $Z_\epsilon \to \mathrm{e}^{-2\lambda_\epsilon}Z_\epsilon$ with rate

$$r_\epsilon^-(X,T) = \frac{\epsilon^{-3/2}}{\sigma}\frac{q}{4}(1+\eta_t(x))(1-\eta_t(x+1)) . \tag{1.113}$$

iii) The function Z_ϵ is subject to a constant drift because of the added term $-\nu_\epsilon \frac{\epsilon^{-3/2}T}{\sigma}$ so that during any instant dT,

$$Z_\epsilon \to Z_\epsilon - Z_\epsilon \nu_\epsilon \frac{\epsilon^{-3/2}}{\sigma} dT \ . \tag{1.114}$$

Thus, the increment of Z_ϵ during dT (which is a random variable) writes

$$dZ_\epsilon = -Z_\epsilon \nu_\epsilon \frac{\epsilon^{-3/2}}{\sigma} dT + Z_\epsilon (\mathrm{e}^{2\lambda_\epsilon} - 1)\ dP_\epsilon^+(X,T) + Z_\epsilon (\mathrm{e}^{-2\lambda_\epsilon} - 1)\ dP_\epsilon^-(X,T) \ . \tag{1.115}$$

where $dP_\epsilon^\pm(X,T)$ are independent Poisson processes with rates $r_\epsilon^\pm(X,T)$, which simply mean that the forward (resp. backward) hopping events occur independently for any X with probabilities $r_\epsilon^+(X,T)$ (resp. $r_\epsilon^-(X,T)$) during a time interval dT. The increment (1.115) can be rewritten as

$$dZ_\epsilon = \Omega_\epsilon Z_\epsilon dT + Z_\epsilon dM_\epsilon \tag{1.116}$$

with

$$\Omega_\epsilon(X,T) = -\nu_\epsilon \frac{\epsilon^{-3/2}}{\sigma} + (\mathrm{e}^{2\lambda_\epsilon} - 1)\ r_\epsilon^+(X,T) + (\mathrm{e}^{-2\lambda_\epsilon} - 1)\ r_\epsilon^-(X,T) \tag{1.117}$$

$$dM_\epsilon(X,T) = (\mathrm{e}^{2\lambda_\epsilon} - 1) dM_\epsilon^+ + (\mathrm{e}^{-2\lambda_\epsilon} - 1) dM_\epsilon^- \tag{1.118}$$

where we defined the new stochastic processes

$$dM_\epsilon^\pm = dP_\epsilon^\pm(X,T) - r_\epsilon^\pm(X,T) dT \tag{1.119}$$

which are the same as $dP_\epsilon^\pm$, centered by removing their average constant drift. Expression (1.116) is strongly reminiscent of the SHE (1.106): the time variation of Z_ϵ is the sum of a deterministic part $\Omega_\epsilon Z_\epsilon dT$ involving spatial variations of Z_ϵ and a random multiplicative term $Z_\epsilon dM_\epsilon$.

Let us first make sense out of the deterministic part. It is indeed possible to choose values of λ_ϵ and ν_ϵ such that the first term in (1.116) writes

$$\Omega_\epsilon Z_\epsilon = \frac{1}{2} D_\epsilon \Delta_\epsilon Z_\epsilon \tag{1.120}$$

where D_ϵ is some new parameter that we will set later, and Δ_ϵ is the discrete Laplacian operator defined by its action on a function $f(X)$ as

$$\Delta_\epsilon f = \frac{1}{\epsilon^2} \left[f(X+\epsilon) + f(X-\epsilon) - 2f(X) \right] \ . \tag{1.121}$$

To fix the values of our parameters, we remark that from definition (1.109) of the height function, we can write

$$Z_\epsilon(X+\epsilon, T) = Z_\epsilon(x+1,t) = Z_\epsilon(x,t) \mathrm{e}^{-\lambda \eta_t(x+1)} \tag{1.122}$$

$$Z_\epsilon(X-\epsilon, T) = Z_\epsilon(x-1,t) = Z_\epsilon(x,t) \mathrm{e}^{\lambda \eta_t(x)} \tag{1.123}$$

Thus, developing the action of the discrete laplacian, equation (1.119) gives four equations on parameters ν_ϵ, λ_ϵ and $_\epsilon$ corresponding to the four possible combination of the values of $\eta_t(x) = \pm 1$ and $\eta_t(x+1) = \pm 1$. Two of these equations are in fact identical and it is straightforward to check that they are solved with

$$\lambda_\epsilon = \frac{1}{2} \log\left(\frac{p}{q}\right) \qquad \nu_\epsilon = p + q - \sqrt{pq} \qquad D_\epsilon = \frac{\epsilon^{1/2}}{\sigma} \sqrt{pq} \tag{1.124}$$

so that (1.116) writes

$$\mathrm{d}Z_\epsilon = \frac{1}{2} D_\epsilon \Delta_\epsilon \mathrm{d}T + Z_\epsilon \mathrm{d}M_\epsilon \ . \tag{1.125}$$

Let us now consider the random multiplicative noise $\mathrm{d}M_\epsilon$. It follows from the definition of a Poisson process that

$$\langle P_\epsilon^\pm(X,T)\rangle = \int r_\epsilon^\pm(X,T)\mathrm{d}T \tag{1.126}$$

so that $\langle \mathrm{d}M_\epsilon^\pm\rangle = 0$ and thus $\langle \mathrm{d}M_\epsilon\rangle = 0$. Regarding the space and time correlations, the local occupation numbers $\eta_t(x)$ being strongly correlated by the exclusion interaction only a few sites apart (at least assuming that the initial configuration was flat or Brownian), the space correlation of the processes $\mathrm{d}M_\epsilon^\pm(X,T)$ are expected to vanish under the scaling $X = \epsilon^{-1}x$, and the absence of time correlation follows from the independence of processes $\mathrm{d}P_\epsilon^\pm(X,T)$, so that $\mathrm{d}M$ can be considered as an uncorrelated white noise [11].

Finally, setting $\sigma = \epsilon^{1/2}$ in (1.124), D_ϵ is finite when $\epsilon \to 0$ and in this limit, (1.125) is exactly the SHE written in terms of the stochastic differentials of Z_ϵ and the noise term.

For finite values of the asymmetry $\sigma = p-q$, the scaling (1.107) is essentially the plain KPZ scaling and the corresponding height function converges to the KPZ fixed point, with a value of the parameter λ depending on the ratio p/q.

1.5.3 Exact expressions for KPZ fixed point fluctuations

Beyond the values of the dynamic exponents α and z, the models in the KPZ universality class are also characterized by the common probability distributions of their rescaled and centered fluctuations, which are known exactly. Before stating their expression, we need to introduce some notions from the theory of random matrices.

Eigenvalue probability distribution for matrix ensembles

A matrix ensemble is defined by a matrix space endowed with a probability measure. Here, we consider a Gaussian probability defined for any $N \times N$ matrix $X = (x_{ij})_{i,j\leq N}$ as

$$P_N[X]\mathrm{d}X = \frac{1}{Z_N}\mathrm{e}^{\mathrm{Tr}(X^2)}\prod_{i=1}^N \mathrm{d}x_{ii}\prod_{i<j}\mathrm{d}\,\mathrm{Re}\,x_{ij}\mathrm{d}\,\mathrm{Im}\,x_{ij} \tag{1.127}$$

where Z_N is a normalization constant. The weight $\mathrm{e}^{\mathrm{Tr}(X^2)}$ depends only of the spectrum of the matrix M and is independent of its eigenvectors. The set of orthogonal matrices $\{M \in \mathcal{M}_n(\mathbb{R}), M^{\mathrm{T}}M = MM^{\mathrm{T}} = \mathrm{Id}\}$ with elements independently drawn with this probability measure is called the Gaussian Orthogonal Ensemble (GOE). Its analogue with unitary matrices $\{M \in \mathcal{M}_n(\mathbb{C}), M^*M = MM^* = \mathrm{Id}\}$ is the Gaussian Unitary Ensemble (GUE).

With this probability measure on matrix elements, the joint probability distribution of the eigenvalues of a random matrix drawn from these ensemble writes

$$P(\lambda_1,...,\lambda_N) = \frac{1}{B_N}\exp\left[-\frac{\beta}{2}\left(\sum_{i=1}^N \lambda_i^2 - \sum_{i\neq j}\log\left(|\lambda_i-\lambda_j|\right)\right)\right] \quad (\lambda_i,...\lambda_N)\in\mathbb{R}^N \tag{1.128}$$

with $\beta = 1$ for the GOE and $\beta = 2$ for the GUE. Interestingly, (1.128) is also the partition function of a one dimensional gas of N particles with Coulomb interactions. Taking various marginal distributions out of (1.128), one can compute several interesting distributions. For instance the average eigenvalue density for both orthogonal and unitary matrices – that is the probability $\rho(\lambda,N)\mathrm{d}\lambda$ that any eigenvalue lies in the interval $[\lambda,\lambda+\mathrm{d}\lambda]$ – follows the celebrated Wigner's semi-circle law for large N:

$$\rho(\lambda,N) = \int_{-\infty}^{+\infty}\mathrm{d}\lambda_2...\mathrm{d}\lambda_N P(\lambda,\lambda_2,...,\lambda_N) \approx \begin{cases} \sqrt{\frac{2}{N\pi^2}}\sqrt{1-\frac{\lambda^2}{2N}} & \text{if} \quad \lambda\in[-\sqrt{2N},\sqrt{2N}] \\ 0 & \text{otherwise} \end{cases} \tag{1.129}$$

[11] This last point requires a much more careful treatment from a mathematical point of view see [8, 21]

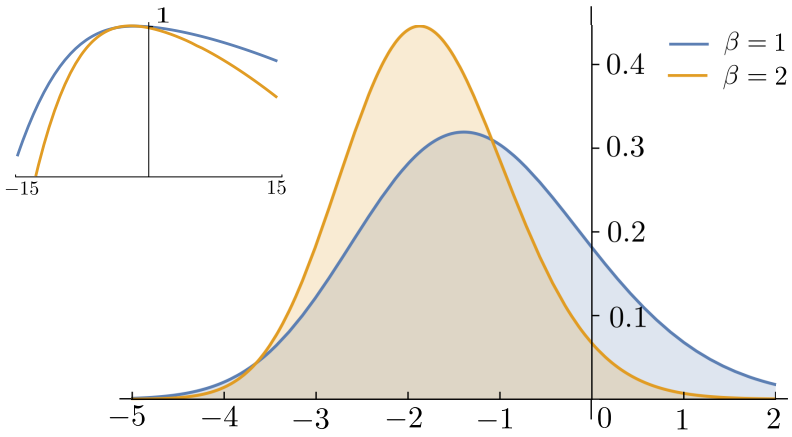

Figure 1.9: Plot of the Tracy-Widom distribution for the orthogonal ($\beta = 1$) and unitary ($\beta = 2$) ensemble (with logarithmic scale on a wider interval in the inset). They divert significantly from a Gaussian distribution. In particular, they are steeper on the left than on the right, which reflects the fact than in order for $\lambda_{\max}$ to have a low value, all other eigenvalues of the matrix have to be pushed toward low values also.

Thus, the maximum eigenvalue of a matrix from GOE or GUE for large N is of order $2N$. What is the complete probability distribution for the largest eigenvalue $\lambda_{\max}$ of random matrices in these ensembles ? One observes that $\lambda_{\max}$ typically fluctuates around $2N$ in a window of size $N^{-1/6}$ (much larger than the average eigenvalue spacing $N^{-1/2}$ on the interval $[-\sqrt{2N}, \sqrt{2N}]$). More precisely the centered and scaled fluctuations of the $\lambda_{\max}$ of random matrices have limit probability distributions for large N :

$$F_\beta(s) = \lim_{N\to\infty} P\left[\sqrt{2}N^{1/6}\left(\lambda_{\max} - \sqrt{2N}\right) \leq s\right] \tag{1.130}$$

where F_β is the *Tracy-Widom* distribution, with $\beta = 1$ for the GOE and $\beta = 2$ for the GUE. The functions F_β have several explicit expressions in terms of Fredholm determinants of kernel operators related to the Airy function, or solutions of Painlevé differential equations, that we do not write here (see figure 1.9 for a plot of the functions).

KPZ fixed point fluctuations on the infinite line

We can now write down the one-point fluctuation functions of the KPZ fixed point height on the real line. The precise form of the scaling – apart from the dynamic exponents and the scaled probability distribution – depends on the model considered, so we will specify it for the ASEP height function $h = h^{\text{ASEP}}$ defined by (1.109) [37]. We will consider two different initial conditions. First, the flat initial height function $h(x, 0) = 0$, which correspond to alternating initial conditions for the exclusion process (see figure 1.1). Then the probability distribution of the fluctuations of the height at $x = 0$ in the large time limit is [49]

$$\lim_{t\to\infty} P\left[\frac{h(0,t) - t/2}{t^{1/3}} \geq -\frac{s}{2}\right] = F_1(s) \tag{1.131}$$

The factor $t^{1/3}$ comes from the fact that for $\epsilon^{-3/2}t$ finite, the fluctuations scale like $\epsilon^{1/2} \sim t^{1/3}$. We can also consider the narrow wedge initial condition, defined by

$$h(x, 0) = \lim_{\delta\to 0} \frac{|x|}{\delta} = \begin{cases} 0 & \text{if} \quad x = 0 \\ \infty & \text{elsewhere} \end{cases} \tag{1.132}$$

it corresponds to the step initial configuration of the ASEP, in which all particles are stacked to the left of bound 0. It is also called the droplet initial condition, as it corresponds (up to the sign of h) to a

curved interface which, under proper rescaling, grows in the radial direction with origin $(x, h) = (0, 0)$. In this case, the fluctuations of the height at $x = 0$ are distributed [68] as

$$\lim_{t\to\infty} P\left[\frac{h(0,t) - t/2}{(t/2)^{1/3}} \geq -s\right] = F_2(s) \; . \tag{1.133}$$

The GUE fluctuations are universally observed for KPZ growth on curved surfaces [86]. Exact expressions for the fluctuations are also known for a random Brownian initial height – that is Poisson initial conditions for the ASEP) and follows the so-called *Baik-Rains* distribution F_0 (which has no known connection to random matrices), as well as for domain wall combinations of flat, wedge, and Brownian joined at $x = 0$ [12]

1.6 KPZ fluctuations of the TASEP in finite volume

In this section we will summarize the main results currently known about the fluctuations of the current and local density in the periodic TASEP. As we just saw, the behaviour that one observes crucially depends on the scaling of time, system size and the limit considered. Let us consider the periodic TASEP on L sites with N particles and average density $\bar{\rho} = N/L$ and occupation numbers $\{n_i\}_{i\leq L}$. The characteristic relaxation time to the steady state for a finite system of size L within the KPZ class is $t_{\text{sat}} \sim L^{3/2}$, which is the time it takes for the correlation length to reach L. Thus three time scales have to be considered: the sub-relaxation scale $t \ll L^{3/2}$, the crossover scale $t \sim L^{3/2}$ and the super-relaxation scale $t \gg L^{3/2}$.

For $x = i/L$, $\tau = t/L$, and density $\rho(x, \tau) = n_i(Lt)$, at leading order (with respect to L) the density on the hydrodynamic (sub-relaxation) time scale $t \sim L$ is described by the inviscid Burger equation

$$\frac{\partial \rho}{\partial \tau} + \frac{\partial}{\partial x}(\rho(1-\rho)) = 0 \; . \tag{1.134}$$

For uniform $\rho(x, 0) = \bar{\rho}$ and Brownian $\rho(x, 0) = \bar{\rho} + (1/\sqrt{L})\xi(x)$ initial conditions (where $\xi(x)$ is a normalized Brownian bridge), the density profile converges to $\rho(x, t) = \bar{\rho}$ in finite time τ. For step initial conditions where $\rho(x, 0) = 1$ on an interval of size $\bar{\rho}$ and 0 elsewhere, the density profile develops a shock in finite τ traveling at velocity $1 - 2\bar{\rho}$ with the density following a linear ramp joining both sides of the discontinuity. Beyond the deterministic hydrodynamic density profile, the exact transition probabilities from the initial configurations we just mentioned to any other configuration are known [1]

On the crossover scale, setting $\tau = t/L^{3/2}$, the fluctuations of the current observed for finite τ belong to the KPZ universality class [72]. As can be seen from (1.23) and (1.66), the functions of interest in a given scaling of time are obtained as sums over the eigenstates corresponding to that scaling, hence the relevant eigenstates of the Markov matrix and its current-counting deformation for the crossover scale are the ones with eigenvalues of real part scaling like $O(1/L^{3/2})$, so that the factors $\mathrm{e}^{E_n t}$ in the decomposition over eigenstates are finite when $L \to \infty$. These states include the gap and all other eigenstates parametrized by a finite set of indices. One defines the rescaled density fluctuation time-integrated current fluctuation (or equivalently the fluctuations of the height function defined above the chain)

$$\xi(\tau) = \frac{Q_i(\tau) - t/4}{\sqrt{L}/2} \tag{1.135}$$

[12] These initial data are the only ones to be invariant under space rescaling $x \to \epsilon^{-1}x$, so they presumably account for all relevant cases

Introducing the functions

$$\chi_r(v) = -\frac{1}{2\pi^{-1/2}}\mathrm{Li}_{5/2}(-\mathrm{e}^v) + \sum_{a\in\mathbb{P}_r}\frac{\omega_a^3(v)}{3} + \sum_{a\in\mathbb{H}_r}\frac{\omega_a^3(v)}{3} \tag{1.136}$$

$$\omega_a(v) = 2(\mathrm{sgn}(a)\mathrm{i}\pi)^{1/2}\left(|a| + \mathrm{sgn}(a)\frac{\mathrm{i}v}{2\pi}\right)^{1/2} \tag{1.137}$$

$$D_r(\nu) = \frac{(\mathrm{i}\pi/2)^{m_r^2}}{(2\pi)^{m_r}}\left(\prod_{a,b\in\mathbb{P}_r}(a-b)\right)\left(\prod_{a,b\in\mathbb{H}_r}(a-b)\right)\exp\left[\lim_{\Lambda\to\infty}\int_{-\Lambda}^{\nu}\mathrm{d}v\frac{\chi_r''(v)^2}{2} - m_r^2\log\Lambda\right] \tag{1.138}$$

where $\mathrm{Li}_{5/2}$ is the polylogarithm function defined (where the power series is convergent) as $\mathrm{Li}_s = \sum_{k\leq 1}\frac{z^k}{k^s}$. The index sets $\mathbb{P}_r$ and $\mathbb{H}_r$ are finite sets of half-integers which fully characterize the r-th eigenstate of the matrices M and $M(\mu)$, and m_r the number of positive (resp. negative) elements in $\mathbb{P}$ (resp. $\mathbb{H}$). The function χ_r is the scaling function of the eigenvalues while D_r gather the contribution from the scalar product of eigenvectors. The physical quantities defined above have then exact expressions in the large system size limit in terms of these functions for different initial conditions. In particular, the moment generating functions of $\xi(\tau)$ are

$$\langle \mathrm{e}^{s\xi(\tau)}\rangle_{\mathrm{stat}} = \sqrt{2\pi}s^2\sum_r\frac{D_r^2(\nu_r)\mathrm{e}^{\tau\chi_r(\nu_r)}}{\mathrm{e}^{\nu_r}\chi_r''(\nu_r)} \tag{1.139}$$

$$\langle \mathrm{e}^{s\xi(\tau)}\rangle_{\mathrm{flat}} = s\sum_{r\ |\ \mathbb{P}=\mathbb{H}}\frac{\mathrm{i}^{m_r}D_r(\nu_r)\mathrm{e}^{\tau\chi_r(\nu_r)}}{\mathrm{e}^{\nu_r/4}(1+\mathrm{e}^{-\nu_r})^{1/4}\chi_r''(\nu_r)} \tag{1.140}$$

$$\langle \mathrm{e}^{s\xi(\tau)}\rangle_{\mathrm{step}} = \sqrt{2\pi}s\sum_r\frac{D_r^2(\nu_r)\mathrm{e}^{\tau\chi_r(\nu_r)}}{\mathrm{e}^{\nu_r}\chi_r''(\nu_r)}\mathrm{e}^{2\mathrm{i}\pi(\sum_{\mathbb{P}_r}a-\sum_{\mathbb{H}_r}a)x} \tag{1.141}$$

where the sums run over all relevant finitely generated eigenstates, that is all finite $\mathbb{H}_r$ and $\mathbb{P}_r$ such that $|\mathbb{H}_+| = |\mathbb{P}_+|$ and $|\mathbb{H}_-| = |\mathbb{P}_-|$ where $\mathbb{H}_\pm$ and $\mathbb{P}_\pm$ denote the subset of positive and negative elements of $\mathbb{H}$ and $\mathbb{P}$ respectively . The parameter ν_r satisfies moreover $\chi_r'(\nu_r) = s$. The generating function are computed for flat, stationary Brownian (stat) and step initial condition. In the latter case, all sites in the initial configuration are filled for $xL - L/2 \leq i \leq xL + L/2$ and empty elsewhere. In the limit $\tau \to 0$, or equivalently in the limit $L \to \infty$ for finite t, the generating functions $\langle \mathrm{e}^{s\xi(\tau)}\rangle_{\mathrm{step}}$, $\langle \mathrm{e}^{s\xi(\tau)}\rangle_{\mathrm{flat}}$, and $\langle \mathrm{e}^{s\xi(\tau)}\rangle_{\mathrm{stat}}$ have been shown numerically to converge to the generating functions of the distribution F_2, F_1 and F_0 respectively, thus connecting KPZ fluctuations in finite volume and on the infinite line.

Let us give an interpretation of the form of these expressions. The sums appearing in expressions (1.139)–(1.141) are sums over all relevant excited states eigenvalues of the deformed Markov matrix $M(\mu)$ indexed by $r \in \mathbb{R}$, according to the generic expression (1.66). The sets $\mathbb{H}_r$ and $\mathbb{P}_r$ describing these eigenstates can be interpreted as the positions in momentum space of holes and excitations respectively removed from and added above a Fermi sea of fermionic quasi-particles from which eigenstates of $M(\mu)$ are constructed. We will present in detail in chapter 2 and chapter 4 how these quasi-particle emerge from the Bethe ansatz diagonalization of $M(\mu)$ for the open TASEP which has a similar structure. The eigenvalue themselves scale like $L^{-3/2}\chi_r$ where the function χ_r given by (1.136) is the sum of a term corresponding to the filled Fermi sea and additional terms $\omega_a^3/3$ which accounts for holes and excitations, see figure 1.10.

Finally, in the super-relaxation regime $t \gg L^{3/2}$, the average density profile converges to the stationary solution of the Burger equation, while the fluctuations saturates to an amplitude $L^{1/2}$ with Gaussian one-point distribution.

1.7 Toward fluctuation of the density and current in the open TASEP

In contrast with the infinite and periodic cases, exact results for the fluctuations of the open (T)ASEP are more sparse. It is the object of the present work to contribute to extend the results just stated

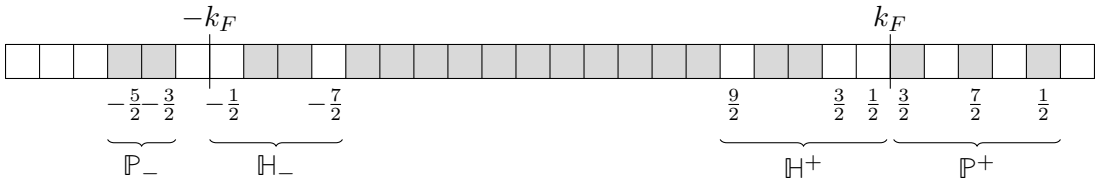

Figure 1.10: Representation of the excitation pattern corresponding to a pair $\mathbb{H}_r$, $\mathbb{P}_r$ of a term in sums (1.139)–(1.141), or equivalently to a spectral gap of $M(\mu)$. The filled square outside the interval $[-k_F, k_F]$ are the elements of $\mathbb{P}$ corresponding to added terms in expression (1.136) and the empty squares within the interval to the elements of $\mathbb{H}$. The total number of momenta in the *Fermi sea* corresponding to $\mathbb{H} = \mathbb{P} = \emptyset$ is equal to N.

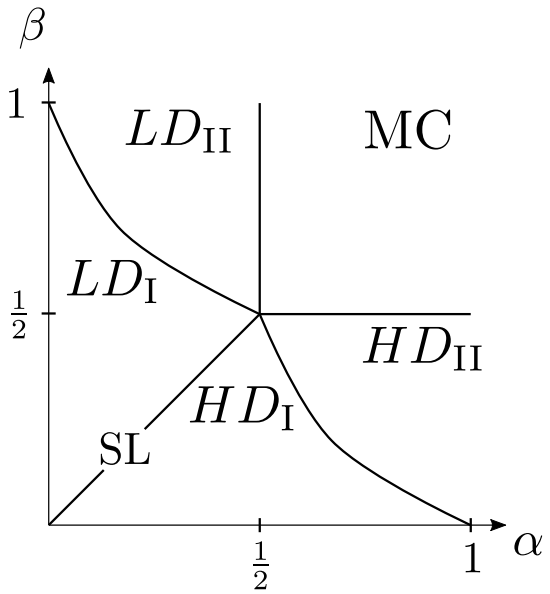

Figure 1.11: Dynamic phase diagram of the open TASEP as function of the boundary parameters α and β. With $a = \frac{1}{\alpha} - 1$, $b = \frac{1}{\beta} - 1$, $\alpha_c = (1 + b^{-1/3})^{-1}$, $\beta_c = (1 + a^{-1/3})^{-1}$, the curve with the hight (resp. low) density phase have equation $\alpha = \alpha_c$ (resp. $\beta = \beta_c$). Regions in the diagram correspond to different scaling of the gap E_1 (eigenvalue of M with second largest real part) with respect to the system size L.

for the periodic TASEP to the open case. The stationary measure on configurations in the stationary state for the open ASEP is known exactly from matrix product ansatz, and yields the same stationary values of J and $\bar{\rho}$ as the mean-filed approach, however, it gives no useful insight on the fluctuations of density and current on the relaxation scale $t \sim L^{3/2}$ where KPZ fluctuations are expected.

In the stationary state, the large deviation functions of the steady current have been computed from the deformed Markov $M(\mu)$ [55] of the ASEP conditioned on large ($\mu \to \infty$) and low current ($\mu \to -\infty$) leading to simplified high and low currents phase diagrams. Exact expressions are also known for the first cumulants of the current in finite size [56, 44]. Regarding the fluctuations of the stationary density profile, the *macroscopic fluctuation theory* [12] has been used to compute large deviation functionals of the steady density function, which has additional local minima, besides the stationary hydrodynamic solution. The principle of macroscopic fluctuation theory is to generalize the mean field approach used in 1.3.3 beyond the deterministic evolution. Adding a random term of the form $\sqrt{\rho(1-\rho)}\xi(x,t)$ to the hydrodynamic current (1.44), the long time limit of the probability of a given density profile is obtained by evaluating the probability of the realization of the noise that gives rise to it, minimizing a large deviation functional of the density. One finds several other optimizing profiles [55] which are interestingly in correspondence with the relaxation modes identified by Bethe ansatz, see below.

For finite values of the current on the crossover scale, exact results have been obtained by Bethe ansatz, see chapter 2. De Gier and Essler computed [28] the gap E_1 of the Markov matrix of the TASEP for all values of the parameters α and β, giving different types of scaling of E_1 with respect to the system size in different regions of the parameter space. In particular, the KPZ universal regime, corresponding to $E_1(\alpha,\beta,L) \sim L^{-3/2}$ is found in the maximal current phase. Considering the scaling of E_1 along with the stationary values of the density and current, several dynamical phases are identified (see figure 1.11):

(MC) Maximal current $-E_1 = e_1 L^{-3/2} + O(L^{-2})$, with $e_1 \approx 3.56$. The characteristic relaxation time $1/L^{3/2}$ of the KPZ class is recovered in the maximal current phase.

(LD_{I}) Massive low/high density phases $-E_1 = \alpha + \beta - \frac{2}{1+\sqrt{ab}} + O(L^{-2})$. In these phases, the gap is finite in the thermodynamic limit so that the relaxation to the stationary state is exponential in time. Identical (except for the value of the mean density) to HD_{I}.

(LD_{II}) Second low density phase, $-E_1 = \alpha + \beta_c - \frac{2}{1+\sqrt{ab_c}} + O(L^{-2})$, the gap is independent of β. The gap in the second hight density phase (HD_{II}) is obtained by the exchange $\alpha \leftrightarrow \beta$, $\alpha_c \leftrightarrow \beta_c$.

(SL) shock line, $-E_1 = \frac{\pi^2 \alpha(1-\alpha)}{1-2\alpha} L^{-2} + O(L^{-2})$. The scaling exponent $z = 2$ correspond to a diffusive system, coherent with the phenomenology of the shock line (domain wall following a Brownian random walk).

As in the case of the infinite ASEP, the height function constructed from the open ASEP is also solution to the KPZ equation in the weak asymmetry limit $p - q \sim 1/\sqrt{L}$ (that is close from LD/MC transition line), with Neumann boundary conditions on the slope of the height function fixed by the boundary parameters [66, 23]. More precisely, with the following scaling of the parameters

$$\alpha = \frac{p^{3/2}(p^{1/2} - \mu_{\tilde{A}} q^{1/2})}{p-q}\,, \qquad \beta = \frac{p^{3/2}(p^{1/2} - \mu_{\tilde{B}} q^{1/2})}{p-q}\,, \tag{1.142}$$

$$\gamma = \frac{q^{3/2}(q^{1/2} - \mu_{\tilde{A}} p^{1/2})}{q-p}\,, \qquad \delta = \frac{q^{3/2}(q^{1/2} - \mu_{\tilde{B}} p^{1/2})}{q-p}\,, \tag{1.143}$$

with $\mu_{\tilde{A}} = 1 - \tilde{A}\epsilon$ and $\mu_{\tilde{B}} = 1 - \tilde{B}\epsilon$, $p = \frac{1}{2}\mathrm{e}^{\sqrt{\epsilon}}$ and $q = \frac{1}{2}\mathrm{e}^{-\sqrt{\epsilon}}$, the rescaled corner growth model height function (see figure 1.4)

$$H^{\epsilon}(x,t) = \epsilon^{1/2} h^{\mathrm{ASEP}}(\epsilon^{-1}X, \epsilon^{-2}T) - \left(\frac{1}{2}\epsilon^{-1} + \frac{1}{24}\right) T \tag{1.144}$$

is solution in the limit $\epsilon \to 0$ to the KPZ equation with $\partial_X H(X=0) = \tilde{A}$ and $\partial_X H(X=1) = \tilde{B}$. Thus, the finite asymmetry case, with the above scaling for the boundary rates can be interpreted as the KPZ fixed point limit in finite volume with fixed boundary conditions. Some other results are also known about the KPZ equation height function with Neumann boundary conditions [22, 20]. In particular it was recently shown [3] that the stationary height function $h(x)$ solution to the KPZ equation (that is for finite λ) could be written as the sum of a Brownian motion and some other independent random process with known measure. These results however do not apply to the KPZ fixed point and do not allow to recover one point statistics.

Chapter 2

Integrability of the exclusion process

In this section, we review the methods used to perform exact computations of the eigenstates and eigenvalues of the exclusion process. Starting with the matrix product ansatz that yields exact expressions for the ground state of the open ASEP, we will validate the results recalled in 1.3.3 obtained by mean-field approximation. We will then introduce the Bethe ansatz formalism, from which most results obtained in this work are directly derived or checked numerically. The reader will be given some intuition on its operation principle by treating the periodic ASEP with the coordinate Bethe ansatz, before moving to the modified algebraic Bethe ansatz formalism and its setting in the open TASEP case. Finally, we will present the so-called Q-operator computation of the ground state eigenvalue of the deformed Markov matrix of the TASEP.

2.1 Matrix product ansatz for the open ASEP

The matrix product ansatz is a method that allows for exact computation of the steady state probability distribution or ground state of various classical and quantum non-equilibrium statistical systems, of which ASEP is the first historical example. Matrix product states are in fact a general category of steady states beyond equilibrium.

In the case of equilibrium steady states, the probability of the microstates of the system depends only on the value of some macroscopic quantity (energy, temperature, total magnetization, etc.).

In the case of some non-equilibrium models defined on a discrete lattice (most notably for the zero-range processes [35]) of size L, probability can be expressed as a product of simple scalar functions depending on each site states, as $P_{\text{stat}} = \prod_{i=1}^{L} f(n_i)$. These *factorized steady states* can be generalized one step further by considering the case where the configuration probabilities are expressed as matrix elements of a product of local operators that depend on the state of each state, as $P_{\text{stat}} = \langle W| \prod_{i=1}^{L} X_{n_i} |V\rangle$, which are matrix product states. An elementary example of a matrix product steady states is given by the computation of the partition function of the $1D$ Ising model by the transfer matrix method, in which case the matrix product reduces in fact to a dependency on the average magnetization (see for instance [4]).

The matrix product ansatz as a computation method was first introduced by Derrida, Evans, Hakim and Pasquier in [30] to compute the stationary density profile of the open ASEP, and has been since generalized to many other models [10].

Let us see how this construction works in the case of the open ASEP. Let us define two vectors $\langle\langle W\|$ and $\|V\rangle\rangle$ and operators E and D acting on them, satisfying the following algebra

$$DE - qED = (1-q)(D+E) \tag{2.1}$$
$$\langle\langle W\|(\alpha E - \gamma D) = (1-q)\langle\langle W\| \tag{2.2}$$
$$(\beta D - \delta E)\|V\rangle\rangle = (1-q)\|V\rangle\rangle \ . \tag{2.3}$$

where α,β,γ, δ and q are the usual parameters of the open ASEP, and p is set to 1 for convenience. The *auxilary space* $\mathcal{A}$ in which $\langle\langle W\|$ and $\|V\rangle\rangle$ live is not physical and should be distinguished from the configuration space of the system (of dimension 2^L). Then the probability of a configuration

$\mathcal{C} = \{n_i\}_{1 \leq i \leq L}$ in the steady state is

$$P^*(\mathcal{C}) = \frac{1}{Z_L} \langle\langle W \| \prod_{i=1}^{L} (n_i D + (1 - n_i) E) \, \| V \rangle\rangle \tag{2.4}$$

where the normalization factor Z_L writes

$$Z_L = \langle\langle W \| (D + E)^L \| V \rangle\rangle \tag{2.5}$$

which contains indeed the terms of the form (2.4) for all 2^L configurations, as a configuration is represented by a product of operators D et E, standing respectively for an occupied or an empty site. Several explicit representations of the algebra (2.1)-(2.3) exist; note that there is no need to dispose of an explicit representation to perform computations for small system size, simply using the relations between E, D, $\| V \rangle\rangle$, $\langle\langle W \|$.

Proof of the matrix product ansatz

Let us now give of proof of the matrix product ansatz, following [54]. We look for an expression of the probability distribution in the stationary state $P^*(n_1, ...n_L)$ such that

$$\left(B_1 + \sum_{i=1}^{L-1} m_{i,i+1} + B_L \right) |P^*(n_1, ...n_L)\rangle = 0 \, . \tag{2.6}$$

Let us assume that we dispose of operators $\{X_0 = D, X_1 = E\}$ and $\{\tilde{X}_0 = \tilde{D}, \tilde{X}_1 = \tilde{E}\}$ and vectors $\langle\langle W \|$ and $\| V \rangle\rangle$ such that the scalar function $P^*(n_1, ...n_L)$ writes

$$P^*(n_1, ..., n_L) = \langle\langle W \| X_{n_1} ... X_{n_L} \| V \rangle\rangle \, . \tag{2.7}$$

Operators E and D are indeed the ones appearing in expressions (2.1)–(2.3) while $\tilde{D}$ and $\tilde{E}$ are auxiliary operators needed for the proof. Defining moreover the vectors (with operators on $\mathcal{A}$ as elements) $X, \tilde{X} \in \mathbb{C}^2 \otimes \mathrm{End}(\mathcal{A})$ by

$$X = \begin{pmatrix} E \\ D \end{pmatrix} \qquad \tilde{X} = \begin{pmatrix} \tilde{E} \\ \tilde{D} \end{pmatrix} \tag{2.8}$$

and denoting by $X^{(i)}$ the vector corresponding to site i, (2.7) rewrites

$$|P^*\rangle = \langle\langle W \| \prod_{i=1}^{L} X^{(i)} \| V \rangle\rangle \tag{2.9}$$

where the product of the $X^{(i)}$ is understood as a tensor product on the configuration spaces $\mathbb{C}^2$ and as an matrix product on the auxilary space $\mathcal{A}$, *i.e.*

$$X^{(i)} X^{(i+1)} = \begin{pmatrix} EE \\ ED \\ DE \\ DD \end{pmatrix} \tag{2.10}$$

Let us assume that E and D are such that the the following relations are satisfied

$$m_{i,i+1} X^{(1)} ... X^{(2)} X^{(i+1)} ... X^{(L)} = X^{(1)} ... [\tilde{X}^{(i)} X^{(i+1)} - X^{(i)} \tilde{X}^{(i+1)}] ... X^{(L)} \tag{2.11}$$

$$B_1 X^{(1)} ... X^{(L)} = -\tilde{X}^{(1)} ... X^{(L)} \tag{2.12}$$

$$B_L X^{(1)} ... X^{(L)} = X^{(1)} ... \tilde{X}^{(L)} \, . \tag{2.13}$$

Inserting vector (2.9) in the master equation with $X^{(i)}$ satisfying these relations, we see that the sum in (2.6) telescopes to zero from site 2 to site $L-1$. Besides, writing explicitely in coordinates the actions of the local update operators on (pairs) of $X^{(i)}$, one finds

$$m_{i,i+1}X^{(i)}X^{(i+1)} = \begin{pmatrix} 0 \\ DE - qED \\ qED - DE \\ 0 \end{pmatrix} \tag{2.14}$$

$$B_1\langle\langle W\|X^{(1)} = \begin{pmatrix} \langle\langle W\|(\gamma D - \alpha E) \\ \langle\langle W\|(\alpha E - \gamma D) \end{pmatrix} \tag{2.15}$$

$$B_L X^{(L)}\|V\rangle\rangle = \begin{pmatrix} (\beta D - \delta E)\|V\rangle\rangle \\ (\delta E - \beta D)\|V\rangle\rangle \end{pmatrix} \tag{2.16}$$

so that (2.11)–(2.13) are indeed satisfied if

$$\tilde{D}D - D\tilde{D} = \tilde{E}E - E\tilde{E} = 0 \tag{2.17}$$

$$DE - qED = \tilde{E}D - E\tilde{D} = -\tilde{D}E + D\tilde{E} \tag{2.18}$$

$$\langle\langle W\|(\gamma D - \alpha E)) = -\langle\langle W\|\tilde{E} = \langle\langle W\|\tilde{D} \tag{2.19}$$

$$(\delta E - \beta D)\|V\rangle\rangle = \tilde{D}\|V\rangle\rangle = -\tilde{E}\|V\rangle\rangle \ . \tag{2.20}$$

Setting $\tilde{D} = -\mathrm{Id}$ and $\tilde{E} = \mathrm{Id}$, these relations are exactly (2.1)-(2.3) and (2.11)–(2.13) are satisfied, so that the relations defining the matrix ansatz algebra are indeed necessary conditions for the distribution P^* as defined by (2.7) to be stationary, which proves the validity of the matrix ansatz.

Phase diagram and correlation functions of the open TASEP from matrix ansatz

Let us first give the expression of the current in terms of the matrix product ansatz objects. Recalling equations (1.42), the steady state current writes

$$J = \langle n_{i-1}(1-n_i)\rangle - q\langle n_i(1-n_{i-1})\rangle \ . \tag{2.21}$$

Since for any $k \geq 0$, the sum of all words in E or D of length k representing all configurations of a section of k sites in the chain writes

$$(E+D)^k = \sum_{\{X_i\}\in\{E,D\}^k} X_1 ... X_k \ , \tag{2.22}$$

the mean value can be computed by inserting powers of $(D+E)$ on the portions of the chain which are averaged, so that

$$J = \frac{1}{Z_L}\left(\langle\langle W\|(D+E)^{i-2}DE(D+E)^{L-i}\|V\rangle\rangle - q\langle\langle W\|(D+E)^{i-2}ED(D+E)^{L-i}\|V\rangle\rangle\right) \tag{2.23}$$

$$= \frac{1-q}{Z_L}\langle\langle W\|(D+E)^{i-2}(D+E)(D+E)^{L-i}\|V\rangle\rangle \tag{2.24}$$

$$= (1-q)\frac{Z_{L-1}}{Z_L} \tag{2.25}$$

where we used (2.1) in the second equality. The computation of the normalization constant Z_L can be done by diagonalizing the matrix $E+D$. Let us first define the operators

$$e = E - \mathrm{Id} \qquad d = D - \mathrm{Id} \tag{2.26}$$

so that (2.1) can be written as

$$de - qed = (1-q)\mathrm{Id} \ . \tag{2.27}$$

This operator identity happens to be the defining relation satisfied by the creation operator e and annihilation operator d of the *q-deformed harmonic oscillator* [77] [1].

Several representations exist for these operators and the boundary vectors $\langle\langle W\|$ and $\|V\rangle\rangle$ that we can use to compute Z_L. They are built by considering basis of orthogonal polynomials [78] satisfying some recursion relations implied for the coordinate of $\langle\langle W\|$ and $\|V\rangle\rangle$ by the algebraic relations (2.1)-(2.3). The simplest of them is the representation based on the q-deformed Hermite polynomials that we present now. Denoting by $\{\|0\rangle\rangle, \|1\rangle\rangle, \|2\rangle\rangle, ...\}$ the infinite orthonormal basis of the representation space with $\langle\langle m\|n\rangle\rangle = \delta_{m,n}$, one can write operators e and d as

$$e = \sum_{n=0}^{\infty} \|n+1\rangle\rangle\langle\langle n\| \ , \tag{2.28}$$

$$d = \sum_{n=1}^{\infty} (1-q^n)\|n-1\rangle\rangle\langle\langle n\| \ . \tag{2.29}$$

Writing the boundary vectors $\|V\rangle\rangle$ and $\langle\langle W\|$ as

$$\|V\rangle\rangle = \sum_{n=0}^{\infty} V_n \|n\rangle\rangle \ , \qquad\qquad \langle\langle W\| = \sum_{n=0}^{\infty} W_n \langle\langle n\| \ , \tag{2.30}$$

the relations (2.2) and (2.3) rewrite as recursion relations on the coefficients V_n and W_n

$$\alpha W_{n+1} + (\alpha - \gamma - 1 + q)W_n - \gamma(1-q^n)W_{n-1} = 0 \ , \tag{2.31}$$

$$\beta(1-q^{n+1})V_{n+1} + (\beta - \delta - 1 + q)V_n - \delta V_{n-1} = 0 \ . \tag{2.32}$$

Defining, along with the parameters a and b (1.48)–(1.49), the new boundary parameters

$$\tilde{a} = \frac{1}{2\alpha}\left[1-q-\alpha+\gamma - \sqrt{(1-q-\alpha+\gamma)^2 + 4\alpha\gamma}\right] \ , \tag{2.33}$$

$$\tilde{b} = \frac{1}{2\beta}\left[1-q-\beta+\delta - \sqrt{(1-q-\beta+\delta)^2 + 4\beta\delta}\right] \ , \tag{2.34}$$

these expressions write

$$W_{n+1} - (a+\tilde{a})W_n + a\tilde{a}(1-q^n)W_{n-1} = 0 \tag{2.35}$$

$$(1-q^{n+1})V_{n+1} - (b+\tilde{b})V_n + b\tilde{b}V_{n-1} = 0 \ . \tag{2.36}$$

We introduce the following notation

$$(x)_n = \prod_{k=0}^{n-1}(1-q^k x) \tag{2.37}$$

and its limit for $n \to \infty$ defined for $q < 1$

$$(x)_\infty = \prod_{k=0}^{\infty}(1-q^k x) \ . \tag{2.38}$$

$(\bullet)_n$ is called the q-Pochhammer symbol. We will use besides the notation $(a,b)_n = (a)_n(b)_n$ for the product of two Pochhammer symbols. We now introduce the q-deformed Hermite polynomials

$$H_n(x,y) = \sum_{k=0}^{n} \frac{(q)_n}{(q)_k(q)_{n-k}} x^k y^{n-k} \tag{2.39}$$

[1] In the limit $q \to 1$, operators d, e and $N = ed$ satisfy the usual commutation relations of the ladder operators of the quantum oscillator harmonic – or of any bosonic algebra $[d,e] = 1$, $[N,e] = e$ and $[N,d] = -d$.

which are defined such that in the limit $q \to 1$,

$$H_n(x,y) = y^n H\left(\frac{x}{y}, 1\right) = x^n H\left(1, \frac{y}{x}\right) \to \mathcal{H}_n\left(\frac{x}{y}\right) \tag{2.40}$$

where $\mathcal{H}_n$ is the usual Hermite polynomial of order n, defined by

$$\mathcal{H}_n(x) = (-1)^n \mathrm{e}^{x^2} \frac{\mathrm{d}^n}{\mathrm{d}x^n} \mathrm{e}^{-x^2} \tag{2.41}$$

which are orthogonal for the probability measure with Gaussian weight $\mathrm{e}^{-x^2/2}\mathrm{d}x$. It can be shown besides that the q-Hermite polynomials satisfy the following identity known as the q-Mehler formula [14]

$$\sum_{n=0}^{\infty} H_n(x,y) H_n(z,t) \frac{u^n}{(q)_n} = \frac{(xyztu^2)_\infty}{(xzu, xtu, yzu, ytu)_\infty} \ . \tag{2.42}$$

which is valid when $xz, xt, yz, yt < 1/u$. The q-deformed Hermite polynomials also satisfy the following recursion relation

$$H_{n+1}(x,y) - (x+y) H_n(x,y) + xy(1-q^n) H_{n-1}(x,y) = 0 \tag{2.43}$$

which is the same as (2.35) and (2.36) by setting $x, y = a, \tilde{a}$ and $x, y = b, \tilde{b}$ respectively, so that

$$W_n = H_n(a, \tilde{a}) \ , \tag{2.44}$$

$$V_n = \frac{H_n(b, \tilde{b})}{(q)_n} \ . \tag{2.45}$$

Now that we have an explicit representation of the matrix ansatz algebra, we are left with computing $Z_L = \langle\!\langle W \| (2+d+e)^L \| V \rangle\!\rangle$. The eigenstates of operator $(e+d)$ can be interpreted as the coherent states of a q-deformed harmonic oscillator, whose ladder operators satisfy the aforementioned q-deformed bosonic algebra. Such eigenstates are known [78] and form a basis of the representation state writing

$$\| z \rangle\!\rangle = \sum_{n=0}^{\infty} \frac{H_n(z, z^{-1})}{(q)_n} \| n \rangle\!\rangle \ , \tag{2.46}$$

$$\langle\!\langle z \| = \sum_{n=0}^{\infty} H_n(z, z^{-1}) \langle\!\langle n \| \ . \tag{2.47}$$

with closure relation

$$\mathrm{Id} = \frac{(q)_\infty}{2} \oint_{|z|=1} \frac{\mathrm{d}z}{2\mathrm{i}\pi z} (z^2, z^{-2})_\infty \| z \rangle\!\rangle \langle\!\langle z \| \ . \tag{2.48}$$

The action of $(e+d)$ on these states write

$$(e+d) \| z \rangle\!\rangle = (z + 1/z) \| z \rangle\!\rangle \ , \tag{2.49}$$

$$\langle\!\langle z \| (e+d) = \langle\!\langle z \| (z + 1/z) \ . \tag{2.50}$$

Inserting the closure relation (2.48) in the expression of Z_L one gets

$$Z_L = \langle\!\langle W \| (e+d) \mathrm{Id} \| V \rangle\!\rangle \tag{2.51}$$

$$= \frac{(q)_\infty}{2} \oint_{|z|=1} \frac{\mathrm{d}z}{2\mathrm{i}\pi z} (z^2, z^{-2})_\infty (2 + z + z^{-1})^L \langle\!\langle W \| z \rangle\!\rangle \langle\!\langle z \| V \rangle\!\rangle \ . \tag{2.52}$$

Using (2.42), one gets

$$\langle\!\langle W \| z \rangle\!\rangle = \sum_{n=0}^{\infty} \frac{H_n(a, \tilde{a}) H_n(z, z^{-1})}{(q)_n} = \frac{(a\tilde{a})_\infty}{(az, az^{-1}, \tilde{a}z, \tilde{a}z^{-1})_\infty} \ , \tag{2.53}$$

$$\langle\!\langle z \| V \rangle\!\rangle = \sum_{n=0}^{\infty} \frac{H_n(b, \tilde{b}) H_n(z, z^{-1})}{(q)_n} = \frac{(b\tilde{b})_\infty}{(bz, bz^{-1}, \tilde{b}z, \tilde{b}z^{-1})_\infty} \tag{2.54}$$

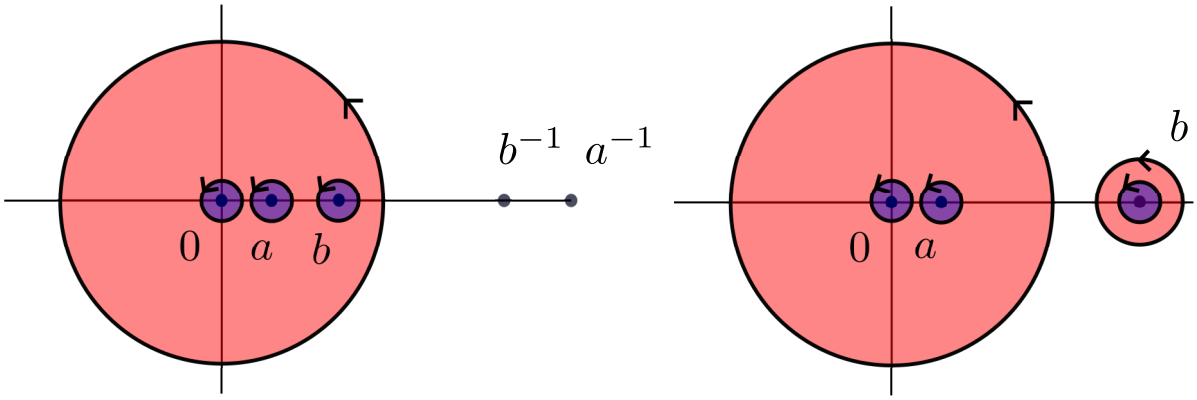

Figure 2.1: Plot of the poles a,b,and 0 of the function $F(z)$ defined in (2.57) for the totally asymmetric case and the corresponding integration contours of (2.55) at two different points of the phase diagram. The integral has to be taken around the poles which are inside the unit disk $|z| < 1$ when $|a| < 1$ and $|b| < 1$, which are trivially a,b and 0 for the TASEP. The red and blue contours are thus equivalent on the figure. In the general case for $q \neq 0$, the set of contributing poles is $\bigcup_{k\in\mathbb{N}}\{0, aq^k, \tilde{a}q^k, bq^k, \tilde{b}q^k\}$

so that finally the normalization constant writes

$$Z_L = \frac{1}{2}\oint_S \frac{\mathrm{d}z}{2\mathrm{i}\pi}\frac{F(z)}{z} \tag{2.55}$$

with

$$F(z) = \frac{(1+z)^L(1+z^{-1})^L(z^2,z^{-2})_\infty}{(az,az^{-1},\tilde{a}z,\tilde{a}z^{-1},bz,bz^{-1},\tilde{b}z,\tilde{b}z^{-1})_\infty}\,. \tag{2.56}$$

This derivation is only rigorous in the case $|a|, |b|, |\tilde{a}|, |\tilde{b}| < 1$ as it is needed to apply the formula (2.42). In this case, the integration contour S in (2.55) is simply the unit circle $|z| = 1$. However the validity of (2.55) can be extended beyond these conditions by analytic continuation, in which case one has to change the integration contour of the integral S so as to include the poles that exit the unit circle, see figure 2.1. In the totally asymmetric case, the function $F(z)$ takes a much simpler form

$$F(z) = \frac{(1+z)^L(1+z^{-1})^L(1-z^2)(1-z^{-2})}{(1-az)(1-az^{-1})(1-bz)(1-bz^{-1})}\,. \tag{2.57}$$

In particular, the function F has only a finite number of poles. This integral can be computed in the large L limit by saddle point approximation, and the computation of the current J according to expression (2.21) gives the same phase diagram as the one obtained by the mean field approach of section 1.3.3.

Validity of the mean-field approximation in the thermodynamic limit

The fact that the mean field derivation gives the exact result for the stationary values arise from the vanishing of nearest neighbour correlations in the thermodynamic limit. The two point correlation density on the ASEP chain of size L writes

$$\langle n_i n_j\rangle = \langle\!\langle W\|(D+E)^{i-1}E(D+E)^{j-i-1}E(D+E)^{L-j}\|V\rangle\!\rangle\,. \tag{2.58}$$

This expression has been computed exactly with another representation of the matrix ansatz algebra using the Askey-Wilson orthogonal polynomials [91]. The connected nearest-neighbor correlation function at leading order in the system size writes

$$\langle n_i n_{i+1}\rangle - \langle n_i\rangle\langle n_{i+1}\rangle \underset{L\to\infty}{\simeq} \frac{1}{\pi L^{1/2}}\left[\frac{i-L/2}{\sqrt{i(L-i)}}\frac{i+1-L/2}{\sqrt{(i+1)(L-i-1)}}\right. \tag{2.59}$$
$$\left. - \frac{1-i^2+i(L-i-1)-(L-i-1)^2}{4\sqrt{i(L-i-1)(i-1)(L-i)}}\right].$$

Casting this expression into (1.44) and taking the large system size limit, one finds

$$J = (1-q)\rho(1-\rho) - \frac{1+q}{2L}\frac{\partial \rho}{\partial x} + \frac{c(x)}{\sqrt{L}} \tag{2.60}$$

where $c(x)$ is a bounded function of order 1 [2] gathering the dependency of the correlation function on the position on the chain. The contribution of nearest neighbors correlations vanishes in the limit $L \to \infty$ so that the mean field approximation is indeed exact for the stationary state in the thermodynamic limit.

2.2 Coordinate Bethe ansatz for the periodic ASEP

We will now present the coordinate Bethe ansatz diagonalization of the periodic ASEP [31], in order to get an intuitive understanding of the Bethe ansatz formalism. The coordinate Bethe ansatz is the first historical form of the Bethe ansatz and was originally applied in [9] to the diagonalization of the Hamiltonian of the XXX spin chain. It consists, roughly speaking, in looking for the wavefunctions of a N-body system under the form of a sum over all permutations of positions and pseudo-momenta of individual particles.

Let us consider the periodic ASEP with L sites and N particle, with current counting deformation on every bond of the system. We denote by $\psi(x_1, ..., x_N)$ the coordinates of the eigenvectors in the configuration basis, or *wavefunctions* and E the associated eigenvalues, with particle positions $1 \leq x_1 \leq ... \leq L$. In particular, for the ground states eigenvalue, the $\psi(x_1, ..., x_N)$ are the stationary probabilities of the configurations. Our goal is to find exact expressions for ψ and E for all eigenstates. The eigenvalue equation $M(\mu)\,|\psi\rangle = E\,|\psi\rangle$ in coordinates writes

$$\begin{aligned} E\psi(x_1, ...x_N) = p\sum_i \left[\mathrm{e}^{\mu}\psi(x_1, ..., x_i - 1, ..., x_N) - \psi(x_1, ..., x_i, ..., x_N)\right]^{\mathrm{ex}} \\ + q\sum_i \left[\mathrm{e}^{-\mu}\psi(x_1, ..., x_i + 1, ..., x_N) - \psi(x_1, ..., x_i, ..., x_N)\right]^{\mathrm{ex}} \end{aligned} \tag{2.61}$$

where the terms in brackets $[...]^{\mathrm{ex}}$ are zero when the terms $\psi(\{x_i\})$ contain two x_i which are equals, so that the exclusion constraint is satisfied. If the particle on the chain were non-interacting, a natural ansatz for the eigenvectors would be to look for them as a linear combination of plane waves $\psi(x_1, ..., x_N) = \prod_i \mathrm{e}^{ip_i x_i}$ with momentum p_i fixed by the periodic boundary conditions. However, it is straightforward to check that this ansatz fails due to the exclusion constraint, thus we need a more sophisticated form for the eigenvectors. By analogy with elastic scattering in one-dimension [3], the interaction of particles at adjacent positions is expected to exchange their momenta. The essence of the Bethe ansatz then consists in looking for the eigenvectors under the form

$$\psi(x_1, ..., x_N) = \sum_{\sigma \in \mathfrak{S}_N} A_\sigma \prod_{i=1}^{N} z_{\sigma(i)}^{x_i} \tag{2.62}$$

which is invariant by construction under particle - momentum permutations. The amplitudes $\{A_\sigma\}$ and the *Bethe roots* $\{z_i\}_{1 \leq i \leq N}$ are parameters that we need to set and $\mathfrak{S}_N$ is the N-th symmetric group, so that the sum runs over all permutations σ of the positions and the Bethe roots z_i. The factors z_i can be equivalently written as $\mathrm{e}^{\mathrm{i}p_i}$ to make the analogy quantum scattering more apparent. In order to completely determine the expression of the wavefunctions and eigenvalues, we will proceed as follow:

i) Solve the eigenvalue equation (2.61) assuming that the particle are well separated, that is $1 \leq x_1 < x_2 < ... < x_N < x_1 + L$ with $x_i < x_{i+1} - 1$ for all pairs of consecutive particles, so that one does not have to bother with adjacency cases on the positions. This will yield a value of E in terms of the Bethe roots.

[2] Assuming that $i = xL$ is of order L. In fact, the predictions of the mean-field approximation for the density profile do break down at the boundaries.

[3] A typical example of a model – also solved by Bethe ansatz – featuring this type of hard-core interaction is the δ-Bose gas, consisting of N bosons on a circle with Hamiltonian $H = -\sum_i \partial_{x_i}^2 + \sum_{i<j} \delta(x_i - x_j)$

ii) Instead of restricting the sums in (2.61) to non-overlapping x_i, we will set the parameters A_σ so as to ensure that the sum of all the terms on the RHS of (2.61) accounting for prohibited transition – *i.e.* those containing wavefunctions $\psi(x_1, ..., x_i, x_i, ..., x_N)$ with equal positions – cancel. Several cases have to be considered, depending on the number of adjacent particles on the LHS of (2.61). The crucial observation at the heart of the integrability of the exclusion process is that the cancellation condition for any k-collision with $\psi(x_1, ..., \underline{x_i, x_i+1, ..., x_i+k}, ..., x_N)$ is expressed as a sum of independent 2-collision conditions.

iii) Finally, we will impose the boundary conditions $\psi(x_1, ..., x_L) = \psi(x_2, ..., x_N, x_1 + L)$ which will yield N independent polynomial equations on the z_i, referred to as the *Bethe equations*. The momenta corresponding to Bethe roots $z_i = \mathrm{e}^{\mathrm{i}p_i}$ are thus quantized for a finite size system. Different solutions of the Bethe equations will correspond to different eigenstates of the Markov matrix.

Let us first work out the cases $N = 1, 2$ and 3, from which the generalization to N particle is straightforward.

The one particle case

For $N = 1$, injecting the Bethe-ansatz wavefunction $\psi(x) = A_1 z_1^x$ in (2.61), one finds immediately

$$E = \frac{\mathrm{e}^{\mu} p}{z_1} + \mathrm{e}^{-\mu} q z_1 - (p + q) \, . \tag{2.63}$$

The periodicity condition reads $z_1^L = 1$ so that the unique Bethe root is simply a L-th root of unity, and A_1 is a global normalization constant. The L eigenstates of $M(\mu)$ then correspond to the L possible values of z_1 and the matrix $M(\mu)$ is completely diagonalized

The two particle case

For $N = 2$, the wavefunction is now

$$\psi(x_1, x_2) = A_{12} z_1^{x_1} z_2^{x_2} + A_{21} z_1^{x_2} z_2^{x_1} \tag{2.64}$$

and the eigenvalue equation, in the generic case where $x_2 > x_1 + 1$, writes

$$\begin{aligned} E\psi(x_1, x_2) = \; & p\mathrm{e}^{\mu} \left[\psi(x_1 - 1, x_2) + \psi(x_1, x_2 - 1)\right] \\ & + q\mathrm{e}^{-\mu} \left[\psi(x_1 + 1, x_2) + \psi(x_1, x_2 + 1)\right] \\ & - 2(p + q)\psi(x_1, x_2) \end{aligned} \tag{2.65}$$

which yields the eigenvalue expression

$$E = \mathrm{e}^{\mu} p \left(\frac{1}{z_1} + \frac{1}{z_2} \right) + \mathrm{e}^{-\mu} q (z_1 + z_2) - 2(p + q) \, . \tag{2.66}$$

Considering now the 2-collision case $x_2 = x_1 + 1$, the eigenvalue equation restricted on allowed transitions reduces to

$$E\psi(x_1, x_1 + 1) = p\mathrm{e}^{\mu} \psi(x_1 - 1, x_1 + 1) + q\mathrm{e}^{-\mu} \psi(x_1, x_1 + 2) - (p + q)\psi(x_1, x_1 + 1) \, . \tag{2.67}$$

In order for the expression (2.66) to hold, we can equivalently impose the generic eigenvalue equation (2.65) on ψ and the cancellation of the terms missing in (2.67), that is

$$p\mathrm{e}^{\mu} \psi(x_1, x_1) + q\mathrm{e}^{-\mu} \psi(x_1 + 1, x_1 + 1) - (p + q)\psi(x_1, x_1 + 1) = 0 \, . \tag{2.68}$$

This 2-collision cancellation condition is satisfied for

$$\frac{A_{21}}{A_{12}} = -\frac{p\mathrm{e}^{\mu} + q\mathrm{e}^{-\mu} z_1 z_2 - (p + q) z_2}{p\mathrm{e}^{\mu} + q\mathrm{e}^{-\mu} z_1 z_2 - (p + q) z_1} \, , \tag{2.69}$$

so that the amplitudes are fixed up to a global normalization factor. Imposing the periodicity $\psi(x_1, x_2) = \psi(x_2, x_1 + L)$, one find

$$z_1^{x_1} z_2^{x_2} + \frac{A_{21}}{A_{12}} z_1^{x_2} z_2^{x_1} = z_1^{x_2} z_2^{x_1+L} + \frac{A_{21}}{A_{12}} z_1^{x_1+L} z_2^{x_2} \tag{2.70}$$

which has to be satisfied for any values of x_1 and x_2 so that $A_{12}/A_{21} = z_2^L = z_1^{-L}$. Using expression (2.69), the Bethe equations for $N = 2$ write

$$z_1^L = -\frac{p\mathrm{e}^{\mu} + q\mathrm{e}^{-\mu} z_1 z_2 - (p+q) z_1}{p\mathrm{e}^{\mu} + q\mathrm{e}^{-\mu} z_1 z_2 - (p+q) z_2} , \tag{2.71}$$

$$z_2^L = -\frac{p\mathrm{e}^{\mu} + q\mathrm{e}^{-\mu} z_1 z_2 - (p+q) z_2}{p\mathrm{e}^{\mu} + q\mathrm{e}^{-\mu} z_1 z_2 - (p+q) z_1} , \tag{2.72}$$

and all free parameters in the wavefunction are set.

The three particle case

The generic eigenvalue equation for well-separated particles is similar to the case with $N = 2$ so let us focus directly on the adjacency case. Two types of collision can occur

- 2-collisions, with two adjacent particles and the third one apart. There are two cases, for positions $(x_1, x_2 = x_1 + 1, x_3 > x_2 + 1)$ and $(x_1, x_2 > x_1 + 1, x_3 = x_2 + 1)$. The case $(x_1, x_2 > x_1 + 1, x_3 = x_1 + L - 1)$ is in fact equivalent to the second one by periodicity. Canceling the missing terms in (2.61) for these types of configuration then yields two equations

$$\begin{aligned} &\text{(A)} \quad \mathrm{e}^{\mu} p\psi(x, x, x_3) + q\mathrm{e}^{-\mu}\psi(x+1, x+1, x_3) - (p+q)\psi(x, x+1, x_3) = 0 \\ &\text{(B)} \quad \mathrm{e}^{\mu} p\psi(x_1, x, x) + q\mathrm{e}^{-\mu}\psi(x_1, x, x) - (p+q)\psi(x_1, x, x+1) = 0 \end{aligned}$$

- 3-collision, with particle positions $(x_1, x_1 + 1, x_1 + 2)$ leading to the cancellation condition

$$\begin{aligned} & p\mathrm{e}^{\mu}\big[\psi(x, x, x+2) + \psi(x, x+1, x+1)\big] \\ + \;& q\mathrm{e}^{-\mu}\big[\psi(x+1, x+1, x+2) + \psi(x, x+2, x+2)\big] \\ - \;& 2(p+q)\psi(x, x+1, x+2) = 0 \end{aligned}$$

  which rewrites as

$$\begin{aligned} & \underbrace{p\mathrm{e}^{\mu}\psi(x, x, x+2) + q\mathrm{e}^{-\mu}\psi(x+1, x+1, x+2) - (p+q)\psi(x, x+1, x+2)}_{\text{(A)}} \\ + \;& \underbrace{p\mathrm{e}^{\mu}\psi(x, x+1, x+1) + q\mathrm{e}^{-\mu}\psi(x, x+2, x+2) - (p+q)\psi(x, x+1, x+2)}_{\text{(B)}} = 0 . \end{aligned} \tag{2.73}$$

Thus, the 3-collision cancellation condition is in fact expressed as the sum of the 2-collision conditions, so that all cancellation conditions are compatible with each other, and our ansatz on the form of the wavefunction is valid. In the parlance of quantum integrability, the 3-body scattering factors into the product of commuting 2-body scattering. This property is the fundamental ingredient needed to apply the Bethe ansatz, and is not satisfied by non-integrable models on lattice. We will now present the rest of the derivation of the Bethe equation for the general case of N particles.

The N particle case

For any value of N, the eigenvalue obtained by solving the generic eigenvalue equation is

$$E = \sum_{i=1}^{N} \left(p\mathrm{e}^{\mu} \frac{1}{z_i} + q\mathrm{e}^{-\mu} z_i \right) - N(p+q) . \tag{2.74}$$

Let us derive the 2-collision conditions on the amplitudes A_σ. They consist of $N-1$ independent equations

$$\begin{aligned} p\mathrm{e}^{\mu}\psi(x_1,...,x_i,x_i,...,x_L)+q\mathrm{e}^{-\mu}\psi(x_1,...,x_i+1,x_i+1,...,x_L) \\ -(p+q)\psi(x_1,...,x_i+1,x_i+1,...,x_L)=0 \end{aligned} \tag{2.75}$$

for $1\leq i\leq L-1$. Developing these equations with the wavefunction (2.62) one obtains

$$\sum_{\sigma\in\mathfrak{S}_N} A_\sigma \left(\prod_{k\neq i,i+1} z_{\sigma(k)}^{x_k}\right)\left(p\mathrm{e}^{\mu}z_{\sigma(i)}^{x}z_{\sigma(i+1)}^{x}+q\mathrm{e}^{-\mu}z_{\sigma(i)}^{x+1}z_{\sigma(i+1)}^{x+1}-(p+q)z_{\sigma(i)}^{x}z_{\sigma(i+1)}^{x+1}\right)=0\,. \tag{2.76}$$

Denoting by $\tau=(i\ \ i+1)$ the transposition permuting i and $i+1$, the sum over the symmetric group can be split in two: the set $\mathfrak{S}_N/\tau$ of permutations such that $\sigma(i)<\sigma(i+1)$ and the set $(\mathfrak{S}_N/\tau)\circ\tau$ of *inversions* the pair of indices $\{i,i+1\}$ such that $\sigma(i)>\sigma(i+1)$. These two sets differ globally by a right composition with τ, which leaves the factor $\prod_{k\neq i,i+1} z_{\sigma(k)}^{x_k}$ invariant. Equation (2.76) then writes

$$\begin{aligned} &\sum_{\sigma\in\mathfrak{S}_N/\tau} A_\sigma\left(p\mathrm{e}^{\mu}z_{\sigma(i)}^{x}z_{\sigma(i+1)}^{x}+q\mathrm{e}^{-\mu}z_{\sigma(i)}^{x+1}z_{\sigma(i+1)}^{x+1}-(p+q)z_{\sigma(i)}^{x}z_{\sigma(i+1)}^{x+1}\right) \\ &\quad+\quad A_{\sigma\circ\tau}\left(p\mathrm{e}^{\mu}z_{\sigma(i)}^{x}z_{\sigma(i+1)}^{x}+q\mathrm{e}^{-\mu}z_{\sigma(i)}^{x+1}z_{\sigma(i+1)}^{x+1}-(p+q)z_{\sigma(i)}^{x+1}z_{\sigma(i+1)}^{x}\right)=0\,. \end{aligned} \tag{2.77}$$

A sufficient condition for the cancellation is then to have for any $\sigma\in\mathfrak{S}_N$ the following relation on amplitudes differing by a transposition

$$\frac{A_{\sigma\circ\tau}}{A_\sigma}=-\frac{p\mathrm{e}^{\mu}+q\mathrm{e}^{-\mu}z_{\sigma(i)}z_{\sigma(i+1)}-(p+q)z_{\sigma(i+1)}}{p\mathrm{e}^{\mu}+q\mathrm{e}^{-\mu}z_{\sigma(i)}z_{\sigma(i+1)}-(p+q)z_{\sigma(i)}}\qquad\forall\sigma\in\mathfrak{S}_N\,. \tag{2.78}$$

Since any permutation can be written as the product of transpositions of consecutive numbers, these conditions set all amplitudes A_σ up to a global normalization factor. Note that this result was derived for generic values of the positions $\{x_k\}$ besides x_i and x_{i+1} so it is still valid if several 2-collisions occur in the same configuration.

We now have to show that the cancellation conditions for k-collision are implied by the conditions we just derived for 2-collisions, as in expression (2.73). Using the shorthand notations

$$\widetilde{\psi}_k(i,j,r)=\psi(x_1,...,\underline{x_i,x_i+1,...,x_i+j+r,...,x_i+k},...,x_N) \tag{2.79}$$

$$\widetilde{\psi}_k(i)=\psi(x_1,...,\underline{x_i,x_i+1,...,x_i+k},...,x_N) \tag{2.80}$$

where the dependency of $\widetilde{\psi}_k$ on the position of the particles outside the cluster of particles j to $j+k$ (underlined) is implicit, the cancellation condition for k-collisions write

$$p\sum_{j=1}^{k-1}[\mathrm{e}^{\mu}\widetilde{\psi}_k(i,j+1,-1)-\widetilde{\psi}_k(i)]+q\sum_{j=1}^{k-1}[\mathrm{e}^{-\mu}\widetilde{\psi}_k(i,j,+1)-\widetilde{\psi}_k(i)]=0\qquad 1\leq i\leq N-k+1\,. \tag{2.81}$$

Since the $\widetilde{\psi}_k$ are in fact special cases of the 2-collisions wave functions $\widetilde{\psi}_2$ evaluated for specific values of the remainder particle positions (outside the two stacked or adjacent particles), the LHS of (2.81) is actually the sum of $k-1$ of the conditions (2.75) shifted in particle indices i. Thus, the k-collisions cancellation conditions are indeed the sum of 2-collision conditions and are automatically satisfied.

Bethe equations

We can finally exploit the periodicity of the wavefunction to obtain the Bethe equations. Expanding the periodicity condition $\psi(x_1, ..., x_N) = \psi(x_2, ..., x_N, x_1 + L)$, we obtain

$$\sum_{\sigma\in\mathfrak{S}_N} A_\sigma z_{\sigma(1)}^{x_1}...z_{\sigma(N)}^{x_N} = \sum_{\sigma\in\mathfrak{S}_N} A_\sigma z_{\sigma(1)}^{x_2}...z_{\sigma(N-1)}^{x_N} z_{\sigma(N)}^{x_1+L} \tag{2.82}$$

$$\sum_{\sigma\in\mathfrak{S}_N} \left(A_\sigma - A_{\sigma\circ C} z_{\sigma(1)}^{L}\right) z_{\sigma(1)}^{x_1}...z_{\sigma(N)}^{x_N} = 0 \tag{2.83}$$

where $C = (2\ \ 3\ ...\ L\ \ 1)$ is the circular permutation that shifts Bethe roots indices by 1. The last expression being satisfied for generic values of the positions, it implies

$$\frac{A_{\sigma\circ C}}{A_\sigma} = z_{\sigma(1)}^{-L}\ . \tag{2.84}$$

The permutation C can be decomposed as a product of transposition $C = (1\ 2)\circ(2\ 3)\circ...\circ(N-1\ N)$, so we can write

$$\frac{A_{\sigma\circ C}}{A_\sigma} = \prod_{k=1}^{N-1} \frac{A_{\sigma\circ(1\ 2)\circ(2\ 3)\circ...\circ(k-1\ k)}}{A_{\sigma\circ(1\ 2)\circ(2\ 3)\circ...\circ(k-2\ k-1)}} \frac{A_{\sigma\circ(1\ 2)}}{A_\sigma}\ . \tag{2.85}$$

Using relation (2.78) to eliminate the successive transpositions, each factor in the product is equal to the ratio $A_{\sigma(1)\circ(1\ k)}/A_\sigma$, and with (2.84), setting $\sigma(1) = i$ we obtain the Bethe equations

$$z_i^L = (-1)^{N-1} \prod_{j=1}^{N} \frac{p\mathrm{e}^{\mu} + q\mathrm{e}^{-\mu} z_i z_j - (p+q) z_i}{p\mathrm{e}^{\mu} + q\mathrm{e}^{-\mu} z_i z_j - (p+q) z_j} \qquad 1 \le i \le N\ . \tag{2.86}$$

We have finally obtained a complete expression for the wavefunction and eigenvalues of the periodic exclusion process. The Bethe equation that we just derived have discrete sets of solutions for the z_i, some unphysical, the other being in one-to-one correspondence with eigenstates of $M(\mu)$.

Several points should be noted. Regarding the completeness of our derivation of the eigenstates, there is *a priori* no reason for the Bethe ansatz approach to yield all the $\binom{L}{N}$ eigenstates of $M(\mu)$. It was only shown recently in [13] to be the case in the undeformed case $\mu = 0$ for generic values of p and q (which might exclude some special cases), and in general, the problem of the completeness of the Bethe ansatz equations is still open for most of the models solved by Bethe ansatz [53, 88], including the open TASEP that we will consider latter.

In order to determine the eigenstates of the system, one still has to solve a system of N polynomial equation of the Lth degree which is analytically not feasible in general. However daunting the task may look, it is yet a huge simplification of the diagonalization problem. First, it is computationally much easier to solve a system of degree L polynomials than to find the roots of the 2^L-th degree characteristic polynomial of $M(\mu)$. The fact that Bethe equation have a fixed form for any system size and number of particle allows for the computation of exact expressions in the thermodynamic limit. As we will see in chapter 4, solving the Bethe equations also leads to a natural classification of eigenstates which is physically meaningful

Simplifications occur in the Bethe equations for some limit cases. Considering the totally asymmetric case $p = 1$, $q = 0$, the Bethe equations become

$$\frac{z_i^L}{(\mathrm{e}^{\mu} - z_i)^N} = (-1)^{N-1} \prod_{j=1}^{N} (\mathrm{e}^{\mu} - z_i)^{-1}\ . \tag{2.87}$$

They have the form $f(z_i) = C$ where C is a parameter that depends symmetrically on all Bethe roots and f is a simple rational function. This separated form is especially convenient to work with as it allows to treat C as a free parameter from which Bethe roots can be obtained directly by inverting function f, and then set by writing down its definition in self-coherent form. It is also insightful to look a the limit $\mu \to \infty$, where the Bethe equations simply become

$$z_i^L = (-1)^{N-1} \tag{2.88}$$

and the Bethe roots are L-th roots of unity or -1 depending on the parity of N, as one would expect for non-interacting particles. Indeed, as already seen in paragraph 1.4.3, solving the dynamics for large values of μ amounts to conditioning the evolution of the system on large values of the current. Since the main limitation to the current comes from the exclusion interaction, which tends to jam the flow of particles, the likely configurations for $\mu \to \infty$ are the ones with all particles well separated, so that the exclusion constraint virtually does not play any role, hence this simplification of Bethe roots expressions.

2.2.1 Ground state eigenvalue $E(\mu)$ from Bethe equations

We can now compute a near explicit expression of the ground state eigenvalue $E(\mu)$ of $M(\mu)$ from the Bethe ansatz equations and the expression of $E(\mu)$ in terms of the Bethe roots. Under the change of variable $z_i = \mathrm{e}^{\mu}(1+y_i)$, the eigenvalue and the Bethe equations for the periodic TASEP rewrite

$$E(\mu) = \sum_{i=1}^{N} \left(\frac{1}{1+y_i} - 1 \right) , \tag{2.89}$$

$$\mathrm{e}^{\mu} \frac{(1+y_i)^L}{y_i^N} = (-1)^{N-1} \left(\prod_{j=1}^{N} y_j \right)^{-1} . \tag{2.90}$$

We also introduce the notations

$$B = (-1)^{N-1} \mathrm{e}^{\mu} \prod_{j=1}^{N} y_j , \tag{2.91}$$

$$h(y) = \frac{(1+y)^L}{y^N} , \tag{2.92}$$

so that the Bethe roots $\{y_i, 1 \leq i \leq N\}$ are roots of the polynomial $1 - Bh(y)$ of degree L, treating B as a free parameter. We know that the ground state eigenvector of the undeformed Markov matrix $\mu = 0$ (*i.e.* the stationary probability distribution on configurations) has uniform entries, which correspond from (2.62) and (2.85) to all $y_i = 1$, so that the corresponding eigenvalue is indeed 0. Considering the small B asymptotic behaviour of the L roots of $1 - Bh(y)$

$$y^N = B(1+y)^L \qquad \text{when} \quad B \to 0 \tag{2.93}$$

we see that the roots have the following scaling [4]

$$y_j \sim B^{1/N} \mathrm{e}^{\frac{2\mathrm{i}\pi j}{N}} \qquad \text{for} \quad 1 \leq j \leq N , \tag{2.94}$$

$$y_j \sim B^{-\frac{1}{L-N}} \mathrm{e}^{\frac{2\mathrm{i}\pi j}{L-N}} \qquad \text{for} \quad N < j \leq L . \tag{2.95}$$

Thus exactly N roots of $1 - Bh(y)$ go to zero, which are then precisely the Bethe roots corresponding to the ground state. In particular for μ and B small enough, they are located within the open unit disk $\{z, |z| < 1\}$. Both $E(\mu)$ and

$$\mu = \sum_{i=1}^{N} \log\Big(-B^{1/N}/y_i \Big) \tag{2.96}$$

are expressed as sums of functions of the Bethe roots. We can then, for μ small enough, write these sums as contour integrals on the unit circle, using the fact that for y_i roots of $P(y) = 1 - Bh(y)$ and any function f,

$$\sum_{i=1}^{N} f(y_i) = \oint_{\{y_i\}} \frac{\mathrm{d}y}{2\mathrm{i}\pi} \, f(y) \frac{P'(y)}{P(y)} . \tag{2.97}$$

[4] We choose here the simplest labeling of the y_j for our purpose. See [73] for a detailed study of the Bethe ansatz equation of the periodic TASEP in finite size

After integration by part we obtain

$$\mu = \oint_{|z|=1} \frac{\mathrm{d}z}{2\mathrm{i}\pi z} \log(1 - Bh(z)) \,, \tag{2.98}$$

$$E(\mu) = \oint_{|z|=1} \frac{\mathrm{d}z}{2\mathrm{i}\pi(1+z)^2} \log(1 - Bh(z)) \,. \tag{2.99}$$

Expanding these expressions in series of B we obtain

$$\mu = -\sum_{k=1}^{\infty} C_k \frac{B^k}{k} \tag{2.100}$$

$$E(\mu) = -\sum_{k=1}^{\infty} D_k \frac{B^k}{k} \tag{2.101}$$

with

$$C_k = \int_{|z|=1} \frac{\mathrm{d}z}{2\mathrm{i}\pi z} h(z)^k = \binom{kL}{kN} \,, \tag{2.102}$$

$$D_k = \int_{|z|=1} \frac{\mathrm{d}z}{2\mathrm{i}\pi(1+z)^2} h(z)^k = \binom{kL-2}{kN-1} \,. \tag{2.103}$$

We finally obtained a parametric expression of $E(\mu)$, the cumulant generating function of the stationary current in the periodic TASEP.

Algebraic Bethe ansatz for the periodic ASEP

There is an alternative and more general route the the above-derived Bethe equations through the *algebraic Bethe ansatz*. The algebraic Bethe ansatz formalism was first elaborated for integrable spin chains and vertex models [4, 36, 52] with periodic boundary conditions. The method is based on the existence of a familly of commuting operators $t(x)$ called the *transfer matrix*, which is a generating function of the operators associated to conserved charges of the model, from which the hamiltonian, partition function or stochastic generator of the model (depending on the setting) can be recovered. The transfer matrix is built from a *monodromy matrix* constructed as a product of local operators satisfying themsleves compatibility relations known as the *Yang-Baxter equation* and *RTT relations*. The monodromy matrix also defines an algebra of operators acting on the configuration space of the model such that eigenvectors of $t(x)$ can be built systematically by application of these operators. The Bethe equations then appear as cancelation conditions on parameters upon which the operators depend for *unwanted* terms in the spectral equality between $t(x)$, its eigenvalues and eigenvectors.

Concerning the exclusion process specifically, the algebraic Bethe ansatz was first formulated for the periodic ASEP [42], relying on the fact that the local update operators (1.13) satisfy the *Temperley-Lieb algebra*, which also plays an important role in the integrability of the XXZ model.

2.3 Modified Algebraic Bethe ansatz for the open TASEP

We have just seen that one can determine all eigenstates of the periodic ASEP by means of the Bethe ansatz. However, the coordinate approach that we used and the usual algebraic Bethe ansatz rely crucially on the conservation of the number of particles and periodicity of the system, features which are absent from the ASEP with open boundary conditions. It is however possible to formulate the Bethe ansatz in a more general framework that allows to account for general boundary conditions, this is the *modified algebraic Bethe ansatz*.

Following the introduction by Sklyanin of the the so-called *boundary algebra* [82], the algebraic Bethe ansatz was extended to systems with open *diagonal* boundary conditions presenting a $U(1)$ symmetry, understood in our context as conservation of the number of particles. The usual algebraic

Bethe ansatz formalism requires indeed the existence of a unique reference state (or pseudo-vacuum), which cannot be properly defined in the absence of such symmetry. This problem was circumvented with the introduction of the modified algebraic Bethe ansatz by Belliard and Crampé [5] that allowed to treat spin chains, and incidentally the exclusion process, with generic non-diagonal boundary condtions.

A generalized coordinate Bethe ansatz was also proposed in [24] for the open ASEP, which allowed the construction of the full set of eigenvectors of $M(\mu)$, although with constraints of the values of the parameters of the model of the form $\pm(\gamma/\alpha)^{\epsilon}(\delta/\beta)^{\epsilon'} = \mathrm{e}^{\mu}(p/q)^n$ with $\epsilon, \epsilon' = 0, 1$ and $1 \leq n \leq L-1$. With this method, the higher eigenstates are obtained by adding excitations on the groundstate of the matrix product ansatz of section 2.1.

In what follows we will first connect the ASEP with open boundaries to the XXZ-chain to justify the applicability of the algebraic Bethe anstaz. We will then construct the transfer matrix of the open ASEP by means of the modified algebraic Bethe ansatz, following [25] and obtain exact expressions for the eigenvalues and eigenvectors of the deformed Markov matrix along with a set of Bethe equations. Finally, we will see that a reformulation the Bethe ansatz in terms of *TQ-relations* yields Bethe equations in a separated form similar to (2.87).

2.3.1 Mapping to the XXZ spin chain

The XXZ spin chain is one of the most studied system in quantum statistical mechanics and arguably the prototype of integrable models on one-dimensional lattices. It is defined as follow. Consider a lattice of L sites each carrying a spin-1/2, that is a local two dimensional Hilbert space $H_i = \mathbb{C}^2$. Those spins are coupled through a nearest neighbour interaction which is isotropic in the directions X and Y and has a different coupling strength in the Z direction. The boundary sites H_1 and H_L are moreover subject to local boundary Hamiltonians B_1 and B_L which have to satisfy some conditions to preserve the integrability of the model. The global Hamiltonian acting on the whole chain Hilbert space $\mathcal{H} = \bigotimes_{i=1}^{L} H_i$ with integrable boundaries then writes

$$H_{\mathrm{XXZ}} = K_1 + K_N - \frac{1}{2}\sum_{j=1}^{L-1}\left(\sigma_j^x\sigma_{j+1}^x + \sigma_j^y\sigma_{j+1}^y - \cos\eta\ \sigma_j^z\sigma_{j+1}^z\right) \tag{2.104}$$

with

$$K_1 = \frac{\sin\eta}{\cos\omega_- + \cos\delta_-}\begin{pmatrix} \frac{\mathrm{i}}{2}(\cos\omega_-\cos\delta_-) - \sin\omega_- & \mathrm{e}^{-\mathrm{i}\theta_1} \\ \mathrm{e}^{\mathrm{i}\theta_1} & \frac{\mathrm{i}}{2}(\cos\omega_+\cos\delta_+) - \sin\omega_+ \end{pmatrix} \tag{2.105}$$

$$K_L = \frac{\sin\eta}{\cos\omega_+ + \cos\delta_+}\begin{pmatrix} -\frac{\mathrm{i}}{2}(\cos\omega_+ - \cos\delta_+) - \sin\omega_+ & \mathrm{e}^{-\mathrm{i}\theta_2} \\ \mathrm{e}^{\mathrm{i}\theta_2} & \frac{\mathrm{i}}{2}(\cos\omega_+\cos\delta_+) - \sin\omega_+ \end{pmatrix} \tag{2.106}$$

where the matrices σ^x, σ^y and σ^z are the Pauli matrices, and the subscripts indicate on which sites the operators act non-trivially. The Markov matrix $M(\mu)$ of the open TASEP with current counting deformation on the first bond is then related to H_{XXZ} by the similarity transformation [27]

$$M(\mu) = -\sqrt{pq}\ U^{-1} H_{\mathrm{XXZ}}\ U \qquad \text{with} \qquad U = \bigotimes_{j=1}^{L}\begin{pmatrix} 1 & 0 \\ 0 & \xi\left(\sqrt{\frac{q}{p}}\right)^{j-1} \end{pmatrix} \tag{2.107}$$

where the parameters of both models are related by

$$\sqrt{\frac{\alpha}{\gamma}} = -\mathrm{i}\mathrm{e}^{\mathrm{i}\omega_-} \qquad \sqrt{\frac{\beta}{\delta}} = -\mathrm{i}\mathrm{e}^{\mathrm{i}\omega_+} \tag{2.108}$$

$$\sqrt{\frac{p}{q}} = -\mathrm{e}^{\mathrm{i}\eta} \qquad \sqrt{\frac{\alpha}{\gamma}}\mathrm{e}^{\mu} = \mathrm{e}^{\mathrm{i}\theta_1} \tag{2.109}$$

$$\sqrt{\frac{\delta}{\beta}}\left(\sqrt{\frac{q}{p}}\right)^{L-1} = \mathrm{e}^{\mathrm{i}\theta_2}\ . \tag{2.110}$$

Due to this mapping, the diagonalization of the open spin chain is then essentially equivalent to that of the exclusion process. One should note that although the mapping is singular in the totally asymmetric

limit $q = 0$, the Bethe equations obtained from the Bethe ansatz on the XXZ chain are still well defined and give the correct expression for the eigenstates. These equations allowed de Gier and Essler [5] to compute the exact value of the gap of the open TASEP in [28]. Let us note moreover that the totally asymmetric case of the ASEP correspond to the infinite anisotropy case of the XXZ chain where the coefficient of the spin interaction on the z-axis goes to infinity.

By analogy with the idea of classical integrability, expressed by Liouville's theorem, that a system is integrable if it possesses enough conserved quantities, the algebraic Bethe ansatz consist in building and diagonalizing a more general, parameter dependent operator $t(x)$ called the *transfer matrix*, of which $M(\mu)$ itself is a special case, that is essentially a generating function of the conserved charges of the system. In what follows we will write this construction directly in terms of the ASEP parameters, following [26].

2.3.2 Transfer matrix of the open TASEP

Since we will be interested only in the totally asymmetric case in the rest of this work, we will concentrate on the TASEP with $p = 1$ to keep the notations light. The protocol for deriving Bethe equations and eigenstates expression by Bethe ansatz unfold as follow

i) Local operators acting on (pairs of) local configuration spaces $\mathbb{C}^2$ are defined: the R-matrix and the boundary operators K and $\overline{K}$. These operators are related, but not equal, to the bulk and boundary jump operators w, B_1 and B_L. They are constructed to satisfy compatibility conditions: the *Yang-Baxter equation* and *reflection equations*, which ensure the integrability of the model.

ii) Global operators, the monodromy matrix T and the transfer matrix $t(x)$ are constructed as tensor products of the aforementioned local operators. As a consequence of the Yang-Baxter and reflection equations, the transfer matrix $t(x)$ satisfies the commutation relation $[t(x), t(y)] = 0$ for generic values of its variable. In particular one has also $-(1/2)t'(1) = M(\mu)$, so that the diagonalization of $M(\mu)$ follows from the derivation of the eigenstates of $t(x)$.

iii) The operators A, B, C and D are defined as block entries of the monodromy matrix T. These operators satisfy a specific algebra, and their defining relation are used to construct the eigenstates of $t(x)$.

R-matrix and the Yang-Baxter equation

Let us first define the R-matrix of the open TASEP as

$$R(x) = \begin{pmatrix} 1 & 0 & 0 & 0 \\ 0 & 0 & x & 0 \\ 0 & 1 & 1-x & 0 \\ 0 & 0 & 0 & 1 \end{pmatrix} \tag{2.111}$$

This matrix acts on the tensor product $\mathbb{C}^2 \otimes \mathbb{C}^2$ with basis $(|00\rangle, |01\rangle, |10\rangle, |11\rangle)$ and depends on a variable x called the *spectral parameter*, that we leave free for now. The operator R can act non-trivially on two sites i and j of the TASEP chain and as the identity else where, which is denoted by $R_{ij}(x)$. Along with the sites of the chain for $1 \leq i, j \leq L$, we consider an additional site with index 0, called the *auxiliary space* [6]. Considering a generic three sites space $\mathbb{C}^2 \otimes \mathbb{C}^2 \otimes \mathbb{C}^2$, the R-matrix satisfies the Yang-Baxter equation

$$R_{12}\left(\frac{z_1}{z_2}\right) R_{13}\left(\frac{z_1}{z_3}\right) R_{23}\left(\frac{z_2}{z_3}\right) = R_{23}\left(\frac{z_2}{z_3}\right) R_{13}\left(\frac{z_1}{z_3}\right) R_{12}\left(\frac{z_1}{z_2}\right) \tag{2.112}$$

[5] It should be noted that the Bethe ansatz equations for the XXZ chain used by de Gier and Essler were obtained by different routes to the generalization of the algebraic Bethe ansatz than the one reviewed in the present work [65]. In particular, they are valid under constraints on the XXZ parameters which account however for all relevant cases in the asymptotics computations of the spectrum of the ASEP.

[6] The introduction of the auxiliary space might seem arbitrary in this context, it has however a natural physical interpretation when considering the Bethe ansatz computation of the partition function of vertex models, see [4, 52]

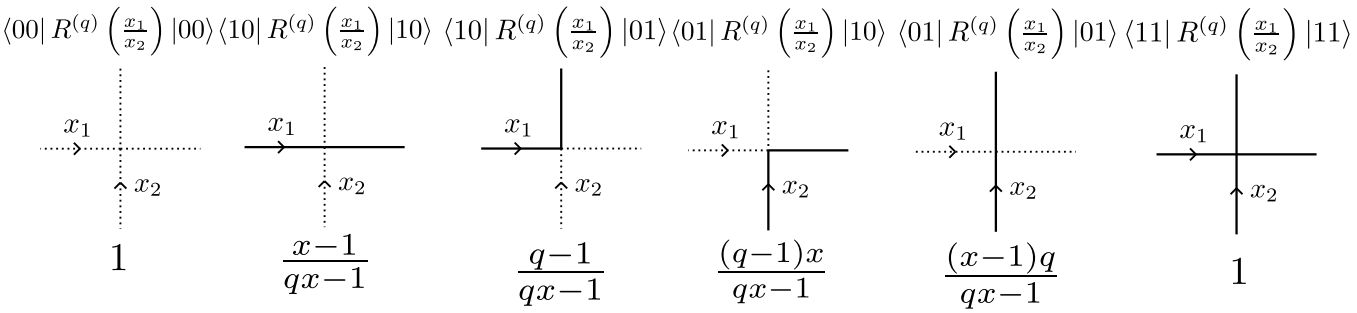

Figure 2.2: Diagrammatic representation of the R-matrix of the open ASEP. Each diagram represent a non-zero entry of operators $R_{ij}^{(q)}(x_1/x_2)$, with each leg of the diagram representing the state of the sites on which the operator acts. Thick lines indicate occupied site and dashed lines empty sites. Lines marked with incoming arrows represent the input states of the operators, while outgoing lines represent output states. In what follows, the horizontal lines while represent states belonging to the auxiliary space, while vertical lines will represent the physical states of spaces 1 to L from left to right. The R-matrix satisfies the so-called *line conservation* property: the number of incoming lines is equal to the number of outgoing lines.

for any values of $z_1, z_2, z_3 \in \mathbb{C}$. As we will see, the Yang-Baxter equation encodes the integrability of the model in the bulk. If we denote by P_{12} the permutation operator acting on the tensor product of two sites as $P_{12}(|u\rangle \otimes |v\rangle) = |v\rangle \otimes |u\rangle$, the R-matrix also satisfies the following properties

- unitarity : $R_{12}(z)R_{21}(1/z) = \mathrm{Id}$
- regularity : $R(1) = P$
- recovering of the local jump operator : $P_{12}R'_{12}(1) = -m\mathrm{Id}$

The last property connects the R-matrix to the Markov matrix of the process. In the course of the computation, we will also need the R matrix of the general ASEP with finite q, writing (with $p = 1$)

$$R^{(q)}(x) = \begin{pmatrix} 1 & 0 & 0 & 0 \\ 0 & \frac{(x-1)q}{qx-1} & \frac{(q-1)x}{qx-1} & 0 \\ 0 & \frac{q-1}{qx-1} & \frac{x-1}{qx-1} & 0 \\ 0 & 0 & 0 & 1 \end{pmatrix} \tag{2.113}$$

The R-matrix has a nice pictorial representation that can be used to represent the calculations in a more intuitive way, see figure 2.2. The R-matrix encodes the integrability of the process in the bulk. We also need operators accounting for the behaviour of the model at the boundaries of the chain.

Matrices K, $\overline{K}$ and the reflection equation

We define the boundary matrices, also know as reflection operators, K for the left boundary and $\overline{K}$ for the right:

$$K(x) = \begin{pmatrix} \frac{x(x+a)}{ax+1} & 0 \\ \frac{1-x^2}{ax+1} & 1 \end{pmatrix} \qquad \overline{K}(x) = \begin{pmatrix} 1 & \frac{x^2-1}{x(x+b)} \\ 0 & \frac{bx+1}{x(x+b)} \end{pmatrix} . \tag{2.114}$$

where the boundary transition rates are parametrized as

$$a = \frac{1}{\alpha} - 1 \qquad b = \frac{1}{\beta} - 1 \tag{2.115}$$

These matrices act on a single state space $\mathbb{C}^2$. As for the R-matrix, when considering the state space of the whole chain (along with the auxiliary space), the sites on which they act non-trivially will be

denoted by an index. Considering a generic tensor product of two sites $\mathbb{C}^2 \otimes \mathbb{C}^2$, the matrix K for the left boundary satisfies the reflection equation

$$R_{12}\left(\frac{x_1}{x_2}\right) K_1(x_1) R_{21}(x_1x_2) K_2(x_2) = K_2(x_2) R_{12}(x_1x_2) K_1(x_1) R_{21}\left(\frac{x_1}{x_2}\right) . \tag{2.116}$$

Regarding the right boundary matrix $\overline{K}$, a similar relation, the *inverse* reflection equation, holds for the general ASEP case but not in the totally asymmetric limit:

$$R_{12}\left(\frac{x_2}{x_1}\right)^{-1} \overline{K}_1(x_1) R_{21}(x_1x_2)^{-1} \overline{K}_2(x_2) = \overline{K}_2(x_2) R_{12}(x_1x_2)^{-1} \overline{K}_1(x_1) R_{21}\left(\frac{x_2}{x_1}\right)^{-1} \tag{2.117}$$

with

$$\overline{K}^{(q)}(x) = \begin{pmatrix} \frac{x(p-q-\beta+x(\beta-\delta)+\delta)}{\beta x^2+(p-q-\beta+\delta)x-\delta} & \frac{(x^2-1)\beta}{\beta x^2+(p-q-\beta+\delta)x-\delta} \\ \frac{(x^2-1)\delta}{\beta x^2+(p-q-\beta+\delta)x-\delta} & \frac{\beta-\delta+x(p-q-\beta+\delta)}{\beta x^2+(p-q-\beta+\delta)x-\delta} \end{pmatrix} . \tag{2.118}$$

The computation will thus be made with this matrix $\overline{K}$ and the limit $\delta, q \to 0$ will be taken at the end, as we need the inverse reflection equation in the course of the construction. The reflection equations generalizes the Yang-Baxter equation for an open system, and are needed to ensure the integrability of the system at the boundaries. The boundary matrices satisfy additional properties:

- unitarity : $K(x)K(1/x) = \overline{K}(x)\overline{K}(1/x) = \mathrm{Id}$
- regularity (for the general ASEP $\overline{K}$): $K(1) = \overline{K}(1) = \mathrm{Id}$
- recovering of the boundary jump operators : $-\frac{1}{2}K'(1) = B_1$ and $\frac{1}{2}\overline{K}'(1) = B_L$.

Here also, the boundary operators K and $\overline{K}$ are related to the physical Markov jump operators at the boundaries of the chain. From the right boundary matrix $\overline{K}$, one also defines the matrix $\tilde{K}$ as

$$\tilde{K}_1(x) = \mathrm{Tr}_0\left[\overline{K}_0(-x)\left(R_{01}^{\mathrm{T}_1}(2x)^{-1}\right)^{\mathrm{T}_1} P_{01}\right] \tag{2.119}$$

$$= \frac{1}{bx+1}\begin{pmatrix} 1 & 1 \\ 0 & bx \end{pmatrix} . \tag{2.120}$$

The matrix $\tilde{K}$ satisfies the *dual* reflection equation

$$\tilde{K}_2(x)\left(R_{21}^{\mathrm{T}_1}(x_1x_2)^{-1}\right)^{\mathrm{T}_1} \tilde{K}_1(x_1) R_{21}\left(\frac{x_2}{x_1}\right) = R_{12}\left(\frac{x_2}{x_1}\right) \tilde{K}_1(z_1)\left(R_{12}^{\mathrm{T}_2}(x_1x_2)^{-1}\right)^{\mathrm{T}_2} \tilde{K}_2(x_2) \tag{2.121}$$

where $\square^{\mathrm{T}_1}$ and $\square^{\mathrm{T}_2}$ denote the partial transposition on spaces 1 and 2. We now dispose of the local operators needed to construct the monodromy and transfer matrices of the TASEP. These operators admit a diagrammatic representation that eases computations. A local operator acting on one or two sites is represented by a set of respectively two or four leged vertices, the form of the legs indicating the state of the considered site.

Mondromy and transfer matrices

The monodromy matrix is defined as

$$T_0(x) = R_{0L}(\frac{x}{z_L})...R_{01}(\frac{x}{z_1})K_0(x)R_{10}(z_1x)...R_{L0}(z_Lx) \tag{2.122}$$

where index 0 indicates action on the auxiliary space. The parameters $(z_1, ..., z_L)$ are called *inhomogeneities*. They are needed to derive the eigenstates of the Markov matrix, which are recovered when taking the limit $(z_1, ..., z_L) = (1, ..., 1)$. In general, we will not write explicitly the dependency of our

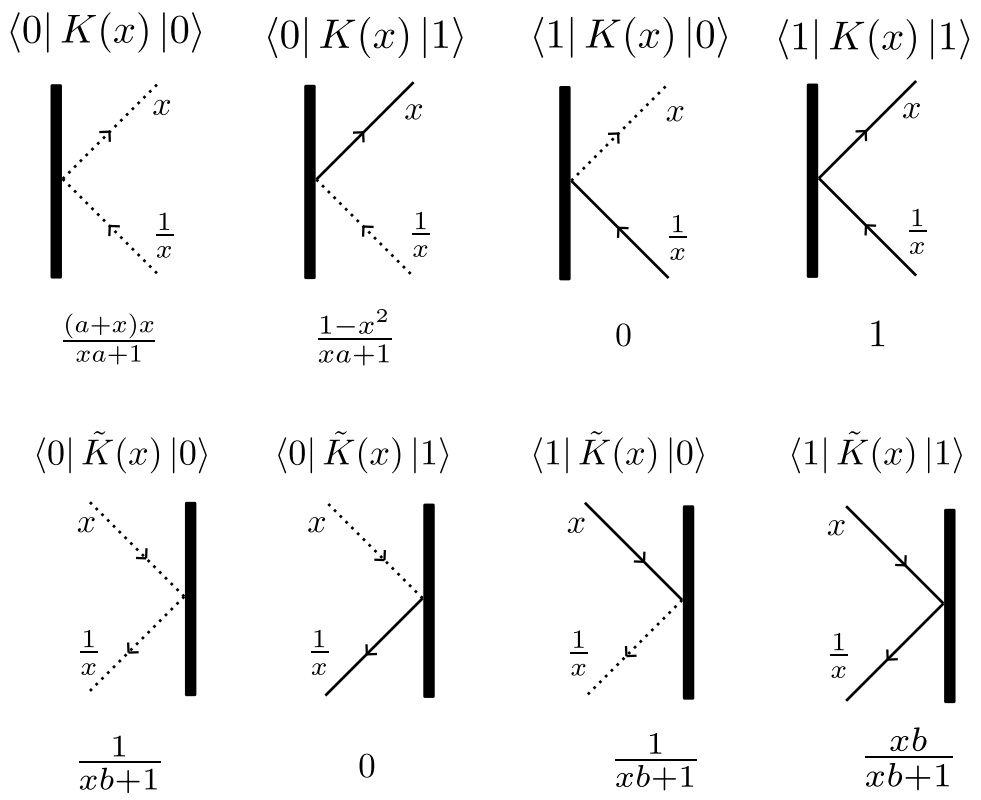

Figure 2.3: Diagrammatic representation of the boundary operators K and $\tilde{K}$.

expression on the inhomogeneity parameters (assuming that they are pairwise distinct), except when needed in the computations. From the monodromy matrix, one also defines the transfer matrix

$$t(x) = \mathrm{Tr}_0 \left[\tilde{K}(x) T(x) \right] \ . \tag{2.123}$$

where the partial trace is taken on the auxiliary space. The main property of the transfer matrix is the commutation relation

$$[t(x), t(y)] = 0 \qquad \forall x, y \in \mathbb{C} \ . \tag{2.124}$$

The proof of this commutation relation [92] is a direct consequence of the reflection equations and of the cyclic property of the trace. Denoting by the index a and b two different copies of the auxiliary space, let us prove (2.124):

$$\begin{aligned}
t(x)t(y) &= \mathrm{Tr}_a \left[\tilde{K}_a(x) T_a(x) \right] \mathrm{Tr}_b \left[\tilde{K}_b(y) T_b(y) \right] && (2.125)\\
&= \mathrm{Tr}_a \left[\tilde{K}_a(x)^{\mathrm{T}_a} T_a(x)^{\mathrm{T}_a} \right] \mathrm{Tr}_b \left[\tilde{K}_b(y) T_b(y) \right] && (2.126)\\
&= \mathrm{Tr}_{a,b} \left[\tilde{K}_a(x)^{\mathrm{T}_a} \tilde{K}_b(y) T_a(x)^{\mathrm{T}_a} T_b(x) \right] && (2.127)\\
&= \mathrm{Tr}_{a,b} \left[\tilde{K}_a(x)^{\mathrm{T}_a} \tilde{K}_b(y) \left(R_{b,a}(xy)^{\mathrm{T}_a} \right)^{-1} \left(R_{b,a}(xy)^{\mathrm{T}_a} \right) T_a(x)^{\mathrm{T}_a} T_b(x) \right] && (2.128)\\
&= \mathrm{Tr}_{a,b} \left[\left(\tilde{K}_b(y) \left(\left(R_{b,a}(xy)^{\mathrm{T}_a} \right)^{-1} \right)^{\mathrm{T}_a} \tilde{K}_a(x) \right)^{\mathrm{T}_a} \left(T_a(x) R_{b,a}(xy) T_b(y) \right)^{\mathrm{T}_a} \right] && (2.129)\\
&= \mathrm{Tr}_{a,b} \left[\left(\tilde{K}_b(y) \left(\left(R_{b,a}(xy)^{\mathrm{T}_a} \right)^{-1} \right)^{\mathrm{T}_a} \tilde{K}_a(x) R_{ba}\left(\frac{y}{x}\right) \right) \left(R_{ab}\left(\frac{x}{y}\right) T_a(x) R_{b,a}(xy) T_b(y) \right) \right] && (2.130)
\end{aligned}$$

where we have used the fact that operators acting on different spaces commute, and inserted the unitarity relation of the R-matrix in the last equality. Besides, one shows by applying several times

(2.116) that the monodromy matrix also satisfies the reflection equation

$$R_{ab}\left(\frac{x}{y}\right) T_a(x) R_{ba}(xy) T_b(y) = T_b(y) R_{ab}(xy) T_a(x) R_{ba}\left(\frac{x}{y}\right) . \tag{2.131}$$

By applying (2.121) and (2.131) to equality (2.130), we can exchange the position of matrices $T_a(x)$ with $T_b(y)$ and $\tilde{K}_a(x)$ with $\tilde{K}_b(y)$. Applying the equalities (2.125)-(2.130) in reverse order, we finally obtain $t(x)t(y) = t(y)t(x)$.

Besides commutation relation (2.124), the Markov matrix is also recovered as the derivative of the transfer matrix:

$$-\frac{1}{2}t'(1) = M(\mu) . \tag{2.132}$$

This is proved by using the regularity property of reflection and R-matrices and the identities connecting them to local update operators:

$$\begin{aligned} t'(1) &= \mathrm{Tr}_0\left[\tilde{K}_0'(1) P_{0L}...P_{01}\ K_0(1)\ P_{10}...P_{L0}\right] && (2.133)\\ &\quad + \sum_{k=1}^{L-1}\left(\mathrm{Tr}_0\left[\mathrm{Id}...P_{0(k+1)}R_{0k}'(1)...\mathrm{Id}...\right] + \mathrm{Tr}_0\left[\mathrm{Id}...\mathrm{Id}...P_{(k+1)0}R_{k0}'(1)...\right]\right)\\ &\quad + \mathrm{Tr}_0\left[\mathrm{Id}\ R_{0L}'(1)...\right] + \mathrm{Tr}_0\left[...R_{L0}'(1)\right] + \mathrm{Tr}_0\left[\tilde{K}_0(1)...K_0'(1)...\right]\\ &= \mathrm{Tr}_0\left[\tilde{K}_0(1)\right] P_{01}K_1'(1) + 2\sum_{k=1}^{L-1}\left(\mathrm{Tr}_0\left[\tilde{K}_0(1)\right] P_{k,k+1}R_{k,k+1}(1)\right) && (2.134)\\ &\quad - \frac{\mathrm{d}}{\mathrm{d}x}\mathrm{Tr}_0\left[\tilde{K}_0\left(\frac{1}{z}\right) R_{0L}\left(\frac{1}{z^2}\right) P_{0L}\right]\Big|_{x=1}\\ &= K_1(1) + 2\sum_{k=1}^{L-1} P_{k,k+1}R_{k,k+1}'(1) - \overline{K}_L'(1) && (2.135)\\ -\frac{1}{2}t'(1) &= B_1 + \sum_{k=1}^{L-1} m_{k,k+1} + B_L = M(\mu) . && (2.136) \end{aligned}$$

Deriving equation (2.124) with respect to one variable, we see that the Markov matrix commutes with the transfer matrix for any value of the spectral parameter, so that they are diagonalizable in the same basis of eigenvectors. We will see that the Bethe ansatz offers a systematic way of constructing the eigenstates of the transfer Matrix. Moreover, defining the operators

$$Q_k = \frac{\mathrm{d}^k}{\mathrm{d}x^k}\log t(x)\Big|_{x=1} , \tag{2.137}$$

commutation relation (2.124) implies that the operators Q_k commute with $M(\mu)$ and commute with each other so that their eigenvalues are independent conserved charges of the system. Thus we dispose of a large family of conserved quantities in analogy with the Liouville integrability of classical Hamiltonian systems. We are now left with diagonalizing the transfer matrix.

2.3.3 Modified Bethe ansatz for the transfer matrix of open TASEP

Recalling the definition of the monodromy matrix, we can write it as a Kronecker product over the auxiliary site 0 with block entries A,B,C and D:

$$T_0(x) = \begin{pmatrix} A(x) & B(x) \\ C(x) & D(x) \end{pmatrix} . \tag{2.138}$$

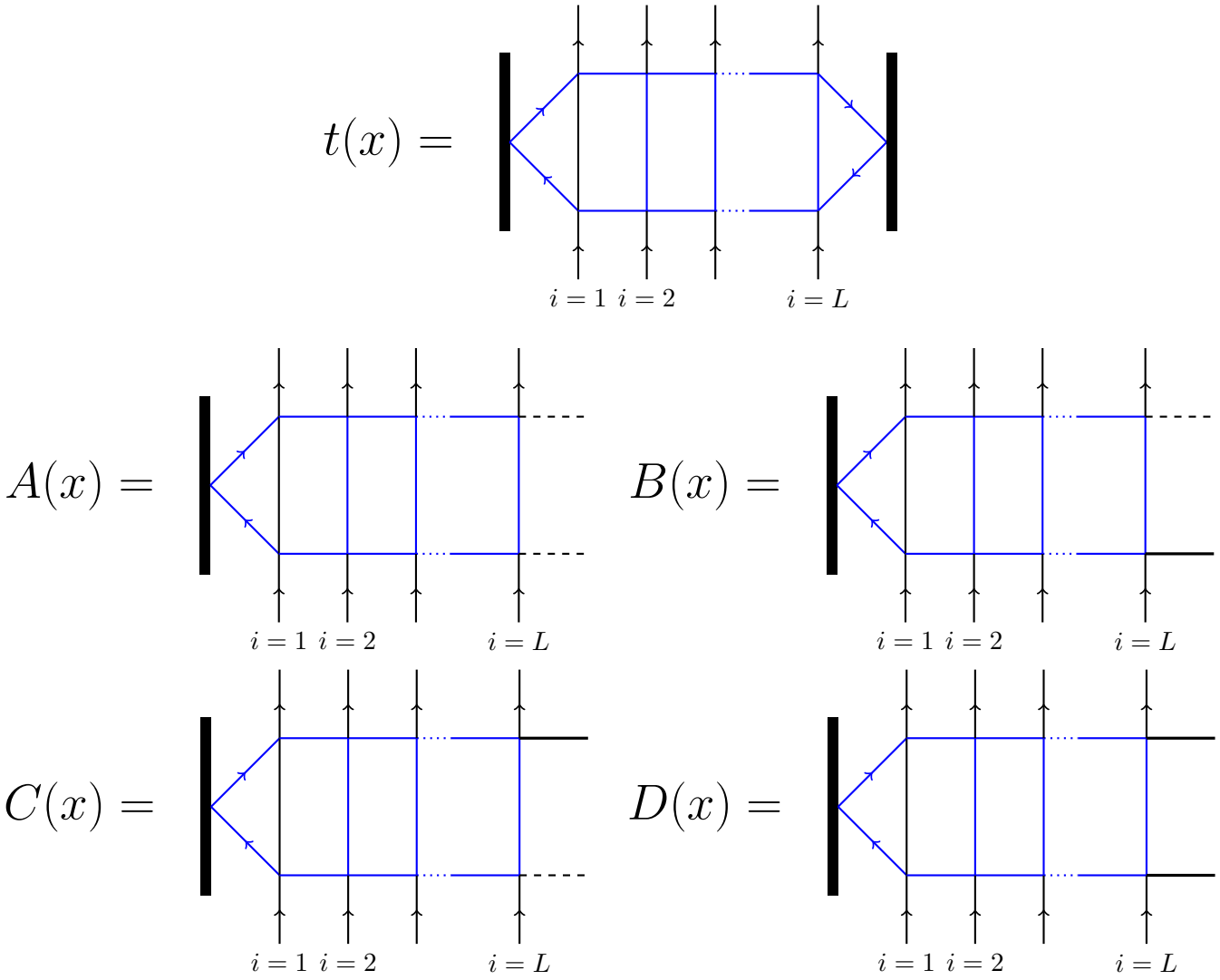

Figure 2.4: Diagrammatic representation of the transfer matrix and block operators of the monodromy matrix. Summation is implied over the possible states of blue edges. The exterior edges are the input and output states of the sites of the chain on which these operators act. Each diagram represents an element of the operators acting on the tensor product $\mathbb{C}^{\otimes L}$, whose value is the product of the values of the elementary vertices

As we mentioned earlier, the monodromy matrix satisfies the reflection equation (2.131), from which one can deduce the following relations between the block operators:

$$[C(x), C(y)] = 0 \tag{2.139}$$

$$D(x)C(y) = \frac{x(xy-1)}{y-x}C(y)D(x) - \frac{y(xy-1)}{y-x}C(y)D(x) - C(y)A(x)\ . \tag{2.140}$$

In the usual formalism of the algebraic Bethe ansatz for periodic systems, operators B and C are naturally interpreted as respectively creation and annihilation operators of one particle excitations and eigenstates are then built by applying repeatedly $B(x)$ on some vacuum state. Here however this approach cannot be used straightforwardly as the open TASEP lacks a proper vacuum state, because the number of particle is not conserved by the evolution.

The modified algebraic Bethe ansatz for the open ASEP as developed in [26] consists in looking for the eigenvectors of $t(x)$ under the form

$$|\Psi(u_1, ..., u_L)\rangle = C(u_1)C(u_2)...C(u_L)\,|\Omega\rangle \tag{2.141}$$

where the pseudo-vacuum state $|\Omega\rangle$ is the state corresponding to the full occupation of the system with probability 1:

$$|\Omega\rangle = |1\rangle_1 \otimes |1\rangle_2 \otimes\ ...\ \otimes |1\rangle_L\ . \tag{2.142}$$

The parameters $(u_1, ..., u_L)$ are the Bethe roots of the algebraic Bethe ansatz, and satisfy a set of polynomial equations that we will derive. As in the case of the periodic ASEP, several sets of solution correspond to different eigenstates of the transfer matrix (or equivalently of the Markov matrix), and the corresponding eigenvalue is expressed as a rational function of the u_j. The transfer matrix writes

$$t(x) = \mathrm{Tr}_0\left[\tilde{K}_0(x)T_0(x)\right] = \frac{1}{bx+1}(A(x) + bxD(x) + C(x))\ . \tag{2.143}$$

We will first compute the action of $t(x)$ by determining the action operators A, B, C and D on $|\Psi\rangle$ with generic values of $(u_1, ..., u_j)$, and then find conditions on them to ensure that $|\Psi\rangle$ is indeed an eigenvector of $t(u_0)$ for a given value of the spectral parameter u_0, which will take the form of the Bethe equations.

Action of operators A, C and D on vector $|\Psi\rangle$

Starting with $A(x)$, there is no convenient relation similar to (2.139) and (2.140) allowing to permute $A(x)$ and $C(x)$ up to additional terms in the totally asymmetric limit. However, there is one for $q \neq 0$. Using now the general ASEP R-matrix

$$R^{(q)}(x) = \begin{pmatrix} 1 & 0 & 0 & 0 \\ 0 & \frac{(x-1)q}{qx-1} & \frac{(q-1)x}{qx-1} & 0 \\ 0 & \frac{q-1}{qx-1} & \frac{x-1}{qx-1} & 0 \\ 0 & 0 & 0 & 1 \end{pmatrix} \tag{2.144}$$

we denote by $T_0^{(q)}(x)$ the monodromy matrix defined using $R^{(q)}(x)$ in place of the totally asymmetric $R(x)$, and $A^{(q)}(x)$, $B^{(q)}(x)$, $C^{(q)}(x)$ the corresponding block operators. From the reflection equation (2.131) which is still satisfied by $T_0^{(q)}(x)$, one deduces the following relation

$$\overline{A}^{(q)}(x)C^{(q)}(x) = \frac{(q^2xy-1)(qx-y)}{q(x-y)(qxy-1)}C^{(q)}(y)\overline{A}^{(q)}(x) - \frac{(q-1)(q^2xy-1)x}{q(x-y)(qx^2-1)}C^{(q)}\overline{A}^{(q)}(y) \tag{2.145}$$

$$+ \frac{xy(q-1)(y^2-1)(q^2x^2-1)}{(qxy-1)(qx^2-1)(qy^2-1)}C^{(q)}(x)D^{(q)}(y) \tag{2.146}$$

with

$$\overline{A}^{(q)} = A^{(q)}(x) + \frac{(1-q)x^2}{qx^2-1} D(x) \ . \tag{2.147}$$

Relation (2.146) is indeed singular when $q \to 0$. Similarly, the generalization of identity (2.140) for $q \neq 0$ writes

$$\begin{aligned} D^{(q)}(x)C^{(q)}(y) = &\frac{(x-qy)(xy-1)}{(qxy-1)(x-y)} C^{(q)}(y)D^{(q)}(x) + \frac{(q-1)(y^2-1)y}{(x-y)(qy^2-1)} C^{(q)}(x)D^{(q)}(y) \\ &+ \frac{q-1}{qxy-1} C^{(q)}(x)A^{(q)}(y) \end{aligned} \tag{2.148}$$

which has (2.140) as limit when $q \to 0$. Let us now compute the action of these operators on $|\Omega\rangle$. It is convenient to use the diagrammatic representation of the operators, see figure 2.4. One easily checks that the only non zero diagram contributing to the action of $D(x)$ on $|\Omega\rangle$ is such that

$D(x)\,|\Omega\rangle =$ 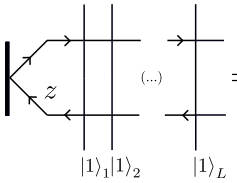

$= |\Omega\rangle$

Similarly, the action of the operator $A^{(q)}$ can be computed by suming all contributing diagrams, as

$A^{(q)}\,|\Omega\rangle =$ 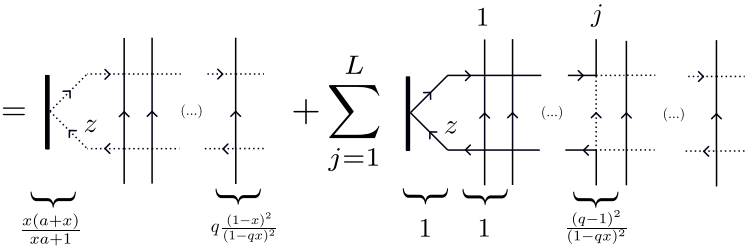

Finally one gets

$$D(x)\,|\Omega\rangle = |\Omega\rangle \tag{2.149}$$

$$\overline{A}^{(q)}\,|\Omega\rangle = q^L \frac{x(x^2-1)(qx+a)}{(xa+1)(qx^2-1)} \left(\frac{(1-x)^2}{(1-qx)^2}\right)^L |\Omega\rangle \ . \tag{2.150}$$

As a side note, using the same diagrammatic reasoning, one easily checks that operator $B(x)$ is in fact 0, so that

$$B(x)\,|\Omega\rangle = 0 \ . \tag{2.151}$$

Knowing the action of $A(x)$ and $D(x)$ on $|\Omega\rangle$ and the relations (2.140) and (2.146), one gets in the limit $q \to 0$:

$$A(u_0)\,|\Psi(u_1,...u_L)\rangle = \sum_{p=0}^{L} \frac{u_0 u_p (u_p^2-1)}{u_p u_0 - 1} \prod_{\substack{k=0 \\ k\neq p}}^{L} \left(\frac{u_p(u_p u_k - 1)}{u_k - u_p} C(u_k)\right) |\Omega\rangle \tag{2.152}$$

$$- \sum_{p=0}^{L} \frac{a u_p (u_p^2-1)}{a u_p + 1} (u_p - 1)^{2L} \prod_{\substack{k=0 \\ k\neq p}}^{L} \frac{u_k}{u_k - u_p} C(u_k)\,|\Omega\rangle \tag{2.153}$$

$$D(u_0)\,|\Psi(u_1,...,u_L)\rangle = \sum_{p=0}^{L} \frac{u_p^2-1}{u_p u_0 - 1} \prod_{\substack{k=0 \\ k\neq p}}^{L} \frac{u_p(u_p u_k - 1)}{u_k - u_p} C(u_k)\,|\Omega\rangle \ . \tag{2.154}$$

The computation of the action of $C(x)$ on $|\psi(u_1,...,u_L)\rangle$ is more involved as many diagrams contribute to the action on $|\Omega\rangle$. In particular, $|\Omega\rangle$ is not an eigenstate of $C(x)$. In order to compute $C(u_0)\,|\Psi(u_1,...,u_L)\rangle$, let us first define the vector

$$\mathcal{V}(x) = \mathrm{e}^{\mu}\frac{1-x^2}{x(ax+1)}\prod_{j=1}^{L}(x-z_j)\left(x-\frac{1}{z_j}\right)\prod_{l=0}^{L}\left(\frac{u_l}{u_l-x}C(u_l)\right)C(x)^{-1}\,|\Omega\rangle\ . \tag{2.155}$$

The inhomogeneity parameters $(z_1,...,z_L)$ are assumed here to be all distinct. Computing the residues of $\mathcal{V}(x)$, we will use the fact the sum of all residues of a rational function is zero to obtain the expression of $C(u_0)\,|\Psi(u_1,...,u_L)\rangle$. We first need to introduce a similarity transformation, or *factorizing twist* of the operator $C(x)$, depending on the inhomogeneities [7]. With

$$F_{j,j+1...L} = 1-\hat{n}_j+\hat{n}_j R_{jL}(z_j/z_L)\ ...\ R_{jj+1}(z_j/z_{j+1}) \qquad \text{with} \qquad \hat{n}=\begin{pmatrix}0&0\\0&1\end{pmatrix} \tag{2.156}$$

one defines the operator

$$F_{12...L} = F_{L-1,L}F_{L-2,L-1L}\ ...\ F_{1,23...L} \tag{2.157}$$

acting on $(\mathbb{C}^2)^{\otimes L}$, and the transformed $C(x)$ operator

$$C^{\mathrm{F}}(x) = F_{12...L}C(x)F_{12...L}^{-1}\ . \tag{2.158}$$

One can show from the results of [60], which originally introduced this change of basis, that $C^{\mathrm{F}}(x)$ and $C^{\mathrm{F}}(x)^{-1}$ have the following explicit coordinate expression

$$\begin{aligned} C^{\mathrm{F}}(x) =& \frac{1-x^2}{ax+1}\left[\sum_{i=1}^{L}x(z_i+a)\sigma_i^+\prod_{\substack{j=1\\j\neq i}}^{L}\left((1-z_ix)\hat{n}_j+\frac{x-z_j}{z_i-z_j}(1-\hat{n}_j)\right)\right. \\ &\left.+\,\mathrm{e}^{\mu}\prod_{j=1}^{L}\left((1-z_jx)\hat{n}_j+\frac{x-z_j}{z_j}(1-\hat{n}_j)\right)\right] \end{aligned} \tag{2.159}$$

$$\begin{aligned} C^{\mathrm{F}}(x)^{-1}\,|\Omega\rangle =& \frac{(ax+1)\mathrm{e}^{-\mu}}{(1-x^2)\prod_{j=1}^{L}(x-z_j)(x-1/z_j)} \\ &\times\sum_{\{n_i\}\in\{0,1\}^L}\left(\prod_{j=1}^{L}\left[(n_i-1)\mathrm{e}^{-\mu}(a+z_i)x+n_i\frac{(z_i-x)}{z_i}\right]\right)\bigotimes_{i=1}^{L}e_{n_i}\ . \end{aligned} \tag{2.160}$$

One checks besides that $F_{12...L}\,|\Omega\rangle = |\Omega\rangle$. Replacing $C(x)$ by $C^{\mathrm{F}}(x)$ in expression (2.155), one finds

$$F_{1...L}\mathcal{V}(x) = \mathrm{e}^{\mu}\frac{1-x^2}{x(ax+1)}\prod_{j=1}^{L}(x-z_j)\left(x-\frac{1}{z_j}\right)\prod_{l=0}^{L}\left(\frac{u_l}{u_l-x}C^{\mathrm{F}}(u_l)\right)C^{\mathrm{F}}(x)^{-1}\,|\Omega\rangle\ . \tag{2.161}$$

As we can see from (2.159) and (2.160), the only poles of $F_{1...L}\mathcal{V}(x)$ – or equivalently of $\mathcal{V}(x)$ – are $x=0$ and $(u_0,...,u_L)$, while $1,-1,-1/a,z_j,1/z_j$ are non-essential singularities and there is no pole at infinity.

The residues of $F_{1...L}\mathcal{V}(x)$ thus write

$$\mathrm{Res}_{x=0}\ \mathcal{V}(x) = \mathrm{e}^{\mu}\prod_{l=0}^{L}C(u_l)C(0)^{-1}\,|\Omega\rangle \tag{2.162}$$

$$\mathrm{Res}_{x=u_p}\ \mathcal{V}(x) = -\mathrm{e}^{\mu}\frac{1-u_p^2}{au_p+1}\prod_{j=1}^{L}\left[(u_p-z_j)\left(u_p-\frac{1}{z_j}\right)\right]\prod_{\substack{k=0\\k\neq p}}\left(\frac{u_k}{u_k-u_p}C(u_k)\right)|\Omega\rangle\ . \tag{2.163}$$

[7] It is necessary to have distinct inhomogeneity parameters in order for the matrix $F_{1...L}$ to be invertible

Finally, using the fact that $\mathcal{V}(x)$ vanishes at infinity, one gets

$$\lim_{R\to\infty}\frac{1}{2\mathrm{i}\pi}\int_{|z|=R}\mathcal{V}(r)\mathrm{d}z=\sum_{x=0,u_1,\dots,u_p}\mathrm{Res}_x\mathcal{V}(x)=0\ . \tag{2.164}$$

Then, using the fact that

$$F_{12\dots L}^{-1}C^F(0)\left|\Omega\right\rangle=C(0)^{-1}\left|\Omega\right\rangle=\mathrm{e}^{-\mu}\left|\Omega\right\rangle\ , \tag{2.165}$$

one deduces, taking all inhomogeneities to 1,

$$C(u_0)\left|\Psi(u_1,...,u_L)\right\rangle=\mathrm{e}^{\mu}\sum_{p=0}^{L}\frac{1-u_p^2}{au_p+1}(u_p-1)^{2L}\prod_{\substack{k=0\\k\neq p}}^{L}\left(\frac{u_k}{u_k-u_p}C(u_k)\right)\left|\Omega\right\rangle\ . \tag{2.166}$$

Now that the action of all non-zero block entries of $T_0(x)$ on the putative eigenvector $\left|\Psi(u_1,...,u_L)\right\rangle$ are known, we can compute the action $t(x)\left|\Psi\right\rangle$ of the transfer matrix and derive the Bethe equations.

Action of the transfer matrix on $\left|\Psi\right\rangle$ and Bethe equations

Using (2.143), the action of the transfer matrix on $\left|\Psi\right\rangle$ writes

$$t(u_0)\left|\Psi(u_1,..,u_L)\right\rangle=\frac{1}{bu_0+1}(A(u_0)+bu_0D(u_0)+C(u_0))\left|\Psi(u_1,...,u_L)\right\rangle \tag{2.167}$$

$$=\Lambda(u_0)\left|\Psi\right\rangle+\sum_{p=1}^{L}\frac{u_0(u_p^2-1)}{(u_0-u_p)(bu_0+1)}U_p\prod_{\substack{k=0\\k\neq p}}^{L}C(u_k)\left|\Omega\right\rangle \tag{2.168}$$

where

$$\Lambda(u_0)=u_0^{L+1}\frac{b+u_0}{bu_0+1}\prod_{k=1}^{L}\frac{u_0u_k-1}{u_k-u_0}-\frac{(au_0+\mathrm{e}^{\mu})(u_0^2-1)}{(au_0+1)(bu_0+1)}(u_0-1)^{2L}\prod_{k=1}^{L}\frac{u_k}{u_k-u_0}\ , \tag{2.169}$$

$$U_p=(b+u_p)u_p^L\prod_{\substack{k=1\\k\neq p}}^{L}\frac{u_pu_k-1}{u_k-u_p}-\frac{au_p+\mathrm{e}^{\mu}}{au_p+1}(u_p-1)^{2L}\prod_{\substack{k=0\\k\neq p}}^{L}\frac{u_k}{u_k-u_p}\ . \tag{2.170}$$

Thus, a necessary condition for $\left|\Psi(u_1,...,u_L)\right\rangle$ to be indeed an eigenvector of $t(u_0)$ is the vanishing of all U_p, that is

$$(au_j+\mathrm{e}^{\mu})(u_j-1)^{2L}=u_j^L(u_j+b)(au_j+1)\prod_{\substack{k=1\\k\neq j}}^{L}\left(u_j-\frac{1}{u_k}\right)\qquad\forall\ 1\leq j\leq L \tag{2.171}$$

which are the Bethe ansatz equations for the open TASEP. In particular, deriving the polynomial Λ, the expression of the eigenvalue of the deformed Markov matrix $M(\mu)$ corresponding to a given solution of the Bethe equations $(u_1,...,u_L)$ writes

$$E(\mu)=-\beta-\sum_{p=1}^{L}\frac{u_p}{u_p-1}\ . \tag{2.172}$$

The main difference between these equation and those of the periodic case (2.86) is the absence of the separability property, which makes their resolution much harder. It is however possible to derive a more convenient set of Bethe equation to work with, by means of the so-called *TQ-relation* formalism.

2.3.4 Polynomial TQ-relation for the open TASEP

The TQ-relation is a way of formulating the Bethe ansatz which allows to compute the eigenvalues of an integrable operator, without however providing a systematic construction of the eigenvectors. The TQ-relation method was originally introduced by Baxter to compute the partition function of the 8-vertex model [76]. We saw that the integrability of the process is essentially expressed by the commutation property of the transfer matrix $[t(x), t(y)] = 0$. Let us suppose that there exists another operator $q(z)$ depending on another spectral parameter such that

$$[t(x), q(z)] = [q(x), q(z)] = 0 \qquad \forall x, z \in \mathbb{C} \tag{2.173}$$

Let us suppose moreover that the eigenvalues of $q(z)$ and $t(z)$ are polynomial in z – or equivalently that the entries of $q(z)$ and $t(z)$ are rational functions of z – and that the following algebraic TQ-relation, written here in its most general form, holds

$$t(z)q(z) = q(z)t(z) = F(z, q(z), q(z^{-1})) \tag{2.174}$$

where F is an operator-valued functional of z and q which has entries meromorphic in z. If we denote by $T(z)$ and $Q(z)$ the eigenvalues of $t(z)$ and $q(z)$ respectively, which are polynomial functions of z, the fact that $q(z)$ and $t(z)$ are commuting operators and thus can be diagonalized in a common basis implies, with relation (2.174), that

$$T(z)Q(z) = F(z, Q(z), Q(z^{-1})) \tag{2.175}$$

which is the polynomial TQ-relation. In particular, denoting by $\{z_1, ..., z_M\}$ the roots of $Q(z)$, the residues of $T(z)$ at the z_i are zero by analyticity, so that one gets

$$f(z_i, Q(z_i), Q(z_i^{-1})) = 0 \qquad \forall\ 1 \leq i \leq M\ , \tag{2.176}$$

which are precisely the Bethe equations in this formalism. The explicit construction of an operator Q satisfying these properties is possible for some integrable models, most notably for the eight-vertex model to which it was first applied. As we will see in next section, it is possible to construct a Q-operator for the open TASEP, however one can immediately cast the expression of the eigenvalue Λ (2.169) and the Bethe equations (2.171) into the form of the polynomial TQ-relation

$$\Lambda(x)Q(x) = x^{2L+1}\frac{b+x}{bx+1}Q(1/x) - \frac{(x-1)^{2L}(ax+\mathrm{e}^{\mu})(x^2-1)}{(ax+1)(bx+1)} \tag{2.177}$$

with

$$Q(x) = \prod_{k=1}^{L}\left(1 - \frac{x}{u_k}\right) \tag{2.178}$$

where the $\{u_j\}_{1\leq j\leq L}$ are the Bethe roots derived by algebraic Bethe ansatz. The right hand side of this relation is indeed the zero term in the Bethe equations (2.171). As Crampé and Nepomechie pointed out in [25], there exists another TQ-relation satisfied by the polynomial Λ and a second polynomial $\overline{Q}$ defined by

$$\overline{Q}(x) = \prod_{k=1}^{L+2}(x - \overline{u}_k) \tag{2.179}$$

writing

$$\Lambda(x)\overline{Q}(x) = x^L(x+b)(x+a)\mathrm{e}^{-\mu} + \overline{Q}(0)\frac{(1-x)^{2L+2}(x+1)^2}{(ax+1)(bx+1)}\mathrm{e}^{\mu} \tag{2.180}$$

	$\Lambda^{(1)}$	$\Lambda^{(2)}$	$\Lambda^{(3)}$	$\Lambda^{(4)}$
$L=1$	$\frac{x^3}{2}-x^2-\frac{x}{2}+1$	$\frac{3x^3}{8}-\frac{x^2}{2}-\frac{3x}{8}+\frac{1}{2}$	$\frac{7x^3}{48}-\frac{x^2}{6}-\frac{7x}{48}+\frac{1}{6}$	$\frac{5x^3}{128}-\frac{x^2}{24}-\frac{5x}{128}+\frac{1}{24}$
$L=2$	$\frac{4x^3}{5}-\frac{4x^2}{5}-\frac{4x}{5}+1$	$\frac{78x^3}{125}-\frac{38x^2}{125}-\frac{78x}{125}+\frac{1}{2}$	$\frac{2366x^3}{9375}-\frac{686x^2}{9375}-\frac{2366x}{9375}+\frac{1}{6}$	$\frac{2189x^3}{31250}-\frac{1187x^2}{93750}-\frac{2189x}{31250}+\frac{1}{24}$
$L=3$	$\frac{13x^3}{14}-\frac{4x^2}{7}-x+1$	$\frac{1965x^3}{2744}-\frac{85x^2}{1372}-\frac{157x}{196}+\frac{1}{2}$	$\frac{229399x^3}{806736}+\frac{20609x^2}{403368}-\frac{4789x}{14406}+\frac{1}{6}$	$\frac{8131699x^3}{105413504}+\frac{4521569x^2}{158120256}-\frac{2132863x}{22588608}+\frac{1}{24}$

Table 2.1: First coefficients of the expansion of polynomial $\Lambda(x)$ in powers of μ for different system sizes, obtained by solving TQ relation (2.177) or (2.180) for $a=b=0$.

and corresponding to the Bethe roots $\{\overline{u}_j\}_{1\leq j\leq L+2}$ and the $L+2$ Bethe equations

$$\overline{u}_j^L(\overline{u}_j+b)(\overline{u}_j+a)(a\overline{u}_j+1)(b\overline{u}_j+1)=(-1)^{L+1}\mathrm{e}^{2\mu}(1-\overline{u}_j)^{2L+2}(\overline{u}_j+1)^2\prod_{k=1}^{L+2}\overline{u}_k\ . \tag{2.181}$$

We see that that these Bethe equation can be written in separated form

$$f(\overline{u}_j)=(-1)^{L+1}\mathrm{e}^{2\mu}\prod_{k=1}^{L+2}\overline{u}_k\ , \tag{2.182}$$

$$f(x)=\frac{x^L(x+a)(x+b)(ax+1)(bx+1)}{(1-x)^{2L+2}(x+1)^2}\ . \tag{2.183}$$

The equivalence between these two relations has not been rigorously proven, but it can be verified by looking at the first orders of the expansion of both relations in powers of μ. We look for the polynomial $\Lambda(x)$ under the form

$$\Lambda(x)=1+\sum_{k=1}^{\infty}\mu^k\Lambda^{(k)}(x) \tag{2.184}$$

$$\Lambda^{(j)}(x)=\frac{1}{(ax+1)(bx+1)}\sum_{k=0}^{L+2}\ell_k^{(j)}x^k \tag{2.185}$$

By taking the limit $x\to 0$ in the first TQ relation (2.177), one checks that $\Lambda(0)=\mathrm{e}^{\mu}$ so that $\ell_0^{(j)}=\frac{1}{j!}$. We also write the series expansion of Q and $\overline{Q}$ as follow

$$Q(x)=\sum_{k=0}^{\infty}\mu^kQ^{(k)}(x) \qquad \overline{Q}(x)=\sum_{k=0}^{\infty}\mu^kQ^{(k)}(x)\ , \tag{2.186}$$

$$Q^{(0)}(x)=\sum_{k=0}^{L}q_k^{(0)}x^k \qquad \overline{Q}^{(0)}(x)=\sum_{k=0}^{L+2}\overline{q}_k^{(0)}x^k\ , \tag{2.187}$$

$$Q^{(j)}(x)=\sum_{k=1}^{L}q_k^{(0)}x^k \qquad \overline{Q}^{(j)}(x)=\sum_{k=0}^{L+2}\overline{q}_k^{(j)}x^k\ . \tag{2.188}$$

This choice of expansion is not the only one possible, yet in the case $\mu=0$, one gets $\Lambda(x)=1$ and the corresponding eigenvalue of the Markov matrix is $E=0$, so that this choice corresponds to the ground state solution of the Bethe equations. Injecting these expression in TQ relations (2.177) and (2.180), one can determine coefficients $\ell_k^{(j)}$, $q_k^{(j)}$ and $\overline{q}_k^{(j)}$ respectively by solving linear equations. The solution of both TQ relations for the coefficients $\ell_k^{(j)}$ of the polynomial $\Lambda(x)$ are indeed the same for the first orders j in μ and small system size (see table 2.1). We thus dispose of a second set of Bethe equations (2.181) which we can exploit to write down an explicit expression of the ground state eigenvalue of $M(\mu)$.

2.3.5 Ground state eigenvalue $E(\mu)$ from Bethe equations

In what follows, we will only use the second set of Bethe equations (2.181) so that the Bethe roots $\overline{u_j}$ will be written u_j for $1\leq j\leq L+2$ in the rest of this work unless stated otherwise. Let us first

compute the explicit expression of $E(\mu)$ as a function of the Bethe roots. From the second TQ-relation (2.180) one gets

$$E(\mu) = \frac{x^L(x+a)(x+b)}{\mathrm{e}^{\mu}\overline{Q}(x)} + \mathrm{e}^{\mu}\frac{\overline{Q}(0)}{\overline{Q}(x)}\frac{(1-x)^{2L+2}(x+1)^2}{(ax+1)(bx+1)} \ . \tag{2.189}$$

Besides, one obtains $\Lambda(1) = 1$ from the first TQ-relation (2.177), which implies

$$Q(1) = \frac{\mathrm{e}^{-\mu}}{\alpha\beta} \tag{2.190}$$

so that the ground state eigenvalue writes

$$E(\mu) = 1 - \frac{\alpha+\beta}{2} + \frac{1}{2}\sum_{j=1}^{L+2}\frac{u_1}{1-u_j} \ . \tag{2.191}$$

From here, we can compute $E(\mu)$ under a more explicit form, following the same procedure as in 2.2.1. We define the following functions and parameters

$$h(z) = \frac{(1-z)^{2L+2}(z+1)^2}{z^L(az+1)(bz+1)(z+a)(z+b)} \tag{2.192}$$

$$B = (-1)^{L+1}\mathrm{e}^{2\mu}\prod_{k=1}^{L+2}u_j \tag{2.193}$$

so that the Bethe roots $\{u_j\}_{j\leq L+2}$ and the definition of parameter B give the following equations

$$1 - Bh(u_j) = 0 \quad 1 \leq j \leq L+2 \ , \tag{2.194}$$

$$\mu = \frac{1}{2}\sum_{i=1}^{L+2}\log\left(-\frac{B^{1/(L+2)}}{y_i}\right) \ . \tag{2.195}$$

Note that the function h defined above is actually equal to $h(z) = -F(-z)$ where F is the function (2.57) that was obtained by matrix ansatz. We see that both $E(\mu)$ and μ are expressed as a sum over the set of Bethe roots. A careful study of the Bethe ansatz equations (that will be done in chapter 3) shows that for μ small enough, the roots of $1 - Bh(z)$ which are indeed the Bethe roots for the ground state are the $L+2$ roots located within the unit disk. For now, we will admit this fact to compute $E(\mu)$, so that these sum may be rewritten as contour integrals on the unit circle:

$$\mu = \frac{1}{2}\sum_{i=1}^{L+2}f(u_i) = -\frac{1}{2}\int_{|z|=1}\frac{\mathrm{d}z}{2\mathrm{i}\pi}f(z)\frac{-Bh'(z)}{1-Bh(z)} \quad \text{with} \quad f(z) = \log\left(-\frac{B^{1/(L+2)}}{z}\right) \ , \tag{2.196}$$

$$E(\mu) = \frac{1}{2}\sum_{i=1}^{L+2}g(u_i) = -\frac{1}{2}\int_{|z|=1}\frac{\mathrm{d}z}{2\mathrm{i}\pi}g(z)\frac{-Bh'(z)}{1-Bh(z)} \quad \text{with} \quad g(z) = \frac{z}{1-z} + \frac{2-\alpha-\beta}{L+2} \ . \tag{2.197}$$

Integrating by part, we get

$$\mu = \frac{1}{2}\int_{|z|=1}\frac{\mathrm{d}z}{2\mathrm{i}\pi z}\log(1-Bh(z)) \ , \tag{2.198}$$

$$E(\mu) = \frac{1}{2}\int_{|z|=1}\frac{\mathrm{d}z}{2\mathrm{i}\pi(1+z)^2}\log(1-Bh(z)) \ . \tag{2.199}$$

Expanding these expression in series of B we obtain the following parametric expressions

$$\mu = -\sum_{k=1}^{\infty}C_k\frac{B^k}{2k} \qquad \text{with} \quad C_k = \int_{|z|=1}\frac{\mathrm{d}z}{2\mathrm{i}\pi z}h(z)^k \tag{2.200}$$

$$E(\mu) = -\sum_{k=1}^{\infty}D_k\frac{B^k}{2k} \qquad \text{with} \quad D_k = \int_{|z|=1}\frac{\mathrm{d}z}{2\mathrm{i}\pi(1+z)^2}h(z)^k \tag{2.201}$$

In the case $\alpha = \beta = 1$, the coefficients C_k and D_k can be computed exactly for finite values of L. The integrand in the expression of coefficient C_k has a single pole of order $k(L+2)+1$ at $z = 0$ and can be computed easily with residues theorem

$$C_k = \int_{|z|=1} \frac{\mathrm{d}z}{2\mathrm{i}\pi z} h(z)^k \tag{2.202}$$

$$= \mathrm{Res}_{z=0}\left(h(z)^k\right) \tag{2.203}$$

$$= \frac{1}{[k(L+2)]!}\frac{\mathrm{d}^{k(L+2)}}{\mathrm{d}z^{k(L+2)}}\left[(1-z)^{k(2L+2)}(z+1)^{2k}\right]\Big|_{x=0} \tag{2.204}$$

$$= (-1)^{k(L+1)}\frac{(2k)!}{k!}\frac{[2k(L+1)]!}{[k(L+1)]![k(L+2)]!}\,. \tag{2.205}$$

Similarly, the integrand of coefficient D_k has a pole of order $k(L+2)$ at $z = 0$ and the computation of D_k gives

$$D_k = \mathrm{Res}_{z=0}\left(\frac{(1-z)^{k(2L+2)}(z+1)^{2(k-1)}}{z^{k(L+2)}}\right) \tag{2.206}$$

$$= \frac{1}{[k(L+2)-1]!}\frac{\mathrm{d}^{k(L+2)-1}}{\mathrm{d}z^{k(L+2)-1}}\left[(1-z)^{k(2L+2)}(z+1)^{2(k-1)}\right]\Big|_{x=0} \tag{2.207}$$

$$= (-1)^{k(L+1)}\frac{(2k)!}{k!}\frac{[2k(L+1)-2]!}{[k(L+1)-1]![k(L+2)-1]!}\,. \tag{2.208}$$

Since B in expressions (2.200)-(2.201) is a dummy parameter that has to be eliminated between the two equations to get E as a function of μ, the factor $(-1)^{k(L+1)}$ can be incorporated in B^k, so that the parametric expression of $E(\mu)$ writes

$$\mu = -\sum_{k=1}^{\infty}\frac{(2k)!}{k!}\frac{[2k(L+1)]!}{[k(L+1)]![k(L+2)]!}\frac{B^k}{2k} \tag{2.209}$$

$$E(\mu) = -\sum_{k=1}^{\infty}\frac{(2k)!}{k!}\frac{[2k(L+1)-2]!}{[k(L+1)-1]![k(L+2)-1]!}\frac{B^k}{2k} \tag{2.210}$$

From these expressions, the exact values of the first cumulant of the current can be obtained, see chapter 4. Let finally us make a remark that relates the open TASEP to the periodic one. Making the change of variables $y_j = 1 - \mathrm{e}^{-\mu} z_j$ in the Bethe equations (2.86) of the periodic case and the corresponding expression of $E(\mu)$, setting the number of particle to $N = L+2$ and the size of the periodic system to $L' = 2L+2$, it is straightforward to check that for $\alpha = 1$ and $\beta = 1/2$, the expression of the eigenvalue and the Bethe roots (*i.e.* the second set of equations (2.181) obtained by the TQ-relation in the open case) are identical for the open TASEP of size L with fugacity $\mu/(L+1)$ [8] and for the periodic TASEP of size $2L+2$ with $L+2$ particles. Thus, the spectrum of the open TASEP on the boundary between the maximal current and the low density phase is a subset of that of the periodic TASEP with appropriate size and number of particles.

2.4 Q operator method for the ground state of the TASEP

In this section we outline the so-called Q-operator construction used by Lazarescu and Pasquier in [57] to compute the exact expression of the ground state eigenvalue of the deformed Markov matrix $M(\mu)$ in an alternate way. This construction is essentially a generalization of the matrix product ansatz to the deformed Markov matrix. Instead of giving an expression for the stationary distribution however,

[8] We recall that the Bethe equation were obtained with a current counting deformation on all bonds for the periodic ASEP and on a single bond for the open case, so that this rescaling of the fugacity by the system size is expected from the similarity relation between both deformations, see equation (1.74)

it will yield an new TQ relation for the ground state eigenvalue of $M(\mu)$. Generalizing operators e and d defined by (2.1) from the matrix product ansatz for the non-deformed Markov matrix, we introduce the following algebra

$$de - qed = (1-q)(1-x^2A^2) \tag{2.211}$$
$$dA - qAd = 0 \tag{2.212}$$
$$Ae - qeA = 0 \tag{2.213}$$

where A is an additional operator and x is a free parameter. One also introduce the current counting deformation of operator A defined by the relations

$$dA_\mu - \mathrm{e}^{-\mu} A_\mu d = 0 \ , \tag{2.214}$$
$$eA_\mu - \mathrm{e}^{\mu} A_\mu e = 0 \ . \tag{2.215}$$

These operators have the following infinite dimensional representation

$$d = \sum_{n=1}^{\infty} (1-q^n) \|n-1\rangle\!\rangle \langle\!\langle n\| \ , \tag{2.216}$$
$$e = \sum_{n=0}^{\infty} (1-x^2 q^n) \|n+1\rangle\!\rangle \langle\!\langle n\| \ , \tag{2.217}$$
$$A = \sum_{n=0}^{\infty} q^n \|n\rangle\!\rangle \langle\!\langle n\| \ , \tag{2.218}$$
$$A_\mu = \sum_{n=0}^{\infty} \mathrm{e}^{-n\mu} \|n\rangle\!\rangle \langle\!\langle n\| \ . \tag{2.219}$$

Let us define the matrix

$$X(x) = \begin{pmatrix} 1+xA & e \\ d & 1+xA \end{pmatrix} \tag{2.220}$$

which can be thought of as acting on the tensor product $\mathbb{C}^2 \otimes \mathcal{A}$ of a single local space of the chain and the infinite representation space $\mathcal{A}$ of the algebra satisfied by d,e,A and A_μ. Generalizing the boundary vectors of the matrix ansatz we introduce two pairs of vectors $\|V\rangle\!\rangle$, $\langle\!\langle W\|$ and $\|\tilde{V}\rangle\!\rangle$, $\langle\!\langle \tilde{W}\|$ such that the following relations hold

$$\langle\!\langle W\| \left[\alpha(e+1+xA) - \gamma(d+1+xA) - (1-q)\mathrm{Id}\right] = 0 \ , \tag{2.221}$$
$$\left[\beta(d+1+xA) - \delta(e+1+xA) - (1-q)\mathrm{Id}\right] \|V\rangle\!\rangle = 0 \ , \tag{2.222}$$
$$\langle\!\langle \tilde{W}\| \left[\alpha(e-1-xA) - \gamma(d-1-xA) + (1-q)xA\right] = 0 \ , \tag{2.223}$$
$$\left[\beta(d-1-xA) - \delta(e-1-xA) + (1-q)xA\right] \|\tilde{V}\rangle\!\rangle = 0 \ , \tag{2.224}$$

which generalize (2.1)-(2.3) for $x \neq 0$. For each of the two aforementioned pairs of boundary vectors we now introduce so-called transfer matrices $U_\mu(x)$ and $T_\mu(x)$ defined as

$$U_\mu(x) = \langle\!\langle W\| A_\mu \prod_{i=1}^{L} X^{(i)}(x) \|V\rangle\!\rangle \ , \tag{2.225}$$
$$T_\mu(x) = \langle\!\langle \tilde{W}\| A_\mu \prod_{i=1}^{L} X^{(i)}(x) \|\tilde{V}\rangle\!\rangle \ , \tag{2.226}$$

with $X^{(i)} = \mathrm{Id} \otimes ... \otimes \underset{i}{X}(x) \otimes ... \otimes \mathrm{Id}$ acting on the tensor product $\left(\mathbb{C}^2\right)^{\otimes L} \otimes \mathcal{A}$. The matrices $U_\mu(x)$ and $T_\mu(x)$ act on the configuration space of the chain. If $\mathcal{C} = \{n_1, ..., n_L\}$ and $\mathcal{C}' = \{n'_1, ..., n'_L\}$ are

two configurations the chain with different sets of occupation numbers, the entries of $U_\mu(x)$ and $T_\mu(x)$ as product of matrix ansatz operators are

$$\left\langle \mathcal{C}' \right| U_\mu(x) \left| \mathcal{C} \right\rangle = \langle\!\langle W \| A_\mu \prod_{i=1}^{L} X_{n'_i,n_i}(x) \| V \rangle\!\rangle \,, \tag{2.227}$$

$$\left\langle \mathcal{C}' \right| T_\mu(x) \left| \mathcal{C} \right\rangle = \langle\!\langle \tilde{W} \| A_\mu \prod_{i=1}^{L} X_{n'_i,n_i}(x) \| \tilde{V} \rangle\!\rangle \,. \tag{2.228}$$

The transfer matrices U_μ and T_μ satisfy the following commutation relations

$$[U_\mu(x)T_\mu(y), U_\mu(x')T_\mu(y')] = 0 \qquad \forall\, x, y \in \mathbb{C} \tag{2.229}$$

$$[U_\mu(x)T_\mu(y), M(\mu)] = 0 \tag{2.230}$$

which are analogous to the commutation relations satisfied by the transfer matrix of the algebraic Bethe ansatz. The proof of these relations is rather lengthy and can be found in [57]. From $T_\mu(x)$ and $U_\mu(x)$ one defines two matrices $P(x)$ and $Q(x)$ as

$$P(x) = U_\mu(x)U_\mu(0)^{-1} \tag{2.231}$$

$$Q(x) = (1 - \mathrm{e}^{-\mu})^{-1} U_\mu(0) T_\mu(x) \tag{2.232}$$

which are such that

$$[P(x), Q(y)] = 0 \,, \tag{2.233}$$

$$U_\mu(x)T_\mu(x) = (1 - \mathrm{e}^{-\mu}) P(x)Q(x) \,. \tag{2.234}$$

By construction, $P(x)$ and $Q(x)$ also commute with $M(\mu)$. Moreover, it is possible to derive a TQ-relation from these two operators as

$$P(x)Q(1/x) = F(x)\mathrm{Id} + \mathrm{e}^{-2\mu} P(qx)Q(q/x) \tag{2.235}$$

where $F(x)$ is in fact the same function as (2.56). One recovers the deformed Markov matrix from operator $Q(x)$ as

$$M(\mu) = \frac{1}{2}(1-q)\frac{\mathrm{d}}{\mathrm{d}x} \log\left(\frac{Q(q/x)}{Q(1/x}\right)\bigg|_{x=-1} \,. \tag{2.236}$$

The commutation of $P(x)$, $Q(x)$ and $M(\mu)$ allows us to diagonalize them in a common basis. We now restrict the expressions obtained above to the sector of the ground state eigenvalue, denoting by $\mathcal{P}(x)$, $\mathcal{Q}(x)$ and E the eigenvalues of $P(x)$, $Q(x)$ and $M(\mu)$ respectively. We also denote by B the eigenvalue in the ground-state sector of operator $-\mathrm{e}^{-\mu}Q(0)^{-1}$. Parameter B plays a similar role as in the previous section. Defining the function

$$\mathcal{W}(x) = -\frac{1}{2}\log\left(\frac{\mathcal{P}(x)\mathcal{Q}(1/x)}{\mathrm{e}^{-2\mu}\mathcal{P}(qx)\mathcal{Q}(q/x)}\right) \,. \tag{2.237}$$

It can be shown that the function $\mathcal{W}$ can be written as a solution to the functional equation

$$\mathcal{W}(x) = -\frac{1}{2}\log\left(1 - BF(x)\exp\left[\oint_{|y|=1} \frac{\mathrm{d}y}{2\mathrm{i}\pi y}\mathcal{W}(y)K(x,y)\right]\right) \tag{2.238}$$

with the convolution kernel

$$K(x,y) = 2\sum_{k=1}^{\infty} \frac{q^k}{1-q^k}\left(\left(\frac{x}{y}\right)^k + \left(\frac{x}{y}\right)^{-k}\right) \,. \tag{2.239}$$

Relation (2.236) can be rewritten as a contour integral for the ground state eigenvalue as

$$E(\mu) = \frac{1}{2}(1-q)\oint_{|z|=1} \frac{\mathrm{d}z}{2\mathrm{i}\pi(1+z)^2} \log\left(\frac{\mathcal{Q}(q/z)}{\mathcal{Q}(1/z)}\right) \tag{2.240}$$

with $\mu = -\mathcal{W}(0)$ fixed by considering the limit $x \to 0$ in the closed form expression (2.237) of $\mathcal{W}(x)$. Here, $\mathcal{W}$ is an unknown function that has to be determined for each value of μ. Assuming now that $\mathcal{P}(x)$ is holomorphic and has no zero within the unit circle, the term $\log(P(x)/P(qx))$ in (2.237) does not contribute in the last integral so that $E(\mu)$ finally has the parametric expression

$$\mu = -\oint_{|z|=1} \frac{\mathrm{d}z}{2\mathrm{i}\pi z}\mathcal{W}(z)\ , \tag{2.241}$$

$$E(\mu) = -(1-q)\oint_{|z|=1} \frac{\mathrm{d}z}{2\mathrm{i}\pi(1+z)^2}\mathcal{W}(z)\ . \tag{2.242}$$

As in last section, formulas have a much simpler form in the totally asymmetric case. In particular, the convolution kernel $K(x,y)$ is zero when $q=0$ and the function $\mathcal{W}$ can be computed explicitly by developing (2.238) in series of B :

$$\mathcal{W}(x) = \sum_{k=1}^{\infty} \frac{F(x)^k}{2k} B^k\ . \tag{2.243}$$

Casting this expansion of $\mathcal{W}$ in (2.241) and (2.242), one recovers the expressions (2.200) and (2.201) that where obtained by Bethe ansatz.[9]

2.5 Determination of the eigenvectors

Our discussion so far has been essentially focused on the computation of the eigenvalues of matrix $M(\mu)$. Recalling the expression of the scaled cumulant generating function of the current at finite time with initial state $|P_0\rangle$ obtained in section 1.4.1

$$\langle \mathrm{e}^{\mu O_t}\rangle = \sum_{n=0}^{2^L-1} \langle 1|\psi_n(\mu)\rangle\, \langle \psi_n(\mu)|P_0\rangle\, \mathrm{e}^{E_n(\mu)t} \tag{2.244}$$

where the $\{|\psi_n\rangle\}$ are the eigenvectors associated with the eigenvalues $\{E_n\}$, we see that the expression of the coordinates of the eigenvectors are needed to compute the statistics of the current. These expressions were already computed for the periodic case, as expressions (2.62) and (2.84) give the coordinate of the eigenvectors (or wavefunctions) up to a global normalizing factor. In the totally asymmetric case, the coordinates of the right and left eigenvectors of the periodic $M(\mu)$ corresponding to a given set of Bethe roots $\vec{z} = (z_1, ..., z_N)$ also have the following expression [61] in terms of determinants

$$\langle x_1, ..., x_N|\psi_{\vec{z}}(\mu)\rangle = \det\Big[(1-z_j\mathrm{e}^{-\mu})^{-k} z_j^{x_k}\Big]_{j,k\in[\![1,N]\!]} \tag{2.245}$$

$$\langle \psi_{\vec{z}}(\mu)|x_1, ..., x_N\rangle = \det\Big[(1-z_j\mathrm{e}^{-\mu})^{k} z_j^{-x_k}\Big]_{j,k\in[\![1,N]\!]} \tag{2.246}$$

where $|x_1, ..., x_N\rangle$ is the basis vector of the configuration space corresponding to particles in the positions $1 < x_1 < ... < x_N$.

Such expressions are currently missing for the eigenvectors of the open TASEP. Our first attempt at getting an expression for the wavefunctions in the open case was to look at the case $\beta = 1$, $\alpha = 1/2$ where the spectrum of $M(\mu)$ for the open chain is as subset of the one of the periodic chain. It appeared however that the eigenvectors corresponding to common eigenvalues do not coincide for generic values

[9] One should note however that the result obtained in [57] where stated some years before the equivalent TQ relation from [25], and have been rigorously derived in the totally asymmetric case.

of μ. In the large fugacity limit $\mu \to \infty$, numerical computations showed that a partial correspondence exist between some coordinates in the configuration basis of the open and periodic systems eigenvectors, but this correspondence could not be exploited in any meaningful way as the Bethe equations in the limit $\mu \to \infty$ are highly degenerate and do not provide a precise enough insight on the expressions for general μ.

The modified algebraic Bethe ansatz construction used above yields an explicit expression of the eigenvectors under the form[10]

$$|\Psi(u_1,...,u_L)\rangle = C(u_1)C(u_2)...C(u_L)\,|\Omega\rangle \tag{2.247}$$

where the pseudo-vacuum state is taken in fact as the configuration where all sites are occupied, $|\Omega\rangle = |1\rangle_1 \otimes ... \otimes |1\rangle_L$. Note that as a result of the non-conservation of the number of particles, this general form for the eigenvectors differs significantly from the expressions obtained with the standard algebraic Bethe ansatz, where the number of so-called creation operators applied on the pseudo-vacuum is equal to the number of physical particles in the system.

Looking at the diagrammatic representation of operator $C(x)$ in figure 2.4, and using the line conservation property of the bulk vertices (broken by the left boundary vertex corresponding to operator $K(x)$) sketched in figure 2.2, we see the operator $C(x)$ acts on $|\Omega\rangle$ by removing at most one particle on the chain, returning a superposition of configurations with L or $L-1$ particles. Applying recursively L times the operators $C(u_j)$ will thus yield a vector $|\Psi(u_1,...,u_L)\rangle$ with finite coordinates for all configuration for generic values of the u_j. It is in principle possible to obtain these coordinates by carefully enumerating and summing all diagrams contributing to a given coordinate $\langle n_1,...,n_L|\Psi(u_1,...,u_L)\rangle$ in the configuration basis, but the computation still has to be done.

This would provide an expression of the eigenvectors in terms of the Bethe roots $\{u_1,...,u_L\}$ solutions to equations (2.171), however our derivation of the asymptotics of the Bethe ansatz expressions, that will be presented in chapter 4 relies crucially on the mean-field-like character of the equations (2.181), with Bethe roots $\{\overline{u}_1,...\overline{u}_{L+2}\}$. It would thus be necessary to obtain an expression of $|\Psi(u_1,...,u_L)\rangle$ directly in terms of the roots $\overline{u}_j$. In this regard, both sets of Bethe root can be related using the TQ-relations (2.177) and (2.180). The polynomial Λ appearing in both relations is the same, so that one can write a direct relation between polynomials Q and $\overline{Q}$

$$\begin{aligned} &Q(x)\big(x^{L+2}\mathrm{e}^{-\mu} + \overline{Q}(0)(1-x)^{2L+2}(x+1)^2\mathrm{e}^{\mu}\big) \\ &\qquad = \overline{Q}(x)\big(x^{2L+2}Q\left(\frac{1}{x}\right) - (x-1)^{2L}(x^2-1)\mathrm{e}^{\mu}\big) \end{aligned} \tag{2.248}$$

where

$$Q(x) = \prod_{k=1}^{L}\left(1-\frac{x}{u_k}\right)\,, \qquad \overline{Q}(x) = \prod_{k=1}^{L+2}(x-\overline{u}_k)\,. \tag{2.249}$$

Introducing now the elementary symmetric polynomials $\{s_k\}_{1\le k\le n}$ in n variables $(X_1,...,X_n)$ defined by

$$s_k(X_1,...X_n) = \sum_{1\le j_1<j_2<...<j_k\le n} X_{j_1}...X_{j_k} \qquad 1\le k\le n\,, \tag{2.250}$$

any factorized polynomial $P(X) = \prod_{k=1}^{n}(X-r_k)$ can be written in terms of elementary symmetric polynomials of its roots as

$$P(x) = X^n + \sum_{k=1}^{n}(-1)^k s_k(r_1,...,r_n)X^{n-k}\,. \tag{2.251}$$

Equality (2.248) thus provides us with relations between elementary symmetric functions of the roots $\{u_j\}_{1\le j\le L}$ and of the roots $\{\overline{u}_j\}_{1\le j\le L+2}$. Using the notation $s_k = s_k(u_1,...,u_L)$ and $\overline{s}_k = s_k(\overline{u}_1,...,\overline{u}_{L+2})$,

[10] In this paragraph we reintroduce the difference in notation between the roots $\{u_j\}_{1\le j\le L}$ of the modified Bethe ansatz and the roots $\{\overline{u}_j\}_{1\le j\le L+2}$ intervening in the alternate polynomial TQ-relation

computation for small system sizes suggest that functions s_k have the following expression in terms of the $\overline{s}_k$

$$s_k = \begin{cases} \left(\sum_{i=1}^{\lfloor \frac{L+2}{2} \rfloor - \frac{k}{2}} \overline{s}_{k+2i} \right) \Big/ \left(\sum_{j=1}^{\lfloor \frac{L+2}{2} \rfloor} \overline{s}_{2j} \right) & k \quad \text{even} \\ \left(\sum_{i=k+2}^{\lfloor \frac{L+2}{2} \rfloor - \frac{k-1}{2}} \overline{s}_{k+2i} \right) \Big/ \left(\sum_{j=1}^{\lfloor \frac{L+2}{2} \rfloor} \overline{s}_{2j} \right) & k \quad \text{odd} \end{cases} \tag{2.252}$$

Note that although the degree of (2.248) is larger that the number of symmetric functions $\overline{s}_k$, all relation obtained are compatible with each others when the $\{\overline{u}_j\}_{1 \leq j \leq L+2}$ are solutions to the Bethe equations (but not for generic values).

Since the wavefunctions and in fact all physical observable of the system are by construction symmetric functions of the Bethe roots, the knowledge of the symmetric elementary polynomials $\{s_k\}_{1 \leq k \leq L}$ is enough to write the eigenstates $|\psi(u_1, ..., u_L)\rangle$ directly in terms of the roots $\{\overline{u}_j\}_{1 \leq j \leq L+2}$, as any symmetric rational function of several variable is also a rational functions of the elementary symmetric polynomial in these variables.

As a side note, exact expressions have been conjectured for the ground state eigenvector of the transfer matrix of the deformed open TASEP, using an alternate formulation of the modified algebraic Bethe ansatz on a *twice deformed* version of the process [38, 16]. It appears that in the undeformed limit (with respect to the second deformation), the ground state can be expressed in terms of symmetric *Koornwinder polynomials*, although no closed form expression for the coordinate of the eigenvector is provided in [38].

Chapter 3

Analytic continuation and Riemann surfaces

Anticipating the results of next chapter, where the asymptotics of the ground state eigenvalues of the periodic and open TASEP will be derived from the Bethe ansatz expressions, the object of this chapter is to compute the analytic continuation of the scaling functions of these eigenvalues with respect to the system size. More precisely, assuming for now that the ground state eigenvalues of $M(\gamma)$ is given for large L under the general parametric form

$$E(\mu) - f(L)\mu = k_1 L^{-3/2}\chi(v)\ , \tag{3.1}$$

$$\mu = k_2 L^{-1/2}\eta(v)\ . \tag{3.2}$$

We will compute the analytic continuation of χ and η, as higher eigenvalues of $M(\gamma)$ will be obtained in chapter 4 by substituting in equations (3.1)–(3.2) the functions χ and η with other branches of their analytic continuation. We can note that the scaling of the eigenvalue given by (3.1) is indeed in accordance with the KPZ time scale $t \sim L^{3/2}$ over which the spectral gaps that we will compute are relevant. The relevance of this study comes from the fact that the eigenvalues of any parameter dependant operator $M(\mu)$ are expected to be generically related to one another by analytic continuation, as can be seen by considering the characteristic polynomial $\det[M(\mu) - \lambda \mathrm{Id}]$ of such operator which defines, as a two variable complex polynomial, an algebraic curve of which the eigenvalues of $M(\mu)$ are local parametrizations, see paragraph 3.1.4.

After a concise mathematical introduction to analytic functions, analytic continuation and Riemann surfaces, we construct the analytic continuation of the ground-state scaling function of the TASEP deformed Markov matrix in different settings. In section 3.2, we present the common features of the functions studied in this chapter and introduce the formalism used afterward to construct their analytic continuation. In section 3.3, we recall the results obtained by Prolhac in [74] for the scaling function of the gaps of the periodic TASEP in the large system size limit. We next compute in section 3.4 the analytic continuation of a different function χ (in the notation of (3.1) involved in the expression of the gaps of the TASEP in the maximal current phase. We finally generalize this computation to the case of the crossover between the low density and maximal current phases of the open TASEP in 3.5. Note that the expressions of the original functions whose analytic continuations are introduced without physical motivation at this stage, and we will make sense of these in chapter 4. The Riemann surfaces upon which these analytic continuation are properly defined are built systematically for each function.

3.1 Mathematical introduction

3.1.1 Analytic and meromorphic functions

A holomorphic function $f : U \to \mathbb{C}$ on some open set $U \subset \mathbb{C}$ is a function such that its derivative defined as

$$f'(z_0) = \lim_{z \to z_0} \frac{f(z) - f(z_0)}{z - z_0} \tag{3.3}$$

exists for all $z_0 \in U$. Looking at f as mapping $(x, y) \mapsto (u, v)$ from the real plane to itself defined by $f(x + \mathrm{i}y) = u(x, y) + \mathrm{i}v(x, y)$, f is holomorphic if the real functions u and v are differentiable and satisfie the additional Cauchy-Riemann equations

$$\frac{\partial u}{\partial x} = \frac{\partial v}{\partial y} \quad \text{and} \quad \frac{\partial u}{\partial y} = -\frac{\partial v}{\partial x} \tag{3.4}$$

so that the differential of f at any point is the composition of a scaling and a rotation, or equivalently that f is a *conformal* transformation of the plane. Complex differentiable, or holomorphic functions are thus much more constrained in their behaviour than their real counterpart. A fundamental consequence of their definition is the fact that holomorphic functions are *analytic*, that is they coincide with their Taylor series on any disk lying in U. Intuitively, the data of f on any open set contains all the information needed to restitute it on its largest possible domain of definition – a notion that will be made precise in what follows. This *rigidity* property of holomorphic functions is at the heart of the analytic continuation protocol that we will use extensively.

A function is said to be meromorphic if it is holomorphic everywhere on a domain U except on a countable set of separated points $\{z_i\} \subset U$ which are poles of f, that is points where f can be locally factorized as $f(z) = g(z)(z - z_i)^{-k}$ where g is holomorphic at z_i and k is called the order of the pole.

It is often convenient to define meromorphic functions on the *Riemann sphere*, $\widehat{\mathbb{C}} = \mathbb{C} \cup \{\infty\}$ which is the usual complex plane compactified by adding a point at infinity. In particular, a meromorphic function f is said to have a pole at infinity if $f(1/z)$ has a pole at $z = 0$.

3.1.2 Analytic continuation

We will now consider functions which are not meromorphic on $\mathbb{C}$. This is the case if these functions have discontinuities or non-analyticities on lines or curve in the complex plane, which typically happens for multivalued inverse functions of non injective analytic functions. Such lines will be called *branch cuts* and their end points, (which may be the point at infinity) *branch points*. The latters are singularities of the considered function. Given such a function f defined and analytic on an open domain Ω, it is often possible to find a new analytic function f_1 defined on a new domain Ω_1 that intersect Ω, such that the function f_1 coincide with f on $\Omega \cap \Omega_1$. The function f_1 is then said to be the *analytic continuation* of f on Ω_1. One can iterate this procedure by continuing a function along a path on successive domains, however, it does not generally yields a unique value of the function f (see 3.1) at the same point, thus giving rise to several *branches* of f. The function obtained by analytic continuation are said to be multivalued.

Let us first consider the prototypical example of the complex nth root function. A complex number $z = r\mathrm{e}^{\mathrm{i}\theta}$ has n different nth roots, so that one can define n different branches of the nth root function

$$f_k(z) = r^{1/n}\mathrm{e}^{\mathrm{i}\theta/n + 2\mathrm{i}k\pi/n} \qquad 0 \leq k < n$$

analytic on $\mathbb{C} \setminus \mathbb{R}^-$, with the usual determination of the argument $-\pi < \theta \leq \pi$. These branches are not continuous on the negative real half-line $\mathbb{R}^-$, however one has

$$f_k(-r + \mathrm{i}0^+) = \begin{cases} f_{k+1}(-r + \mathrm{i}0^-) & \text{if } k \geq 1 \\ f_0(-r + \mathrm{i}0^-) & \text{if } k = n - 1 \end{cases} \qquad r > 0 \tag{3.5}$$

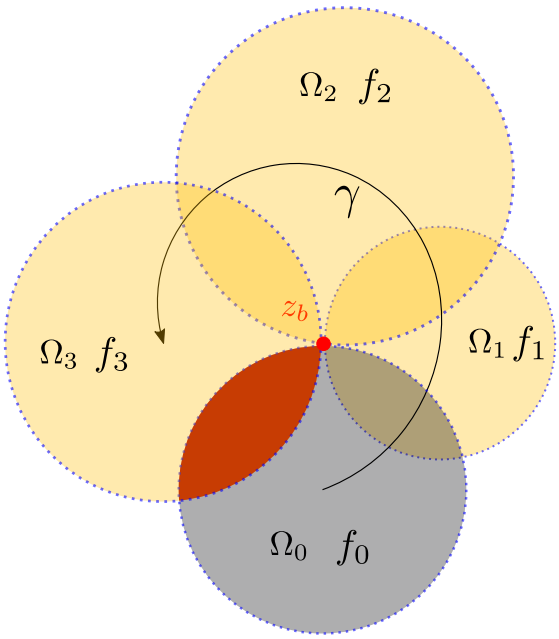

Figure 3.1: A function f defined on a original domain Ω_0 is analytically continued step by step along a path γ into functions f_i defined on domains Ω_i, here open disks centered on points of γ. If γ circles around a branch points z_b of f, then the analytic continuation f_3 on Ω_3 in general does not coincides with f_0 on $\Omega_0 \cap \Omega_3$

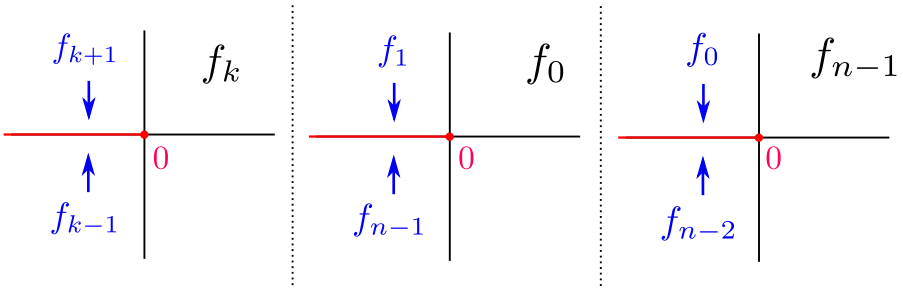

Figure 3.2: Schematic representation of the analytic continuation pattern of the nth root function. The blue labels indicate the analytic continuation of the corresponding branch when crossing the branch cut $\mathbb{R}^-$ in the direction indicated by the arrow.

were the terms $\mathrm{i}0^{\pm}$ denote the limits taken from above or below the branch cut, so that the function defined as

$$f(z) = \begin{cases} f_k(z) & \text{if } \operatorname{Im} z \leq 0 \\ f_{k-1}(z) & \text{if } \operatorname{Im} z > 0 \end{cases} \tag{3.6}$$

is continuous and in fact analytic on the open domain $\operatorname{Re} z < 0$, and f_{k-1} is said to be the analytic continuation of f_k when crossing the cut $\mathbb{R}_-$ from below. Continuing the branch f_k from above the cut yields the branch f_{k+1} (see figure 3.2). Thus it is always possible to find a determination of the nth root function which is locally analytic around any point in $\mathbb{C}^*$, but not globally.

The reader should be aware there is no reason for the branches obtained by analytic continuation to have the same branch points and branch cuts as the original function. This however will be the case in all the examples considered in the present work. One should also note that the position of the branch cut of the f_k on the negative real line comes from the choice of determination of the argument in the interval $[-\pi, \pi]$, which is arbitrary. This is a general fact that branch cuts of a multivalued function are in fact arbitrary an can be moved in the complex plane by changing the definition of the branches (but not the set of values they take altogether at a given point), however their ending branch

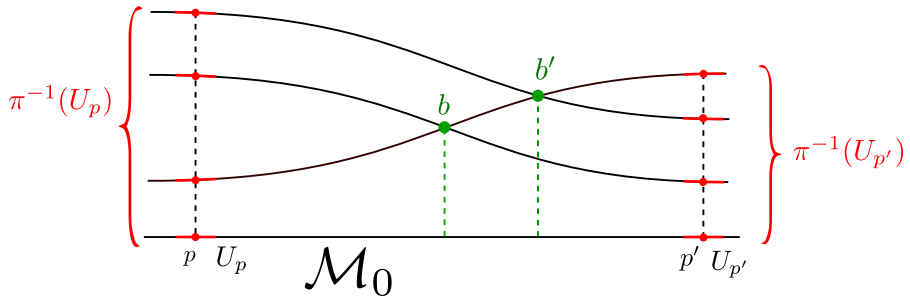

Figure 3.3: Schematic representation of a section of a branched covering. Generically (as shown here for points p and p'), any point $p \in \mathcal{M}_0$ have a discrete set of points as preimage, with distinct open neighborhoods such that the projection π is locally a homeomorphism upon each. In contrast,there is no open neighborhood V_b, $V_{b'}$ of the branch branch points b and b' so that the restrictions of the projection $\pi|_{V_b}$ and $\pi|_{V_{b'}}$ are homeomorphisms onto $\mathcal{M}_0$.

points are fixed.

Another way of dealing with multivalued functions is, instead of considering various branches defined on the complex plane, to define a larger domain of definition upon which the functions is analytic and single-valued, namely, a Riemann surface.

3.1.3 Riemann surfaces

A Riemann surface $\mathcal{M}$ is a complex manifold of complex dimension one, that is a topological space endowed with a collection of open sets U_i such that $\mathcal{M} = \bigcup_i U_i$ and applications $\phi_i : U_i \to \mathbb{C}$ called *charts* which are homeomorphism (continuous and bijective) onto their images. One requires moreover that for any two open sets U_i and U_j of the open cover with non-empty intersection, the *transition map*

$$\phi_i \circ \phi_j^{-1} : \phi_j(U_i \cap U_j) \subset \mathbb{C} \to \phi_i(U_i \cap U_j) \subset \mathbb{C} \tag{3.7}$$

are bijective and holomorphic. Intuitively, $\mathcal{M}$ is a space which locally looks like $\mathbb{C}$ but not globally. In what follows we will be interested in Riemann surfaces which are *branched* (or *ramified*) *coverings* of the complex plane. A Riemann surface $\mathcal{M}$ is a branched covering of a given *base space* $\mathcal{M}_0$ if there is a map $\pi : \mathcal{M} \to \mathcal{M}_0$ such that for any point $p \in \mathcal{M}_0$ except a for a discrete subset of *branch points* in $\mathcal{M}_0$, there is an open neighborhood U_p of p such that $\pi^{-1}(U_p)$ is the union of disjoint open sets of $\mathcal{M}$, so that π is a homeomorphism upon each of them. One can think of a branched covering as a collection of distinct sheets, which are copies of $\mathcal{M}_0$ stacked one upon the other and glued together along common lines, the branch points being the points where several sheets come together (see figure 3.3).

On any open set of $U \subset \mathcal{M}$ away from a branch point, the points of U can be parametrized by a complex coordinate $z = \phi(p)$ by choosing an appropriate chart $\phi : U \to \mathbb{C}$. On a neighborhood of a branch point $U \ni b$, several situations may occur. If the branch point is *algebraic*, then there exist an integer $e_b \in \mathbb{N}^*$ such that points $p \in U$ can be parametrized with a coordinate $y \in \mathbb{C}$ and points $\pi(p) \in \pi(U)$ with a coordinate z, so that $z = y^{e_b}$. If the branch point is *logarithmic*, then on can choose y and z such that $z = \log(y)$.

Branched covering of the complex plane $\mathbb{C}$ are the natural domain of definition of multivalued functions obtained by analytic continuations. The original domain of definition of a function f_0 is identified with a sheet $\mathcal{M}_0$ of a Riemann surface $\mathcal{M}$, biholomorphic to the base space of the covering that defines $\mathcal{M}$ [1]. If the domains of definition of the other branches f_k of the analytic continuation of f_0 are identical to $\mathcal{M}_0$ (that is if the other branches f_k have the same branch cuts and branch points as the original function), the Riemann surface $\mathcal{M}$ is constructed by considering a copy $\mathcal{M}_k$ of $\mathcal{M}_0$ for

[1] By a slight abuse of notation we identify the base space of the covering $\pi : \mathcal{M} \to \mathcal{M}_0$ with a specific sheet of $\mathcal{M}$, in such way that the covering map can be seen as a projection onto the sheet acting base space

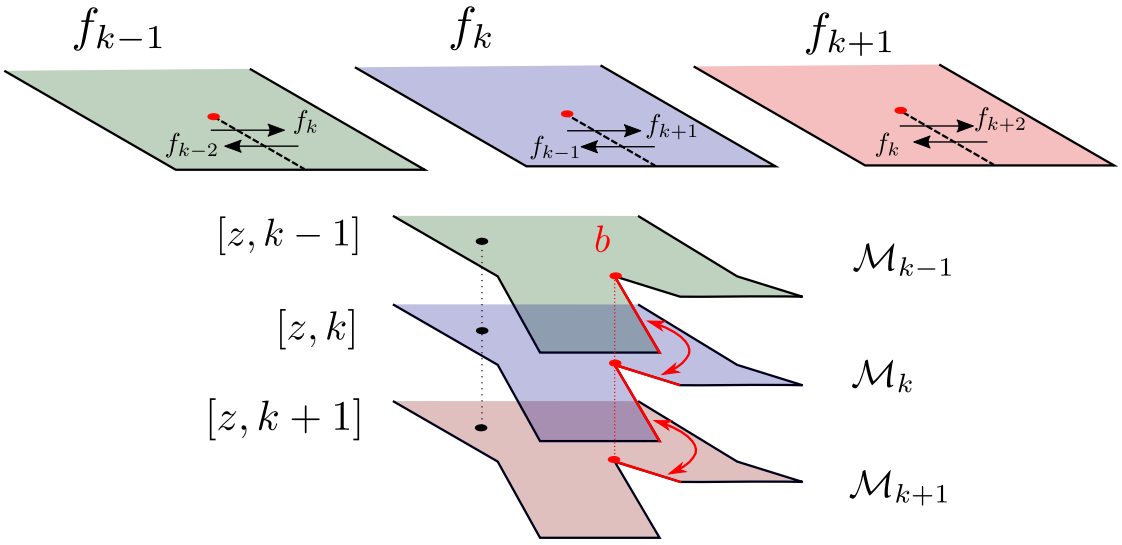

Figure 3.4: Construction of the Riemann surface associated to the analytic continuation of a function f with branches f_k having a branch point b and a single branch cut.

each branch f_k, and gluing them along the branch cuts in such way that two sheets are connected if the corresponding branches are related to one another by analytic continuation across the cut (see figure 3.4). In the process, the branch points lying in several sheets are identified as one point in $\mathcal{M}$.

If the original domain of f is $\mathbb{D}$, we will denote by $[z, k] \in \mathcal{M}$ the unique point belonging to the sheet $\mathbb{D}_k$ labeled by the index k that projects itself onto $\mathbb{D}$ as $\pi([z, k]) = z$. Then, one can define a single valued function of the Riemann surface

$$\begin{aligned} \mathfrak{F} : \ \mathcal{M} &\to \mathbb{C} \\ [z, k] &\mapsto f_k(z) \end{aligned}$$

The function $\mathfrak{F}$ is then the analytic continuation of f on $\mathcal{M}$, which is the largest possible domain of definition of f. Here again, given a Riemann surface $\mathcal{M}$, its partitions into sheets $\mathcal{M}_k$ is somewhat arbitrary, however its topology is of course an intrinsic characteristic. In particular if $\mathcal{M}$ is obtained as the domain of definition of a multivalued function, the sheets are in correspondence with the branches of the function, and different partitions correspond to different choices of branch cut, but the topology of $\mathcal{M}$ is uniquely defined by the function itself.

Before moving forward to the actual computation of the eigenstate scaling functions of the exclusion process, let us mention another general result of importance that justifies our interest in analytic continuations.

3.1.4 Analytic continuations of eigenvalues

Let $P \in \mathbb{C}[X, Y]$ be a two variable complex polynomial, then the *algebraic curve*

$$V(P) = \{(y, z) \in \mathbb{C}^2 \mid P(y, z) = 0\}$$

defines a Riemann surface. More precisely if P is such that there is no singular point (x_0, y_0) such that

$$P(x_0, y_0) = \frac{\partial P}{\partial x}(x_0, y_0) = \frac{\partial P}{\partial y}(x_0, y_0) = 0 \ , \tag{3.8}$$

then $V(P)$ is said to be *smooth*, and is a Riemann surface that can be endowed with various sets of charts, see [17]. If P has singular points, then it is possible to construct a smooth algebraic curve $V'(P)$ – thus a Riemann surface – that maps properly onto $V(P)$ by various methods of *resolutions of singularities* [83, 13]. If the polynomial P can be factorized into a product of non-trivial factors in

$\mathbb{C}[X,Y]$, then in general $V(p)$ will possess several disjoint connected components (in correspondence with irreducible factors in P).

As a consequence, given a parameter dependent matrix $M(u)$ with entries polynomial in u, its characteristic polynomial $\chi(z,u)$ defines a Riemann surface, so that its eigenvalues $E_k(u)$ seen as functions of the parameter u are all related to one another by analytic continuations, provided $\chi(z,u)$ does not have a non-trivial factorization.

Thus, if one disposes of an expression for a single eigenvalue $E_i(u)$ of $M(u)$, it is possible in some cases to obtain the full spectrum of $M(u)$ by computing the analytic continuation of the function $E_i(u)$. To illustrate this, let us consider the simplest example of a 2×2 matrix with parameter dependent complex coefficients

$$M(u) = \begin{pmatrix} a(u) & b(u) \\ c(u) & d(u) \end{pmatrix} . \tag{3.9}$$

Its two eigenvalues write

$$\lambda_\pm(u) = \frac{1}{2}(a(u)+d(u)) \pm \sqrt{\Delta(u)} . \tag{3.10}$$

with $\Delta(u) = (\operatorname{Tr} M(u))^2 - 4\det M(u)$. If the entries of the matrix M are analytic in u, and $\Delta(z)$ has a single zero for $z\in\mathbb{C}$, then both functions λ_+ and λ_- have a single branch cut in the u-plane on the curve $\{u \mid \Delta(u)\in\mathbb{R}_-\}$ due to the square root function. Since the analytic continuation of the square root across its cut is obtained by flipping its sign $\sqrt{z}\to -\sqrt{z}$, we see that λ_+ and λ_- are analytic continuation of each other across their common branch cut. In the case $c(u)=b(u)=0$, the characteristic polynomial of $M(u)$ is factorized as $\chi(u,X) = (X-a(u))(X-d(u))$, with eigenvalues $a(u)=d(u)$ unrelated by analytic continuation.

Considering now the block-diagonal matrix

$$N(u) = \begin{pmatrix} a(u) & b(u) & 0 \\ c(u) & d(u) & 0 \\ 0 & 0 & \mu(u) \end{pmatrix} \tag{3.11}$$

with eigenvalues $\lambda_\pm(u)$ and $\mu(u)$, then $\mu(u)$ is generically not related by analytic continuations to the two other eigenvalues, and the Riemann surface defined by the spectrum of $N(u)$ is disconnected. Thus we expect the various connected components of the Riemann surface associated to an operator to be in correspondence with its physical sectors characterized, for instance, by conserved quantities. The Riemann surface of the eigenstates of the deformed Markov matrix $M(\mu)$ of the periodic TASEP with finite size L (with fixed number of particle) is indeed split [73] into connected components corresponding to states with different values of the total momentum, in the case where the Markov matrix is deformed with respect to all bonds (see 1.4.2) of the chain. In the case where the current counting deformation is added on a single bond, the translation invariance of the system is broken and eigenstates of $M(\mu)$ are no longer momentum eigenstates, so that all eigenvalues do belong to a connected Riemann surface.

One should note that although the argument we outlined above is valid only for operators acting on finite dimensional spaces, this underlying analytic structure of eigenvalues may also exist for infinite dimensional operators. The idea that the analytic continuation of some eigenstate of an operator – typically the ground state of a Hamiltonian or stochastic generator – can be used to compute its spectrum has seen several applications in Physics. A first historical example is the partial computation by Bender and Wu in [6, 7] of the excited energies of the quantum quartic oscillator, with Hamiltonian

$$H(\lambda) = \frac{p^2}{2m} + \frac{1}{2}kx^2 + \frac{1}{4}\lambda x^4 \tag{3.12}$$

by analytic continuation of the perturbative expansion of the ground-state with respect to the coefficient λ of the quartic term.

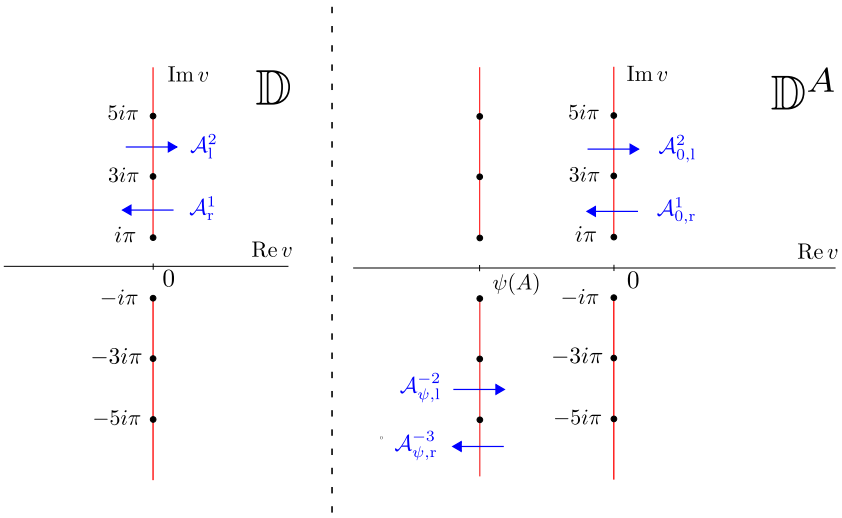

Figure 3.5: Sketch of the domains $\mathbb{D}$ and $\mathbb{D}^A$

3.2 Continuable functions with singularities on the imaginary line

In this work, we will consider special classes of functions analytic on the domains

$$\mathbb{D} = \mathbb{C} \setminus (\mathrm{i}(-\infty, -\pi] \cup \mathrm{i}[\pi, \infty)) \tag{3.13}$$

$$\mathbb{D}^A = \mathbb{C} \setminus (\mathrm{i}(-\infty, -\pi] \cup \mathrm{i}[\pi, \infty) \cup (\psi(A) + \mathrm{i}(-\infty, -\pi])) \cup (\psi(A) + \mathrm{i}[\pi, \infty)) \tag{3.14}$$

where $A \in \mathbb{R}$ and $\psi(A)$ is a negative decreasing function of A. These functions moreover have their singularities in the respective sets

$$\mathcal{S} = 2\mathrm{i}\pi \left(\frac{1}{2} + \mathbb{Z}\right) \tag{3.15}$$

$$\mathcal{S}^A = 2\mathrm{i}\pi \left(\frac{1}{2} + \mathbb{Z}\right) \cup \left(\psi(A) + 2\mathrm{i}\pi \left(\frac{1}{2} + \mathbb{Z}\right)\right) \tag{3.16}$$

some of these singularities being branch points, although not all in general. The branch cuts of these functions are in general the intervals between two consecutive branch points

$$2\mathrm{i}\pi \left[n - \frac{1}{2}, n + \frac{1}{2}\right] \qquad \text{for} \qquad n \in [\![-\infty, -1]\!] \cup [\![1, \infty]\!] \tag{3.17}$$

$$\psi(A) + 2\mathrm{i}\pi \left[n - \frac{1}{2}, n + \frac{1}{2}\right] \qquad \text{for} \qquad n \in [\![-\infty, -1]\!] \cup [\![1, \infty]\!] \tag{3.18}$$

We will denote by $\mathcal{F}$ (respectively $\mathcal{F}^A$) the set of functions defined on the domain $\mathbb{D}$ (respectively $\mathbb{D}^A$) such that each of their branches obtained by analytic continuation have the same branch points and branch cuts, *i.e.* are also defined on $\mathbb{D}$ or $\mathbb{D}^A$.

Given a function $f \in \mathcal{F}$, we will denote by $\mathcal{A}_{\mathrm{l}}^n f$ (respectively $\mathcal{A}_{\mathrm{r}}^n f$) the function obtained by analytic continuation from the left (respectively from the right) through the cut $2\mathrm{i}\pi \left[n - \frac{1}{2}, n + \frac{1}{2}\right]$.

Similarly, given a function $f \in \mathcal{F}^A$, we will denote by $\mathcal{A}_{0,\mathrm{l}f}^n$ (respectively $\mathcal{A}_{0,\mathrm{r}}^n f$) the function obtained by analytic continuation from the left (respectively from the right) through the cut $2\mathrm{i}\pi \left[n - \frac{1}{2}, n + \frac{1}{2}\right]$ and by $\mathcal{A}_{\psi,\mathrm{l}f}^n$ (respectively $\mathcal{A}_{\psi,\mathrm{r}}^n f$) the function obtained by analytic continuation from the left (respectively from the right) through the cut $\psi(A) + 2\mathrm{i}\pi \left[n - \frac{1}{2}, n + \frac{1}{2}\right]$, see figure 3.5. It will be useful in what follows to consider translations of their domain parallel to the imaginary axis. For $f \in \mathcal{F}$, we define the translation operators acting on f as

$$\mathcal{T}_{\mathrm{r}}^n f(v) = f(v + 2\mathrm{i}\pi n) \quad \text{if} \quad \mathrm{Re}\, v > 0\,, \tag{3.19}$$

$$\mathcal{T}_{\mathrm{l}}^n f(v) = f(v + 2\mathrm{i}\pi n) \quad \text{if} \quad \mathrm{Re}\, v < 0\,. \tag{3.20}$$

where the action of these operators outside the domains specified by expressions (3.19) and (3.20) follows by analytic continuation as $\mathcal{T}_{\mathrm{r}}^n f$ and $\mathcal{T}_{\mathrm{l}}^n f$ are required to be in $\mathcal{F}$ also, which uniquely determines $\mathcal{T}_{\mathrm{l}}^n f$ for $\mathrm{Re}\, v > 0$ and $\mathcal{T}_{\mathrm{r}}^n f$ for $\mathrm{Re}\, v < 0$. Similarly for a function $f \in \mathcal{F}^A$, we define the translation operators

$$\mathcal{T}_{\mathrm{r}}^n f(v) = f(v + 2\mathrm{i}\pi n) \quad \text{if} \quad \mathrm{Re}\, v > 0 \tag{3.21}$$
$$\mathcal{T}_{\mathrm{m}}^n f(v) = f(v + 2\mathrm{i}\pi n) \quad \text{if} \quad \psi(A) < \mathrm{Re}\, v < 0 \tag{3.22}$$
$$\mathcal{T}_{\mathrm{l}}^n f(v) = f(v + 2\mathrm{i}\pi n) \quad \text{if} \quad \mathrm{Re}\, v < \psi(A)\ . \tag{3.23}$$

We will see that the branches of multivalued functions in $\mathcal{F}$ and $\mathcal{F}^A$ – or equivalently the sheets of the Riemann surfaces upon which they are defined – are conveniently indexed by sets of integers $P \subset \mathbb{Z}$ or half integers $P \subset \mathbb{Z} + 1/2$, so that the analytic continuation and translation operators defined above amount to set theoretical operations on the indexing sets. The operations on indexing sets corresponding to the function operators $\mathcal{A}$ and $\mathcal{T}$ will be denoted in Latin font A and T such that for a given branch $f_P \in \mathcal{F}$ of a multivalued function f with branch indexing set $P \subset \mathbb{Z}$,

$$\mathcal{A} f_P = f_{AP}\ , \tag{3.24}$$
$$\mathcal{T} f_P = f_{TP}\ . \tag{3.25}$$

Finally, the translation operators $\mathcal{T}_{\mathrm{r|l}}^n$ and analytic continuation operators $\mathcal{T}_{\mathrm{r|l}}^n$ are connected by the identities

$$\mathcal{A}_{\mathrm{l}}^{m+n} = \mathcal{T}_{\mathrm{r}}^{-m} \mathcal{A}_{\mathrm{l}}^n \mathcal{T}_{\mathrm{l}}^m \tag{3.26}$$
$$\mathcal{A}_{\mathrm{r}}^{m+n} = \mathcal{T}_{\mathrm{l}}^{-m} \mathcal{A}_{\mathrm{r}}^n \mathcal{T}_{\mathrm{r}}^m\ . \tag{3.27}$$

Since the function in $\mathcal{F}$ are analytic for $-\pi < \mathrm{Im}\, v < \pi$, operators $\mathcal{A}_{\mathrm{r|l}}^0$ is are fact identity, so that

$$\mathcal{A}_{\mathrm{l}}^n = \mathcal{T}_{\mathrm{r}}^{-n} \mathcal{T}_{\mathrm{l}}^n \tag{3.28}$$
$$\mathcal{A}_{\mathrm{r}}^n = \mathcal{T}_{\mathrm{l}}^{-n} \mathcal{T}_{\mathrm{r}}^n\ . \tag{3.29}$$

Thus we can express the analytic continuations of $\mathcal{F}$ functions in terms of translations, which will make the actual computations much easier. Similarly for $\mathcal{F}^A$ functions,

$$\mathcal{T}_{\mathrm{r}}^{-n} \mathcal{A}_{0,\mathrm{l}}^m \mathcal{T}_{\mathrm{m}}^n = \mathcal{A}_{0,\mathrm{l}}^{m+n} \tag{3.30}$$
$$\mathcal{T}_{\mathrm{m}}^{-n} \mathcal{A}_{0,\mathrm{r}}^m \mathcal{T}_{\mathrm{r}}^n = \mathcal{A}_{0,\mathrm{r}}^{m+n} \tag{3.31}$$
$$\mathcal{T}_{\mathrm{m}}^{-n} \mathcal{A}_{\psi,\mathrm{l}}^m \mathcal{T}_{\mathrm{l}}^n = \mathcal{A}_{\psi,\mathrm{l}}^{m+n} \tag{3.32}$$
$$\mathcal{T}_{\mathrm{l}}^{-n} \mathcal{A}_{\psi,\mathrm{r}}^m \mathcal{T}_{\mathrm{m}}^n = \mathcal{A}_{\psi,\mathrm{r}}^{m+n}\ . \tag{3.33}$$

and for the same reason we obtain

$$\mathcal{A}_{0,\mathrm{l}}^n = \mathcal{T}_{\mathrm{r}}^{-n} \mathcal{T}_m^n \tag{3.34}$$
$$\mathcal{A}_{0,\mathrm{r}}^n = \mathcal{T}_{\mathrm{m}}^{-n} \mathcal{T}_{\mathrm{r}}^n \tag{3.35}$$
$$\mathcal{A}_{\psi,\mathrm{l}}^n = \mathcal{T}_{\mathrm{m}}^{-n} \mathcal{T}_{\mathrm{l}}^n \tag{3.36}$$
$$\mathcal{A}_{\psi,\mathrm{r}}^n = \mathcal{T}_{\mathrm{l}}^{-n} \mathcal{T}_{\mathrm{m}}^n\ . \tag{3.37}$$

3.3 Riemann surface of the periodic TASEP

In this section we will recall – without physical motivation at this stage, the construction of the Riemann surface $\mathcal{R}^{\mathrm{Per}}$ associated with the computation of the spectral gaps of the TASEP with periodic boundary conditions in the thermodynamic limit by analytic continuation of the ground state eigenvalue of its

deformed Markov matrix, following [74]. The physical meaning of this function will be explained in chapter 4. Explicitly, we will compute the analytic continuation of the function

$$\chi_\emptyset(v) = \frac{\mathrm{Li}_{5/2}\left(-\mathrm{e}^{v}\right)}{\sqrt{2\pi}} \tag{3.38}$$

where Li_s is the polylogarithm function defined for $|z| < 1$ by its series expansion as

$$\mathrm{Li}_s(z) = \sum_{k=1}^{\infty} \frac{z^k}{k^s} \ . \tag{3.39}$$

In the notations of (3.1)-(3.2), the role of the function $\eta(v)$ is played by $\chi'(v)$.

The polylogarithm function

The Taylor expansion (3.39) defining the polylogarithm function is not convergent for $|z| \geq 1$. However the function Li_s can be analytically continued beyond the unit disk into a function on $\mathbb{C} \setminus [1, \infty)$ with a single branch point at $z = 1$ and a branch cut usually taken as the half line of real numbers larger than 1. The analytic continuation of the the polylogarithm function across the cut $[1, \infty)$ is

$$\mathrm{Li}_s(z) \to \mathrm{Li}_s(z) - 2\mathrm{i}\pi \frac{\log(z)^{s-1}}{\Gamma(s)} \qquad \text{from below} \ , \tag{3.40}$$

$$\mathrm{Li}_s(z) \to \mathrm{Li}_s(z) + 2\mathrm{i}\pi \frac{\log(z)^{s-1}}{\Gamma(s)} \qquad \text{from above} \ . \tag{3.41}$$

The introduction of the logarithm function adds a branch point at $z = 0$ and a branch cut $(-\infty, 0]$. This is not the case however when considering the function $\mathrm{Li}_s\left(-\mathrm{e}^{v}\right)$. This function has an infinite number of branch points $2\mathrm{i}\pi(n + 1/2)$ and branch cuts $2\mathrm{i}\pi(n + 1/2) + [0, \infty)$, corresponding to all the points mapped by $v \mapsto -\mathrm{e}^{v}$ on the conventional cut of $\mathrm{Li}_s(z)$. Of course this setting of cuts is arbitrary and depends on the original choice of branch cuts of the polylogarithm. We will choose rather a determination of the polylogarithm which makes $\chi_\emptyset(v)$ belong to the class $\mathcal{F}$ of analytically continuable functions defined on $\mathbb{D}$.

The function $\chi_\emptyset(v)$ admits another representation

$$\chi_\emptyset(v) = \frac{8\pi^{3/2}}{3}\left(\mathrm{e}^{\mathrm{i}\pi/4}\zeta\left(-\frac{3}{2}, \frac{1}{2} + \frac{v}{2\mathrm{i}\pi}\right) + \mathrm{e}^{-\mathrm{i}\pi/4}\zeta\left(-\frac{3}{2}, \frac{1}{2} - \frac{v}{2\mathrm{i}\pi}\right)\right) \tag{3.42}$$

where $\zeta(s, a)$ is the Hurwitz zeta function defined as

$$\zeta(a, z) = \sum_{n=0}^{\infty} \frac{1}{(n + a)^z} \ , \tag{3.43}$$

which is known to be analytically continuable as a function of z on the domain $\mathbb{C} \setminus \mathbb{R}_-$ for any $s \neq 1$. The equality (3.42) between the original function $\mathrm{Li}_{5/2}/\sqrt{2\pi}$ and the right hand side with ζ functions is only satisfied for $\mathrm{Re}\, v > 0$, however choosing this definition of $\chi_\emptyset$ simply amounts to change its branch cuts, so that it belongs to $\mathcal{F}$. It is now left to compute the analytic continuation of $\chi_\emptyset$ across its cuts.

The square root function $\kappa_a(v)$

The other branches of $\chi_\emptyset$ when crossing its cuts are obtained as a sum of $\chi_\emptyset$ and a finite numbers of additional terms depending of which cut is crossed. These additional terms essentially consist in shifted and scaled square roots of v defined by

$$\kappa_a(v) = \sqrt{\mathrm{sgn}(a)\mathrm{i}}\sqrt{|4\pi a| + \mathrm{sgn}(a)2\mathrm{i}v} = \begin{cases} \sqrt{4\mathrm{i}\pi a - 2v} & \text{if} \quad \mathrm{Re}\, v < 0 \\ \mathrm{sgn}(a)\mathrm{i}\sqrt{2v - 4\mathrm{i}\pi a} & \text{if} \quad \mathrm{Re}\, v > 0 \end{cases} \tag{3.44}$$

where the square root is understood as its principal value with branch cut $\mathbb{R}_-$, so that $\kappa_a(v)$ has a single branch point $2i\pi a$ and a branch cut $\mathrm{sgn}(a)[|a|,\infty)$, and κ_a is a class $\mathcal{F}$ function.

Shifting v by $\pm 2ni\pi$ is equivalent to shifting a by n, up to a change in sign if $\mathrm{Re}\, v > 0$ that is if the branch cut of the square root is crossed in the process, so that

$$T_{\mathrm{l}}^n \kappa_a = \kappa_{a-n} \tag{3.45}$$
$$T_{\mathrm{r}}^n \kappa_a = \sigma_a(B_n)\kappa_{a-n} \tag{3.46}$$

with

$$B_n = \begin{cases} \{1/2, 3/2, ..., n-1/2\} & \text{if} \quad n > 0 \\ \{n+1/2, ... -3/2, -1/2\} & \text{if} \quad n > 0 \\ \emptyset & \text{if} \quad n = 0 \end{cases} \tag{3.47}$$

$$\sigma_a(P) = \begin{cases} -1 & \text{if} \quad a \in P \\ 1 & \text{if} \quad a \notin P \end{cases} \tag{3.48}$$

Using relations (3.28)-(3.29) we obtain

$$\mathcal{A}_{\mathrm{l}}^n \kappa_a = \mathcal{A}_{\mathrm{r}}^n \kappa_a = \sigma_a(B_n)\kappa_a \tag{3.49}$$

where the equality between left and right analytic continuation comes from the fact that the complex square root has only two branches. We can now compute the whole analytic continuation of $\chi_\emptyset$.

Analytic continuation of function $\chi_\emptyset$

Using the fact that $\zeta(a, z+1) = \zeta(a,z) - z^{-1}$ (which is true wherever $\zeta(a,z)$ is defined, and outside the domain of definition of (3.43)) along with appropriate asymptotic expansion of the ζ function, it is possible to show that

$$\chi_\emptyset(v) = \lim_{M\to\infty} \left(-\frac{4(2\pi M)^{5/2}}{15\pi} - \frac{2v(2\pi M)^{3/2}}{3\pi} + \frac{(\pi^2 + 3v^2)\sqrt{2\pi M}}{6\pi} - \sum_{a=-M+1/2}^{M-1/2} \frac{\kappa_a^3(v)}{3} \right) . \tag{3.50}$$

Thus, analytically continuing $\chi_\emptyset$ across any branch cut amounts to changing the sign of a finite number of κ_a^3 function according to (3.49) so that the difference between $\chi_\emptyset$ and its analytic continuation consist of the sum of the κ_a functions whose sign were flipped, indexed by a set $P \ni a$. Again, there is no difference between analytic continuation from the left and from the right of any cut.

$$\mathcal{A}_{\mathrm{l}}^n \chi_\emptyset = \mathcal{A}_{\mathrm{r}}^n \chi_\emptyset = \chi_P = \chi_\emptyset + \sum_{a\in P} \frac{\kappa_a^3}{3} . \tag{3.51}$$

The set P indexing additional terms is determined by (3.49), and writing the action of $\mathcal{A}_{\mathrm{l|r}}^n$ on any branch χ_P of χ as the action of $A_{\mathrm{l|r}}^n$ on its indexing set P one obtains

$$A_{\mathrm{l}}^n P = A_{\mathrm{r}}^n P = P \ominus B_n \tag{3.52}$$

where $\ominus$ is the symmetric difference operator defined for two sets A and B as

$$A \ominus B = (A \setminus B) \cup (B \setminus A) . \tag{3.53}$$

The functions χ_P for any $P \subset \mathbb{Z} + 1/2$ thus describes all branches of the analytic continuation of $\chi_\emptyset$. Since any set P of half-integers can be built by iterated applications of A^n, each finite set of half integers correspond to a branch of χ. One can similarly work out the action of the translation operators $T_{\mathrm{l|r}}$ on χ_P as

$$T_{\mathrm{l}}^{-n} P = P + n , \tag{3.54}$$
$$T_{\mathrm{r}}^{-n} P = (P + n) \ominus B_n \tag{3.55}$$

Riemann surface $\mathcal{R}^{\mathrm{Per}}$

As explained above, the analytic continuation of the multivalued scaling function χ can be defined on a Riemann surface $\mathcal{R}^{\mathrm{Per}}$ whose sheets are in one-to-one correspondence with the branches of χ, that will be denoted χ_P^{Per} from now on to differentiate it from its analogues in other settings. The Riemann surface is constituted of an infinite number of copies of $\hat{\mathbb{D}} = \mathbb{D} \cup \{\infty\}$, the domain $\mathbb{D}$ compactified by adding a point at infinity. This point being a branch point of all branches of χ^{Per}, it is identified as a single point in $\mathcal{R}^{\mathrm{Per}}$. Defining

$$\begin{aligned} \chi: \quad & \mathcal{R}^{\mathrm{Per}} \to \hat{\mathbb{C}} \\ & [z, P] \mapsto \chi_P^{\mathrm{Per}}(z) \end{aligned} \tag{3.56}$$

where $[z, P] \in \mathcal{R}^{\mathrm{Per}}$ is the only point on sheet P that projects to $z \in \mathbb{D}$ under the covering map $\pi : \mathcal{R}^{\mathrm{Per}} \to \mathbb{D}$, the structure of $\mathcal{R}^{\mathrm{Per}}$ understood as the connectivity pattern of its sheets is determined by above-defined analytic continuation operators $A_{\mathrm{l}}^n = A_{\mathrm{r}}^n$. Every point $2\mathrm{i}(n + 1/2) \in \mathcal{S}$ is a branch point, and one checks that for any $n \in \mathbb{Z}$, and $P \subset (\mathbb{Z} + 1/2)$,

$$(A_{\mathrm{l}}^n \; A_{\mathrm{r}}^{n+1})^2 \; P = (A_{\mathrm{r}}^n \; A_{\mathrm{l}}^{n+1})^2 \; P = P \tag{3.57}$$

so that every branch point of $\mathcal{R}^{\mathrm{Per}}$ is of square root type [2]. As a side note, $\mathcal{R}^{\mathrm{Per}}$ is, from a purely topological point of view, the limit with infinite genus of a family of surfaces which are homeomorphic to the graphs of N-dimensional hypercubes thickened by replacing the edges with cylinder and vertices by spheres.

As we will explain in chapter 4, the relevant physical quantities obtained from the function χ are in fact the solutions $E(\mu)$ to the parametric equations (3.1)-(3.2), with these solution being invariant under the shift $v \to v + 2\mathrm{i}\pi$ for $\mathrm{Re}\, v > 0$. Equivalently, we know from (3.54)-(3.55) that translating a branch χ_P amounts to consider another branch $\chi_{P'}$. Thus replacing functions χ and η in (3.1)-(3.2) by any of their branches obtained by right translation will yield the same solutions for $E(\mu)$.

The translation operator $\mathcal{T}_{\mathrm{r}}$ generates a group acting on the branches of χ^{Per} or equivalently on the sheets of $\mathcal{R}^{\mathrm{Per}}$. Thus, the relevant objects to consider are not the sheets of surface $\mathcal{R}^{\mathrm{Per}}$ itself but rather equivalence classes under the group or right translation $\mathfrak{t}_{\mathrm{r}} = \{\mathcal{T}_{\mathrm{r}}^n, \; n \in \mathbb{Z}\}$. Looking at expressions (3.55), one easily checks that for any $P \in (\mathbb{Z} + 1/2)$,

$$|(P + m) \ominus B_m|_+ - |(P + m) \ominus B_m|_- = |P|_+ - |P|_- + m \tag{3.58}$$

where $|P|_+$ and $|P|_-$ denote respectively the the number of positive and negative elements of P. Thus, the set $P^* = T_{\mathrm{r}}^{|P|_+ - |P|_-} \; P$ has as much positive elements as negative elements. There is a unique element in each orbit under $\mathfrak{t}_r$ such that $|P|_+ = |P|_-$ that will be used to represent the corresponding orbit, and we will denote by P^* the unique element in the orbit of P satisfying this property.

3.4 Riemann surface of the open TASEP in the maximal current phase

We now move on to the computation of the analytic continuation of the scaling function of the spectral gaps of the deformed matrix of the open TASEP in the maximal current phase, with $\alpha = \beta = 1$. We use the same notation for χ in this section as in the previous one for its analogue for the periodic case. If the two functions need to be distinguished, we will write χ^{Per} for the eigenvalue scaling function of the periodic case and χ^{MC} for the function that we are considering now. The role of function η in the notation of (3.1) is played again by χ'. The derivation of its expression will be done in chapter 4. For now, we just write its explicit form [3]

$$\chi(v) = \frac{1}{3\pi} \int_{-\infty}^{\infty} \mathrm{d}y \; \frac{(1 - y^2)(3 - y^2)}{1 + y^{-2} \; \mathrm{e}^{y^2 - v - 1}} \; . \tag{3.59}$$

[2] meaning that their ramification index is $e_p = 2$, which is in general unrelated to the presence of actual square root functions, as we will see in next section

[3] In the notations of (3.2), the role of function $\eta(v)$ is again played by $\chi'(v)$

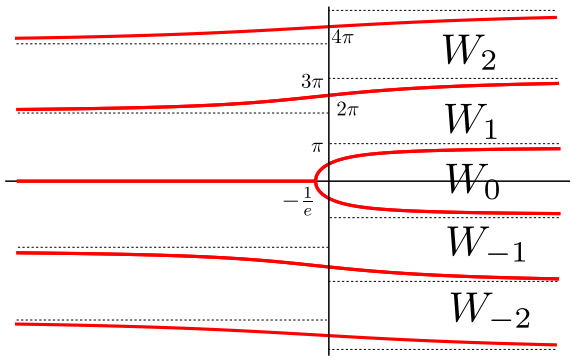

Figure 3.6: Plot of the images of the first Lambert functions in the complex plane. The red lines separate the codomains of W_j with consecutive indices j, expect for W_{-1} and W_1 which are directly related to one another by analytic continuation

The first step of the computation will be to construct a new determination $\chi_\emptyset$ of this function χ that will be a class $\mathcal{F}$ function. Then, we will compute the analytic continuation of $\chi_\emptyset$ and its various branches χ_P in the same way we did for the function χ^{Per}.

Before, we need to introduce the Lambert W_j functions, which plays a role analogue to square root functions of last section.

The Lambert W_j functions and functions w_j

The Lambert functions $W_j(z)$ are the branches of the multivalued inverse function of $z \mapsto z\mathrm{e}^z$ or equivalently the solutions to the equation

$$W_j(z)\mathrm{e}^{W_j(z)} = z\ , \tag{3.60}$$

There is generically an infinite number of such solutions so that the W_j are defined such that

$$W_j(z) + \log W_j(z) = \log z + 2\mathrm{i}\pi j \tag{3.61}$$

with log denoting the principal value of the complex logarithm with branch cut $\mathbb{R}_-$. The codomains $W_j(\mathbb{D})$ of all W_j functions form a partition of the complex plane (see figure 3.6) The Lambert functions for $j \neq 0$ have a branch cut $(-\infty, 0]$ and a branch point at $z = 0$. Moreover, W_{-1} and W_1 have an additional branch point at $z = -1/e$. Since this branch point lies on the cut $(-\infty, 0]$, one has to pay attention to which side of the cut the branch point is on. As for W_1, the branch point lies on the bottom side of the cut at $-1/e + \mathrm{i}0^-$ while for W_{-1} it lies on the top side at $-1/e + \mathrm{i}0^+$. W_0 has a single branch point $-1/e$ and a corresponding cut $(-\infty, -1/e]$. For any $j \neq -1, 1$, the analytic continuation of W_j when crossing the cut from below is W_{j-1} while crossing from above yields W_{j+1}. For W_1, crossing the cut from above leads to W_2, while crossing from below gives W_0 across the cut $(-\infty, -1/e]$ and W_{-1} across the segment $[-1/e, 0]$. Similarly, analytically continuing W_{-1} from below the cut $(-\infty, 0]$ yields W_{-2}, from above across $(-\infty, -1/e]$ gives W_0 and from above across $[-1/e, 0]$ gives W_1. All this is summarized in figure 3.7 We now introduce the functions $w_j(v)$, $j \in \mathbb{Z}$, defined from Lambert functions for $j = 0$ as

$$w_0(v) = \begin{cases} W_{-[\frac{\mathrm{Im}\ v}{2\pi}]}(\mathrm{e}^{-1-v}) & \text{if} \quad \mathrm{Re}\ v < 0 \\ W_0(\mathrm{e}^{-1-v}) & \text{if} \quad \mathrm{Re}\ v > 0 \end{cases} \tag{3.62}$$

and for $j \in \mathbb{Z}^*$ as

$$w_j(v) = \begin{cases} W_{j-[\frac{\mathrm{Im}\ v}{2\pi}]-\mathrm{sgn}(j)}(\mathrm{e}^{-1-v}) & \text{if Re } v < 0 \text{ and } \mathrm{sgn}(j)\,\mathrm{Im}(v) > 2\pi(|j| - \frac{1}{2}) \\ W_{[\frac{\mathrm{Im}\ v}{2\pi}]}(\mathrm{e}^{-1-v}) & \text{otherwise} \end{cases} . \tag{3.63}$$

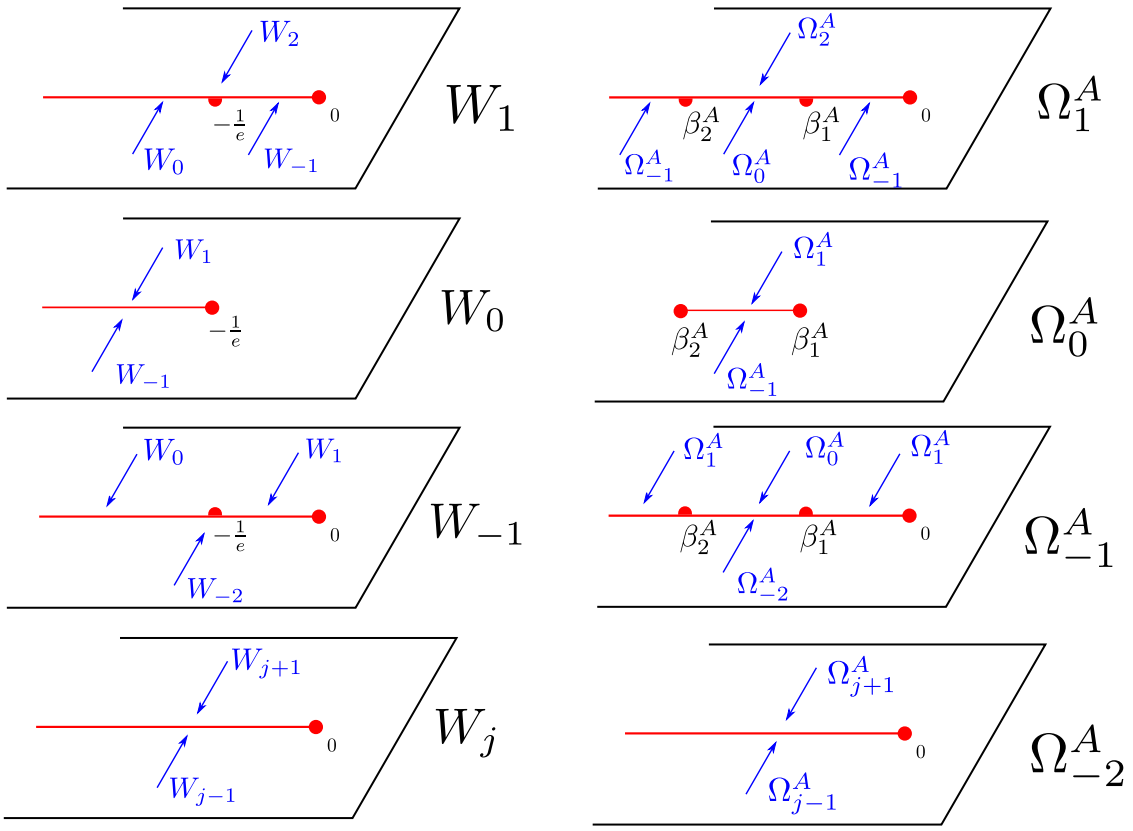

Figure 3.7: Sketch of the analytic continuation structure of the Lambert W_j functions (left column) and their generalized analogues Ω_j^A (right column) in the complex plane across their cuts on the real axis. Red lines represent the cuts and red dots branch points. Half red dots indicate that a branch point lies only on the corresponding side of the cut. Blue labels indicate the function obtained by analytic continuation when crossing the cut in the direction indicated by the corresponding arrow.

where the square brackets $[\bullet]$ denote rounding to the nearest integer. The functions w_j are $\mathcal{F}$ functions which coincides with $W_j(\mathrm{e}^{-1-v})$ for $-\pi < \mathrm{Im}\, v < \pi$. By construction, they transform under the action of $\mathcal{T}_\mathrm{l}$ and $\mathcal{T}_\mathrm{r}$ as

$$\mathcal{T}_\mathrm{l} w_j = w_{j-1} \tag{3.64}$$

$$\mathcal{T}_\mathrm{r} w_j = \begin{cases} w_0 & j = 0 \\ w_{-1} & j = 1 \\ w_{j-1} & j \notin \{0,1\} \end{cases} . \tag{3.65}$$

Using relations (3.28)-(3.29), one can then deduce the action of $\mathcal{A}^n_\mathrm{l}$ and $\mathcal{A}^n_\mathrm{r}$

From function χ to $\chi_\emptyset$

The function χ defined by (3.59) has horizontal branch cuts which correspond to the values of v for which the poles of the integrand of (3.59) take real values, that is

$$y^2 \mathrm{e}^{y^2-1} = -\mathrm{e}^{-v} . \tag{3.66}$$

Since $0 \leq y^2 \mathrm{e}^{y^2-1} \leq 1$ for $y \in \mathbb{R}$, the branch cuts of χ are the half-lines $2\mathrm{i}\pi(n+1/2) + \mathbb{R}_-$.

In order to relate χ to its analogue for the periodic case, and to make the computation of its analytic continuation easier and more systematic, we will now construct a new determination of χ analytic on $\mathbb{D}$ by rotating its cuts of $\pm\pi/2$ around the branch points $2\mathrm{i}\pi(n+1/2)$. Defining

$$f_v(y) = \frac{(1-y^2)(3-y^2)}{1 + y^{-2}\ \mathrm{e}^{y^2-v-1}} \tag{3.67}$$

the integrand of expression (3.59), the poles of $f_v(y)$ can be expressed as square roots of Lambert functions

$$-y^2 \mathrm{e}^{-y^2} = \mathrm{e}^{-v-1} \tag{3.68}$$

$$\Rightarrow y = \sqrt{-W_j(\mathrm{e}^{-v-1})} . \qquad j \in \mathbb{Z} . \tag{3.69}$$

As these roots will appear in the final expression of $\chi_\emptyset$, we need first to relabel them in such way that the solutions of equation (3.68) are analytic on $\mathbb{D}$. We define the functions $y_j(v)$ as

$$y_j(v) = \begin{cases} \mathrm{sgn}(\mathrm{Im}\ v - 2\pi j)\sqrt{-w_j(v)} & \mathrm{Re}\ v < 0 \\ (-1)^{-[\frac{\mathrm{Im}\ v}{2\pi}]}\sqrt{-w_0(v)} & \mathrm{Re}\ v > 0 \quad \text{and} \quad j = 0 \\ -\mathrm{sgn}(j)\sqrt{-w_j(v)} & \mathrm{Re}\ v > 0 \quad \text{and} \quad j \neq 0 \end{cases} , \tag{3.70}$$

which are $\mathcal{F}$ functions. They transform under translation as

$$\mathcal{T}_\mathrm{l} y_j = y_{j-1} \tag{3.71}$$

$$\mathcal{T}_\mathrm{r} y_j = \begin{cases} -y_0 & j = 0 \\ -y_{-1} & j = 1 \\ y_{j-1} & j \notin \{0,1\} \end{cases} . \tag{3.72}$$

so that their analytic continuations across their cuts on the imaginary line write

$$\mathcal{A}^n_\mathrm{l} y_j = \begin{cases} (-1)^n y_0 & \text{if} \quad j = n \\ -y_{j+\mathrm{sgn}(n)} & \text{if} \quad j \in \{0\} \cup B_{n-\mathrm{sgn}(n)} \\ y_j & \text{if} \quad j \notin \{0\} \cup B_n \end{cases} \tag{3.73}$$

$$\mathcal{A}^n_\mathrm{r} y_j = \begin{cases} (-1)^n y_n & \text{if} \quad j = 0 \\ -y_{j-\mathrm{sgn}(n)} & \text{if} \quad j \in B_n \\ y_j & \text{if} \quad j \notin \{0\} \cup B_n \end{cases} \tag{3.74}$$

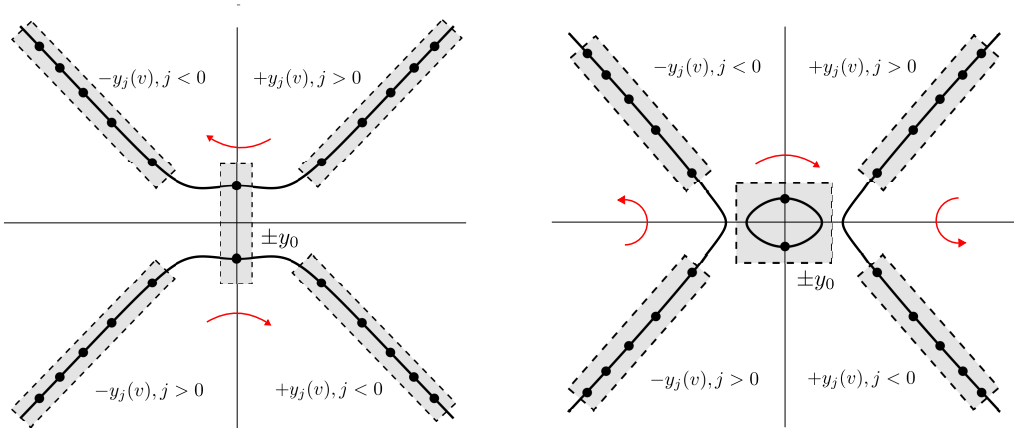

Figure 3.8: Plot of the poles $y_j(v)$ of $f_v(y)$ given by (3.67) in the complex plane for $v = r + \mathrm{i}\pi t$ with $r < 0$ (left) and $r > 0$ (right). The $y_j(v)$ move along the solid black line as t is varied, the red arrows represent the direction in which $y_j(v)$ move for increasing t.

where

$$B_n \begin{cases} \{1, \dots, n\} & \text{if} \quad n > 0 \\ \emptyset & \text{if} \quad n = 0 \\ \{n, \dots, -1\} & \text{if} \quad n < 0 \end{cases} . \tag{3.75}$$

Now that we have analytic expressions of the poles, we can define a function $\chi_\emptyset$ analytic on $\mathbb{D}$. In order to construct it from χ we need to perform the analytic continuation of χ across its horizontal cuts along path $v + \mathrm{i}t$, $t \in \mathbb{R}$. χ is analytic for $\mathrm{Re}\, v < 0$ and one observe that for $\mathrm{Re}\, v > 0$, when $\mathrm{Im}\, v = 2\mathrm{i}\pi(j + 1/2)$, the four poles $\pm y_0(v)$ and $\pm y_j(v)$ of $f_v(y)$ take real values, see figure 3.8.

Taking the analytic continuation of χ across the cut $2\mathrm{i}\pi(j + 1/2) + \mathbb{R}_+$ then simply consist in continuously deforming the integration contour in (3.59) so as to avoid the poles or equivalently to add the residues of $f_v(y)$ at these poles while keeping the same integration path, see figure 3.9. The discontinuity of χ when crossing the cut $2\mathrm{i}\pi(j + 1/2) + \mathbb{R}_+$ thus writes

$$\lim_{\epsilon \to 0} \chi(v + \mathrm{i}\epsilon) - \chi(v - \mathrm{i}\epsilon) = 2\mathrm{i}\pi \Big(\mathrm{res}(f_v, y_j(v)) - \mathrm{res}(f_v, -y_0(v)) \tag{3.76}$$

$$+ \mathrm{res}(f_v, y_0(v)) - \mathrm{res}(f_v, -y_j(v)) \Big) . \tag{3.77}$$

The computation of these residues is straightforward and adding the appropriate terms on each sector $2\mathrm{i}\pi(n - 1/2) < \mathrm{Im}\, v < 2\mathrm{i}\pi(n + 1/2)$ we obtain for $\mathrm{Re}\, v > 0$

$$\chi_\emptyset(v) = \chi(v) - 2i \left(\frac{1 - (-1)^{[\mathrm{Im}\, \frac{v}{2\pi}]}}{2} \eta_0(v) + \sum_{j \in B_{[\mathrm{Im}\, \frac{v}{2\pi}]}} \eta_j(v) \right) , \tag{3.78}$$

with

$$\eta_j(v) = \frac{y_j(v)^3}{3} - y_j(v) . \tag{3.79}$$

For $\mathrm{Re}\, v < 0$, one simply has $\chi_\emptyset(v) = \chi(v)$. Let us stress once more that the difference between χ and $\chi_\emptyset$ is merely a different convention choice for its branch cuts. We are now in position to compute the analytic continuation $\chi_\emptyset$ across the cuts $[2\mathrm{i}\pi(n - 1/2), 2\mathrm{i}\pi(n + 1/2)]$

Analytic continuation of $\chi_\emptyset$

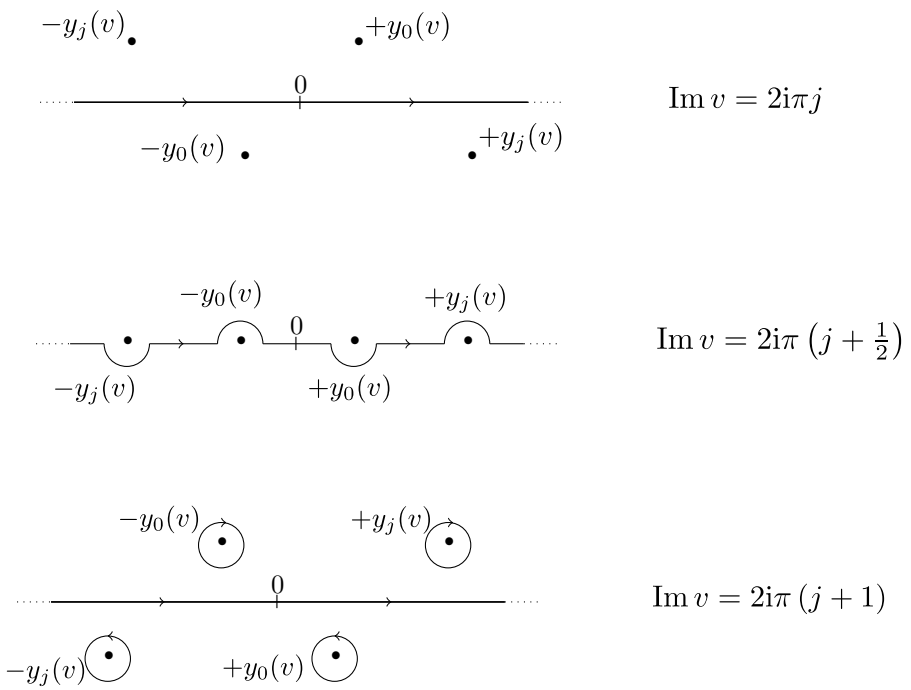

Figure 3.9: Deformation of the integration contour of the integral in (3.59) when crossing the cut $2\mathrm{i}\pi(j+1/2)+\mathbb{R}_+$ along a path $v+\mathrm{i}t$ for increasing t. The dots represent the four poles that take real value on the cut. The analytic continuation of function χ across this cut is obtained by adding the residues of the integrand at these poles, corresponding to the loop of the integration path circling around them

The function χ is analytic for $\operatorname{Re} v < 0$ and on all strips $2\mathrm{i}\pi(n-1/2) < \operatorname{Im} v < 2\mathrm{i}\pi(n+1/2), j \in \mathbb{Z}$, so the analytic continuation of $\chi_\emptyset$ from the left is obtained by removing all the additional terms from (3.78):

$$\mathcal{A}^{\mathrm{l}}_n \chi_\emptyset = \chi_\emptyset + 2i\left(\frac{1-(-1)^n}{2}\eta_0 + \sum_{j\in B_n}\eta_j\right). \tag{3.80}$$

Considering now the analytic continuation from the right, one has to take care of all terms η_j on the right hand side of (3.78), and one gets

$$\mathcal{A}^{\mathrm{r}}_n \chi_\emptyset = \chi_\emptyset + 2i\left(\eta_0 - \frac{1+(-1)^n}{2}\eta_n + \sum_{j\in B_n}\eta_j\right). \tag{3.81}$$

Applying repeatedly the operators $\mathcal{A}^n_{\mathrm{l}}$ and $\mathcal{A}^n_{\mathrm{r}}$ on $\chi_\emptyset$ for any path avoiding the branch points, we obtain in any case a function of the form

$$\chi_P = \chi_\emptyset + 2\mathrm{i}\sum_{j\in P}\eta_j(v) \tag{3.82}$$

where $P \subset \mathbb{Z}$ is a finite set indexing the branch of the analytic continuation of $\chi_\emptyset$. The function $\chi_\emptyset$ belongs to the class $\mathcal{F}$, so we can use again the expression of the analytic continuation operators in terms of translation by multiples of $2\mathrm{i}\pi$. The translation to the left of the imaginary axis writes, in terms of operations on indexing sets

$$\mathcal{T}_{\mathrm{l}}^{-n} P = P + n\,. \tag{3.83}$$

Similarly, the action of the right translation operator on the right writes

$$T_{\rm r}^{-n}P = \begin{cases} ((P+n)\setminus C_n)\cup(B_n\setminus(P+n+\mathrm{sgn}\ n))\cup\{0\} & \begin{array}{l}0\in P\ \&\ n \text{ even}\\ 0\notin P\ \&\ n \text{ odd}\end{array}\\ ((P+n)\setminus C_n)\cup(B_n\setminus(P+n+\mathrm{sgn}\ n)) & \begin{array}{l}0\in P\ \&\ n \text{ odd}\\ 0\notin P\ \&\ n \text{ even}\end{array}\end{cases} \tag{3.84}$$

with $C_n = B_n\cup\{0\}$. Using (3.28)-(3.29), we obtain the analytic continuation operators $\mathcal{A}_{\rm l}^n\chi_P = \chi_{\mathcal{A}_{\rm l}^n P}$ and $\mathcal{A}_{\rm r}^n\chi_P = \chi_{\mathcal{A}_{\rm r}^n P}$ for $n\neq 0$ as

$$A_n^{\rm l}P = \begin{cases} (P\setminus C_n)\cup(B_n\setminus(P+\mathrm{sgn}\ n))\cup\{0\} & \begin{array}{l}n\in P\ \&\ n \text{ even}\\ n\notin P\ \&\ n \text{ odd}\end{array}\\ (P\setminus C_n)\cup(B_n\setminus(P+\mathrm{sgn}\ n)) & \begin{array}{l}n\in P\ \&\ n \text{ odd}\\ n\notin P\ \&\ n \text{ even}\end{array}\end{cases} \tag{3.85}$$

$$A_n^{\rm r}P = \begin{cases} (P\setminus C_n)\cup(C_{n-\mathrm{sgn}\ n}\setminus(P-\mathrm{sgn}\ n))\cup\{n\} & \begin{array}{l}0\in P\ \&\ n \text{ even}\\ 0\notin P\ \&\ n \text{ odd}\end{array}\\ (P\setminus C_n)\cup(C_{n-\mathrm{sgn}\ n}\setminus(P-\mathrm{sgn}\ n)) & \begin{array}{l}0\in P\ \&\ n \text{ odd}\\ 0\notin P\ \&\ n \text{ even}\end{array}\end{cases}. \tag{3.86}$$

The structure of the branches of χ_P is more complex here than in the periodic case. In particular, the left and right analytic continuation are not identical.

Riemann surfaces $\mathcal{R}^{\rm MC}$

Using the same definition as (3.56), we can lift the function χ (that we will denote by $\chi^{\rm MC}$ to distinguish it from its analogue $\chi^{\rm Per}$ for the periodic TASEP) to a Riemann surface $\mathcal{R}^{\rm MC}$ whose structure is entirely determined by the analytic continuation of $\chi^{\rm MC}$ encoded in the operators $\mathcal{A}_{\rm l|r}^n$. It appears that $\mathcal{R}^{\rm MC}$ has a more complex structure than that of $\mathcal{R}^{\rm Per}$. Not all points in $\mathcal{S}$ are branch points depending on the branch $\chi_P^{\rm MC}$; for instance points $2{\rm i}\pi(n+1/2)$ with odd n are not branch points for the branch $P=\emptyset$.

As in the case of $\chi^{\rm Per}$, the solutions $E(\mu)$ of (3.1)-(3.2) in the MC case are invariant under translation $v\to v+2{\rm i}n\pi$ for $\mathrm{Re}\, v$, so we will consider, instead of the sheets of $\mathcal{R}^{\rm MC}$, equivalence classes of sheets constituted of orbits under the action of the group $\mathfrak{t}_r$ of discrete translations on the right of the cuts. We will first check that there exist in each orbit a unique element $P_\star$ such that $|P|_+ = |P|_-$, then that if P is the index of a sheet connected to $\emptyset$ (that is if χ_P is obtained from $\chi_\emptyset$ by analytic continuation), then $0\notin P_\star$. This way, solutions to the parametric equations (3.1)-(3.2) will be uniquely characterized by a sets $P\in\mathbb{Z}^*$ with $|P|_+ = |P|_-$.

Let $P\subset\mathbb{Z}$ be a finite set of integers, with positive elements $P_+ = \{k_1^+,\dots,k_h^+\}$, $0<k_1^+<\ldots<k_h^+$ and negative elements $P_- = \{k_\ell^-,\dots,k_1^-\}$, $k_\ell^-<\ldots<k_1^-<0$. Then, the action on P of the operator T_r computed with (3.84) writes

$$T_rP = \begin{cases} \{k_\ell^-+1,...,k_2^-+1,k_1^++1,...,k_h^++1\} & \text{if}\quad 0\in P\ \&\ -1\in P\\ \{k_\ell^-+1,...,k_1^-+1,1,k_1^++1,...,k_h^++1\} & \text{if}\quad 0\in P\ \&\ -1\notin P\\ \{k_\ell^-+1,...,k_2^-+1,0,k_1^++1,...,k_h^++1\} & \text{if}\quad 0\notin P\ \&\ -1\in P\\ \{k_\ell^-+1,...,k_1^-+1,0,1,k_1^++1,...,k_h^++1\} & \text{if}\quad 0\notin P\ \&\ -1\notin P\end{cases}. \tag{3.87}$$

In any case, the application of T_r increases the excess number of positive elements in P by exactly 1, so that for any P, the set $P^* = T_r^{|P_-|-|P_+|}P$ is such that $|P_+^*| = |P_-^*|$. Moreover, there is a unique element P^* satisfying this property in the orbit $\mathfrak{t}_rP$ by construction.

With P^* the unique representative with $|P_+^*| = |P_-^*|$ in the orbit of any finite set $P\subset\mathbb{Z}$ under the action of T_r, we want to show that for any P such that the function χ_P may be obtained from $\chi_\emptyset$ by analytic continuations, i.e. any P that can be obtained from the empty set $\emptyset$ by repeated action of the operators $A_n^{\rm l|r}$, $n\in\mathbb{Z}$, the corresponding set P^* does not contain 0.

Since by construction $(T_r^n P)^* = P^*$, the identities

$$\begin{aligned} A_n^{\mathrm{l}} &= T_{\mathrm{r}}^{-n} T_{\mathrm{l}}^n \\ A_n^{\mathrm{r}} &= T_{\mathrm{l}}^{-n} T_{\mathrm{r}}^n \ , \end{aligned} \tag{3.88}$$

imply that we only need to prove that the collection of all $P \subset \mathbb{Z}$ such that $0 \notin P^*$ is globally stable under the action of T_{l}, defined by $T_{\mathrm{l}}^n P = P - n$. But we observe from (3.87) that $0 \in P^*$ is equivalent to $0 \in P$ (respectively $0 \notin P$) if $|P_+| - |P_-|$ is even (resp. odd). The fact that under the replacement $P \to T_{\mathrm{l}} P$, $|P_+| - |P_-|$ is left unchanged if $0 \notin P$ and is decreased by one otherwise concludes the proof.

The fact that all sheets indexed by P such that $0 \in P^*$ is stable under $A_n^{\mathrm{l|r}}$ means that these sheets belong to a (not necessarily connected) component $\mathcal{R}_*^{\mathrm{MC}}$ of $\mathcal{R}^{\mathrm{MC}}$. We will now prove that $\mathcal{R}_*^{\mathrm{MC}}$ is in fact constituted of an infinite number of connected components $\mathcal{C}_k$. Defining

$$C_k = \left\{ P \subset \mathbb{Z}, \left| |P^*_{\mathrm{odd}}| - |P^*_{\mathrm{even}}| \right| = 2k \right\} \tag{3.89}$$

where P_{odd} and P_{even} are the subsets of respectively odd and even elements of $P \subset \mathbb{Z}^*$, one easily checks that the action of T_{r}^n and T_{l}^n on a set P do not change the excess number of elements of a given parity $|\ |P^*_{\mathrm{odd}}| - |P^*_{\mathrm{even}}|\ |$ in the corresponding set P^*. Each C_k is then stable under T_{r}^n and T_{l}^n, and thus under A_n^{l} and A_n^{r}. The corresponding components $\mathcal{C}_k$ gathering the sheets indexed by all $P \in C_k$ are thus disconnected from one another for different $k \in \mathbb{N}$. It is now left to prove that the $\mathcal{C}_k$ are connected. Let

$$P_k = \{2j - 1, 1 \leq j \leq 2k\} \cup \{-2j + 1, 1 \leq j \leq 2k\} \ . \tag{3.90}$$

P_k is an element of C_k which can be constructed by repeated applications of operators A_{l}^n and A_{r}^n on any set $P \in C_k$. This is proved by remarking that the action of A_{l}^n on $P \ni n$ removes the element n if $n - 1 \in P$ while the action of A_{r}^n removes n from P if $0 \in P$ (respectively $0 \notin P$) if n is odd (respectively n is even). Hence, starting from P^* in the orbit O_P, one can reach P_k by successive substitutions $P \to A_{\mathrm{l|r}}^n P$, so that the components $\mathcal{C}_k$ are indeed connected.

One should note that, strictly speaking, most spectral gaps (i.e. relevant solutions to the parametric equations (3.1)-(3.2)) are not obtained by analytic continuation of the ground state, as $\mathcal{R}_*^{\mathrm{MC}}$ is not connected. For instance, the sheet $P = \{-1, 1\}$, corresponding to the gap of $M(\mu)$, does not belong to the same connected component as $P = \emptyset$ which is the ground-state sheet. However, our systematic construction of the branches of χ^{MC} does provide us exact expression for all spectral gaps of $M(\mu)$.

3.5 Riemann surface of the open TASEP in the MC/HD crossover

We have computed the analytic continuation of the eigenvalue scaling function of the periodic TASEP and that of the open TASEP in the maximal current phase, and constructed the Riemann surface upon which these functions are defined. We will now consider the eigenvalue scaling function of the TASEP in the crossover regime between the maximal current and the high density phases, which interpolates between the two former cases. These functions depend now on an additional parameter $A > 0$ related to the scaling of the left boundary rate α. Defining

$$\eta^A(v) = \int_{-\infty}^{\infty} \mathrm{d}y \, \frac{(A+4)y^2 \left(4A\left(y^2-4\right) + y^4\right)}{2\left(4A + y^2\right)\left(\left(4A + y^2\right) e^{-v - v_0^A + \frac{y^2}{4}} + (A+4)y^2\right)} \ , \tag{3.91}$$

$$\chi^A(v) = \frac{1}{16} \int_{-\infty}^{\infty} \mathrm{d}y \, \frac{(A+4)y^4 \left(4A\left(y^2-4\right) + y^4\right)}{2\left(4A + y^2\right)\left(\left(4A + y^2\right) e^{-v - v_0^A + \frac{y^2}{4}} + (A+4)y^2\right)} \ . \tag{3.92}$$

where

$$v_0^A = \frac{2\sqrt{A}}{\sqrt{A} + \sqrt{A+4}} - 2\log\left(\frac{2\sqrt{A+4}}{\sqrt{A} + \sqrt{A+4}}\right) , \tag{3.93}$$

we now compute the full analytic continuation of both χ^A and η^A for $0 \leq A \leq \infty$. The function χ^{Per} is recovered (up to a constant factor) as the limit of χ^A when $A \to 0$ and one obtains similarly χ^{MC} when $A \to \infty$. We will show that the family of Riemann surfaces parametrized by A corresponding to the analytic continuation of χ^A is a continuous deformation of the Riemann surface $\mathcal{R}^{\mathrm{Per}}$ into $\mathcal{R}^{\mathrm{MC}}$.

The following computation is mostly a generalization of the χ^{MC} case, and we will use the same approach. First we will construct determinations of η^A and χ^A in the class $\mathcal{F}^A$ of functions analytically continuable on the domain $\mathbb{D}^A$ defined by (3.14), then we will construct their various branches with the help of the above defined translation operators. Since η^A and χ^A have very similar structure, we will denote by $\varphi^A(v)$ any of the two functions when an expression is valid for both.

Generalized Lambert functions $W_j^A(z)$ and $\Omega_j^A(z)$ and functions $w_j^A(v)$

We first introduce the generalized Lambert functions W_j^A as the solutions to

$$\mathrm{e}^{W_j^A(z)} \frac{W_j^A(z)}{A - W_j^A(z)} = z \ , \tag{3.94}$$

for $A > 0$. As in the case of plain Lambert functions, the branches are indexed by taking the logarithm of (3.94) so that for $j \in \mathbb{Z}$, W_j^A is the unique solution to

$$W_j^A(z) + \log\Big(\frac{W_j^A(z)}{A - W_j^A(z)}\Big) = \log z + 2\mathrm{i}\pi j \tag{3.95}$$

with the same convention as before for the branch cuts of the logarithm. For any $j \in \mathbb{Z}$,

$$\lim_{A\to\infty} W_j^A(z/A) = W_j(z) \tag{3.96}$$

where W_j is a regular Lambert function, while for $A \to 0$, $W_j^A(v)$ converge to a branch of the complex logarithm equal to the principal value of the log shifted by $2\mathrm{i}\pi j$.

The W_j^A can be seen equivalently as the branches of the multivalued inverse function of $f(y) = \mathrm{e}^y \frac{y}{A-y}$. It is a general result that for a meromorphic function f, the branch points z_* of the inverse functions f^{-1} are equal to $z_* = f(y_*)$ where y_* is one of the solution to $f'(y_*) = 0$ [4] . There are three solution $y_* = -\infty$, $y_* = \frac{1}{2}(A \pm \sqrt{A}\sqrt{A+4})$ corresponding to three possible branch points on the real axis $z_* = 0$, $z_* = b_1^A$ and $z_* = b_2^A$ with

$$b_1^A = -\tfrac{1}{4}(\sqrt{A+4} - \sqrt{A})^2\, e^{\frac{1}{2}(A - \sqrt{A}\sqrt{A+4})} \tag{3.97}$$

$$b_2^A = -\tfrac{1}{4}(\sqrt{A+4} + \sqrt{A})^2\, e^{\frac{1}{2}(A + \sqrt{A}\sqrt{A+4})} \ . \tag{3.98}$$

In order to make the correspondence with the function χ^{MC} clearer, we will work instead with the modified functions

$$\Omega_k^A(z) = W_j^A\left(\frac{z}{4+A}\right) \ , \tag{3.99}$$

which have branch points among 0, $\beta_1^A = (4+A)b_1^A$ and $\beta_2^A = (4+A)b_2^A$.

For $j \notin \{-1, 0, 1\}$, Ω_j^A has a single branch point $z = 0$ and a corresponding branch cut that we choose to be the negative real axis. The function Ω_0^A has branch points β_1^A and β_2^A and we set the branch cut on the real interval $[\beta_1^A, \beta_2^A]$. Finally the function Ω_1^A (respectively) Ω_{-1}^A) has branch points 0, $\beta_1^A - \mathrm{i}0^+$ and $\beta_2 - \mathrm{i}0^+$ (respectively $\beta_1^A + \mathrm{i}0^+$ and $\beta_2 + \mathrm{i}0^+$) meaning that β_1^A and β_2^A are only branch points when analytically continuing the function from below (respectively above) the cut. The way the Ω_j^A relate to one another by analytic continuation is more complex than in the case of the plain Lambert functions and is summarized in figure 3.7.

[4] More precisely, the branch points of each of the branches of f^{-1} are among the set of the $f(y_*)$ where y_* is a singular point of f, however, not all branches have the same branch points and not all singular points of f correspond to branch points of f^{-1} in general

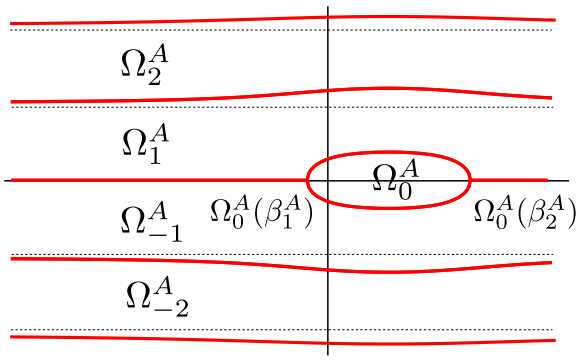

Figure 3.10: Images in the complex plane of the branches of the modified Lambert functions Ω_j^A for $A = 10$.

In the limit $A \to \infty$, one has $\beta_2^A \to \infty$ and $\beta_1^A \to -\frac{1}{e}$ so that the analytic structure of the usual Lambert W_j functions is recovered. Similarly, when $A \to 0$, both branch points β_1^A and β_2^A goes to 0, and the branch Ω_0^A is uniformly 0 so that the structure of the analytic continuation of functions Ω^A is that of the logarithm, as expected.

In a similar way we defined the functions w_j in section 3.4 as analytic determination of $W_j(\mathrm{e}^{-v-1})$ in the space $\mathcal{F}$, we now define the functions $w_j^A(v)$ as functions in the space $\mathcal{F}^A$ analytic on $\mathbb{D}^A$ which coincide with $\Omega_j^A(\mathrm{e}^{-v-v_0})$ on the strip $-\pi < \operatorname{Im} v < \pi$. They write

$$w_0^A(v) = \begin{cases} \Omega^A_{-[\frac{\operatorname{Im}\{v\}}{2\pi}]}(\mathrm{e}^{-v-v_0^A}) & \psi(A) < \operatorname{Re}\{v\} < 0 \\ \Omega_0^A(\mathrm{e}^{-v-v_0^A}) & \text{otherwise} \end{cases} \tag{3.100}$$

$$w_j^A(v) = \begin{cases} \Omega^A_{j-[\frac{\operatorname{Im}\{v\}}{2\pi}]-\operatorname{sgn}(j)}(\mathrm{e}^{-v-v_0^A}) & \psi(A) < \operatorname{Re}\{v\} < 0 \quad \& \quad \operatorname{sgn}(j)\operatorname{Im}\{v\} > 2\pi\left(|j| - \frac{1}{2}\right) \\ \Omega^A_{j-[\frac{\operatorname{Im}\{v\}}{2\pi}]}(\mathrm{e}^{-v-v_0^A}) & \text{otherwise} \end{cases}$$

The translation operators act on the w_j^A as follow

$$\mathcal{T}_{\mathrm{m}}\, w_j^A = w_{j-1}^A\,, \tag{3.101}$$

$$\mathcal{T}_{\mathrm{r}}\, w_j^A = \mathcal{T}_{\mathrm{l}}\, w_j^A = \begin{cases} w_0^A & j = 0 \\ w_{-1}^A & j = 1 \\ w_{j-1}^A & j \notin \{0, 1\} \end{cases}\,, \tag{3.102}$$

The w_j^A have two sets of branch points and branch cuts at $\operatorname{Re} v = 0$ and $\operatorname{Re} v = \psi(A) = \log\left(\beta_1^A/\beta_2^A\right)$, where ψ writes explicitly

$$\psi(A) = -\sqrt{A}\sqrt{A+4} - 4\log\left(\frac{\sqrt{A} + \sqrt{A+4}}{2}\right)\,, \tag{3.103}$$

corresponding to the branch points β_1^A and β_2^A of the Ω_j^A mapped by $v \to \mathrm{e}^{-v-v_0^A}$, since v_0^A defined in (3.93) is actually equal to $v_0^A = -\log\left(-\beta_1^A\right)$. From expressions (3.101)-(3.102), we see that the behaviour of the w_j^A at these cuts is in fact identical under left $\leftrightarrow$ right symmetry. We can now get back to the analytic continuation of χ^A and η^A

From function χ^A and η^A to $\chi_\emptyset^A$ and $\eta_\emptyset^A$

Let us first construct determination $\eta_\emptyset^A$ and $\chi_\emptyset^A$ of η^A and χ^A analytic and analytically continuable on $\mathbb{D}^A$. The function χ^A and η^A are analytic for $\operatorname{Re} v < 0$ and have branch cuts for $v \in 2\mathrm{i}\pi(\mathbb{Z} + 1/2)$. As in the case of χ^{MC}, branch cuts of $\eta(v)$ and $\chi(v)$ correspond to values of v for which the integrands

$f_\eta^{A,v}(y)$ and $f_\chi^{A,v}(y)$ of (3.91) and (3.92) given by

$$f_\eta^{A,v}(y) = \frac{(A+4)y^2\left(4A\left(y^2-4\right)+y^4\right)}{2\left(4A+y^2\right)\left(\left(4A+y^2\right)e^{-v-v_0^A+\frac{y^2}{4}}+(A+4)y^2\right)} \tag{3.104}$$

$$f_\chi^{A,v}(y) = \frac{y^2}{16} f_\eta^{A,v}(v) \tag{3.105}$$

have real poles. The two points $\pm 2\mathrm{i}\sqrt{A}$ do not take real values, and the other poles of $f_\eta^{A,v}(y)$ and $f_\chi^{A,v}(y)$ are the solutions to

$$\left(4A+y^2\right)e^{-v-v_0^A+\frac{y^2}{4}}+(A+4)y^2 = 0\ . \tag{3.106}$$

These poles are given by the square roots of modified Lambert functions as

$$\pm 2\sqrt{-W_j^A\Big(\frac{\mathrm{e}^{-v-v_0^A}}{4+A}\Big)} = \pm 2\sqrt{-\Omega_j^A(\mathrm{e}^{-v-v_0^A})}\ . \tag{3.107}$$

Again, we construct $\mathcal{F}^A$ determinations $y_j^A(v)$ of these poles from functions w_j^A, defined by

$$y_0^A(v) = \begin{cases} (-1)^{-[\frac{\mathrm{Im}\, v}{2\pi}]}\sqrt{-w_0^A(v)} & \mathrm{Re}\{v\} > 0 \\ \mathrm{sgn}(\mathrm{Im}\ v - 2\pi j)\sqrt{-w_0^A(v)} & \psi(A) < \mathrm{Re}\{v\} < 0 \\ \sqrt{-w_0^A(v)} & \mathrm{Re}\{v\} < \psi(A) \end{cases}\ , \tag{3.108}$$

$$y_j^A(v) = \begin{cases} -\mathrm{sgn}(j)\sqrt{-w_j^A(v)} & \mathrm{Re}\{v\} > 0 \\ \mathrm{sgn}(\mathrm{Im}\ v - 2\pi j)\sqrt{-w_j^A(v)} & \mathrm{Re}\{v\} < 0 \end{cases}\ . \tag{3.109}$$

From the properties of the square root and function w_j^A we deduce the action of translation operators

$$\mathcal{T}_{\mathrm{m}}\ y_j^A = y_{j-1}^A\ , \tag{3.110}$$

$$\mathcal{T}_{\mathrm{r}}\ y_j^A = \begin{cases} -y_0^A & j = 0 \\ -y_{-1}^A & j = 1 \\ y_{j-1}^A & j \notin \{0,1\} \end{cases}\ , \tag{3.111}$$

$$\mathcal{T}_{\mathrm{l}}\ y_j^A = \begin{cases} y_0^A & j = 0 \\ y_{-1}^A & j = 1 \\ y_{j-1}^A & j \notin \{0,1\} \end{cases}\ , \tag{3.112}$$

from which the action of the analytic continuation operators across the cuts $\mathrm{i}[2\pi(n-1/2), 2\pi(n+1/2)]$ and $\psi(A) + \mathrm{i}[2\pi(n-1/2), 2\pi(n+1/2)]$ follows as

$$\mathcal{A}_{0,\mathrm{l}}^n\ y_j^A = \begin{cases} (-1)^n y_0^A & \text{if} \quad j = n \\ -y_{j+\mathrm{sgn}(n)}^A & \text{if} \quad j \in \{0\} \cup B_{n-\mathrm{sgn}(n)} \\ y_j^A & \text{if} \quad j \notin \{0\} \cup B_n \end{cases} \tag{3.113}$$

$$\mathcal{A}_{0,\mathrm{r}}^n y_j^A = \begin{cases} (-1)^n y_n^A & \text{if} \quad j = 0 \\ -y_{j-\mathrm{sgn}(n)}^A & \text{if} \quad j \in B_n \\ y_j^A & \text{if} \quad j \notin \{0\} \cup B_n \end{cases}\ , \tag{3.114}$$

$$\mathcal{A}_{\psi,\mathrm{l}}^n\ y_j^A = \begin{cases} y_n^A & \text{if} \quad j = 0 \\ -y_{j-\mathrm{sgn}(n)}^A & \text{if} \quad j \in B_n \\ y_j^A & \text{if} \quad j \notin \{0\} \cup B_n \end{cases} \tag{3.115}$$

$$\mathcal{A}_{\psi,\mathrm{r}}^n y_j^A = \begin{cases} y_0^A & \text{if} \quad j = n \\ -y_{j+\mathrm{sgn}(n)}^A & \text{if} \quad j \in \{0\} \cup \in B_{n-\mathrm{sgn}(n)} \\ y_j^A & \text{if} \quad j \notin \{0\} \cup B_n \end{cases}\ . \tag{3.116}$$

The poles y_j^A take real values when $v \in \mathbb{R}_+ + 2\mathrm{i}\pi(\mathbb{Z}+1/2)$ which correspond to the cuts of χ^A and η^A, with corresponding branch points in the set $\mathcal{S}$ of (3.15). As in the case of χ^{MC}, only the four poles $\pm y_0^A(v)$ and $\pm y_j^A(v)$ take real values for $\mathrm{Im}\, v = 2\mathrm{i}\pi(j+1/2)$. We can now construct the functions $\eta_\emptyset^A$ and $\chi_\emptyset^A$ from analytic continuation of χ^A and η^A by adding the residues of $f_\eta^{A,v}$ and $f_\chi^{A,v}$ at these poles using the fact that

$$\lim_{\epsilon\to 0} \varphi^A(v+\mathrm{i}\epsilon) - \varphi^A(v-\mathrm{i}\epsilon) = 2\mathrm{i}\pi\Big(\mathrm{res}(f_{\eta|\chi}^{A,v}(v), y_j^A(v)) - \mathrm{res}(f_{\eta|\chi}^{A,v}(v), -y_0^A(v)) \tag{3.117}$$

$$+\mathrm{res}(f_{\eta|\chi}^{A,v}(v), y_0^A(v)) - \mathrm{res}(f_{\eta|\chi}^{A,v}(v), -y_j^A(v))\Big)\,. \tag{3.118}$$

where $f_{\eta|\chi}^{A,v}(v)$ stands for either $f_\eta^{A,v}(v)$ or $f_\chi^{A,v}(v)$. Adding this discontinuities on each strip $2\mathrm{i}\pi(n+1/2) < \mathrm{Im}\, v < 2\mathrm{i}\pi(n+3/2)$ above the corresponding cut, we obtain for $\mathrm{Re}\, v >$ the expressions

$$\eta_\emptyset^A(v) = \eta^A(v) - 2i\left(\frac{1-(-1)^{[\mathrm{Im}\,\frac{v}{2\pi}]}}{2}\, y_0^A(v) + \sum_{j\in B_{[\mathrm{Im}\,\frac{v}{2\pi}]}} y_j^A(v)\right) \tag{3.119}$$

$$\chi_\emptyset^A(v) = \chi^A(v) - 2i\left(\frac{1-(-1)^{[\mathrm{Im}\,\frac{v}{2\pi}]}}{2}\, y_0^A(v)^3 + \sum_{j\in B_{[\mathrm{Im}\,\frac{v}{2\pi}]}} y_j^A(v)^3\right) \tag{3.120}$$

which belong to the space $\mathcal{F}^A$. For $\mathrm{Re}\, v < 0$, $\eta_\emptyset^A(v)$ and $\chi_\emptyset^A(v)$ are equal to $\eta^A(v)$ and $\chi^A(v)$.

Analytic continuation of functions $\eta_\emptyset^A$ and $\chi_\emptyset^A$: functions χ_P^A and η_P^A

We can now compute the analytic continuation of χ_P^A and η_P^A across the cuts $2\mathrm{i}\pi(n-1/2, n+1/2)$ and $\psi(A) + 2\mathrm{i}\pi(n-1/2, n+1/2)$, $n \in \mathbb{Z}^*$ [5]. Both functions have the same analytic structure, so we will denote by φ^A either η^A and χ^A and by λ^A the additional terms y_j^A (respectively $(y_j^A)^3$) appearing in the analytic continuation of η^A (respectively χ^A) in expressions (3.119) and (3.120).

The structure of the analytic continuation of $\varphi_\emptyset^A$ across the cuts on the imaginary line $\mathrm{Re}\, v = 0$ is identical to that of the function $\chi_\emptyset^{\mathrm{MC}}(v)$ so we can directly transpose expressions (3.80) and (3.81) in this context

$$\mathcal{A}_{0,l}^n\ \varphi_\emptyset^A(v) = \varphi_\emptyset^A(v) + 2i\left(\frac{1-(-1)^{[\mathrm{Im}\,\frac{v}{2\pi}]}}{2}\, \lambda_0^A(v) + \sum_{j\in B_{[\mathrm{Im}\,\frac{v}{2\pi}]}} \lambda_j^A(v)\right), \tag{3.121}$$

$$\mathcal{A}_{0,r}^n\ \varphi_\emptyset^A(v) = \varphi_\emptyset^A(v) + 2i\left(\frac{1+(-1)^{[\mathrm{Im}\,\frac{v}{2\pi}]}}{2}\, \lambda_n^A(v) + \sum_{j\in B_{[\mathrm{Im}\,\frac{v}{2\pi}]}} \lambda_j^A(v)\right). \tag{3.122}$$

The set of functions λ_j^A being, by construction, closed under analytic continuation, the continuation of all branches of $\varphi_\emptyset^A$ across theirs cuts are obtained under the form

$$\varphi_P^A = \varphi_\emptyset^A(v) + 2\mathrm{i}\sum_{j\in P} \lambda_j^A(v) \tag{3.123}$$

where $P \subset \mathbb{Z}$, similar to (3.82). Knowing the action of translations operators $T_{\mathrm{l|m|r}}$ from (3.110), (3.111), and (3.112), we can painstakingly compute the action of translation operators on φ_P^A in terms

[5] The functions χ^A and η^A originally have their branch points on the imaginary line $\mathrm{Re}\, v = 0$. The branch points at $\mathrm{Re}\, v = \psi(A)$ of $\eta_\emptyset^A(v)$ and $\chi_\emptyset^A(v)$ are the result of the introduction of the additional terms $\pm y_j^A(v)$

of set-theoretic operation on the indexing set P:

$$T_{\rm m}^{-n}P = P + n \tag{3.124}$$

$$T_{\rm r}^{-n}P = \begin{cases} ((P+n)\setminus C_n)\cup(B_n\setminus(P+n+\mathrm{sgn}\ n))\cup\{0\} & \begin{array}{llll} 0\in P & \& & n & \text{even}\\ 0\notin P & \& & n & \text{odd}\end{array}\\ ((P+n)\setminus C_n)\cup(B_n\setminus(P+n+\mathrm{sgn}\ n)) & \begin{array}{llll} 0\in P & \& & n & \text{odd}\\ 0\notin P & \& & n & \text{even}\end{array}\end{cases} \tag{3.125}$$

$$T_{\rm l}^{-n}P = \begin{cases} ((P+n)\setminus C_n)\cup((P\cap B_{-n})+n+\mathrm{sgn}\ n)\cup\{0\} & 0\in P\\ ((P+n)\setminus C_n)\cup((P\cap B_{-n})+n+\mathrm{sgn}\ n) \& & 0\notin P\end{cases}. \tag{3.126}$$

Using the relations (3.34)-(3.37) between translation operators and analytic continuations on $\mathcal{F}^A$, we obtain

$$A_{0,\rm l}^n P = \begin{cases} (P\setminus C_n)\cup(B_n\setminus(P+\mathrm{sgn}\ n))\cup\{0\} & \begin{array}{llll} n\in P & \& & n & \text{even}\\ n\notin P & \& & n & \text{odd}\end{array}\\ (P\setminus C_n)\cup(B_n\setminus(P+\mathrm{sgn}\ n)) & \begin{array}{llll} n\in P & \& & n & \text{odd}\\ n\notin P & \& & n & \text{even}\end{array}\end{cases} \tag{3.127}$$

$$A_{0,\rm r}^n P = \begin{cases} (P\setminus C_n)\cup(C_{n-\mathrm{sgn}\ n}\setminus(P-\mathrm{sgn}\ n))\cup\{n\} & \begin{array}{llll} 0\in P & \& & n & \text{even}\\ 0\notin P & \& & n & \text{odd}\end{array}\\ (P\setminus C_n)\cup(C_{n-\mathrm{sgn}\ n}\setminus(P-\mathrm{sgn}\ n)) & \begin{array}{llll} 0\in P & \& & n & \text{odd}\\ 0\notin P & \& & n & \text{even}\end{array}\end{cases} \tag{3.128}$$

$$A_{\psi,\rm l}^n P = \begin{cases} (P\setminus C_n)\cup((P\cap B_n)-\mathrm{sgn}\ n)\cup\{n\} & 0\in P\\ (P\setminus C_n)\cup((P\cap B_n)-\mathrm{sgn}\ n) & 0\notin P\end{cases}, \tag{3.129}$$

$$A_{\psi,\rm r}^n P = \begin{cases} (P\setminus C_n)\cup((P\cap C_{n-\mathrm{sgn}\ n})+\mathrm{sgn}\ n)\cup\{0\} & n\in P\\ (P\setminus C_n)\cup((P\cap C_{n-\mathrm{sgn}\ n})+\mathrm{sgn}\ n) & n\notin P\end{cases}. \tag{3.130}$$

Riemann surface $\mathcal{R}^A$

We now consider the Riemann surface $\mathcal{R}^A$, covering the domain $\mathbb{D}^A$, to which the branches of χ^A and η^A are lifted as single valued functions. As we can see, operators $A^n_{\rm l|r}$ (3.85)-(3.86) for the maximal current phase and $A^n_{0,\rm l|r}$ (3.127)-(3.128) for the MC/HD crossover are in fact identical. The same symmetry of the solutions of (3.1) and (3.2) under translations on the right sector $\mathrm{Re}\, v > 0$ mentioned in the two previous cases also exist for χ^A and η^A. Thus, we look for a canonical representative of the orbits of finite subsets of integer under the right translation group $\mathfrak{t}_r$.

Using the shorthand notations $T_{\rm r} = T_{\rm r}^{-1}$, $T_{\rm m} = T_{\rm m}^{-1}$, $T_{\rm l} = T_{\rm l}^{-1}$, we also denote by $O_P = \mathfrak{h}_r P$ the orbit of set P. The existence for any $P \subset \mathbb{Z}$ of a single $P^* \in O_P$ such that $|P^*|_+ = |P^*|_-$ has already been proved for the case of $\mathcal{R}^{\rm MC}$, as operators $T_{\rm r}$ have the same expression in both contexts. Defining

$$\mathbb{P}^0 = \{P \subset \mathbb{Z}, 0 \in P^*\}\,, \tag{3.131}$$

$$\mathbb{P}^* = \{P \subset \mathbb{Z}, 0 \notin P^*\}\,. \tag{3.132}$$

we now prove that $\mathbb{P}^*$ is globally stable under the action of analytic continuation operators $A^n_{\psi|0,r|l}$. Due to the relations (3.34)-(3.37) connecting translation and analytic continuations, we only need to prove that $\mathbb{P}^*$ is stable under the action of $T_{\rm m}$ and $T_{\rm l}$.

We observe from (3.87) that $0 \in P^*$ is equivalent to $0 \in P$ (respectively $0 \notin P$) if $|P_+| - |P_-|$ is even (resp. odd). Under the replacement $P \to T_{\rm m}^{-1}P$, $|P_+| - |P_-|$ is left unchanged if $0 \notin P$ and is decreased by one otherwise, which proves the stability under $T_{\rm m}$.

Similarly, writing down the action of $T_{\rm l}$ on a set $P \in \mathbb{P}^*$, wee see that in every case, under the replacement $P \to T_{\rm m}^{-1}P$, $|P_+| - |P_-|$ is left unchanged or decreased by two, which concludes the proof. The collections of sets $\mathbb{P}^0$ and as a consequence its complement $\mathbb{P}^*$ are thus stable under the action of analytic continuation operators so that the associated Riemann surfaces $\mathcal{R}^A_0$ and $\mathcal{R}^A_*$ form two disjoint components of $\mathcal{R}^A$. We can thus, as in the MC case, index solutions for the eigenvalue $E(\mu)$ by finite sets $P \subset \mathbb{Z}^*$ with as many positive as negative elements, corresponding to sheets of $\mathcal{R}^A_*$.

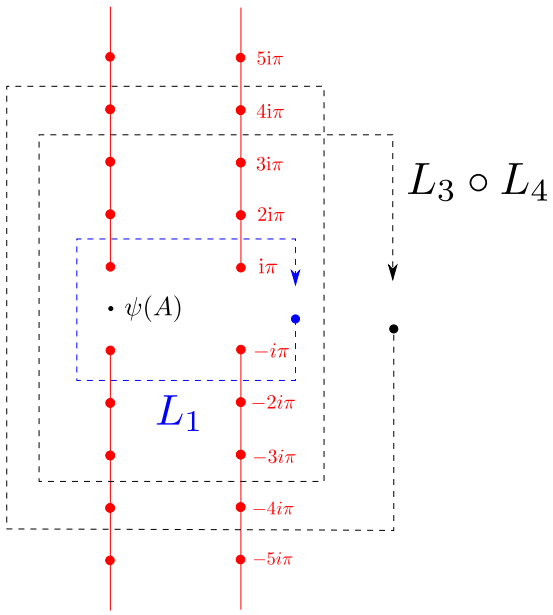

Figure 3.11: Representation of the path corresponding to the action of operator L_n (3.133)

.

We will now prove that the Riemann surface $\mathcal{R}_*^A$ representing physical solutions to equations (3.1) and (3.2) is connected for $0 \leq A < \infty$. Since the structure of the Riemann surface $\mathcal{R}^A$ is similar to that of $\mathcal{R}^{\rm MC}$ in the vicinity of the cuts at $\mathrm{Re}\, v = 0$, the connected components $\mathcal{C}_k$, indexed by sets $P \in C_k$ defined by (3.89) are also defined by the same sets of integers in $\mathcal{R}_*^A$ and are each connected. To prove that $\mathcal{R}_*^A$ itself is connected, we just need to prove that the base domain $P =$ is connected to a sheet in each $\mathcal{C}_k$. Let us define the operator

$$L_n = A_{0,\mathrm{l}}^n A_{\psi,\mathrm{l}}^n A_{\psi,\mathrm{r}}^{-n} A_{0,\mathrm{r}}^{-n} \tag{3.133}$$

which correspond to the analytic continuation of χ_P^A along a path represented in figure 3.11. Recaling the definition of P_k from (3.90), we know that $P_k \in C_k$ so that the corresponding sheet belongs the collection of sheets $\mathcal{C}_k$. The set P_k is obtained from the empty set as

$$P_k = L_1 \circ L_2 \circ ... \circ L_n \, \emptyset \, , \tag{3.134}$$

so that all components $\mathcal{C}_k$ are connected to each other, which proves the connectedness of $\mathcal{R}_*^A$.

Limits of χ^A, η^A and $\mathcal{R}^A$ for $A \to 0$ and $A \to \infty$

We expect the family of Riemann surfaces $\{\mathcal{R}^A, 0 \leq A < \infty\}$ to interpolate between the two surfaces $\mathcal{R}^{\rm Per}$ for $A \to 0$ and $\mathcal{R}^{\rm MC}$ for $A \to \infty$ [6].

Let us first consider the case $A \to 0$. We make the change of variable $y = 2\sqrt{t}$ in the integrals (3.91) and (3.92) defining functions η^A and χ^A. Using the identity

$$\int_0^\infty \mathrm{d}t \frac{t^{s-1}}{\mathrm{e}^{t-v}-1} = \Gamma(s)\mathrm{Li}_s(\mathrm{e}^v) \tag{3.135}$$

where Γ is the Euler gamma function, we obtain for $A = 0$ in terms of the variable $c = v/(2\pi)$

$$\eta^0(c) = 2\sqrt{\pi}\,\mathrm{Li}_{3/2}(-\mathrm{e}^{2\pi c}) \tag{3.136}$$

$$\chi^0(c) = 12\sqrt{\pi}\,\mathrm{Li}_{5/2}(-\mathrm{e}^{2\pi c}) \, . \tag{3.137}$$

[6] These two cases corresponding respectively to the periodic TASEP and the open TASEP in the maximal current. This correspondence is expected from the similarity of the Bethe equations of the periodic TASEP at half filling and of the open TASEP on the MC/HD boundary

For $A = 0$, the functions Ω_j^A become

$$\Omega_j^0(z) = \log(-z/4) + 2\mathrm{i}\pi(j + 1/2) \; . \tag{3.138}$$

For $j \neq 0$ the functions $y_j^A(v)$ write

$$y_j^0(c) = -\mathrm{sgn}(j)\sqrt{2\pi}\sqrt{c + \mathrm{i}\left(j - \mathrm{sgn}(j)\frac{1}{2}\right)} \; , \tag{3.139}$$

and for $j = 0$, $y_j^0(v) \to 0$. Thus, the function $\chi_\emptyset^A(v)$ (resp. $\eta_\emptyset^A(v)$) have limits $\chi_\emptyset^{\mathrm{Per}}(v)$ (resp. $\chi^{\mathrm{Per}'}(v)$) when $A \to 0$. Looking now at the structure of the Riemann surface $\mathcal{R}^A$, the function $\psi(A)$ defined in (3.103) is negative and monotonically goes to 0 when $A \to 0$, so that the two lines of branch cuts of η_P^A and χ_P^A collapse into one. Analytic continuations across the resulting cuts are realized by the product of operators $A_{0,\mathrm{r}}^n A_{\psi,\mathrm{r}}^n$ and $A_{\psi,\mathrm{l}}^n A_{0,\mathrm{l}}^n$ corresponding to continuations along a path crossing to successive branch cuts. For any finite $P \subset \mathbb{Z}$, one gets

$$A_{0,\mathrm{r}}^n A_{\psi,\mathrm{r}}^n P = A_{\psi,\mathrm{l}}^n A_{0,\mathrm{l}}^n P = \begin{cases} P \ominus C_n & n \text{ odd} \\ P \ominus B_n & \text{otherwise} \end{cases} \; , \tag{3.140}$$

where $\ominus$ is the symmetric difference, and $C_n = B_n \cup \{0\}$. Since $y_0^A(v) \to 0$ when $A \to 0$, then the branches $\chi_{P\cup\{0\}}^A$ (respectively $\eta_{P\cup\{0\}}^A$) are equal to χ_P^A (respectively η_P^A) in this limit, so that (3.140) coincides with the action of $A_{\mathrm{r}}^n = A_{\mathrm{l}}^n$ on the branches of χ^{Per} for $A = 0$.

Considering now the limit $A \to \infty$, we saw that the analytic continuation through the cuts at $\mathrm{Re}\, v = 0$ is similar for $\mathcal{R}^{\mathrm{MC}}$ and $\mathcal{R}^A$. Since $\psi(A) \to -\infty$ when $A \to \infty$, the second set of branch cuts of $\chi_P^A(v)$ and $\eta_P^A(v)$ disappears (it gets identified as the point at infinity on each sheet), and the structure of $\mathcal{R}^{\mathrm{MC}}$ is recovered. Since the path through the cuts at $\mathrm{Re}\, v = \psi(A)$ do not exist anymore when $A \to \infty$, the Riemann surface indeed get split in an infinite number of connected components $\mathcal{C}_k$.

Chapter 4

Asymptotics computation of the spectral gaps of the exclusion process

We have reviewed in chapter 2 the methods used to obtain, both in the periodic and open cases, exact expressions for the eigenvalues and eigenstates of the TASEP deformed Markov matrix $M(\mu)$ in finite size. These expressions are written in terms of the solutions to the polynomial Bethe equation. We dispose moreover of explicit expressions for the ground state eigenvalue of $M(\mu)$. In this chapter, we will compute the asymptotic of these expression in the large system size limit.

In the first part of the chapter we compute the large system size limit of the ground state eigenvalues (2.209)–(2.210) of the open TASEP in the maximal current phase and at the MC/HD boundary. We will in particular recover the expressions of functions χ^{Per}, χ^{MC} and χ^{A} which were the object of all attention in chapter 3. The second part of the chapter is devoted to the asymptotic analysis of the Bethe roots solutions to the Bethe equations (2.181), from which a complete classification of the spectral gaps of $M(\mu)$ in the thermodynamic limit will be deduced, and related to the analytic structure constructed in chapter 3.

4.1 Asymptotics of the ground state eigenvalues

4.1.1 Ground state of the periodic TASEP

We have recalled in section 2.2 the expression of the ground state eigenvalue $E(\mu)$ of the deformed Markov matrix $E(\mu)$ of the periodic TASEP under the form of a parametric equation involving two series in a parameter B:

$$\mu = -\sum_{k=1}^{\infty} \binom{kL}{kN} \frac{B^k}{k} , \tag{4.1}$$

$$E(\mu) = -\sum_{k=1}^{\infty} \binom{kL-2}{kN-1} \frac{B^k}{k} . \tag{4.2}$$

We mentioned in 2.3.5 that the spectrum of the open TASEP at the boundaries of the maximal current phase is a subset of that of the periodic TASEP at half-filling, so we will restrict ourselves to the case $N = L/2$ to keep notations light. Being interested in the large system size limit of $E(\mu)$, as it is the case relevant to KPZ universality, we first compute the asymptotic equivalent of the coefficients of these sums using the Stirling equivalent of the factorial $n! \sim \sqrt{2\pi n} n^n \mathrm{e}^{-n}$. It is straightforward to check that for $L \to \infty$,

$$\mu \simeq -\frac{1}{2\sqrt{\pi L}} \sum_{k=1}^{\infty} \frac{B^k}{k^{3/2}} , \tag{4.3}$$

$$E(\mu) - \frac{\mu}{4} \simeq \frac{1}{\sqrt{\pi} L^{3/2}} \sum_{k=1}^{\infty} \frac{B^k}{k^{5/2}} . \tag{4.4}$$

We recognize the polylogarithm functions $\mathrm{Li}_s(z) = \sum_{k=1}^{\infty} z^k/k^s$. With the change of variable $B = -\mathrm{e}^v$, we define the function that we already studied in chapter 3,

$$\chi^{\mathrm{Per}}(v) = \frac{1}{\sqrt{2\pi}}\mathrm{Li}_{5/2}(-\mathrm{e}^v) \ , \tag{4.5}$$

so that the parametric expression of $E(\mu)$ writes

$$\mu = \frac{1}{\sqrt{2L}}\chi^{\mathrm{Per}\prime}(v) \ , \tag{4.6}$$

$$E(\mu) - \frac{\mu}{4} = \frac{\sqrt{2}}{L^{3/2}}\chi^{\mathrm{Per}}(v) \ . \tag{4.7}$$

4.1.2 Ground-state of the open TASEP in the maximal current phase

We recall the parametric expression of the ground state eigenvalue $E(\mu)$ of the open TASEP for $\alpha = \beta = 1$ stated in section 2.3

$$\mu = -\sum_{k=1}^{\infty} \frac{(2k)!}{k!}\frac{[2k(L+1)]!}{[k(L+1)]![k(L+2)]!}\frac{B^k}{2k} \ , \tag{4.8}$$

$$E(\mu) = -\sum_{k=1}^{\infty} \frac{(2k)!}{k!}\frac{[2k(L+1)-2]!}{[k(L+1)-1]![k(L+2)-1]!}\frac{B^k}{2k} \ . \tag{4.9}$$

This expression was obtained in two different ways. First, using the separability [1] of the conjectural Bethe equations (2.181), its was possible to write $E(\mu)$ and μ as contour integrals on the unit circle, assuming that all Bethe roots were located therewithin. The same expression was also obtained before [44, 56] by explicit construction of a Q operator in [57]. As explained in the introduction, $E(\mu)$ is by construction the scaled cumulant generating function of the current in the TASEP chain. One can immediately use these expression to compute the first cumulants of the integrated current Q_t by eliminating the parameter B at the appropriate order between equations (4.8) and (4.9). One obtains for instance [56]

$$\lim_{t\to\infty} \frac{\langle Q_t\rangle}{t} = \frac{L+2}{2(2L+1)} \tag{4.10}$$

$$\lim_{t\to\infty} \frac{\langle Q_t^2\rangle - \langle Q_t\rangle^2}{t} = \frac{3}{2}\frac{(4L+1)![L!(L+2)!]^2}{[(2L+1)!]^3(2L+3)!} \tag{4.11}$$

$$\lim_{t\to\infty} \frac{1}{t}\left\langle \left(\frac{Q_t - \langle Q_t\rangle}{\langle Q_t^2\rangle - \langle Q_t\rangle}\right)^3 \right\rangle = 12\frac{[(L+1)!]^2[(L+2)!]^4}{(2L+1)[(2L+2)!]^3}\left[9\frac{(L+1)!(L+2)!(4L+2)!(4L+4)!}{(2L+1)![(2L+2)!]^2[(2L+4)!]^2}\right. \tag{4.12}$$

$$\left. - 20\frac{(6L+4)!}{(3L+2)!(3L+6)!}\right]$$

Aiming at the computation of the cumulant generating function of the current in the thermodynamic limit, we will take the asymptotic equivalent when $L \to \infty$ of these expressions. We compute the asymptotic equivalent of the coefficients in sums (4.8) and (4.9) using again Stirling's equivalent of the factorial:

$$\mu = -\frac{L^{-1/2}}{2\sqrt{\pi}}\sum_{k=1}^{\infty}\frac{(2k)!}{k!k^{k+3/2}}B^k \tag{4.13}$$

$$E - \frac{\mu}{4} = \frac{L^{-3/2}}{8\sqrt{\pi}}\sum_{k=1}^{\infty}\frac{(2k)!(k+1/2)}{k!k^{k+5/2}}B^k \tag{4.14}$$

$$E - \left(\frac{1}{4} + \frac{1}{4L}\right)\mu = \frac{L^{-3/2}}{8\sqrt{\pi}}\sum_{k=1}^{\infty}\frac{(2k)!k}{k!k^{k+5/2}}B^k \tag{4.15}$$

[1] Also sometimes referred to as the *mean-field* or *decoupled* character of the Bethe equations, as each root depends solely on a global symmetric functions of all others.

where all common powers to the k in both equalities have been incorporated into B. Using the change of variable [2] $B = -\mathrm{e}^{v+1}/4$, we define the function

$$\chi(v) = -\frac{1}{4\sqrt{\pi}} \sum_{k=1}^{\infty} \frac{(2k)!}{k! k^{k+5/2}} (-\mathrm{e}^{v+1}/4)^k \ , \tag{4.16}$$

so that at leading order when $L \to \infty$, the parametric equation giving the ground state eigenvalue writes

$$\mu \simeq \frac{2\,\chi'(v)}{\sqrt{L}} \ , \tag{4.17}$$

$$E - \Big(\frac{1}{4} + \frac{1}{4L}\Big)\mu \simeq \frac{\chi(v)}{4\,L^{3/2}} \ . \tag{4.18}$$

The series (4.16) is convergent only for Re $v < 0$. A first step in the analytic continuation of χ is then to find an alternate representation of the function coinciding with (4.16) on the negative complex half plane. The combinatoric coefficients in the series expansion of χ can be written in terms of a Gaussian integral. Using the fact that for even $n \in \mathbb{N}^*$,

$$\int_{-\infty}^{\infty} y^n \mathrm{e}^{-ay^2} \mathrm{d}y = \frac{\Gamma\left(\frac{n+1}{2}\right)}{a^{\frac{n+1}{2}}} \tag{4.19}$$

one gets, wherever the left hand side is defined

$$-\sum_{k=1}^{\infty} \frac{(2k)!}{k! k^{k+5/2}} (-\mathrm{e}^{v+1}/4)^k = 2 \sum_{k=1}^{\infty} \int_{-\infty}^{\infty} (1-y^2) y^{2k} \mathrm{e}^{-ky^2} \mathrm{d}y \ (-\mathrm{e}^{v+1}/4)^k \tag{4.20}$$

and, permuting the sum and integral,

$$\chi(v) = -\frac{1}{2\pi} \int_{-\infty}^{\infty} \mathrm{d}y \ (1-y^2) \log\left(1 + y^2 \mathrm{e}^{1-y^2+v}\right) \tag{4.21}$$

where the integral on the right hand side is well defined and analytic for $v \in \mathbb{C} \setminus \{\mathbb{R}^+ + 2\mathrm{i}\pi(n+1/2), n \in \mathbb{Z}\}$. Finally, integrating by part, $\chi(v)$ writes

$$\chi(v) = \frac{1}{3\pi} \int_{-\infty}^{\infty} \mathrm{d}y \, \frac{(1-y^2)(3-y^2)}{1 + y^{-2}\,\mathrm{e}^{y^2-v-1}} \tag{4.22}$$

which is the representation used in chapter 3, from which function $\chi_\emptyset$ is computed.

4.1.3 Ground-state of the open TASEP at the edge of the maximal current phase

As explained in 1.7, a solution of the KPZ equation on a finite interval is built from the ASEP with open boundary conditions under the weak asymmetry scaling $p - q \sim 1/\sqrt{L}$. The Neumann boundary conditions for the KPZ height function are fixed by the boundary parameters of the ASEP as specified by the scaling (1.142). The scaling of the boundary parameters α, β and of the bulk parameters p and q can be in fact set independently, so that taking the totally asymmetric $q = 0$ limit within the bulk and keeping a dependency in L in the boundary rates, we choose the following scaling

$$\alpha = \frac{1}{2} + \sqrt{\frac{A}{4L}} \ , \qquad \beta = \frac{1}{2} + \sqrt{\frac{B}{4L}} \ . \tag{4.23}$$

It corresponds, on the phase diagram of TASEP to a crossover between the maximal current phase and the triple point $\alpha, \beta = 1/2$ joining the three phases of the system. One should note that the parameters A and B are not directly related to the parameters $\tilde{A}$ and $\tilde{B}$ of (1.142). In terms of the ASEP height function, the slope at the left and right boundaries $\partial_X h(X = 0, T)$ and $\partial_X h(X = 1, T)$

[2] The shit $+1$ in the exponential ensures, for convenience, that the branch points of χ are on the imaginary line.

are increasing functions of A and B respectively. This choice of parameters correspond to a height function described by the KPZ fixed point with general Neumann boundary conditions.

As explained in chapter 2, the general form of $E(\mu)$, valid whenever the parameters $a = 1/\alpha - 1$, $b = 1/\beta - 1$ and 0 are located within the unit disk is

$$\mu = \frac{1}{2}\oint_{|z|=1} \frac{\mathrm{d}z}{2i\pi z} \log(1 - ZF(z)) \,, \tag{4.24}$$

$$E = \frac{1}{2}\oint_{|z|=1} \frac{\mathrm{d}z}{2i\pi(1+z)^2} \log(1 - ZF(z)) \,. \tag{4.25}$$

The function F here is defined by (2.57), and these expression were independently obtained by modified Bethe ansatz and Q-operator method (the same function F appears in both derivations, up to a sign)[3]. Parameters a and b are indeed in the interior of the integration contour as $A, B > 0$. Integrating by part and using changing the parameter $Z \to 4^L Z$, one gets

$$\mu = -\frac{1}{2}\int_{|z|=1} \frac{\mathrm{d}z}{2\pi} \log(z) \frac{-ZF'(z)}{4^L - Z} \,, \tag{4.26}$$

$$E(\mu) = -\frac{1}{2}\int_{|z|=1} \frac{\mathrm{d}z}{2\pi(1+z)} \frac{-ZF'(z)}{4^L - Z} \,. \tag{4.27}$$

These integrals are dominated in the large L limit by the value they take close to $z = 1$ on a support scaling like $z - 1 \sim L^{-1/2}$, so that with the change of variable $z = 1 + \mathrm{i}y/\sqrt{L}$, and function F being asymptotically equivalent to

$$F(z) \simeq -\frac{4y^2 \mathrm{e}^{\frac{y^2}{4}}}{(y-4A)(4A+y)(y-4B)(4B+y)} \tag{4.28}$$

these integrals can be evaluated at leading order for $L \to \infty$ as

$$\mu \simeq -\frac{1}{4\pi\sqrt{L}}\int_{-\infty}^{\infty} \mathrm{d}y \left(1 + \frac{y^2}{3L}\right) \frac{\left(\frac{16i\sqrt{A}}{y-4i\sqrt{A}} - \frac{16i\sqrt{A}}{y+4i\sqrt{A}} + \frac{16i\sqrt{B}}{y-4i\sqrt{B}} - \frac{16i\sqrt{B}}{y+4i\sqrt{B}} + 2y^2 + 8\right)}{\frac{e^{\frac{y^2}{4}}((4\sqrt{A}-iy)(4\sqrt{A}+iy)(4\sqrt{B}-iy)(4\sqrt{B}+iy))}{Zy^2} - 4} \tag{4.29}$$

$$E(\mu) \simeq -\frac{1}{4\pi\sqrt{L}}\int_{-\infty}^{\infty} \mathrm{d}y \left(\frac{1}{4} + \frac{y^2}{16L}\right) \frac{\left(\frac{16i\sqrt{A}}{y-4i\sqrt{A}} - \frac{16i\sqrt{A}}{y+4i\sqrt{A}} + \frac{16i\sqrt{B}}{y-4i\sqrt{B}} - \frac{16i\sqrt{B}}{y+4i\sqrt{B}} + 2y^2 + 8\right)}{\frac{e^{\frac{y^2}{4}}((4\sqrt{A}-iy)(4\sqrt{A}+iy)(4\sqrt{B}-iy)(4\sqrt{B}+iy))}{Zy^2} - 4} \,. \tag{4.30}$$

In order to make further computation simpler, we take the limit $B \to \infty$, so that we consider the system in the vicinity of the low density/maximal current phase boundary. In terms of KPZ height function, we let the left boundary slope take any value. We also make the change of parameter

$$Z = -16B^2(1 + A^2)\mathrm{e}^{v + v_0^A} \,, \tag{4.31}$$

with

$$v_0^A = \frac{2\sqrt{A}}{\sqrt{A} + \sqrt{A+4}} - 2\log\left(\frac{2\sqrt{A+4}}{\sqrt{A} + \sqrt{A+4}}\right) \,, \tag{4.32}$$

to ensure that our expressions have a finite limit in both limits $A \to 0$ and $A \to \infty$ and that the final functions χ^A and η^A have their branch points on the imaginary line as in the MC case. Defining

$$\eta^A(v) = \int_{-\infty}^{\infty} \mathrm{d}y \frac{(A+4)y^2\left(4A\left(y^2-4\right)+y^4\right)}{2\left(4A+y^2\right)\left(\left(4A+y^2\right)e^{-v-v_0^A+\frac{y^2}{4}} + (A+4)y^2\right)} \,, \tag{4.33}$$

$$\chi^A(v) = \frac{1}{16}\int_{-\infty}^{\infty} \mathrm{d}y \frac{(A+4)y^4\left(4A\left(y^2-4\right)+y^4\right)}{2\left(4A+y^2\right)\left(\left(4A+y^2\right)e^{-v-v_0^A+\frac{y^2}{4}} + (A+4)y^2\right)} \,. \tag{4.34}$$

[3]We denote by Z the dummy parameters in equations (4.24)–(4.25) that was previously written B to avoid ambiguities with the scaling parameter corresponding to the boundary rate β

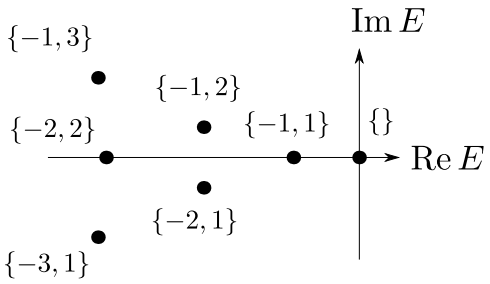

Figure 4.1: Plot of the first spectral gaps of the open TASEP for $\alpha = \beta = 1$ in the complex plane with the corresponding labeling set P of the branch of χ^{MC} appearing in equations (4.37)-(4.38).

the asymptotic expression of the ground state eigenvalue in the phase crossover scaling of the left boundary rate is

$$\mu \simeq \frac{\eta^A(v)}{4\pi\sqrt{L}} , \tag{4.35}$$

$$E - \frac{\mu}{4} \simeq \frac{\chi^A(v)}{12\pi L^{3/2}} , \tag{4.36}$$

so that we recover the functions η^A and χ^A studied in chapter 3. One also checks that when $A \to \infty$, the relations (4.29) and (4.30) reduce to their analogue (4.17) and (4.18) in the maximal current phase. Similarly, considering the limit $A \to 0$, up to a change of parameter $v \to 2\pi v$, (4.29) and (4.30) have limits expressions (4.6) and (4.7) which are their analogue for the periodic TASEP at half-filling with zero total momentum. This result is expected from the fact, noted in section 2.3.5, that the spectral gaps of the open TASEP on the transition line between low density and maximal current phases is a subset of that of the periodic TASEP.

4.1.4 Spectral gaps from analytic continuation

We now dispose of the ground state eigenvalues of matrices $M(\mu)$ in the large L limit. In this limit, the eigenvalues of $M(\mu)$ follow various scaling with respect to the system size. Among the $\mathrm{e}^{\kappa L}$ eigenstates of $M(\mu)$ – where κ depends on the geometry and filling of the system – the extensive part scales proportionally to L, forming the *bulk* of the eigenvalues [75]. Other subsets of the spectrum of $M(\mu)$ follow different scaling. Of special interest to us are the *spectral gaps* of $M(\mu)$, which are the first eigenvalues larger than the ground state in real part and scaling like $L^{-3/2}$. They form a discrete subset of the spectrum $M(\mu)$, and as noted in chapter 1, they are the relevant eigenstates on the KPZ time scale $t \sim L^{3/2}$.

We observe that all spectral gaps of $M(\mu)$ in the three contexts considered can be obtained by solving the above-derived parametric equations, substituting the functions χ^{Per}, χ^{MC} and χ^A by other branches χ_P^{Per}, χ_P^{MC} and χ_P^A respectively of their analytic continuations. The ground state corresponds, given the way we defined these functions, to the indexing set $P = \emptyset$. Let us consider the example of the open TASEP in the maximal current phase. For any $P \subset \mathbb{Z}^*$ with the same number of positive and negative elements and $\mu \in \mathbb{R}$, we observe that there exist a single solution to the parametric equation

$$\mu_P \simeq \frac{2\,\chi_P^{\mathrm{MC}\prime}(v)}{\sqrt{L}} , \tag{4.37}$$

$$E_P(\mu) - \Big(\frac{1}{4} + \frac{1}{4L}\Big)\mu_P \simeq \frac{\chi_P^{\mathrm{MC}}(v)}{4\,L^{3/2}} . \tag{4.38}$$

such that $E_P(\mu)$ is a higher spectral gap of $M(\mu)$ for $L \to \infty$, see figure 4.1. In particular the first gap

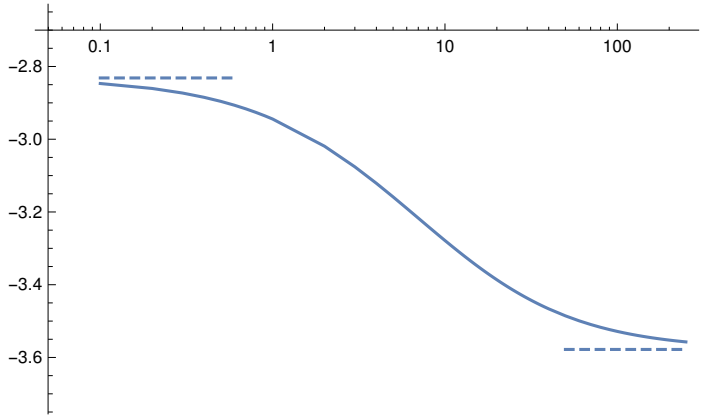

Figure 4.2: Plot of the value of the first gap e_1 of the deformed Markov matrix in the LD/MC crossover for $P = \{-1, 1\}$ as a function of A. The horizontal dashed lines are the asymptotic values of e_1 for $A \to 0$ (left) and $A \to \infty$ (right) corresponding respectively to the second largest real value of the periodic $M(\mu)$ (which is not strictly speaking the gap of the process as the eigenvalues with second largest real part are two complex conjugates) and the gap of the maximal current TASEP, also solution to (4.37)–(4.38) with $P = \{-1, 1\}$.

E_1 of the process is obtained with the label $P = \{-1, 1\}$, with functions χ and χ' writing explicitly

$$\chi_{\{-1,1\}}(v) = \chi(v) + 2\left(\frac{(W_1(\mathrm{e}^{-1-v}))^{3/2}}{3} + \sqrt{W_1(\mathrm{e}^{-1-v})}\right) + 2\left(\frac{(W_{-1}(\mathrm{e}^{-1-v}))^{3/2}}{3} + \sqrt{W_{-1}(\mathrm{e}^{-1-v})}\right) \tag{4.39}$$

$$\chi'_{\{-1,1\}}(v) = \chi'(v) - \sqrt{W_1(\mathrm{e}^{-1-v})} - \sqrt{W_{-1}(\mathrm{e}^{-1-v})}\,. \tag{4.40}$$

Solving (4.37) and (4.38) with these branches for $\mu = 0$ gives $E_1 = e_1 L^{-3/2}$ with $e_1 \approx -3.5780646$, which matches perfectly the numerical value obtained by de Gier and Essler in [39] by solving numericaly the Bethe ansatz equations. Similarly, the spectral gaps of $M(\mu)$ on the edge of the maximal current phase satisfy the following equations

$$\mu_P \simeq \frac{\eta_P^A(v)}{4\pi\sqrt{L}}\,, \tag{4.41}$$

$$E_P - \frac{\mu_P}{4} \simeq \frac{\chi_P^A(v)}{12\pi L^{3/2}}\,. \tag{4.42}$$

They are continuous functions of A and are converging to spectral gaps of the periodic ASEP with zero momentum when $A \to 0$ and to the spectral gaps on the maximal current open TASEP with $\alpha = 1/2$, $\beta = 1$ for $A \to \infty$. See figure 4.2 for a plot of the gap of $M(\mu)$ as a function of A. In what follows, we will justify these results from Bethe ansatz in the maximal current open TASEP case.

Analogous result were already known [70] for the periodic case in terms of the function χ^{Per}. The spectral gaps with zero total momentum of $M(\mu)$ for the periodic TASEP at half-filling $N = L/2$ verify

$$\mu_P = \frac{1}{\sqrt{2L}}\chi_P^{\mathrm{Per}\prime}(v)\,, \tag{4.43}$$

$$E_P(\mu) - \frac{\mu}{4} = \frac{\sqrt{2}}{L^{3/2}}\chi_P^{\mathrm{Per}}(v)\,. \tag{4.44}$$

with sets $P \subset \mathbb{Z} + \frac{1}{2}$ satisfying the same constraint $|P_+| = |P_-|$. Note that this constraint specifically ensures that the eigenstates obtained have zero total momentum. These eigenstates are the one contributing to the cumulant generating function of the current (1.140). Other spectral gaps may be obtained by allowing more general sets P, however, the branches corresponding to these sets are

not directly related to $\chi_{\emptyset}^{\mathrm{Per}}$ by analytic continuation, as expected from the fact, noted in 3.1.4 that sectors conserved by the dynamics should belong to different connected components of the analytic continuation of eigenstates. Only these gaps are recovered by taking the limit $A \to 0$ in equations (4.41)–(4.42).

4.2 Asymptotics of the Bethe roots for the open TASEP in the maximal current phase

We now compute the Bethe roots u_j, solutions to the Bethe equations (2.181) in the large system size limit, in order to prove the results just stated in terms of analytic continuation. Starting from the Bethe equation obtained by TQ-relation for $1 \leq j \leq L+1$

$$u_j^L(u_j+b)(u_j+a)(au_j+1)(bu_j+1) = (-1)^{L+1}\mathrm{e}^{2\mu}(1-u_j)^{2L+2}(u_j+1)^2\prod_{k=1}^{L+2}u_k\ , \tag{4.45}$$

we will first study their solutions for finite L, writing the roots of (4.45) $u_j = \mathfrak{u}_j(C)$ as a function of the parameter $C = -\mathrm{e}^{2\mu}\prod_{k=1}^{L+2}u_k$. We will study the analytic continuation structure of functions $\mathfrak{u}_j$ and find a consistent labeling of the eigenstates for any system size, in correspondence with the labeling of the sheets of $\mathcal{R}^{\mathrm{MC}}$. The value of $E(\mu)$ corresponding to a given set of solutions of the Bethe equation will be obtained by fixing C as a function of μ. As a byproduct, we will show that this indexing of eigenstates has a physical interpretation in terms of fermionic pseudo-particle, as customary for Bethe ansatz integrable models. Finally, we will study the large L asymptotics of the Bethe ansatz expression of the eigenvalues $E(\mu)$, allowing us to recover (4.37)–(4.38).

Labeling of Bethe roots in finite size : functions $\mathfrak{u}_j(C)$ and $\mathfrak{u}_j^*(C)$

Let us define the polynomial

$$R(u,C) = u^L(u+a)(u+b)(au+1)(bu+1) - (-1)^L C(1-u)^{2L+2}(u+1)^2\ , \tag{4.46}$$

the $L+2$ Bethe roots describing an eigenstate of the system are among the solutions to $R(u,C)=0$, which has generically $2L+4$ solutions. All roots belong to the curve

$$\Gamma_C : |u|^L|u+a|\,|u+b|\,|au+1|\,|bu+1| = |C|\,|1-u|^{2L+2}|u+1|^2\ . \tag{4.47}$$

The curve Γ_C has self intersection points in the complex u plane when $R(u,C)=0$ and $\partial_u R(u,C)=0$ simultaneously. For finite C, the solutions for u verify

$$\frac{L}{u}+\frac{1}{u+a}+\frac{1}{u+b}+\frac{1}{u+a^{-1}}+\frac{1}{u+b^{-1}} = \frac{2L+2}{u-1}+\frac{2}{u+1}\ . \tag{4.48}$$

There are six solutions in u, corresponding to pairs of double points occurring for three critical values $C_\pm$ and C_* of the parameter C, see figure 4.3. For $\alpha=\beta=1$, the points $C_\pm$ are zero, and the the critical point C_* has the following scaling with respect to the system size

$$C_* \simeq -\frac{\mathrm{e}\,(1-a)^2(1-b)^2}{4^{L+2}}\Big(L+\frac{3}{2}+\frac{4a}{(1-a)^2}+\frac{4b}{(1-b)^2}\Big)\ , \tag{4.49}$$

which reduces to

$$C_* = -\frac{(L+2)^{L+2}}{4^{L+2}(L+1)^{L+1}} \tag{4.50}$$

when $\alpha=\beta=1$. We observe moreover that for any $\alpha,\beta \geq 1/2$, $C_\pm < C$ and $C_\pm \to 0$ when $L\to\infty$. As we will see next, the values of C corresponding to eigenstates of $M(\mu)$ in the large system size limit will be of order C_* so we will restrict ourselves to the case $\alpha=\beta=1$ in what follows, as the other self-intersections points $C_\pm$ are irrelevant for our purpose.

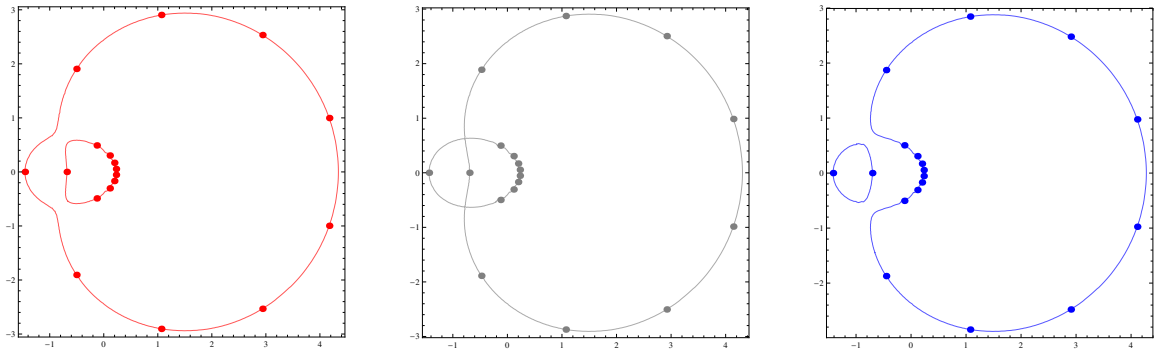

Figure 4.3: Curve Γ_C defined in (4.47), plotted for $L = 7$, $\alpha = \beta = 1$, with $C = 0.9\,C^*$ (left), $C = C^*$ (middle) and $C = 1.1\,C^*$ (right).

For $0 \leq j \leq L+1$ we now introduce the functions $\mathfrak{u}_j(C)$ and $\mathfrak{u}_j^*(C)$ as the the $2L+4$ roots of $R(u, C) = 0$, see figure 4.4. These functions are not analytic as varying C will lead to permutations of roots (in particular, changing the phase of C for constant $|C|$ causes a circular permutations of the roots along the closed components of Γ_C). The branch points of $\mathfrak{u}_j$ and $\mathfrak{u}_j^*$ correspond to the multiple points of Γ_C, which happen for $C \in \{\infty, C_*, 0\}$, where $C_* < 0$, so that we can take the branch cuts of the $\mathfrak{u}_j$ and $\mathfrak{u}_j^*$ to be the intervals $(-\infty, C_*]$ and $[C_*, 0]$.

To fix the labeling of the roots we first consider the small C behaviour of the Bethe roots for $\alpha = \beta = 1$. Considering (4.45) in the limit $C \to 0$, $L+2$ roots go to zero while $L+2$ go to infinity with a phase that is a roots of unity. We choose to set

$$\mathfrak{u}_j \underset{C\to 0}{\simeq} C^{\frac{1}{L+2}} \mathrm{e}^{\frac{2\mathrm{i}\pi j}{L+2}} \tag{4.51}$$

$$\mathfrak{u}_j^* \underset{C\to 0}{\simeq} C^{-\frac{1}{L+2}} \mathrm{e}^{-\frac{2\mathrm{i}\pi j}{L+2}} \tag{4.52}$$

where fractional powers are understood with branch cut $\mathbb{R}^-$. Away from the branch cuts, these asymptotic expressions can be extended for any $\alpha, \beta > \frac{1}{2}$ by continuity. Considering now the large C asymptotics of the roots,

$$\begin{aligned}
1 + \mathfrak{u}_0(C) &\underset{C\to\infty}{\simeq} \frac{(1-a)(1-b)}{2^{L+1}\sqrt{C}} \\
1 + \mathfrak{u}_0^*(C) &\underset{C\to\infty}{\simeq} -\frac{(1-a)(1-b)}{2^{L+1}\sqrt{C}} \\
1 - \mathfrak{u}_j(C) &\underset{C\to\infty}{\simeq} \frac{\mathrm{e}^{-\frac{2\mathrm{i}\pi(j-1-L/2)}{2L+2}}}{(4\alpha^2\beta^2 C)^{\frac{1}{2L+2}}} \qquad \text{for } j = 1, \ldots, L+1 \\
1 - \mathfrak{u}_j^*(C) &\underset{C\to\infty}{\simeq} \frac{\mathrm{e}^{-\frac{2\mathrm{i}\pi(j+L/2)}{2L+2}}}{(4\alpha^2\beta^2 C)^{\frac{1}{2L+2}}} \qquad \text{for } j = 1, \ldots, L+1\,.
\end{aligned} \tag{4.53}$$

We can now explicit the analytic continuations of the $\mathfrak{u}_j$ and $\mathfrak{u}_j^*$ across their branch cuts. We denote by $\mathcal{A}_{\text{in}}$ the analytic continuation from above the cut $[C_*, 0]$ and by $\mathcal{A}_{\text{out}}$ from above $(-\infty, C_*]$. We obtain

$$\mathcal{A}_{\text{out}}\mathfrak{u}_j = \mathfrak{u}_{j+1} \qquad 0 \leq j \leq L \tag{4.54}$$

$$\mathcal{A}_{\text{out}}\mathfrak{u}_{L+1} = \mathfrak{u}_0 \qquad j = L+1 \tag{4.55}$$

$$\mathcal{A}_{\text{out}}\mathfrak{u}_j^* = \mathfrak{u}_{j+1}^* \qquad 0 \leq j \leq L \tag{4.56}$$

$$\mathcal{A}_{\text{out}}\mathfrak{u}_{L+1}^* = \mathfrak{u}_0^* \qquad j = L+1 \tag{4.57}$$

and

$$\mathcal{A}_{\text{in}}\mathfrak{u}_0 = \mathfrak{u}_0^* \qquad j=0 \tag{4.58}$$
$$\mathcal{A}_{\text{in}}\mathfrak{u}_0^* = \mathfrak{u}_0 \qquad j=0 \tag{4.59}$$
$$\mathcal{A}_{\text{in}}\mathfrak{u}_j = \mathfrak{u}_{j+1} \qquad 1\leq j\leq L \tag{4.60}$$
$$\mathcal{A}_{\text{in}}\mathfrak{u}_{L+1} = \mathfrak{u}_1^* \qquad j=L+1 \tag{4.61}$$
$$\mathcal{A}_{\text{in}}\mathfrak{u}_j^* = \mathfrak{u}_{j+1}^* \qquad 1\leq j\leq L \tag{4.62}$$
$$\mathcal{A}_{\text{in}}\mathfrak{u}_{L+1}^* = \mathfrak{u}_1 \qquad j=L+1 \tag{4.63}$$

Construction of spectral gaps

Now that we have an identification for all L of the roots of polynomial $R(u,C)$, we can determine the expression of the various spectral gaps of $M(\mu)$ in terms of the $\mathfrak{u}_j(C)$ and $\mathfrak{u}_j^*(C)$. An eigenstate is characterized by the choice of $L+2$ Bethe roots $\{u_j\}_{0\leq j\leq L+1}$ among the $2L+4$ roots $\{\mathfrak{u}_j(C),\mathfrak{u}_j^*(C)\}$, with the eigenvalue

$$E = 1-\frac{\alpha+\beta}{2}+\frac{1}{2}\sum_{j=0}^{L+1}\frac{u_j}{1-u_j}\,. \tag{4.64}$$

There are $\binom{2L+4}{L+2}$ such choices and only 2^L eigenstates of $M(\mu)$ so the relevant choices of roots have to be identified. We take the $2L+2$-th root of the Bethe equations (4.45),

$$\frac{(1-u_j)(1+u_j)^{\frac{1}{L+1}}C^{\frac{1}{2L+2}}}{u_j^{\frac{L}{2L+2}}(u_j+a)^{\frac{1}{2L+2}}(u_j+b)^{\frac{1}{2L+2}}(1+au_j)^{\frac{1}{2L+2}}(1+bu_j)^{\frac{1}{2L+2}}} = \mathrm{e}^{-\frac{2\mathrm{i}\pi k_j}{2L+2}}\,, \qquad 0\leq j\leq L+1 \tag{4.65}$$

where k_j is an integer if L is even and half-integer if L is odd. The fractional powers are still considered with their branch cuts on $\mathbb{R}^-$. The choice of the numbers k_j for each of the $L+2$ Bethe equation thus determines the choice of Bethe roots in the set $\{\mathfrak{u}_j(C),\mathfrak{u}_j^*(C)\}$. Considering the large C of (4.65) limit [4] we can relate the numbers $\{k_j\}_{0\leq j\leq L+1}$ to the labels of roots $\mathfrak{u}_j$ and $\mathfrak{u}_j^*$. In particular, the ground-state eigenvalue for large C writes, for $\alpha=\beta=1$,

$$E \underset{C\to\infty}{\simeq} 2^{\frac{1}{L+1}-1}C^{\frac{1}{2L+2}}\sum_{j=0}^{L+1}\mathrm{e}^{-\frac{\mathrm{i}\pi k_j}{L+1}}\,. \tag{4.66}$$

The sum in this expression is real and has maximal real part for $\{k_j,\ j=1...L+1\}=\{-L/2,-L/2+1,...,L/2-1,L/2\}$ (see figure 4.5), in which case it yields the ground state of $M(\mu)$. It corresponds to a choice of roots $u_0=\mathfrak{u}_0(C)$ and $u_j=\mathfrak{u}_j(C)$ [5]. Interpreting the $\{k_j\}$ as pseudo-momenta of $L+2$ fermionic quasi-particles, the ground state corresponds to a filled *Fermi sea* where the momenta are stacked one upon the other. More generally, every eigenstate of $M(\mu)$ for finite L is defined in terms of a finite set $P\subset\mathbb{Z}^*$ corresponding to the following choice of Bethe roots

$$\begin{aligned} &u_0=\mathfrak{u}_0(C)\\ &u_j=\mathfrak{u}_j(C) \qquad \text{for} \quad j\in[\![1,L+1]\!]\setminus((-P_-)\cup(L+2-P_+))\\ &u_j=\mathfrak{u}_j^*(C) \qquad \text{for} \quad j\in(-P_-)\cup(L+2-P_+)\end{aligned}$$

[4] This is equivalent to take the large μ limit where Bethe roots are known to simplify to roots of (minus) unity, as we noted in section 1.4.3

[5] Since the roots $\{\mathfrak{u}_j(C)\}$ are the $L+2$ roots going to zero for small C, the ansatz we made in 2.3.5 on the position of the Bethe roots for the computation of the ground state is validated.

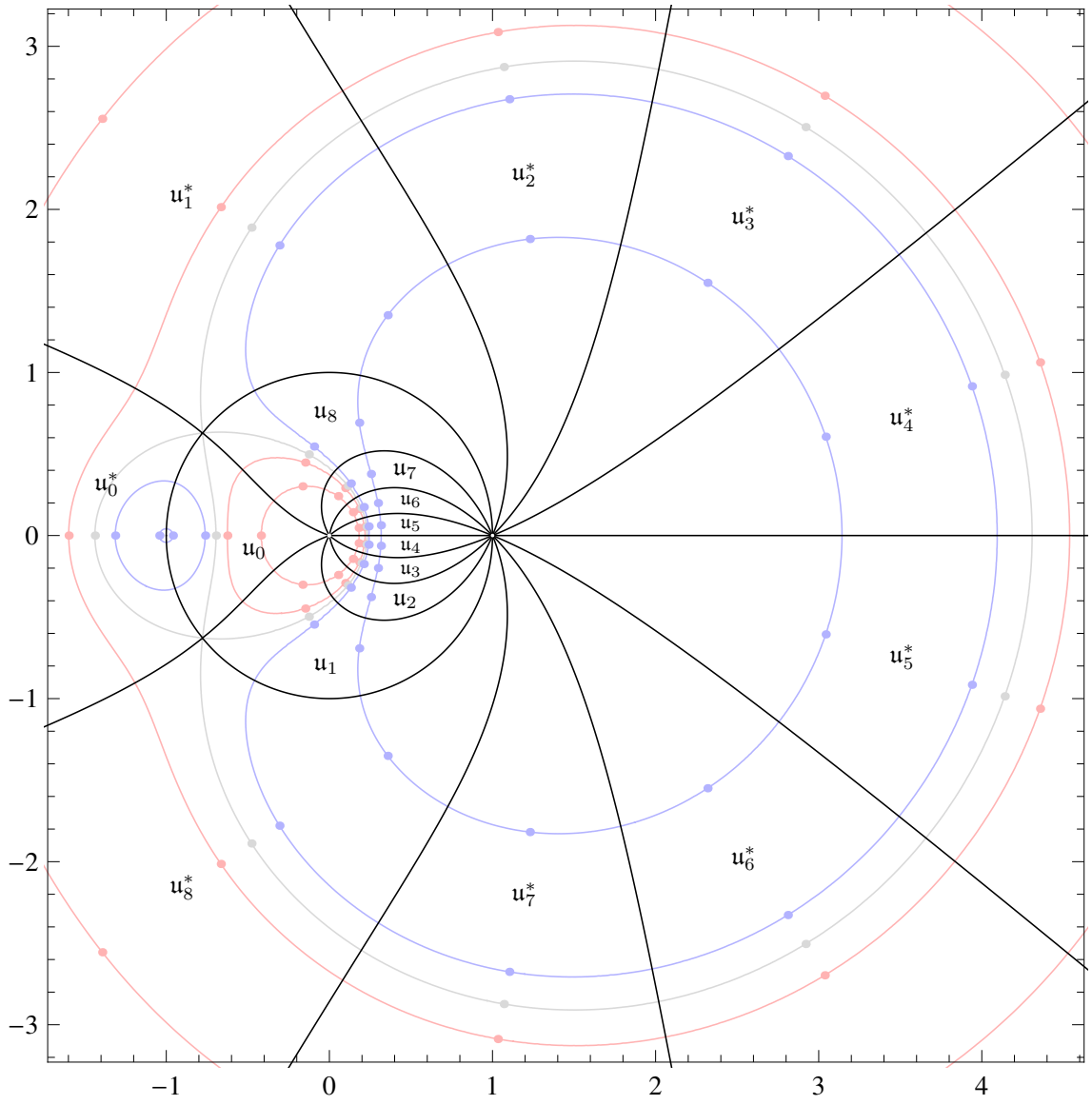

Figure 4.4: Plot of the $2L+2$ solutions u of $R(u,C)=0$ in terms of functions $\mathfrak{u}_j(C)$ and $\mathfrak{u}_j^*(C)$, $j=0,\dots,L+1$ for $L=7$ and $\alpha=\beta=1$. The images $\mathfrak{u}_j(\mathbb{C}\setminus\mathbb{R}^-)$ and $\mathfrak{u}_j^*(\mathbb{C}\setminus\mathbb{R}^-)$ are delimited by the black curves. The lighter, blue, grey and red curves correspond to the curves Γ_C for $|C/C^*|\in\{1/20,1/2,1,2,100\}$ respectively, with C_* defined by (4.50). The dots represent the corresponding solutions of $R(u,C)=0$ with $C>0$.

Figure 4.5: Position on the unit circle of the terms $e^{-2i\pi k_j/(2L+2)}$ for even L. The ground state (left) correspond to the choice $\{k_j,\ j = 1...L+1\} = \{-L/2, -L/2+1, ..., L/2-1, L/2\}$ maximizing the real part of the sum (4.66). The gap (right) is obtained by inverting the extremal k_j at both end of the interval.

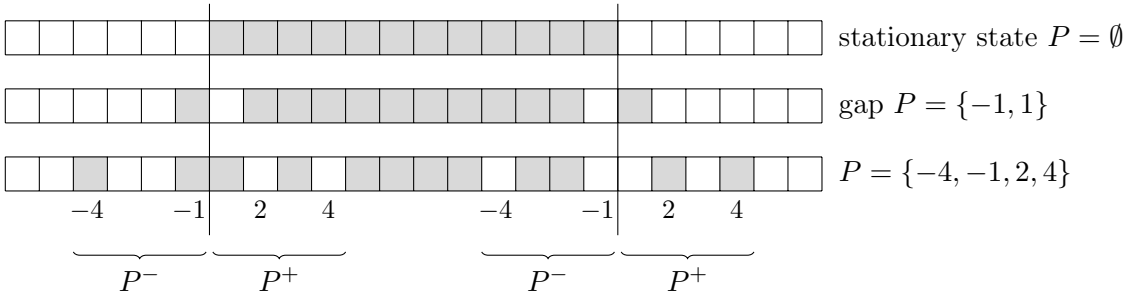

Figure 4.6: Choices of momenta k_j corresponding to some eigenstates of $M(\mu)$. The filled gray square represent the k_j corresponding to selected Bethe roots, and the vertical bars represent the limits $\pm\frac{L}{2}$ of the Fermi sea.

where P_+ and P_- are the subsets of respectively positive and negative elements of P. Thus, the set of the momenta $\{-k_1,\ j = 1...L+1\}$ of the quasi-particles is

$$\Big(\{-L/2, \dots, L/2\} \cup (L/2 + P_+) \cup (-L/2 + P_-)\Big) \setminus \Big((-L/2 - 1 + P_+) \cup (L/2 + 1 + P_-)\Big)\,. \tag{4.67}$$

The elements of P index pairs of excitations and holes in the Fermi sea. We observe moreover from numerical computations (see next section) that in the limit $L \to \infty$, the spectral gaps contributing to the KPZ part of the spectrum scaling in $L^{-3/2}$ are obtained for sets P such that $|P_+| = |P_-|$. This condition implies that the total pseudo-momentum of the quasi particles constituting the eigenstates is zero:

$$\sum_{k=1}^{L+1} k_j = 0 \mod 2L+2\,. \tag{4.68}$$

We see that the spectral gaps of TASEP are obtained as the sum of two contributions, one coming from the filled Fermi sea corresponding to the ground state and the other from the hole-excitations pairs defining higher eigenstates. Splitting the sum (4.64) into both contributions we obtain

$$E = 1 - \frac{\alpha+\beta}{2} + \frac{1}{2}\sum_{j=0}^{L+1} \frac{\mathfrak{u}_j(C)}{1-\mathfrak{u}_j(C)} + \frac{1}{2}\sum_{j\in L+2-P^+} \Big(\frac{\mathfrak{u}_j^*(C)}{1-\mathfrak{u}_j^*(C)} - \frac{\mathfrak{u}_j(C)}{1-\mathfrak{u}_j(C)}\Big) + \frac{1}{2}\sum_{j\in -P^-} \Big(\frac{\mathfrak{u}_j^*(C)}{1-\mathfrak{u}_j^*(C)} - \frac{\mathfrak{u}_j(C)}{1-\mathfrak{u}_j(C)}\Big)\,. \tag{4.69}$$

Taking the logarithm of the parameter $C = -\mathrm{e}^{2\mu}\prod_{k=0}^{L+1} u_k$, we obtain a similar expression for the fugacity μ

$$\begin{aligned}\mu = &-\log(\alpha\beta) - \sum_{j=0}^{L+1}\log(1-\mathfrak{u}_j(C)) \\ &- \sum_{j\in L+2-P^+}\big(\log\big(1-\mathfrak{u}_j^*(C)\big) - \log(1-\mathfrak{u}_j(C))\big) \\ &- \sum_{j\in -P^-}\big(\log\big(1-\mathfrak{u}_j^*(C)\big) - \log(1-\mathfrak{u}_j(C))\big)\ .\end{aligned} \tag{4.70}$$

We remark at this stage that these expressions are reminiscent of the expressions obtained by analytic continuation where the eigenvalue corresponding to some excited state is obtained as the sum of the ground state branch $\chi_\emptyset$ and additional functions η_j indexed by a set of integers. We now compute the large L asymptotics of the sums (4.69) and (4.70)

Large L asymptotics

Considering first the contribution of the filled Fermi sea for the eigenvalue

$$1 - \frac{\alpha+\beta}{2} + \frac{1}{2}\sum_{j=0}^{L+1}\frac{\mathfrak{u}_j(C)}{1-\mathfrak{u}_j(C)} \tag{4.71}$$

and the fugacity

$$-\log(\alpha\beta) - \sum_{j=0}^{L+1}\log(1-\mathfrak{u}_j(C))\ , \tag{4.72}$$

these expressions have been already evaluated by residues in section 2.3 an their large L asymptotics at the beginning of this chapter for $\alpha=\beta=1$. We can perform the same computation for general values of $\alpha,\beta>1/2$ by expanding the summands of the last expressions in series of L, obtaining

$$\sum_{j=0}^{L+1}\frac{\mathfrak{u}_j(C)}{1-\mathfrak{u}_j(C)} \simeq \alpha+\beta-2+\frac{\chi'(v)}{\sqrt{L}} - \Big(\frac{2a}{(1-a)^2}+\frac{2b}{(1-b)^2}\Big)\frac{\chi'(v)}{L^{3/2}} + \frac{3\chi(v)}{8L^{3/2}}\ , \tag{4.73}$$

$$\sum_{j=0}^{L+1}\log(1-\mathfrak{u}_j(C)) \simeq -\log(\alpha\beta) - \frac{2\chi'(v)}{\sqrt{L}} + \Big(2+\frac{4a}{(1-a)^2}+\frac{4b}{(1-b)^2}\Big)\frac{\chi'(v)}{L^{3/2}} + \frac{\chi(v)}{4L^{3/2}}\ , \tag{4.74}$$

with the change of variable $C=\mathrm{e}^v|C_*|$, so that the relevant values of C for the eigenvalues under the KPZ scaling are indeed scaling like $|C_*|$. Of course χ stands here for the specific function χ^{MC}.

We consider now the contribution of the particle-hole excitations. We observe that for large system size L, the Bethe roots at the edge of the Fermi asymptotically get closer to -1 with $u_j+1\sum 1/\sqrt{L}$. Setting $C=\mathrm{e}^v|C_*|$ as above and casting $u=-1-\frac{\lambda}{\sqrt{L}}$ in the equation $R(u,C)=0$, we obtain at leading order in L the following condition on λ

$$\frac{\lambda^2}{4}\mathrm{e}^{\lambda^2/4} = \mathrm{e}^{-v-1} \tag{4.75}$$

so that λ is expressed as the square root of a Lambert function of e^{-1-v}, that is in terms of the functions $\pm y_j(v)$ defined in chapter 3. Tracking the roots $\mathfrak{u}_j$ and $\mathfrak{u}_j^*$ from their large C asymptotic

behaviour, we obtain the following asymptotics at leading order

$$\mathfrak{u}_j(C) \simeq -1 - 2\mathrm{i}\frac{y_{-j}(v)}{\sqrt{L}} \qquad \text{for} \quad j > 0 \tag{4.76}$$

$$\mathfrak{u}_j^*(C) \simeq -1 + 2\mathrm{i}\frac{y_{-j}(v)}{\sqrt{L}} \qquad \text{for} \quad j > 0 \tag{4.77}$$

$$\mathfrak{u}_{L+2+j}(C) \simeq -1 - 2\mathrm{i}\frac{y_{-j}(v)}{\sqrt{L}} \qquad \text{for} \quad j < 0 \tag{4.78}$$

$$\mathfrak{u}_{L+2+j}^*(C) \simeq -1 + 2\mathrm{i}\frac{y_{-j}(v)}{\sqrt{L}} \qquad \text{for} \quad j < 0 \tag{4.79}$$

Pushing the expansion of the equation $R(u, C) = 0$ up to order $L^{-3/2}$ we find that the cancellation of the higher order terms implies only algebraic expressions in λ so that the roots have the following expansion for $j < 0$

$$\mathfrak{u}_{-j}(C) \simeq -1 - \frac{2\mathrm{i}y_j(v)}{\sqrt{L}} + \frac{2y_j(v)^2}{L} + \frac{3\mathrm{i}y_j(v)^3}{2L^{3/2}} + \frac{\mathrm{i}y_j(v)}{L^{3/2}}\Big(\frac{3}{2} + \frac{4a}{(1-a)^2} + \frac{4b}{(1-b)^2}\Big) \tag{4.80}$$

$$\mathfrak{u}_{-j}^*(C) \simeq -1 + \frac{2\mathrm{i}y_j(v)}{\sqrt{L}} + \frac{2y_j(v)^2}{L} - \frac{3\mathrm{i}y_j(v)^3}{2L^{3/2}} - \frac{\mathrm{i}y_j(v)}{L^{3/2}}\Big(\frac{3}{2} + \frac{4a}{(1-a)^2} + \frac{4b}{(1-b)^2}\Big)\,. \tag{4.81}$$

For $j > 0$ one finds the same expressions for $\mathfrak{u}_{L+2-j}(C)$ and $\mathfrak{u}_{L+2-j}^*(C)$ respectively. Casting these expansions into (4.69) and (4.70) and subtracting the term $(1/(4L) + 1/4)\mu$ to $E(\mu)$, one checks that we recover equations (4.37) and (4.38).

4.3 Numerical checks by extrapolation

In order to check the validity of the results we just stated, they have to be compared with the numerical computation of the eigenvalues of matrix $M(\mu)$. This comparison is also needed to establish some more conjectural results in the absence of *a priori* theoretical reason. Most notably, the fact, for the maximal current TASEP, that only excitations parametrized by sets $P \subset \mathbb{Z}^*$ with $|P_+| = |P_-|$ lead to actual spectral gaps for $L \to \infty$ has no clear physical explanation at the time. The diagonalization of a $2^L \times 2^L$ matrix being practically impossible on a conventional computer for a system size larger than a few sites, the asymptotic values of the eigenvalues of $M(\mu)$ cannot be inferred from its direct diagonalization large L. These eigenvalues can be obtained by solving Bethe ansatz equations numerically in finite size with Newton's method. Writing the Bethe equation in separate form

$$u_j(b) = g^{-1}\left(\mathrm{e}^{\frac{2\mathrm{i}\pi k_j}{2L+2}} + b\right) \qquad 1 \le j \le L+2 \tag{4.82}$$

$$b = \frac{2\mu}{2L+2} + \frac{1}{2L+2}\sum_{k=1}^{L+2}\log u_k \tag{4.83}$$

with

$$g(y) = \frac{y^{\frac{L}{2L+2}}[(y+a)(y+b)(ay+1)(by+1)]^{\frac{1}{2L+2}}}{(1-y)(y+1)^{\frac{1}{L+1}}} \tag{4.84}$$

One compute recursively numerical approximations $b^{(n)}$ of b

$$b^{(n+1)} = b^{(n)} - \frac{b^{(n)} - 2\mu/(2L+2) - 1/(2L+2)\sum_{k=1}^{L+2}\log u_k(b)}{1 - \frac{1}{2L+2}\sum_{k=1}^{L+2}\frac{u_j'(b)}{u_j(b)}} \tag{4.85}$$

where $u_j(b)$ is computed at each step by inverting the function g also using Newton's method. Note that the numbers k_j have to be fixed prior to the computation of the numerical solution

In order to compute efficiently the asymptotic values of the spectral gaps $E_P(\mu) = e_P(\mu)L^{-3/2}$, one can make use of the Richardson extrapolation to accelerate the convergence of a sequence to its limit from a sample of its first terms. Its working principle is the following. Let $A(h)$ be a function with limit A^*, behaving at leading order in h as

$$A(h) = A^* - a_0 h^{k_0} + O(h^{k_1}) \qquad \text{with} \quad k_1 > k_0 > 0 \tag{4.86}$$

Let $r > 0$ be some real parameter. One has

$$A\left(\frac{h}{r}\right) = A^* - a_0 \left(\frac{h}{r}\right)^{k_0} + O(h^{k_1}) \tag{4.87}$$

so that

$$A^* = \frac{r^{k_0} A(h/r) - A(h)}{r^{k_0} - 1} + O(h^{k_1}) \, . \tag{4.88}$$

Thus, computing $A_1(h) = \frac{r^{k_0} A(h/r) - A(h)}{r^{k_0} - 1}$ in place of $A(h)$, the rate of convergence is increased to the next order. Considering the full expansion of the function $A(h) = A^* - \sum_i a_i h^{k_i}$, one can define recursively the functions

$$A_{i+1}(h) = \frac{r^{k_i} A_i(h/r) - A_i(h)}{r^{k_i} - 1} \tag{4.89}$$

so that $A^* = A_{i+1}(h) + O(h^{k_{i+1}})$. It is thus computationally more efficient and reliable to compute the limit A^* from the A_i for some reasonable value of h than directly from $A(h)$ for small values of h.

We consider now the case where the limit quantity one is interested in has the form

$$A(h) = A^* - \sum_{k=1}^{\infty} a_k z^{\theta k} \tag{4.90}$$

which applies indeed to the rescaled spectral gaps e_P of TASEP in the variable $z = 1/L$ with $\theta = 1$. The Richardson extrapolation method described above can be adapted to this case by using a more general recursion known as the *Bullirsch-Stoer* algorithm [47, 71]. Starting with a finite sequence of values $h_0 < h_1 < ... < h_n$ and defining $A_i^{(0)} = A(h_i)$, one construct recursively the array

$$\begin{array}{ccccc} A_0^{(0)} & A_1^{(0)} & \cdots & A_{n-1}^{(0)} & A_n^{(0)} \\ A_0^{(1)} & A_1^{(1)} & \cdots & A_{n-1}^{(1)} & \\ \cdots & \cdots & \cdots & & \\ A_0^{(n)} & & & & \end{array}$$

with

$$A_m^{(p)} = A_{m+1}^{(p-1)} + \frac{A_{m+1}^{(p-1)} - A_m^{(p-1)}}{\left(\frac{h_{m+1}}{h_{m+p+1}}\right)^{\theta} \left(1 - \frac{A_{m+1}^{(p-1)} - A_m^{(p-1)}}{A_{m+1}^{(p-1)} - A_{m+1}^{(p-2)} - 1}\right)} \, . \tag{4.91}$$

The extrapolated value of A^* is then $A_0^{(n)}$. An estimation of the order of magnitude of the error is

$$|A^* - A_0^{(n)}| \sim |A_1^{(n)} - A_1^{(n-1)}| + |A_1^{(n)} - A_2^{(n-1)}| + |A_1^{(n-1)} - A_2^{(n-1)}| \, . \tag{4.92}$$

Note that the absence of convergence of the Bullirsch-Stoer algorithm on some numerical quantity is also a good indicator of the presence of subleading terms of the form $z^k \log(z)^l$ in the asymptotic expansion of $A(h)$. See table 4.1 for an illustration of the difference in speed of convergence between the finite size computation of eigenvalue and their extrapolated values. Using the Bullirsch-Stoer extrapolation, all other gaps can be computed and checked against their expression obtained by analytic continuation. See table 4.2 for the numerical values of the first gaps in the maximal current phase

L	$e_1(L)$	e_1 extrapolated
3	-3.15590	$-0.$
4	-3.31254	$-0.$
5	-3.39823	$-4.$
6	-3.44972	$-4.$
7	-3.48286	-3.58
8	-3.50533	-3.578
9	-3.52119	-3.5780
10	-3.53277	-3.5781
	...	...
15	-3.56073	-3.578064664
	...	...
20	-3.57038	-3.5780646644761799
	...	...
25	-3.57460	$-3.5780646644761798418219$
	...	...
30	-3.57672	$-3.5780646644761798418218703 6$
	...	...
35	-3.57787	$-3.5780646644761798418218703582326693543$
	...	...
40	-3.57854	$-3.5780646644761798418218703582326693543$

Table 4.1: Numerical evaluation of the spectral gap $e_{\{-1,1\}}$ of the open TASEP with $\alpha = \beta = 1$ from solutions of the Bethe ansatz equation by Newton's method, directly computed for a given size of the system (left column) and extrapolated (right column). The extrapolated values are obtained by from a sample of values $\{A_i^{(0)}\}$ ranging from $L = 3$ to the system size of the current line. The values are truncated at the order of magnitude of the error estimator (4.92).

P	v	$\chi_P(v)$
$\emptyset$	$-\infty$	0
$\{-1,1\}$	4.22823	-3.57806
$\{-2,1\}$	$6.02264 - 0.593574\mathrm{i}$	$-8.46731 - 1.64993\mathrm{i}$
$\{-1,2\}$	$6.02264 + 0.593574\mathrm{i}$	$-8.46731 + 1.64993\mathrm{i}$
$\{-2,2\}$	7.47802	-13.782
$\{-3,1\}$	$7.28709 - 1.07616\mathrm{i}$	$-14.2212 - 4.34068\mathrm{i}$
$\{-1,3\}$	$7.28709 + 1.07616\mathrm{i}$	$-14.2212 + 4.34068\mathrm{i}$
$\{-2,-1,1,2\}$	8.96685	-19.1775
$\{-3,2\}$	$8.58003 - 0.505733\mathrm{i}$	$-19.8304 - 2.67093\mathrm{i}$
$\{-2,3\}$	$8.58003 + 0.505733\mathrm{i}$	$-19.8304 + 2.67093\mathrm{i}$
$\{-4,1\}$	$8.29833 - 1.49364\mathrm{i}$	$-20.6905 - 7.8732\mathrm{i}$
$\{-1,4\}$	$8.29833 + 1.49364\mathrm{i}$	$-20.6905 + 7.8732\mathrm{i}$
$\{-3,-1,1,2\}$	$9.94552 - 0.418264\mathrm{i}$	$-25.4766 - 2.56307\mathrm{i}$
$\{-2,-1,1,3\}$	$9.94552 + 0.418264\mathrm{i}$	$-25.4766 + 2.56307\mathrm{i}$
$\{-3,3\}$	9.59118	-26.1022
$\{-4,2\}$	$9.48765 - 0.946301\mathrm{i}$	$-26.5289 - 6.17958\mathrm{i}$
$\{-2,4\}$	$9.48765 + 0.946301\mathrm{i}$	$-26.5289 + 6.17958\mathrm{i}$
$\{-5,1\}$	$9.15505 - 1.86586\mathrm{i}$	$-27.788 - 12.1323\mathrm{i}$
$\{-1,5\}$	$9.15505 + 1.86586\mathrm{i}$	$-27.788 + 12.1323\mathrm{i}$

Table 4.2: Numerical values when $L \to \infty$ of higher gaps $4L^{3/2}E_P \simeq \chi_P^{\mathrm{MC}}(v)$, $\chi_P'(v) = 0$ in the maximal current phase with fugacity $\mu = 0$, with corresponding indexing sets. The ground state eigenvalue cannot be obtained as a solution of equations (4.37)–(4.38) for $\mu = 0$ as the corresponding value of v goes to $-\infty$. We observe however that for all other branches of χ^{MC} the exist a single finite value of v for which the equations are satisfied for finite μ.

Conclusion

We have studied the totally asymmetric exclusion process, focusing on the process with open boundary conditions. We have derived exact expressions for the first excited eigenvalues (spectral gap) of its deformed Markov matrix in the maximal current phase [41] and on the boundaries between the maximal current and high/low density phases [40], the later case connecting the results derived for the maximal current phase and previously known for the periodic ASEP chain. These expressions were obtained under the form of parametric expressions involving a multivalued complex function, whose branches were found to be in correspondence with eigenstates. Although these results were obtained directly from Bethe ansatz equation in the periodic case [75], or justified *a posteriori* by Bethe ansatz in the open case, the expressions themselves could be derived by a purely analytic method, simply computing the analytic continuation of a previously known expression for the ground state eigenvalue.

Strictly speaking, the completeness of this approach, *i.e.* the fact that all spectral gaps can be obtained this way, is still a conjecture based on numerical computations; yet the existence of this nice analytic structure appears to be a common feature of the exclusion process in finite volume in all settings.

The interest we have in spectral gaps is justified by the fact they control the relaxation of the system on the time scale $t \sim L^{3/2}$ over which the KPZ universal behaviour is observed for finite volume variants of the ASEP. In this regard, the present work is only a partial contribution to a better understanding of the KPZ fixed point on a interval since exact expressions for the fluctuations and correlation of the KPZ height function would require the knowledge of the eigenvectors of the deformed matrices, which we were not able to determine until now for the open process. In particular, one would need as simple as possible scalar expressions for the coordinates of these eigenvectors $\langle \mathcal{C}|\psi_n\rangle$ in the configuration basis, as well as for the scalar products of two eigenvectors $\langle \psi_n|\psi_m\rangle$.

The Riemann surfaces we constructed in chapter 3 were introduced as the natural domains of functions χ^{Per}, χ^{MC} and χ^{A}, η^{A}. However, the interest of explicitly constructing these surfaces would be eventually to express various probability distributions of the KPZ height function as contour integrals over these surfaces. Such results were obtained in [73] for the KPZ fixed point with periodic boundary conditions for several classes of initial conditions. For instance, the one-point probability distributions of the fluctuations of the KPZ height functions, recalled here in section 1.6, were obtained as contour integrals over the base space of covering maps constructed from the Riemann surface $\mathcal{R}^{\mathrm{Per}}$ considered in chapter 3, involving the sum over all branches of generalizations of the function χ^{Per}. The extension of this construction to KPZ with open boundary conditions would be the next step after the complete determination of the spectral gaps eigenstates of the open exclusion process.

The Neumann boundary conditions of the corner-growth height function constructed from the open ASEP under weak asymmetry scaling are fixed by relations (1.142). In the totally asymmetric limit, that is for a height function corresponding to the KPZ fixed point, we justified that the boundary parameters of the exclusion process were expected to scale like $\alpha, \beta - 1/2 \sim 1/\sqrt{L}$, without however a precise relation between TASEP and KPZ parameters in the phase crossover considered in section 4.1.3. Such connection would be needed to obtain exact expression for KPZ fluctuations on an interval with variable Neumann boundary condition.

Another interesting problem would be the generalization of our computation to the partially asymmetric case $q \neq 0$. It is conjectured in [54] that the parametric equations for the eigenvalues of the deformed Markov matrix are essentially similar, up to constant numerical factors, which would not impact the analytic structure derived in this work for the totally asymmetric case. The structure of the Bethe equations is however expected to be much more involved, in particular no decoupled equations

are known.

A striking feature of the expressions presented or derived in chapter 4 for the gaps of the periodic and open TASEP is that, for the undeformed case $\mu = 0$, the eigenvalues are obtained by evaluating a function $\chi(v)$ at a point such that $\chi'(v) = 0$, which is reminiscent of the evaluation of an integral by the saddle point approximation. What is more, this presumed saddle point approximation here is exact, meaning that in the development over spectral gaps of the generating function $\langle \mathrm{e}^{\mu Q_t} \rangle = \sum_n K_n \mathrm{e}^{E_n t}$ where the coefficients K_n gather the contributions of the eigenstates, no subleading factors polynomial in t^{-1} are found, which would be expected if the saddle-point evaluation was the leading term of a more general asymptotic expansion. It would be interesting to understand the reason for this structure to appear.

Résumé de la thèse

Introduction

L'objet de cette thèse est l'étude du proccessus d'exclusion simple asymétrique (ASEP) avec conditions aux bords ouvertes et plus spécifiquement dans le cas particulier du processus totalement asymétrique (TASEP). Le processus d'exclusion est un modèle stochastique défini sur un réseau unidimensionel [84, 31, 81] dans lequel des particules présentant des interactions de contact se déplacent aléatoirement, avec une direction privilégiée.

Le processus d'exclusion est devenu un objet d'étude central en physique statistique. Il s'agit en effet d'un des modèles les plus simples évoluant vers un état stationnaire hors équilibre, caractérisé par des courants de probabilités non-nuls entre les configurations du système. Le modèle d'exclusion peut également être interprété comme un modèle de croissance d'interface appartenant à la classe d'universalité KPZ, un ensemble de modèles décrivant l'évolutions d'une fonction de hauteur définie sur un substrat unidimensional, caractérisés par des lois d'échelle et des distributions de probabilité communes pour les fluctuations de ces fonctions de hauteurs. Le processus d'exclusion est de plus intégrable par ansatz de Bethe, ce qui permet en principe le calcul exact de son état stationnaire et de la dyamique de sa relaxation en temps fini.

Si de nombreux résultats sont connus pour le processus d'exclusion sur un réseau infini, les connaissances disponibles sur le processus en volume fini, avec conditions aux bords périodiques ou ouvertes, sont plus parcellaires. Le but de cette thèse est de dériver des expressions exactes pour les fluctuations du courant de particules en temps fini dans le cas du TASEP ouvert.

Considérant un opérateur $M(\mu)$ appellé *matrice de Markov déformée* du modèle donnant accès aux fluctuations du courant de particules, nous calculons dans ce qui suit les valeurs propres de $M(\mu)$ pour différentes valeurs des paramètres du modèles dans la limite des grandes tailles de système, et plus particulèrement la partie du spectre de $M(\mu)$ correspondant au régime universel KPZ.

Ce expressions sont obtenues par prolongement analytique d'expressions déjà connues pour la valeur propre $E(\mu)$ de plus grande partie réelle de $M(\mu)$. Les différentes branches des fonctions complexes multivaluées obtenues par prolongement analytique de la valeur propre fondamentale sont mises en correspondance avec les valeurs propres des états excités de la matrice de Markov déformée.

Le modèle d'exclusion totalement asymétrique, état stationnaire, fluctuations du courant

Définition du modèle

Le modèle d'exclusion simple asymétrique est un modèle stochastique dans lequel des particules sautent aléatoirement d'un site à l'autre sur une chaîne discrète de taille L avec des taux de transitions définis (voir fig. 4.7). Ces particules sont en interaction, en effet un site ne peut être occupé par plus d'une particule (contrainte d'exclusion, ou interaction de type *sphères dures*) Nous nous intéresserons dans la suite exclusivement au cas totalement asymétrique (TASEP), où le mouvement des particules est unidirectionnel. On peut alors sans perte de généralité fixer la probabilité de transition dans le bulk (hors des sites extrémaux) à $p = 1$.

Une configuration $\mathcal{C}$ de la chaîne est donnée par l'ensemble des nombres d'occupations des sites $\mathcal{C} = (\tau_1, ..., \tau_L)$, avec $\tau_i = 0$ si le site est vide ou 1 s'il est occupé. Par analogie avec les modèles

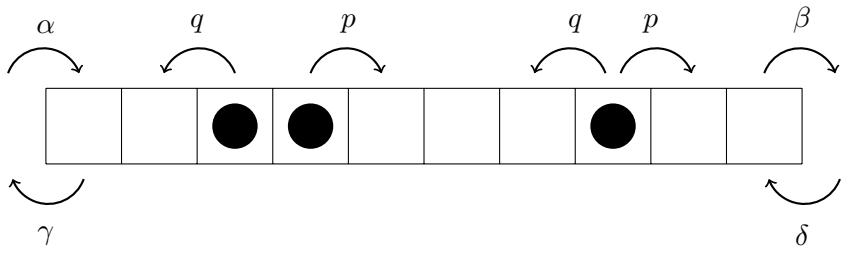

Figure 4.7: ASEP avec conditions aux bords ouvertes. Sur une chaine discrète de L site, chaque particule à l'intérieur de la chaîne (en dehors des sites extrémaux) a une probabilité par unité de temps p de sauter sur le site voisin de droite, et q de sauter sur le site de gauche, si le site d'arrivée est libre (un site est occupé par au plus une particule). Pour les sites extrémaux une particule peut entrer au premier site avec un taux α si il est libre et en sortir avec un taux δ s'il est occupé. De même pour le L-ième site avec des taux β et δ. Dans le cas particulier du TASEP, $p = 1$ et $q = \delta = \gamma = 0$. On peut également définir le processus pour des conditions aux limites périodiques, le nombre de particules est alors conservé, et les sites L et 1 sont considérés comme liés.

quantiques sur réseau comme les chaînes de spin, on peut représenter l'état local de chaque site par un espace de dimension 2 $\mathbb{C}_i^2$ dont une base est $(|0\rangle_i, |1\rangle_i)$ (site vide/site occupé). L'espace des états du systèmes est donc un espace de dimension 2^L

$$\Omega = \bigotimes_{i=1}^{L} \mathbb{C}_i^2$$

On prend comme base de cet espace l'ensemble des suites binaires de longueur L (suite des nombres d'occupations) rangées dans l'ordre lexicographique. A un instant t donné, l'état du système est représenté par un vecteur d'état $|S_t\rangle$ dont les coordonées sont les probabilités de chaque configuration. On note $P_t(\mathcal{C}) = \langle \mathcal{C}|S_t\rangle$ la probabilité que le système soit dans la configuration $\mathcal{C}$ à l'instant t. L'évolution des probabilités de chaque configuration est donnée par l'équation maitresse

$$\frac{d}{dt}P_t(\mathcal{C}) = \sum_{\mathcal{C}'\neq\mathcal{C}} M(\mathcal{C},\mathcal{C}')P_t(\mathcal{C}') \tag{4.93}$$

$$= \sum_{\mathcal{C}\neq\mathcal{C}'} \big(w(\mathcal{C}'\to\mathcal{C})P_t(\mathcal{C}') - w(\mathcal{C}\to\mathcal{C}')P_t(\mathcal{C})\big) \tag{4.94}$$

où M est la matrice de Markov du modèle. Ses coordonées $M(\mathcal{C},\mathcal{C}')$ sont les taux de transition $\mathcal{C}'\to\mathcal{C}$ d'une configuration à une autre, avec $M(\mathcal{C},\mathcal{C}) = -\sum_{\mathcal{C}\neq\mathcal{C}'} M(\mathcal{C},\mathcal{C}')$. Dans le formalisme quantique décrit plus haut, la matrice de Markov est analogue à un hamiltonien effectif du système. Au temps long, la mesure de probabilité des configurations tend vers une mesure stationnaire $P_\infty(\mathcal{C})$ (le processus d'exclusion étant ergodique, cette distribution est unique et toutes les configuration initiales convergent vers elle). Une caractéristique de l'état stationnaire du TASEP est qu'il ne vérifie pas la condition de bilan détaillé, c'est-à-dire qu'en général

$$\frac{M(\mathcal{C},\mathcal{C}')}{M(\mathcal{C}',\mathcal{C})} \neq \frac{P_\infty(\mathcal{C}')}{P_\infty(\mathcal{C})}$$

Ceci a notamment pour conséquence que le spectre de M n'est pas réel. On définit par ailleurs la variable aléatoire Q_t égale au nombre total de particule étant entrée de l'extérieur vers le site 1 au temps t depuis $t = 0$. Aucune particule n'étant créée ou détruite dans le bulk, Q_t est aussi égale, quand $t\to\infty$, au nombre de particules sorties du système par le site L, ou ayant traversé n'importe quelle liaison entre deux sites consécutifs. On peut ainsi définir le courant stationnaire dans le système comme

$$J(\alpha,\beta,L) = \lim_{t\to\infty} \frac{\langle Q_t\rangle}{t}\ . \tag{4.95}$$

On définit également la densité moyenne de particule dans la chaîne

$$\rho = \lim_{t\to\infty} \frac{N_t}{L} \tag{4.96}$$

où N_t est le nombre de particule dans le système à l'instant t. Selon les valeurs des paramètres de bords α et β, le système peut se trouver dans trois phases, caractérisées par des valeurs distinctes de ρ et J (discontinues dans l'espace des paramètres), voir fig. 4.8.

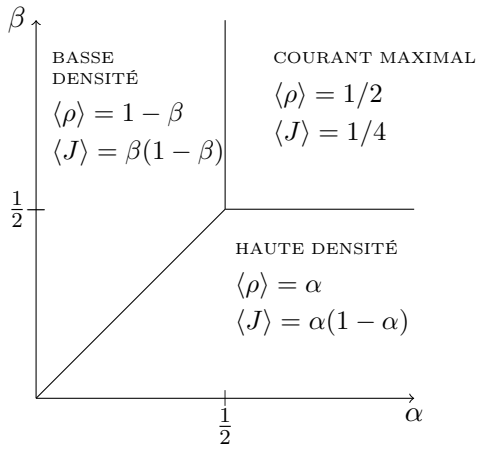

Figure 4.8: Diagramme de phase du TASEP ouvert en fonction des taux d'entrées sorties. Les transitions entre la phase de courant maximal et les phases de haute et basse densité sont du second ordre. La transition entre la phase de haute et la phase de basse densité (dite ligne de choc) est continue pour le courant et discontinue pour la densité. Pour cette dernière transition, le système est divisé en une phase de basse densité et une phase de haute densité, la discontinuité entre les deux suivant un mouvement brownien le long de la chaîne.

Fluctuations du courant, matrice de Markov déformée

Nous allons maintenant introduire la matrice de Markov déformée du système, qui sera l'objet principal considéré dans la suite. Toute l'information sur la statistique du courant stationnaire est contenue dans la suite des moments de sa distribution de probabilité. On peut calculer l'ensemble des moments de la variable Q_t grace à sa fonction génératrice $\langle \exp(\gamma Q_t)\rangle$. Pour la déterminer, on sépare la matrice de Markov du processus en deux termes

$$M(\mathcal{C}', \mathcal{C}) = M_0(\mathcal{C}', \mathcal{C}) + M_1(\mathcal{C}', \mathcal{C})$$

Où la matrice M_1 contient tous les éléments correspondant à des transitions $\mathcal{C}' \to \mathcal{C}$ au cours desquelles une particule rentre dans le système par le site 1. On appelle $M(\gamma)$ la matrice de Markov déformée du modèle. On peut alors montrer que la fonction génératrice des moments du courant pour tout temps t s'écrit

$$\langle \mathrm{e}^{\mu Q_t}\rangle = \langle 1| \left(\sum_{n=0}^{2^L-1} |\psi_n(\mu)\rangle \langle\psi_n(\mu)| \, \mathrm{e}^{E_n(\mu)t} \right) |P_0\rangle \ . \tag{4.97}$$

où les $\{E_n(\mu)\}$ sont les valeurs propres de $M(\mu)$ et $\{|\psi_n\rangle\}$ les vecteurs propres correspondants. Pour $t \to \infty$, cette expression est dominé par l'état propre de plus grande valeur propre en partie réelle $E_0(\mu)$, de sorte que

$$\lim_{t\to\infty} \frac{1}{t} \log\langle \mathrm{e}^{\mu O_t}\rangle \approx E_0(\mu) \ . \tag{4.98}$$

La valeur propre fondamentale est donc la fonction génératrice des cumulants du courant dans l'état stationnaire :

$$E(\gamma) = \frac{\langle Q_t \rangle}{t}\gamma + \frac{\langle Q_t^2 \rangle - \langle Q_t \rangle^2}{t}\gamma^2 + ...$$

Pour obtenir des informations sur la dynamique du courant hors de l'état stationnaire, il est nécessaire de diagonaliser entièrement $M(\gamma)$. On trouvera une introduction détaillée au processus d'exlcusion et une démonstration de ces résultats dans chapitre 1 de la thèse, sections 1 à 4.

Universalité KPZ

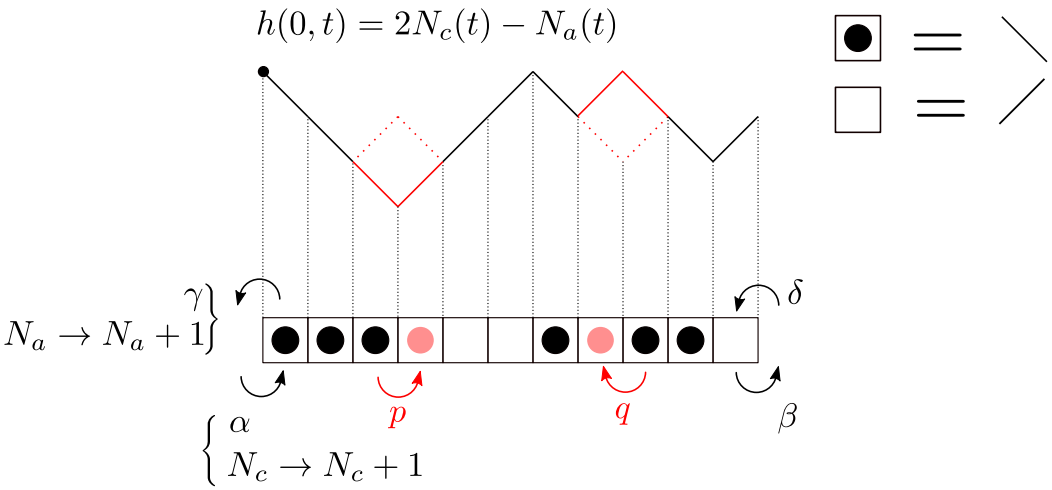

Figure 4.9: Correspondance entre le processus d'exclusion et un modèle de croissance d'interface. Pour chaque lien entre deux sites consécutifs de la chaine de l'ASEP, la fonction $h(x,t)$ au dessus du lien considéré est égale au nombre de particule ayant traversé ce lien: on ajoute un bloc carré dans un minimum local pour un saut vers la gauche et on enlève un bloc d'un maximum local pour un saut vers la droite. Chaque site est associé à une pente positive ou négative, la pente totale de la chaîne étant conservée par l'évolution.

L'équation KPZ est une équation différentielle stochastique introduite en 1986 par Kardar, Parisi et Zhang pour décrire les fluctuations d'une fonction de hauteur $h(x,t)$ modélisant la dynamique d'une interface à une dimension entre une phase stable croissant dans une phase métastable d'un même milieu.

$$\frac{\partial h}{\partial t} = \nu \frac{\partial^2 h}{\partial x^2} + \lambda \left(\frac{\partial h}{\partial x} \right)^2 + \eta(x,t) \tag{4.99}$$

où η est un bruit blanc gaussien en temps et en espace: $\langle \eta(x,t)\eta(x',t') \rangle = 2D\delta(x-x')\delta(t-t')$. L'équation KPZ décrit une large classe de modèles de croissance de surfaces (la classe d'universalité KPZ [21]), qui se caractérisent par une même distribution de probabilité stationnaire pour h, et par des exposants critiques communs pour le comportement de $h(x,t)$ aux temps longs: exposant dyamique $z = 3/2$, exposant de rugosité $\alpha = 1/2$. Si l'on note $w(\ell,t)$ l'écart-type des fluctuations de $h(x,t)$ sur une fenêtre $x \in [x_0, x_0 + \ell]$, on a les lois d'échelles suivantes:

$$w(\ell,t) \sim \begin{cases} \ell^\alpha & \text{pour } \ell \ll t^{1/z} \\ \ell^{\alpha/z} & \text{pour } \ell \gg t^{1/z} \end{cases} \tag{4.100}$$

Il existe un mapping permettant de définir une fonction $h_{ASEP}(x,t)$ à partir de l'ASEP ouvert en intégrant le courant de particule à travers chaque liaison entre deux sites adjacents (voir fig. **??**). Cette fonction est solution de l'équation KPZ dans la limite faiblement asymétrique de l'ASEP: on

fixe $q-p=\sqrt{\epsilon}$, et on note $h^{\epsilon}_{ASEP}(x,t)$ le profil de hauteur obtenu. Alors $\sqrt{\epsilon}h^{\epsilon}_{ASEP}(\epsilon^{-1}x,\epsilon^{-2}t)$ est solution de KPZ dans la limite $\epsilon\sim 1/L$, $L\to\infty$ [66], pour $\nu=1/2$, $\lambda=D=1$.

Dans le cas du TASEP, pour $t\sim L^{3/2}$ les fluctuations du courant (donc de de la hauteur h définie à partir du processus) suivent le régime KPZ à la limite thermodynamique, dans le cas où le paramètre correspondant au terme non-linéaire de l'équation KPZ λ tend vers l'infini. Dans la limite $\lambda\to\infty$, les distributions de probabilités pour $h(x,t)$ existent. De façon équivalente, cette valeur du paramètre correspond à un point fixe de l'équation KPZ pour la renormalisation de la fonctions de hauteur $\mathfrak{h}(x,t)=\lim_{\epsilon\to 0}\epsilon^{1/2}h(\epsilon^{-1}x,\epsilon^{-3/2}t)$, appelé point fixe KPZ. L'ensemble des modèles convergeant vers ce point fixe sous renormalisation forment la classe d'universalité KPZ.

Ainsi, en considérant (4.97), les états propres correspondant à ce régime sont ceux associé à des valeurs propres suivant la loi d'échelle $E\sim 1/L^{3/2}$ quand $L\to\infty$. Ce sont ces valeurs propres, ou *gaps spectraux*, que nous allons calculer explicitement dans la limite thermodynamique.

Outre le modèle d'exclusion, de nombreux modèles sont désormais connus pour appartenir à la classe d'universalité KPZ, issus de domaines variés de la physique. On peux notamment citer des modèles de croissance d'interface comme le modèle de déposition ballistique ou de croissance polynucléaire [2], des chaines de spin intégrables dans certains régimes [58], des réseau de spins désordonnés [69], ou des chaines d'oscillateurs classiques non-linéaires [85]. Les statistiques universelles des fluctuations des quantités pertinentes pour ces modèles sont connues, et issues de la théorie des matrices aléatoires. Du point de vue des réalisations expérimentales, des comportements caractéristique de l'univeralité KPZ sont observés dans des contextes variés, tels que la croissance de colonies de cellules cancéreuses [48], la combustion lente de feuilles de papier [63], ou la croissance de phase turbulentes dans des écoulements bidimensionels de cristaux liquides.

Une brève introduction à l'universalité KPZ dans le contexte du processus d'exclusion est donnée dans la section 1.5 du manuscrit.

Ansatz de Bethe pour le processus d'exclusion

Le processus d'exclusion possède la propriété d'être intégrable par ansatz de Bethe, c'est-à-dire que que sa dynamique peut-être calculée de façon exacte. Plus spécifiquement, il est possible de diagonaliser la matrice $M(\mu)$ et d'en déduire des résultats sur toutes les quantités physiquement intéressante du modèle pour tout temps.

La distribution de probabilité des configurations du modèle dans l'état stationnaire peut-être calculé au moyen de l'*ansatz matriciel* introduit par Derrida *et al.* [30], d'où l'on peut déduire notamment le diagramme de phase 4.8. Ici cependant, nous cherchons à obtenir les valeurs propres contribuant à la relaxation du processus vers l'équilibre, donc en temps fini.

Ces valeurs propres peuvent être obtenues au moyen de l'ansatz de Bethe algébrique. Nous utilisons en particulier une version récente des équations de l'ansatz de Bethe pour le processus d'exclusion ouvert obtenue par Crampé et Nepomechie [25] qui présente plusieurs avantages calculatoires. Ces équations de Bethe sont obtenues au moyen de *relations TQ* qui permet le calcul direct des valeurs propres de $M(\mu)$, sans toutefois fournir de construction systématique des vecteurs propres comme l'ansatz de Bethe algébrique usuelle, développée par exemple dans [26].

On peut montrer qu'il existe $L+2$ paramètres $(u_1,...,u_{L+2})$ appelés racines de Bethe vérifiants le système d'équations polynomiales

$$\overline{u}_j^L(\overline{u}_j+b)(\overline{u}_j+a)(a\overline{u}_j+1)(b\overline{u}_j+1)=(-1)^{L+1}\mathrm{e}^{2\mu}(1-\overline{u}_j)^{2L+2}(\overline{u}_j+1)^2\prod_{k=1}^{L+2}\overline{u}_k\ . \tag{4.101}$$

pour $1\leq j\leq L+2$ tel que la valeur propre correspondant à une solution de ces équations s'écrit

$$E(\mu)=1-\frac{\alpha+\beta}{2}+\frac{1}{2}\sum_{j=1}^{L+2}\frac{u_1}{1-u_j}\ , \tag{4.102}$$

avec $a=1/\alpha-1$ et $b=1/\beta-1$. Les solutions de ces équations conduisant à des états propres de $M(\mu)$ sont indicées par des ensembles d'entier ou demi-entiers $(k_1,...,k_{L+2})$ définis modulo $2L+2$ (voir

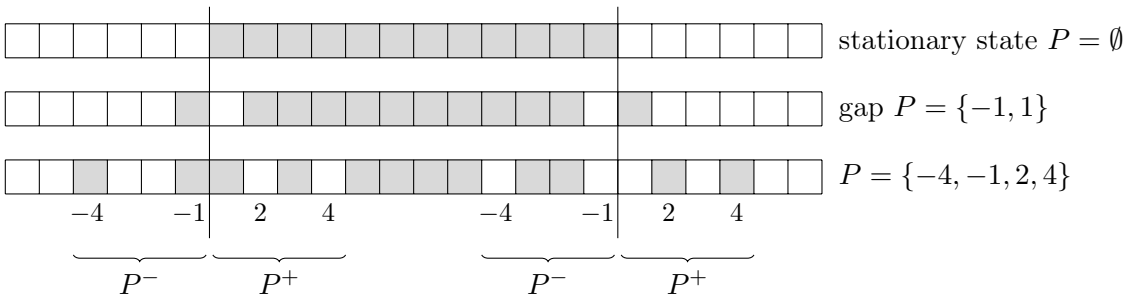

Figure 4.10: Choix de nombres k_j correspondant à quelques états propres de $M(\mu)$. Les cases grises représentent les nombres k_j correspondant à une solution. Le fondamental est obtenu pour $(k_1, ..., k_{L+2}) = (-L/2, ..., L/2)$. On peut de façon équivalente indexer les états excités par des ensembles $P_\pm$ représentantes les nombres enlevés de cet intervalle (*trous*) et ajoutés en dehors (*excitations*). On remarque l'analogie avec un système de fermions, dont les barres verticale sur ce schéma représentent le niveau de Fermi.

fig. 4.10. L'indexation des états propres exposée dans la figure 4.10 au moyen des ensembles d'entiers $P_\pm$ est en particulier indépendante de la taille du système, on peut donc identifier un même état propre dans la limite $L \to \infty$. Les gaps spectraux dont nous allons donner l'expression dans la suite sont obtenus dans cet limite pour un nombre fini d'excitations, c'est-à-dire pour $P_+, P_- \subset \mathbb{Z}$ finis.

Une propriété remarquable des équations (4.101) est qu'une racine de Bethe u_j ne dépend des autres que par leur produit global, ce qui facilite grandement le calcul de leur expressions asymptotiques pour $L \to \infty$. La dérivation complète des équations de Bethe se trouve dans le chapitre 2 du présent document.

Expression de états excités par prolongement analytique

Prolongements analytiques et fonctions complexes multivaluées

Les principaux résultats énoncés dans cette thèse sont obtenus par prolongement analytique de fonctions complexes analytiques sur un sous-ensemble du plan complexe. Plus précisément, les valeurs propres sont obtenues sous la forme d'équations paramétriques faisant intervenir une fonction χ analytique sur $\mathbb{C}$ privés de segments (*coupures*) correspondant aux discontinuités de χ dont les extrémités (*points de branchement*) sont des singularités de χ.

En utilisant les propriétés des fonctions holomorphes, il est possible de construire de nouvelles fonctions, ou *prolongements analytiques*, holomorphes au voisinage d'une coupure de la fonction originale correspondant avec la fonction originale sur une partie de son domaine. Cette procédure conduit à la construction de plusieurs déterminations (*branches*) de la fonction χ, prenant des valeurs différentes en un même point de $\mathbb{C}$. L'exemple le plus simple d'une telle fonction multivaluée est celui de la fonction racine n-ième complexe, voire figure 4.11. Considérant des fonctions χ analytique sur $\mathbb{D} \subset \mathbb{C}$ et χ^A analytique sur $\mathbb{D}^A$ correspondant respectivement à la valeur fondamentale de $M(\mu)$ dans la phase de courant maximal et dans le crossover entre la phase de basse densité et de courant maximal, nous construisons systématiquement toutes les branches χ_P et χ^A_P de ces fonctions, indicées par des ensembles d'entiers $P \subset \mathbb{Z}$. La résolution des équations paramétriques donant la valeur propre fondamentale obtenues en substituant à χ une des branches de son prolongement analytique permet d'obtenir toutes les autres valeurs propres de $M(\mu)$ suivant la loi d'échelle $E_n \sim e_n L^{-3/2}$.

Le domaine de définition naturel d'une fonction complexe multivaluée est une *surface de Riemann* $\mathcal{R}$, c'est-à-dire une variété complexe de dimension 1 localement homéomorphe à $\mathbb{C}$ mais pas globalement. Etant donné une partition de $\mathcal{R}$ en feuillets, copies du domaine de définition $\mathbb{D}$ original de chaque branche, et soit $[z, k] \in \mathcal{R}$ le point appartenant au k-ième feuillet de $\mathcal{R}$ se projetant en $z \in \mathbb{D}$ où $\mathbb{D}$, on peut relever les différentes branches f_k d'une fonction complexe multivaluée en une unique fonction f définie sur $\mathcal{R}$ par $f([z, k]) = f_k(z)$.

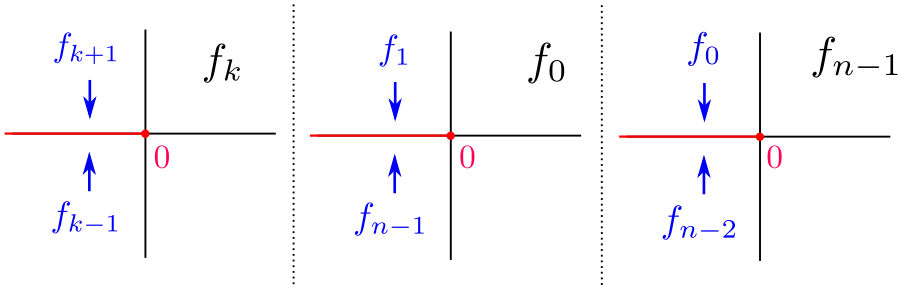

Figure 4.11: Représentation schématique du prolongement analytique des fonctions racines n-ièmes complexes $f_n(re^{i\theta}) = r^{1/n}e^{i\left(\frac{\theta}{n}+\frac{2\pi k}{n}\right)}$. Il existe n déterminations différentes de la fonction racine n-ième, discontinues sur l'axe réel négatif. La fonction définie par $f_k(z)$ pour $\mathrm{Re}\, z > 0$ et $f_{k+1}(z)$ pour $\mathrm{Re}\, z < 0$ est localement holomorphe sur l'axe réel négatif pour $k < n$, on dit que f_{k+1} est le prolongement analytique de f_k en franchissant la coupure par le haut.

On trouvera au chapitre 3 une introduction détaillé au formalisme des fonctions complexes multi-valuées.

Premiers états excités dans la phase de courant maximal

En utilisant les equations de Bethe (4.101), on peut montrer que la valeur propre fondamentale $E(\mu) = E_0(\mu)$ pour le TASEP ouvert de taille L avec taux de bords $\alpha = \beta = 1$ (soit dans la phase de courant maximal) a l'expression paramétrique suivante

$$\mu = -\sum_{k=1}^{\infty} \frac{(2k)!}{k!} \frac{[2k(L+1)]!}{[k(L+1)]![k(L+2)]!} \frac{B^k}{2k} \tag{4.103}$$

$$E(\mu) = -\sum_{k=1}^{\infty} \frac{(2k)!}{k!} \frac{[2k(L+1)-2]!}{[k(L+1)-1]![k(L+2)-1]!} \frac{B^k}{2k} \tag{4.104}$$

Ce résultat avait déjà été dérivé dans [44] au moyen d'une généralisation de l'ansatz matriciel. Pour $L \to \infty$, cette expression devient pour $B = -\mathrm{e}^{-v-1}/4$

$$\mu = \frac{2}{\sqrt{L}} \chi'(v) \tag{4.105}$$

$$E(\mu) - \left(\frac{1}{4} + \frac{1}{4L}\right)\mu = \frac{L^{-3/2}}{4}\chi(v) \tag{4.106}$$

avec

$$\chi(v) = \frac{1}{3\pi} \int_{-\infty}^{+\infty} dy \frac{(1-y^2)(3-y^2)}{1 + y^{-2} e^{y^2-1} e^{-v}} \tag{4.107}$$

où le paramètre v doit être éliminé entre les deux équations pour obtenir l'expression de E en fonction de μ.

La fonction χ n'est pas holomorphe sur l'ensemble du plan complexe, elle possède des discontinuités (coupures) sur l'axe imaginaire, correspondant aux intervalles $\mathrm{i}[2\pi(n-1/2), 2\pi(n+1/2)]$ séparées par les points $2\mathrm{i}\pi(n+1/2)$, pour $n \in \mathbb{Z}$ (points de branchements). Il est cependant possible de prolonger la fonction $\chi(v)$ à travers ses coupures en une nouvelle fonction $A\chi(v)$ analytique sur un voisinage de la coupure franchie. Schématiquement, le prolongement analytique de χ au franchissement d'une coupure est obtenu en ajoutant les résidus aux poles de l'intégrande de (4.107) qui prennent des valeurs réelles pour v situés sur une coupure On peut montrer qu'en itérant cette procédure en prolongeant la fonction χ le long d'un chemin traversant plusieurs coupures, on obtient de nouvelles déterminations (ou *branches*) de χ de la forme

$$\chi_P(v) = \chi(v) + 2\mathrm{i} \sum_{j \in P} \eta_i(v) \tag{4.108}$$

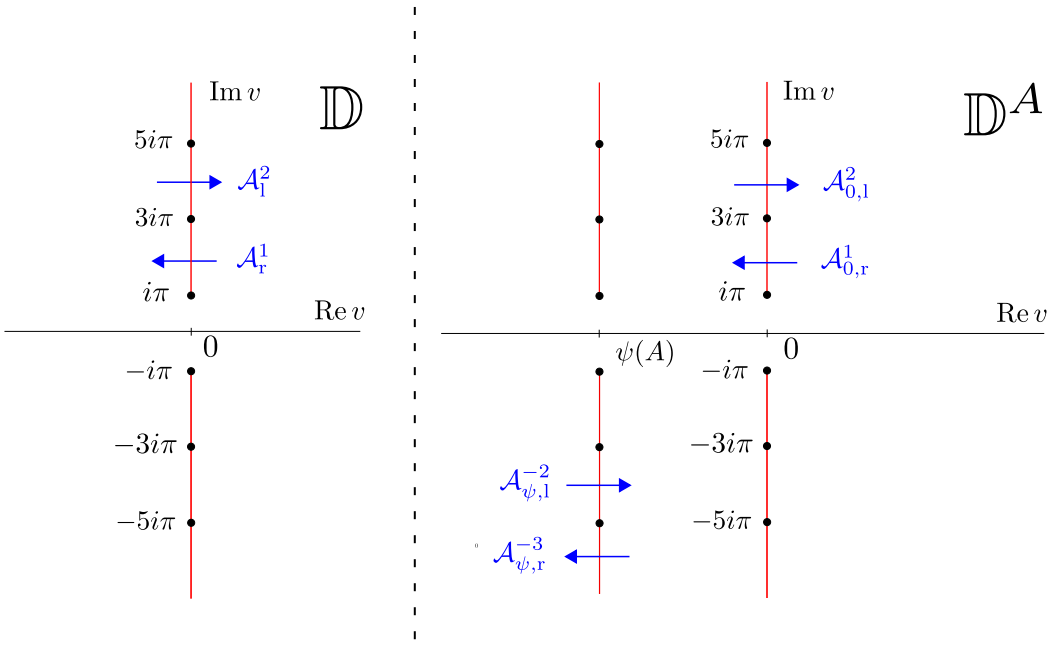

Figure 4.12: Représentation des coupures de la fonction χ dans le plan complexe exclues du domaine $\mathbb{D}$ (gauche) et de la fonction χ^A pour le domaine $\mathbb{D}^A$. On note $A^n_{l|r}$ l'opérateur de prolongement analytique agissant sur une fonction à travers la coupure $\mathrm{i}[2\pi(n-1/2), 2\pi(n+1/2)]$ depuis la gauche ou la droite de la coupure. Ainsi pour une f fonction discontinue sur l'axe imaginaire, la fonction définie par $F(v) = f(v)$ pour $\mathrm{Re}\, v > 0$ et $F(v) = A^n_r f(v)$ pour $\mathrm{Re}\, v < 0$ est continue au voisinage de l'intervalle $\mathrm{i}[2\pi(n-1/2), 2\pi(n+1/2)]$. Dans le cas d'une fonction analytique sur $\mathbb{D}^A$ possédant un second ensemble de coupure en $\mathrm{Re}\, v = \psi(A)$ on définit de façon analogue des opérateurs de prolongement analytique $A^n_{0,l|r}$ et $A^n_{\psi,l|r}$.

où les termes additionnels η_i sont construit à partir de la racine des fonctions W_j de Lambert, solutions de l'équation $W_j(z)\mathrm{e}^{W_j(z)} = z$ telle que

$$\log W_j(z) + W_j(z) = \log z + 2\mathrm{i}j\pi \ .$$

Plus précisément, les fonctions η_j sont des déterminations analytiques sur $\mathbb{D}$ de la fonction $\sqrt{-W_j(\mathrm{e}^{-1-v})}$. On peut montrer qu'en remplaçant la fonction χ par une de ces branches χ_P dans les équations (4.105)–(4.106), on obtient une solution $E(\mu)$ correspondant à l'état excité de $M(\mu)$ indexé par des pairs trous-excitations P_+ et P_- (voir figure 4.10) correspondant aux éléments positifs et négatifs respectivement de l'ensemble P caractérisant la branche de χ choisie. L'ensemble d'indice $P' = A_n^{\mathrm{l}|\mathrm{r}}$ caractérisant le prolongement analytique $\chi_{P'}$ d'une branche χ_P lors du franchissement d'une coupure est obtenu par des opérations ensemblistes sur l'ensemble original $P \subset \mathbb{Z}$, dont les expressions explicites sont

$$A_n^{\mathrm{l}} P = \begin{cases} (P \setminus C_n) \cup (B_n \setminus (P + \operatorname{sgn} n)) \cup \{0\} & \begin{array}{l} n \in P \ \& \ n \text{ even} \\ n \notin P \ \& \ n \text{ odd} \end{array} \\ (P \setminus C_n) \cup (B_n \setminus (P + \operatorname{sgn} n)) & \begin{array}{l} n \in P \ \& \ n \text{ odd} \\ n \notin P \ \& \ n \text{ even} \end{array} \end{cases} \tag{4.109}$$

$$A_n^{\mathrm{r}} P = \begin{cases} (P \setminus C_n) \cup (C_{n-\operatorname{sgn} n} \setminus (P - \operatorname{sgn} n)) \cup \{n\} & \begin{array}{l} 0 \in P \ \& \ n \text{ even} \\ 0 \notin P \ \& \ n \text{ odd} \end{array} \\ (P \setminus C_n) \cup (C_{n-\operatorname{sgn} n} \setminus (P - \operatorname{sgn} n)) & \begin{array}{l} 0 \in P \ \& \ n \text{ odd} \\ 0 \notin P \ \& \ n \text{ even} \end{array} \end{cases} . \tag{4.110}$$

Ce resultat a fait l'objet d'une publication dans [41], où l'on démontre les expressions précédente directement à partir de l'ansatz de Bethe. Voir aussi les chapitres 3 et 4 de la thèse.

Premiers états excités dans le crossover courant maximal/basse densité

Dans un second temps de la thèse, nous avons généralisé ces résultats (valable pour α, β à l'intérieur de la phase de courant maximal) à limite entre les phases de courant maximal et de haute/basse densité. Selon le scaling exact des paramètres de bords α, β en fonction de la taille du système, le modèle de croissance de la figure 4.9 est également décrit par l'universalité KPZ avec des conditions aux bords variables sur la fonction de hauteur. Ces résultats ont été publiés dans [40] et sont détaillés dans le chapitre 4. Nous considérons ici le scaling des taux de bords

$$\alpha = \frac{1}{2} + \frac{1}{2\sqrt{A}} \qquad \beta = \frac{1}{2} + \frac{1}{2\sqrt{B}} \tag{4.111}$$

de sorte que les conditions aux bords de Neumann sur la pente de la fonction de hauteur associées au TASEP sont des fonctions affines des paramètres A et B, d'après [66]. En prenant la limite $B \to \infty$ pour simplifier les calculs, on obtient à partir des expressions obtenues par ansatz de Bethe (ou de façon équivalente par ansatz matriciel généralisé) les équations suivantes, analogue de (4.105)–(4.106)

$$\mu \simeq \frac{\eta^A(v)}{4\pi\sqrt{L}} \ , \tag{4.112}$$

$$E - \frac{\mu}{4} \simeq \frac{\chi^A(v)}{12\pi L^{3/2}} \ , \tag{4.113}$$

où l'on a défini les fonctions

$$\eta^A(v) = \int_{-\infty}^{\infty} \mathrm{d}y \, \frac{(A+4)y^2\left(4A\left(y^2-4\right)+y^4\right)}{2\left(4A+y^2\right)\left(\left(4A+y^2\right)e^{-v-v_0^A+\frac{y^2}{4}}+(A+4)y^2\right)} \ , \tag{4.114}$$

$$\chi^A(v) = \frac{1}{16}\int_{-\infty}^{\infty} \mathrm{d}y \, \frac{(A+4)y^4\left(4A\left(y^2-4\right)+y^4\right)}{2\left(4A+y^2\right)\left(\left(4A+y^2\right)e^{-v-v_0^A+\frac{y^2}{4}}+(A+4)y^2\right)} \ . \tag{4.115}$$

Le prolongement analytique des fonctions χ^A et η^A et la détermination de l'ensemble de leurs branches peuvent être réalisés de façon essentiellement analogue au cas $\alpha = \beta = 1$, en considérant cette fois ci des fonctions de Lambert généralisées, solutions multivaluées de l'équation

$$\mathrm{e}^{W_j^A(z)} \frac{W_j^A(z)}{A - W_j^A(z)} = z \ . \tag{4.116}$$

La structure du prolongement analytique (c'est-à-dire la connectivité des différentes branches au travers des coupures) des fonctions χ^A et η^A sont similaires. On obtient pour les branches de ces prolongements des expressions analogues à (4.108):

$$\eta_P^A(v) = \eta^A(v) + 2\mathrm{i} \sum_{j \in P} \lambda_i^A(v) \tag{4.117}$$

$$\chi_P^A(v) = \chi^A(v) + 2\mathrm{i} \sum_{j \in P} \left(\lambda_i^A(v)\right)^3 \tag{4.118}$$

En substituant ces fonctions à χ^A et η^A dans (4.112) et (4.113), on obtient de nouvelles valeurs propres de $M(\mu)$. On obtient également des expressions similaires à

De façon remarquable, le spectre du TASEP ouvert à L sites sur la ligne de transition basse densité/courant maximal est un sous ensemble de celui du TASEP avec conditions aux bords périodiques pour $2L + 2$ sites et $L + 1$ particules, de sorte que la famille de surfaces de Riemann $\mathcal{R}^A$ fournit une déformation continue de la surface $\mathcal{R}^{\mathrm{Per}}$ précédement construite dans pour le TASEP avec conditions aux bords périodiques pour $A \to 0$ en la surface de Riemann $\mathcal{R}^{\mathrm{MC}}$ correspondant au cas courant maximal. Il est donc vraisemblable que les expressions dérivées dans [73] pour les distributions de probabilités des fluctuations de la fonction de hauteur KPZ avec conditions au bords périodiques en terme d'intégrale de contour sur la surface $\mathcal{R}^{\mathrm{Per}}$ se généralisent au cas ouvert.

Correspondance avec l'ansatz de Bethe

Les expressions dérivées par prolongement analytique peuvent être partiellement démontrées directement à partir du calcul des racines des Bethe pour des grandes tailles de système dans le cas $\alpha = \beta = 1$. On peut en effet exprimer les racines de Bethe $\{u_j, 1 \leq j \leq L + 2\}$ en fonctions du paramètre global $C = \mathrm{e}^{\mu} \prod_{k=1}^{L+2} u_k$,

$$u_j = \mathfrak{u}_j(C) \qquad 1 \leq j \leq L + 2 \ , \tag{4.119}$$

D'où l'on peut ensuite déduire des expressions asymptotique à l'ordre voulu en la taille du système, faisant intervenir les fonctions de Lambert W_j, de sorte que l'expression de la valeur propre (4.102) est effectivement égale pour $L \to \infty$ à l'expression (4.106), et les termes additionnels obtenus par prolongement analytique s'interprètent naturellement comme des contributions des pairs trou excitations ajouté à un état fondamental. L'expression (4.105) est ensuite obtenue simplement en écrivant le paramètre C sous forme auto-cohérente.

Conclusion et perspectives

Nous avons au cours de cette thèse dérivé des expressions exactes pour les valeurs propres de la matrice de Markov déformée du TASEP ouvert contribuant au régime universel KPZ. Ce travail n'est cependant qu'une première étape vers le calcul des statistiques des fluctuations du courant, ou de façon équivalente de la fonction hauteur autour du profil moyen associée au processus d'exclusion via le modèle de croissance présenté à la figure 4.9. En effet, d'après (4.97), la détermination complète de la fonction génératrice des cumulants du courant intégré requiert également la conaissance des vecteurs propres, qui sont encore inconus à la fin de cette thèse. Il devrait ensuite être possible de reformuler ces résultats sous forme plus compact au moyen d'intégrales sur les surfaces de Riemann construites par le calcul du prolongement analytiques des fonctions χ et χ^A.

References

[1] J. Baik and Z. Liu. "TASEP on a Ring in Sub-relaxation Time Scale". In: *Journal of Statistical Physics* 165.6 (2016), pp. 1051–1085. ISSN: 0022-4715, 1572-9613. DOI: 10.1007/s10955-016-1665-y.

[2] A. L. Barabási and H. E. Stanley. *Fractal Concepts in Surface Growth*. First. Cambridge University Press, 1995. ISBN: 978-0-521-48308-7 978-0-521-48318-6 978-0-511-59979-8. DOI: 10.1017/CBO9780511599798.

[3] G. Barraquand and P. Le Doussal. "Steady State of the KPZ Equation on an Interval and Liouville Quantum Mechanics". In: *Europhysics Letters* 137.6 (2022), p. 61003. ISSN: 0295-5075, 1286-4854. DOI: 10.1209/0295-5075/ac25a9.

[4] R. J. Baxter. "Exactly Solved Models in Statistical Mechanics". In: *Integrable Systems in Statistical Mechanics*. Vol. 1. World Scientific, 1985, pp. 5–63. ISBN: 978-9971-978-11-2 978-981-4415-25-5. DOI: 10.1142/9789814415255_0002.

[5] S. Belliard and N. Crampé. "Heisenberg XXX Model with General Boundaries: Eigenvectors from Algebraic Bethe Ansatz". In: *Symmetry, Integrability and Geometry: Methods and Applications* (2013). ISSN: 18150659. DOI: 10.3842/SIGMA.2013.072.

[6] C. M. Bender and T. T. Wu. "Anharmonic Oscillator". In: *Physical Review* 184.5 (1969), pp. 1231–1260. ISSN: 0031-899X. DOI: 10.1103/PhysRev.184.1231.

[7] C. M. Bender and T. T. Wu. "Anharmonic Oscillator. II. A Study of Perturbation Theory in Large Order". In: *Physical Review D* 7.6 (1973), pp. 1620–1636. ISSN: 0556-2821. DOI: 10.1103/PhysRevD.7.1620.

[8] L. Bertini and G. Giacomin. "Stochastic Burgers and KPZ Equations from Particle Systems". In: *Communications in Mathematical Physics* 183.3 (1997), pp. 571–607. ISSN: 0010-3616, 1432-0916. DOI: 10.1007/s002200050044.

[9] H. Bethe. "Zur Theorie der Metalle: I. Eigenwerte und Eigenfunktionen der linearen Atomkette". In: *Zeitschrift fur Physik* 71.3-4 (1931), pp. 205–226. ISSN: 1434-6001, 1434-601X. DOI: 10.1007/BF01341708.

[10] R. A. Blythe and M. R. Evans. "Nonequilibrium Steady States of Matrix-Product Form: A Solver's Guide". In: *Journal of Physics A: Mathematical and Theoretical* 40.46 (2007), R333–R441. ISSN: 1751-8113, 1751-8121. DOI: 10.1088/1751-8113/40/46/R01.

[11] T. Bodineau and B. Derrida. "Current Fluctuations in Nonequilibrium Diffusive Systems: An Additivity Principle". In: *Physical Review Letters* 92.18 (2004), p. 180601. ISSN: 0031-9007, 1079-7114. DOI: 10.1103/PhysRevLett.92.180601.

[12] T. Bodineau and B. Derrida. "Current Large Deviations for Asymmetric Exclusion Processes with Open Boundaries". In: *Journal of Statistical Physics* 123.2 (2006), pp. 277–300. ISSN: 0022-4715, 1572-9613. DOI: 10.1007/s10955-006-9048-4.

[13] E. Brattain, N. Do, and A. Saenz. "The Completeness of the Bethe Ansatz for the Periodic ASEP". In: *arXiv:1511.03762 [cond-mat, physics:math-ph, physics:nlin]* (2017). arXiv: 1511.03762 [cond-mat, physics:math-ph, physics:nlin].

[14] D. Bressoud. "A Simple Proof of Mehler's Formula for q-Hermite Polynomials". In: *Indiana University Mathematics Journal* 29.4 (1980), pp. 577–580.

[15] P. Calabrese, P. L. Doussal, and A. Rosso. "Free-Energy Distribution of the Directed Polymer at High Temperature". In: *EPL (Europhysics Letters)* 90.2 (2010), p. 20002. ISSN: 0295-5075, 1286-4854. DOI: 10.1209/0295-5075/90/20002.

[16] L. Cantini. "Asymmetric Simple Exclusion Process with Open Boundaries and Koornwinder Polynomials". In: *Annales Henri Poincaré* 18 (2015), pp. 1121–1151.

[17] R. Cavalieri and E. Miles. *Riemann Surfaces and Algebraic Curves: A First Course in Hurwitz Theory*. London Mathematical Society Student Texts 87. Cambridge, United Kingdom ; New York, NY, USA: Cambridge University Press, 2016. ISBN: 978-1-107-14924-3 978-1-316-60352-9.

[18] T. Chou, K. Mallick, and R. K. P. Zia. "Non-Equilibrium Statistical Mechanics: From a Paradigmatic Model to Biological Transport". In: *Reports on Progress in Physics* 74.11 (2011), p. 116601. ISSN: 0034-4885, 1361-6633. DOI: 10.1088/0034-4885/74/11/116601.

[19] T. Chou. "Water Alignment, Dipolar Interactions, and Multiple Proton Occupancy during Water-Wire Proton Transport". In: *Biophysical Journal* 86.5 (2004), pp. 2827–2836. ISSN: 00063495. DOI: 10.1016/S0006-3495(04)74335-0.

[20] I. Corwin. *Some Recent Progress on the Stationary Measure for the Open KPZ Equation*. 2022. arXiv: 2202.01836 [math].

[21] I. Corwin. "The Kardar-Parisi-Zhang Equation and Universality Class". In: *Random Matrices: Theory and Applications* 01.01 (2012), p. 1130001. ISSN: 2010-3263, 2010-3271. DOI: 10.1142/S2010326311300014.

[22] I. Corwin and A. Knizel. *Stationary Measure for the Open KPZ Equation*. 2021. arXiv: 2103.12253 [cond-mat, physics:math-ph].

[23] I. Corwin and H. Shen. "Open ASEP in the Weakly Asymmetric Regime". In: *Communications on Pure and Applied Mathematics* 71.10 (2018), pp. 2065–2128. ISSN: 00103640. DOI: 10.1002/cpa.21744.

[24] N. Crampe, E. Ragoucy, and D. Simon. "Matrix Coordinate Bethe Ansatz: Applications to XXZ and ASEP Models". In: *Journal of Physics A: Mathematical and Theoretical* 44.40 (2011), p. 405003. ISSN: 1751-8113, 1751-8121. DOI: 10.1088/1751-8113/44/40/405003.

[25] N. Crampe and R. I. Nepomechie. "Equivalent T-Q Relations and Exact Results for the Open TASEP". In: *Journal of Statistical Mechanics: Theory and Experiment* 2018.10 (2018), p. 103105. ISSN: 1742-5468. DOI: 10.1088/1742-5468/aae2e0.

[26] N. Crampé. "Algebraic Bethe Ansatz for the Totally Asymmetric Simple Exclusion Process with Boundaries". In: *Journal of Physics A: Mathematical and Theoretical* 48.8 (2015), 08FT01. ISSN: 1751-8113, 1751-8121. DOI: 10.1088/1751-8113/48/8/08FT01.

[27] N. Crampé, E. Ragoucy, and D. Simon. "Eigenvectors of Open *XXZ* and ASEP Models for a Class of Non-Diagonal Boundary Conditions". In: *Journal of Statistical Mechanics: Theory and Experiment* 2010.11 (2010), P11038. ISSN: 1742-5468. DOI: 10.1088/1742-5468/2010/11/P11038.

[28] J. de Gier and F. H. L. Essler. "Bethe Ansatz Solution of the Asymmetric Exclusion Process with Open Boundaries". In: *Physical Review Letters* 95.24 (2005), p. 240601. ISSN: 0031-9007, 1079-7114. DOI: 10.1103/PhysRevLett.95.240601.

[29] J. de Gier and F. H. L. Essler. "Large Deviation Function for the Current in the Open Asymmetric Simple Exclusion Process". In: *Physical Review Letters* 107.1 (2011), p. 010602. ISSN: 0031-9007, 1079-7114. DOI: 10.1103/PhysRevLett.107.010602.

[30] B. Derrida et al. "Exact Solution of a 1D Asymmetric Exclusion Model Using a Matrix Formulation". In: *Journal of Physics A: Mathematical and General* 26.7 (1993), pp. 1493–1517. ISSN: 0305-4470, 1361-6447. DOI: 10.1088/0305-4470/26/7/011.

[31] B. Derrida. "An Exactly Soluble Non-Equilibrium System: The Asymmetric Simple Exclusion Process". In: *Physics Reports* 301.1-3 (1998), pp. 65–83. ISSN: 03701573. DOI: 10.1016/S0370-1573(98)00006-4.

[32] B. Derrida and M. R. Evans. "Exact Correlation Functions in an Asymmetric Exclusion Model with Open Boundaries". In: *Journal de Physique I* 3.2 (1993), pp. 311–322. ISSN: 1155-4304, 1286-4862. DOI: 10.1051/jp1:1993132.

[33] B. Doyon. "Lecture Notes on Generalised Hydrodynamics". In: *SciPost Physics Lecture Notes* (2020), p. 18. ISSN: 2590-1990. DOI: 10.21468/SciPostPhysLectNotes.18.

[34] D. J. Evans, E. G. D. Cohen, and G. P. Morriss. "Probability of Second Law Violations in Shearing Steady States". In: *Physical Review Letters* 71.15 (1993), pp. 2401–2404. ISSN: 0031-9007. DOI: 10.1103/PhysRevLett.71.2401.

[35] M. R. Evans and T. Hanney. "Nonequilibrium Statistical Mechanics of the Zero-Range Process and Related Models". In: *Journal of Physics A: Mathematical and General* 38.19 (2005), R195–R240. ISSN: 0305-4470, 1361-6447. DOI: 10.1088/0305-4470/38/19/R01.

[36] L. D. Faddeev. "How Algebraic Bethe Ansatz Works for Integrable Model". In: *arXiv:hep-th/9605187* (1996). arXiv: hep-th/9605187.

[37] P. L. Ferrari. "From Interacting Particle Systems to Random Matrices". In: *Journal of Statistical Mechanics: Theory and Experiment* 2010.10 (2010), P10016. ISSN: 1742-5468. DOI: 10.1088/1742-5468/2010/10/P10016.

[38] C. Finn and M. Vanicat. "Matrix product construction for Koornwinder polynomials and fluctuations of the current in the open ASEP". In: *Journal of Statistical Mechanics: Theory and Experiment* 2017.2 (2017), p. 023102. DOI: 10.1088/1742-5468/aa569b. URL: https://doi.org/10.1088/1742-5468/aa569b.

[39] J. de Gier and F. H. L. Essler. "Exact Spectral Gaps of the Asymmetric Exclusion Process with Open Boundaries". In: *Journal of Statistical Mechanics: Theory and Experiment* 2006.12 (2006), P12011–P12011. ISSN: 1742-5468. DOI: 10.1088/1742-5468/2006/12/P12011.

[40] U. Godreau and S. Prolhac. "Riemann Surface Crossover for the Spectral Gaps of Open TASEP". In: *Journal of Statistical Mechanics: Theory and Experiment* 2021.8 (2021), p. 083219. ISSN: 1742-5468. DOI: 10.1088/1742-5468/ac1662.

[41] U. Godreau and S. Prolhac. "Spectral Gaps of Open TASEP in the Maximal Current Phase". In: *Journal of Physics A: Mathematical and Theoretical* 53.38 (2020), p. 385006. ISSN: 1751-8113, 1751-8121. DOI: 10.1088/1751-8121/aba575.

[42] O. Golinelli and K. Mallick. "The Asymmetric Simple Exclusion Process: An Integrable Model for Non-Equilibrium Statistical Mechanics". In: *Journal of Physics A: Mathematical and General* 39.41 (2006), pp. 12679–12705. ISSN: 0305-4470, 1361-6447. DOI: 10.1088/0305-4470/39/41/S03.

[43] S. Gopalakrishnan and R. Vasseur. "Kinetic Theory of Spin Diffusion and Superdiffusion in X X Z Spin Chains". In: *Physical Review Letters* 122.12 (2019), p. 127202. ISSN: 0031-9007, 1079-7114. DOI: 10.1103/PhysRevLett.122.127202.

[44] M. Gorissen et al. "Exact Current Statistics of the Asymmetric Simple Exclusion Process with Open Boundaries". In: *Physical Review Letters* 109.17 (2012), p. 170601. ISSN: 0031-9007, 1079-7114. DOI: 10.1103/PhysRevLett.109.170601.

[45] T. Halpin-Healy and Y.-C. Zhang. "Kinetic Roughening Phenomena, Stochastic Growth, Directed Polymers and All That. Aspects of Multidisciplinary Statistical Mechanics". In: *Physics Reports* 254.4-6 (1995), pp. 215–414. ISSN: 03701573. DOI: 10.1016/0370-1573(94)00087-J.

[46] D. Helbing. "Traffic and Related Self-Driven Many-Particle Systems". In: *Reviews of Modern Physics* 73.4 (2001), pp. 1067–1141. ISSN: 0034-6861, 1539-0756. DOI: 10.1103/RevModPhys.73.1067.

[47] M. Henkel and G. Schutz. "Finite-Lattice Extrapolation Algorithms". In: *Journal of Physics A: Mathematical and General* 21.11 (1988), pp. 2617–2633. ISSN: 0305-4470, 1361-6447. DOI: 10.1088/0305-4470/21/11/019.

[48] M. A. C. Huergo et al. "Growth Dynamics of Cancer Cell Colonies and Their Comparison with Noncancerous Cells". In: *Physical Review E* 85.1 (2012), p. 011918. ISSN: 1539-3755, 1550-2376. DOI: 10.1103/PhysRevE.85.011918.

[49] K. Johansson. "Shape Fluctuations and Random Matrices". In: *Communications in Mathematical Physics* 209.2 (2000), pp. 437–476. ISSN: 0010-3616, 1432-0916. DOI: 10.1007/s002200050027.

[50] M. Kardar, G. Parisi, and Y.-C. Zhang. "Dynamic Scaling of Growing Interfaces". In: *Physical Review Letters* 56.9 (1986), pp. 889–892. ISSN: 0031-9007. DOI: 10.1103/PhysRevLett.56.889.

[51] A. Kolmogoroff. "Zur Theorie der Markoffschen Ketten". In: *Mathematische Annalen* 112.1 (1936), pp. 155–160. ISSN: 0025-5831, 1432-1807. DOI: 10.1007/BF01565412.

[52] J. Lamers. "A Pedagogical Introduction to Quantum Integrability, with a View towards Theoretical High-Energy Physics". In: *Proceedings of 10th Modave Summer School in Mathematical Physics — PoS(Modave2014)* (2015), p. 001. DOI: 10.22323/1.232.0001. arXiv: 1501.06805.

[53] R. P. Langlands and Y. Saint-Aubin. "Algebro-Geometric Aspects of the Bethe Equations". In: *Strings and Symmetries*. Ed. by G. Aktaş, C. Saçlioğlu, and M. Serdaroğlu. Vol. 447. Berlin, Heidelberg: Springer Berlin Heidelberg, 1995, pp. 40–53. ISBN: 978-3-540-59163-4 978-3-540-49204-7. DOI: 10.1007/3-540-59163-X_254.

[54] A. Lazarescu. "Exact Large Deviations of the Current in the Asymmetric Simple Exclusion Process with Open Boundaries". PhD Thesis. Université Pierre et Marie Curie Paris VI, 2011.

[55] A. Lazarescu. "The Physicist's Companion to Current Fluctuations: One-Dimensional Bulk-Driven Lattice Gases". In: *Journal of Physics A: Mathematical and Theoretical* 48.50 (2015), p. 503001. ISSN: 1751-8113, 1751-8121. DOI: 10.1088/1751-8113/48/50/503001.

[56] A. Lazarescu and K. Mallick. "An Exact Formula for the Statistics of the Current in the TASEP with Open Boundaries". In: *Journal of Physics A: Mathematical and Theoretical* 44.31 (2011), p. 315001. ISSN: 1751-8113, 1751-8121. DOI: 10.1088/1751-8113/44/31/315001.

[57] A. Lazarescu and V. Pasquier. "Bethe Ansatz and Q -Operator for the Open ASEP". In: *Journal of Physics A: Mathematical and Theoretical* 47.29 (2014), p. 295202. ISSN: 1751-8113, 1751-8121. DOI: 10.1088/1751-8113/47/29/295202.

[58] M. Ljubotina, M. Žnidarič, and T. Prosen. "Kardar-Parisi-Zhang Physics in the Quantum Heisenberg Magnet". In: *Physical Review Letters* 122.21 (2019), p. 210602. ISSN: 0031-9007, 1079-7114. DOI: 10.1103/PhysRevLett.122.210602.

[59] C. T. MacDonald, J. H. Gibbs, and A. C. Pipkin. "Kinetics of Biopolymerization on Nucleic Acid Templates". In: *Biopolymers* 6.1 (1968), pp. 1–25. ISSN: 0006-3525, 1097-0282. DOI: 10.1002/bip.1968.360060102.

[60] J. M. Maillet and J. S. de Santos. "Drinfel'd Twists and Algebraic Bethe Ansatz". In: *arXiv:q-alg/9612012* (1996). arXiv: q-alg/9612012.

[61] K. Mallick. "Some Exact Results for the Exclusion Process". In: *Journal of Statistical Mechanics: Theory and Experiment* 2011.01 (2011), P01024. ISSN: 1742-5468. DOI: 10.1088/1742-5468/2011/01/P01024.

[62] K. Matetski, J. Quastel, and D. Remenik. "The KPZ Fixed Point". In: *Acta Mathematica* 227.1 (2021), pp. 115–203. ISSN: 00015962, 18712509. DOI: 10.4310/ACTA.2021.v227.n1.a3.

[63] J. Maunuksela et al. "Kinetic Roughening in Slow Combustion of Paper". In: *Physical Review Letters* 79.8 (1997), pp. 1515–1518. ISSN: 0031-9007, 1079-7114. DOI: 10.1103/PhysRevLett.79.1515.

[64] A. Nahum et al. "Quantum Entanglement Growth under Random Unitary Dynamics". In: *Physical Review X* 7.3 (2017), p. 031016. ISSN: 2160-3308. DOI: 10.1103/PhysRevX.7.031016.

[65] R. Nepomechie. "Bethe ansatz solution of the open XXZ chain with nondiagonal boundary terms". In: *Journal of Physics A: Mathematical and General* 37.2 (2003), pp. 433–440. DOI: 10.1088/0305-4470/37/2/012. URL: https://doi.org/10.1088/0305-4470/37/2/012.

[66] S. Parekh. "The KPZ Limit of ASEP with Boundary". In: *Communications in Mathematical Physics* 365.2 (2019), pp. 569–649. ISSN: 0010-3616, 1432-0916. DOI: 10.1007/s00220-018-3258-x.

[67] A. Parmeggiani, T. Franosch, and E. Frey. "Totally Asymmetric Simple Exclusion Process with Langmuir Kinetics". In: *Physical Review E* 70.4 (2004), p. 046101. ISSN: 1539-3755, 1550-2376. DOI: 10.1103/PhysRevE.70.046101.

[68] M. Prähofer and H. Spohn. "Universal Distributions for Growth Processes in 1 + 1 Dimensions and Random Matrices". In: *Physical Review Letters* 84.21 (2000), pp. 4882–4885. ISSN: 0031-9007, 1079-7114. DOI: 10.1103/PhysRevLett.84.4882.

[69] J. Prior, A. M. Somoza, and M. Ortuño. "Conductance Fluctuations and Single-Parameter Scaling in Two-Dimensional Disordered Systems". In: *Physical Review B* 72.2 (2005), p. 024206. ISSN: 1098-0121, 1550-235X. DOI: 10.1103/PhysRevB.72.024206.

[70] S. Prolhac. "Current Fluctuations and Large Deviations for Periodic TASEP on the Relaxation Scale". In: *Journal of Statistical Mechanics: Theory and Experiment* 2015.11 (2015), P11028. ISSN: 1742-5468. DOI: 10.1088/1742-5468/2015/11/P11028.

[71] S. Prolhac. "Extrapolation Methods and Bethe Ansatz for the Asymmetric Exclusion Process". In: *Journal of Physics A: Mathematical and Theoretical* 49.45 (2016), p. 454002. ISSN: 1751-8113, 1751-8121. DOI: 10.1088/1751-8113/49/45/454002. arXiv: 1604.08843 [cond-mat, physics:math-ph, physics:nlin].

[72] S. Prolhac. "Finite-Time Fluctuations for the Totally Asymmetric Exclusion Process". In: *Physical Review Letters* 116.9 (2016), p. 090601. ISSN: 0031-9007, 1079-7114. DOI: 10.1103/PhysRevLett.116.090601.

[73] S. Prolhac. "Riemann Surface for TASEP with Periodic Boundaries". In: *Journal of Physics A: Mathematical and Theoretical* 53.44 (2020), p. 445003. ISSN: 1751-8113, 1751-8121. DOI: 10.1088/1751-8121/abb389.

[74] S. Prolhac. "Riemann surfaces for KPZ with periodic boundaries". In: *SciPost Phys.* 8 (2020), p. 008. DOI: 10.21468/SciPostPhys.8.1.008. URL: https://scipost.org/10.21468/SciPostPhys.8.1.008.

[75] S. Prolhac. "Spectrum of the Totally Asymmetric Simple Exclusion Process on a Periodic Lattice—Bulk Eigenvalues". In: *Journal of Physics A: Mathematical and Theoretical* 46.41 (2013), p. 415001. ISSN: 1751-8113, 1751-8121. DOI: 10.1088/1751-8113/46/41/415001.

[76] B. R. "Partition function of the Eight-Vertex lattice model". In: *Annals of Physics* 70.1 (1972), pp. 193–228. ISSN: 0003-4916. DOI: https://doi.org/10.1016/0003-4916(72)90335-1. URL: https://www.sciencedirect.com/science/article/pii/0003491672903351.

[77] T. Sasamoto. "Density Profile of the One-Dimensional Partially Asymmetric Simple Exclusion Process with Open Boundaries". In: *Journal of the Physical Society of Japan* 69.4 (2000), pp. 1055–1067. ISSN: 0031-9015, 1347-4073. DOI: 10.1143/JPSJ.69.1055.

[78] T. Sasamoto. "One-Dimensional Partially Asymmetric Simple Exclusion Process with Open Boundaries: Orthogonal Polynomials Approach". In: *Journal of Physics A: Mathematical and General* 32.41 (1999), pp. 7109–7131. ISSN: 0305-4470, 1361-6447. DOI: 10.1088/0305-4470/32/41/306.

[79] A. Scheie et al. "Detection of Kardar–Parisi–Zhang Hydrodynamics in a Quantum Heisenberg Spin-1/2 Chain". In: *Nature Physics* 17.6 (2021), pp. 726–730. ISSN: 1745-2473, 1745-2481. DOI: 10.1038/s41567-021-01191-6.

[80] C. Schiffmann, C. Appert-Rolland, and L. Santen. "Shock Dynamics of Two-Lane Driven Lattice Gases". In: *Journal of Statistical Mechanics: Theory and Experiment* 2010.06 (2010), P06002. ISSN: 1742-5468. DOI: 10.1088/1742-5468/2010/06/P06002.

[81] G. Schütz. "Exactly Solvable Models for Many-Body Systems Far from Equilibrium". In: *Phase Transitions and Critical Phenomena*. Vol. 19. Elsevier, 2001, pp. 1–251. ISBN: 978-0-12-220319-0. DOI: 10.1016/S1062-7901(01)80015-X.

[82] E. K. Sklyanin. "Boundary Conditions for Integrable Quantum Systems". In: *Journal of Physics A: Mathematical and General* 21.10 (1988), pp. 2375–2389. ISSN: 0305-4470, 1361-6447. DOI: 10.1088/0305-4470/21/10/015.

[83] K. E. Smith, ed. *An Invitation to Algebraic Geometry*. Universitext. New York: Springer, 2000. ISBN: 978-0-387-98980-8.

[84] F. Spitzer. "Interaction of Markov Processes". In: *Advances in Mathematics* 5.2 (1970), pp. 246–290. ISSN: 00018708. DOI: 10.1016/0001-8708(70)90034-4.

[85] H. Spohn. "Nonlinear Fluctuating Hydrodynamics for Anharmonic Chains". In: *Journal of Statistical Physics* 154.5 (2014), pp. 1191–1227. ISSN: 0022-4715, 1572-9613. DOI: 10.1007/s10955-014-0933-y.

[86] K. A. Takeuchi. "An Appetizer to Modern Developments on the Kardar–Parisi–Zhang Universality Class". In: *Physica A: Statistical Mechanics and its Applications* 504 (2018), pp. 77–105. ISSN: 03784371. DOI: 10.1016/j.physa.2018.03.009.

[87] K. A. Takeuchi and M. Sano. "Universal Fluctuations of Growing Interfaces: Evidence in Turbulent Liquid Crystals". In: *Physical Review Letters* 104.23 (2010), p. 230601. ISSN: 0031-9007, 1079-7114. DOI: 10.1103/PhysRevLett.104.230601.

[88] V. Tarasov. "Completeness of the Bethe Ansatz for the Periodic Isotropic Heisenberg Model". In: *Reviews in Mathematical Physics* 30.08 (2018), p. 1840018. ISSN: 0129-055X, 1793-6659. DOI: 10.1142/S0129055X18400184.

[89] H. Touchette. "Introduction to Dynamical Large Deviations of Markov Processes". In: *Physica A: Statistical Mechanics and its Applications* 504 (2018), pp. 5–19. ISSN: 03784371. DOI: 10.1016/j.physa.2017.10.046.

[90] H. Touchette. "The Large Deviation Approach to Statistical Mechanics". In: *Physics Reports* 478.1-3 (2009), pp. 1–69. ISSN: 03701573. DOI: 10.1016/j.physrep.2009.05.002.

[91] M. Uchiyama and M. Wadati. "Correlation Function of Asymmetric Simple Exclusion Process with Open Boundaries:" in: *Journal of Nonlinear Mathematical Physics* 12.Supplement 1 (2005), p. 676. ISSN: 1776-0852. DOI: 10.2991/jnmp.2005.12.s1.52.

[92] M. Vanicat. "An integrabilist approach of out-of-equilibrium statistical physics models". Theses. Université Grenoble Alpes, 2017. URL: https://tel.archives-ouvertes.fr/tel-01688587.